

**Field relationships and petro-chemical investigation of mafic sills and dykes in
the vicinity of the Uitkomst Complex, Mpumalanga, South Africa**

Marie-Luise Pecher

May 2011



SUBMITTED IN ACCORDANCE WITH THE REQUIREMENTS FOR THE DEGREE OF MAGISTER SCIENTIAE
IN THE FACULTY OF NATURAL AND AGRICULTURAL SCIENCES, DEPARTMENT OF GEOLOGY AT THE
UNIVERSITY OF THE FREE STATE.

Affirmation

I, Marie-Luise Pecher, declare that this thesis is my own, unaided work and was written without any illegitimate help by a third party and without the use of any other literature and data than indicated in the thesis. Thoughts that were taken directly or indirectly from literature sources are indicated as such. It is being submitted for the Degree of Master of Science at the University of the Free State, Bloemfontein, South Africa and has not been submitted before for any degree or examination in any other University.

Halle, the 25th May 2011

Marie-Luise Pecher

Acknowledgement

I would like to thank and show my appreciation to Prof. Dr. Ch. Gauert and Prof. Dr. G. Borg for their supervision and support of this thesis. I wish to express my gratitude towards Prof. Dr. Ch. Gauert for his help on the ground, advice and encouraging words during the stay at the Nkomati Mine and for the fruitful discussions while writing the thesis. I would also like to thank Prof. Dr. G. Borg for his helpful critics and encouraging words.

A special and very heartfelt “Thank you” is given to Kelvin Mwamba as well as to his crew from Nkomati Mine for their help and support during the field work on the property of Nkomati Mine.

I would like to thank Prof. Dr. Willem v. d. Westhuizen for his effort concerning the realization of this study. Also I thank Mrs. Rina Immelmann from the University of the Free State, Bloemfontein for taking care of the accommodation and other formalities during the stay in Bloemfontein. I want to express thanks to the lab crew at the University of the Free State for their support on sample preparation.

Furthermore I wish to show my gratitude towards Dr. Michiel De Kock and Tumelo Mokgatle for the palaeomagnetic measurements at the laboratories of the University of Johannesburg as well as for their support with regards to the palaeomagnetic study.

I would like to thank Michael Schmidt, Janine Kottke-Levin, Marco Fiedler, Jens Kirste and all the people, who contributed to the success of this work. Finally, I am deeply grateful to my parents and my brother. Without their invaluable moral as well as financial support this work could not have been carried out. I value and appreciate their help exceptionally.

Abstract

Numerous mafic sills and dykes intruded into the Lower Transvaal sediments and the Archaean Basement in the vicinity of the Uitkomst Complex, which is assumed to be a satellite intrusion of the Bushveld Complex. Investigations on mafic sill intrusions near the Eastern Bushveld Complex described sills of pre-, syn- and post-Bushveld age and assigned the syn-Bushveld sills to the corresponding marginal rocks of the Bushveld Complex.

Purpose of the presented combined diploma thesis was to map the mafic sills and dykes in the vicinity of the Uitkomst Complex as basis for a petrographical and geochemical characterization. The geological mapping as well as the petrographic description distinguishes three groups of mafic intrusive rocks: **microgabbro sills**, **gabbronorite sills** and **gabbronoritic basement dykes**. The group of elongated microgabbro sills shows a widespread spatial as well as stratigraphic distribution within the study area, whereas the gabbronorite sills form huge sill bodies within a main stratigraphic position between the Upper Timeball Hill Shale and the Klapperkop Quartzite. The gabbronoritic basement dykes intruded into the Archaean granite gneiss and represent the oldest of the investigated mafic rocks.

Evaluation of the obtained geochemical data from about 160 samples verifies the classification into the three main groups. Based on incompatible element contents and element ratios different magma derivations are interpreted for the gabbronoritic sills, basement dykes and microgabbro sills. The basement dykes and gabbronorites sills are derived from a primitive partial melt, whereas the microgabbro sills show an evolved magma composition. Additional contamination with crustal material also changed the magma composition of each group as reflected by changing Ti/Zr ratios within the groups. The gabbronorite sills and basement dykes are probably contaminated with SiO₂-rich material from quartzites and granite gneiss (highest SiO₂ and Zr values), whereas the microgabbro sills show possible contaminations with dolomitic material (highest variation in CaO contents).

The comparison to Bushveld related marginal rocks shows a similar composition of the gabbronorite sills and basement dykes to the B1 quenched textured microproxenites, whereas the microgabbro sills indicate little correlation with the composition of one of the Bushveld marginal rocks (B1 to B3). Furthermore the microgabbro sills are nearly conformable in composition of selected trace elements with the Basal Gabbro chilled margins at Uitkomst and Slaaihoek, which is supported by a possible palaeomagnetic age relationship in some extent. The geochemical fingerprints of the investigated sills and dykes compared to the Uitkomst Complex have identified no direct correlation between them and show only low contents of exploration relevant elements for microgabbro sills, gabbronorite sills as well as basement dykes.

Table of contents

Affirmation	I
Acknowledgement	II
Abstract	III
Table of contents	IV
Abbreviations	VII
1. Introduction	1
1.1 Preface	1
1.2 Scientific context and motivation	2
1.3 Mining and exploration history	3
1.4 Previous work	4
1.5 Aims of the project	9
2. Geological Setting	10
2.1 Regional Geology	10
2.2 Local Stratigraphy	17
2.2.1 Nelshoogte Pluton	17
2.2.2 Lower Transvaal Supergroup	18
2.2.3 Uitkomst Complex	21
2.2.4 Diabase intrusions	23
3. Methods of investigation	26
3.1 Mapping	26
3.2 Sampling	26
3.3 XRF - Analysis	30
3.4 Microscopy	31
4. Geological mapping	33
4.1 Working area	33
4.2 Lithology of the country rocks	35
4.2.1 Nelshoogte granite gneiss/Archaean basement	35
4.2.2 Lower Transvaal Supergroup	37
4.2.2.1 Black Reef Quartzite	37
4.2.2.2 Malmani Dolomite	38
4.2.2.3 Rooihoogte Quartzite and Conglomerate	40

4.2.2.4 Timeball Hill Shale	40
4.2.2.5 Klapperkop Quartzite	42
4.3 Metamorphism	44
4.4 Tectonic and Structural Features	46
5. Petrography	53
5.1 Rock Classification	53
5.2 Microgabbro	55
5.2.1 Characteristics	55
5.2.2 Uitkomst Sill 1	59
5.2.3 Vaalkop Sill 1 & 2	63
5.2.4 Subgroup of small microgabbro sills	66
5.3 Gabbronorite	69
5.3.1 Characteristics	69
5.3.2 Hofmeyr Sill 1	73
5.3.3 Houtboschloop Sill 1	77
5.3.4 Houtboschloop Sill 3	80
5.3.5 Uitkomst Sill 4	83
5.3.6 Weltevreden Sill 1	85
5.3.7 Uitkomst Sill 3	88
5.4 Basement Dykes	91
5.4.1 Characteristics	91
5.5 Summary of Petrography	95
5.5.1 Basic petrographic features	95
5.5.2 Modal composition	96
5.5.3 Semi-quantitative rock classification	97
6. Geochemistry	98
6.1 Rock Classification	98
6.2 Alteration	101
6.3 Geochemical characterization of the mafic sills and dykes	102
6.4 Geotectonic environment and magma derivation	108
6.5 Comparison with Bushveld marginal rocks	111

7. Palaeomagnetic investigations	115
7.1 Sample sites	115
7.2 Palaeomagnetic methods	115
7.3 Palaeomagnetic results	117
7.4 Comparison with other palaeomagnetic poles	127
8. Discussion	130
9. Conclusion	138
10. References	140
Appendix	149

Attachments

- 1** - Geological map of regional mafic sills and dykes in the vicinity of the Uitkomst Complex, South Africa (1:75.000)
- 2** - Profiles (A – A', B – B', C' – C) (1:10.000)
- 3** - Data CD (includes XRF analyses, geological maps and profiles, thin section spreadsheets)

Abbreviations*Minerals*

Act	actinolite
Amp	amphibole
An	anorthite
Bt	biotite
Chl	chlorite
Cpx	clinopyroxene
Epi	epidote
Fsp	feldspar
Hbl	hornblende
Hem	hematite
Ilm	ilmenite
Magn	magnetite
Ol	olivine
Opx	orthopyroxene
Plag	plagioclase
Px	pyroxene
Py	pyrite
Qz	quartz
Srp	serpentine
Zr	zircon

Local farm names

BD	Basement Dykes
D	Doornhoek
EN	Engelschedraai
HB	Houtboschloop
HM	Hofmeyr
LM	Little Mamre
M	Mamre
SH	Slaaihoek
U	Uitkomst
UZ	Uitzicht
VK	Vaalkop
W	Weltevreden
<i>other</i>	
XRF	X-ray fluorescence spectroscopy
XP view	crossed polarisers
PP view	parallel polarisers
MORB	Mid ocean ridge basalt
MSL	Mean sea level
PM	Palaeomagnetic sample site
NRM	Natural remanent magnetization

Further abbreviations are explained within the individual chapters.

1. Introduction

1.1 Preface

The Uitkomst Complex is a mafic to ultramafic layered intrusion situated 200 km east of Pretoria in the Mpumalanga Province, more precisely 30 km north of Badplaas and 80 km northwest of Barberton (fig. 1.1). It is widely accepted that the Uitkomst Complex with a U-Pb SHRIMP age of 2044 ± 8 Ma (De Waal et al., 2001) is coeval with the Bushveld Igneous Complex. The tubular-shaped Uitkomst Complex with a total extension of 9 km in length and a thickness of up to 800 m intruded into the sediments of the Lower Transvaal Supergroup. The sulphide mineralisation of the Uitkomst Complex is mined at the Nkomati Mine, a joint venture between ARM Platinum and Norilsk Nickel. The high amount of nickel sulphides within the mineralisation, which occurs as a massive sulphide body as well as disseminated sulphides, established the Nkomati Mine as the first primary nickel mine of South Africa (Woolfe, 1996). Numerous mafic to ultramafic sills and dykes intruded in the Lower Transvaal sediments near the Uitkomst Complex. They could be similar to the sills and dykes in the vicinity of the Bushveld Complex, but analogical investigations are rather rare. The petrography and geochemistry of these sills and dykes represent the main objective of this study.

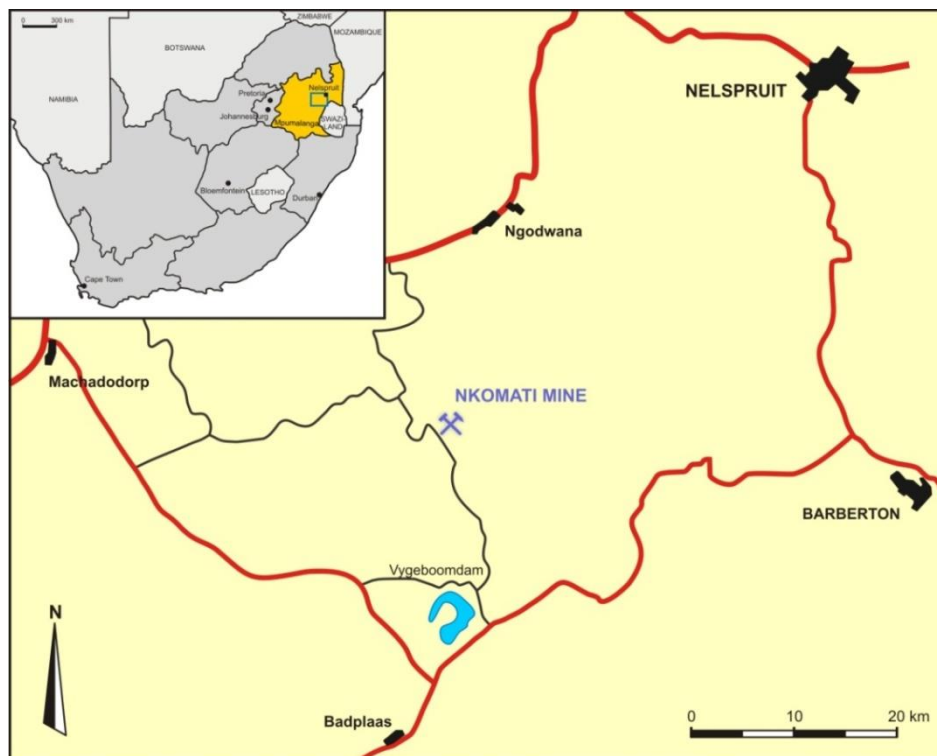


Figure 1.1: Geographical situation of the Uitkomst Complex, whose sulphide mineralisation is mined at the Nkomati Mine, a joint venture between ARM Platinum and Norilsk Nickel.

1.2 Scientific context and motivation

In the course of a regional brownfields exploration program carried out by the Doornhoek Joint Venture, the vicinity of the Nkomati Mine is currently being explored. Initial drilling projects proved the existence of gabbroic sills of several meters in thickness located southeast of the mine within the Oaktree and Black Reef Quartzites. Pilot surveys on these sills offered similarities to the Uitkomst Complex, such as the related stratigraphic position and several distinct rock types. However, none of the sills seemed to be macroscopically identical to one of the units at the Uitkomst Complex (Woolfe, 1996). To identify the Ni-Cu-PGE bearing potential of the mafic sills for further exploration an exact characterization, inclusive detailed mapping, petrographic description and geochemical interpretation, is required. These investigations were planned as a master's thesis, the most suitable option in relation to time and costs. The study was initiated between the coordinator from Norilsk Nickel for the Doornhoek Joint Venture exploration project, Kelvin C. Mwamba, and Prof. Christoph D.K. Gauert, from the Department of Geology at the University of the Free State, Bloemfontein in cooperation with Prof. Dr. Gregor Borg, from the Institute for Geosciences, Research Group for Petrology and Economic Geology at the Martin-Luther-University Halle-Wittenberg. On the basis of the Cooperation and the Memorandum of Understanding between both universities it is purposed to accomplish a diploma thesis as well as a master thesis.

This research is to be contributed to the Doornhoek Joint Venture exploration campaign of Norilsk Nickel Pty./ARM Pty. as well as to the scientific understanding for the correlation of mafic intrusive sills and mafic layered intrusions.

1.3 Mining and exploration history

The first description of sulphide bearing ultramafic rocks at the farm Uitkomst 541 JT is known from Wagner (1929). Upon his reference Anglo American Corporation of South Africa Ltd. (AAC) recognized in 1970 the potential for further exploration. During the seventies and eighties several drilling programs were operated becoming continuously deeper, but still in the region of disseminated mineralization. The results showed no promise amounts of sulphides and additionally serpentine and talc within the rocks caused problems in the extraction, so that a mining operation was abandoned (Woolfe, 1996).

Since 1939 Anglovaal's daughter company Eastern Transvaal Consolidated Mines Ltd. (ETC) held the mineral rights to the adjacent farms Slaaihoek and Mamre in order to mine epithermal gold within the Timeball Hill shale. After a preliminary feasibility study and a drilling program on Slaaihoek 540 JT from 1990 to 1992, the ETC discovered a massive sulphide body at the base of the Uitkomst Complex (Hornsey, 1999). For further exploration on Slaaihoek the Nico Joint Venture was formed in 1993 between two Anglovaal subsidiaries, ETC and Middle Witwatersrand (Western Areas) Ltd.. In order to open up the whole complex and to reduce the development costs, it was necessary to combine the holdings on the farm Slaaihoek and Uitkomst. In June 1995 the Nkomati Joint Venture was created as a partnership between the Nico Joint Venture and Kaffrarian Metal Holdings Ltd., an AAC subsidiary. Until 1996 a total of about 153.000 meters in 746 holes have been drilled and a massive sulphide reserve of 7 Mt @ 2.2 % Ni, 0.9 % Cu, 0.5 % Co and ca. 7 g/t PGE's, and chromite reserves have been determined (Woolfe, 1996). In 1997 South Africa's first primary nickel mine entered production with a predicted life time of ten years. During that time the evaluation of the massive sulphide bodies (MSB) and the exploration and feasibility of the other mineralized zone was going on. In 2004 African Rainbow Minerals (ARM), successor of the Anglovaal properties, purchased the Nkomati nickel operation. In June 2007 Norilsk Nickel acquired 50 % from ARM and the Nkomati Mine Joint Venture was established. In a large scale expansion project ARM and Norilsk Nickel intent to increase the annual nickel production by additional open pit mining and to extend the life of the mine into 2027.

The exploration in the vicinity of the Uitkomst Complex along the Mpumalanga escarpment started contemporaneous with the mining operation in 1996. An intensive greenfields exploration campaign, named Kransberg survey, was carried out until 1998. This comprised airborne magnetics over an area of 100 x 50 km, remote sensing, sampling (1500 stream sediment samples, 150 soil samples and several water samples) and litho geochemistry (XRF and XRD analyses). In 2007 the license area of the Nkomati Mine was expanded to explore the surrounding farms. Therefore the Doornhoek Joint Venture was formed by Norilsk Nickel and ARM to carry out a regional brownfields exploration program. This included airborne magnetics, radiometrics, regional stream sediment and regolith sampling, diamond drilling as well as more detailed prospecting over the farms Engelschedraai and Doornhoek, where anomalies were located by previous exploration campaigns.

During an initial drilling project gabbroic sills of a few to tens of meters in thickness were pointed out southeast of the mine within the Oaktree and Black Reef Quartzites. Preliminary investigations showed similarities as well as differences to the Uitkomst Intrusion (Woolfe, 1996).

1.4 Previous work on the sills and dykes

Since the discovery of the Uitkomst Complex by P. Wagner (1927), who described ‘a big sill of highly altered Pyroxenite carrying platinum in association with magmatic nickel-copper-iron sulphides’, the investigations had occurred rather sparse until the late eighties of the last century, when Gauert et al. (1995) saw a correlation to the Bushveld Complex. The major part of the publications about the Uitkomst Complex is due to the economic potential of the Ni-Co-Cu-PGE bearing Complex itself.

The investigation by Kenyon et al. (1986) confirmed the sill-like form of the Complex based on borehole information. Furthermore four distinct zones were recognized, which become progressively more ultrabasic upwards, so that Kenyon et al. (1986) proposed the model of the geochemical inverse layering of the Uitkomst Complex. On the basis of a single Rb-Sr determination on biotite within the Basal Gabbro Unit, Kenyon et al. (1986) suggested a 2025 Ma age of the Uitkomst Complex, coeval with the mafic phase of the Bushveld Igneous Complex.

Another petrogenetic model was proposed by Von Scheibler et al. (1995), who suggested that the Uitkomst body was formed by lateral flow of Bushveld-related magma. Assimilation of the Timeball Hill sulphidic and graphitic shale increased the sulphur content and the most contaminated magma was richest in sulphide, mainly in the lower pyroxenite zone. Von Scheibler et al. (1995) explained the “inverse layering” of Kenyon et al. (1986) by multiple magma impulses, whereas the magma follows established channels undergo less contamination and consequently become more ultramafic. Gauert et al. (1995) interpreted the elongated Uitkomst body as a magma conduit in which open and closed system conditions dominated different parts of a magma chamber based on the large proportion of sulphide and chromite to silicate and the lack of differentiation in the ultramafic units. They also proposed the first entire magmatic stratigraphy of the Uitkomst Complex. Following geochemical studies of Gauert et al. (1995), De Waal & Gauert (1997) presented a petrogenetic model for the Basal Gabbro Unit that reveals that parental magma (referred to as the Uitkomst Bu magma) is chemically identical to a mixture of Bushveld B2 magma and a fractionated variant of Bushveld B1 magma (fig. 1.2). In a further elaboration Gauert (2001) explained the large quantity of sulphides compared to the thickness of the Complex by separation from a larger magma pool at depth, followed by entrapment in the ascending magma and deposition in the conduit. He also compared the origin of mineralization, due to country rock assimilation at Uitkomst, with that of the Platreef portion of the Potgietersrus Limb of the Bushveld Complex.

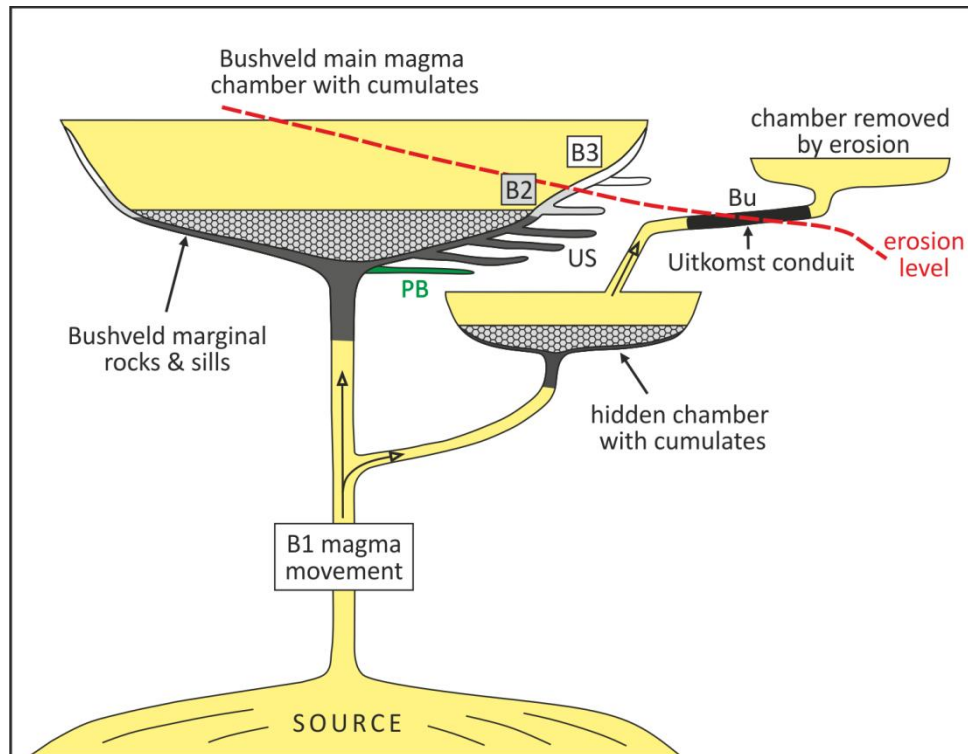


Figure 1.2: Schematically illustration shows the relation between Uitkomst and Bushveld Complex. The B1 magma is injected in the Bushveld main magma chamber as well as in a smaller hidden magma chamber, from which the Uitkomst Bu magma evolved (Gauert, 2001).

Hornsey (1999) argued that the Basal Gabbro was the first of a series of sills, followed by the Lower Harzburgite, intruding and dilating the country rocks. The massive sulphide mineralization was generated from a localized immiscibility event that occurred within the Lower Harzburgite. The Uitkomst Complex has been subject to diabase sill intrusion and layer parallel thrust faulting after cooling of the Complex, resulting from the intrusion and lateral propagation of the Bushveld Complex (Hornsey, 1999). With a concordant $^{207}\text{Pb}/^{206}\text{Pb}$ zircon age of 2044 ± 8 Ma for the upper Gabbronorite Unit De Waal et al. (2001) gave evidence for the relation to the Bushveld Complex. Therefore the Uitkomst Complex seems to be later than the Rustenburg Layered Suite (2059 Ma) of the Bushveld Complex. The most previous studies about mafic to ultramafic sills and dykes are associated with the intrusion of the Bushveld Complex whereas investigations at the Uitkomst Complex are sparse so far.

The research of numerous sills related to the Bushveld Complex was the objective by several authors such as Willemse (1959), Frick (1973), Sharpe (1978, 1981 & 1984), Cawthorn et al. (1981) and Sharpe & Hulbert (1985) due to the assumption that the composition of certain sills conforms to the parental magma composition of the Complex. One of the first who recognized different types of sills in the eastern part of the Bushveld Complex was Willemse (1959). He classified the Lydenburg type of diabase, a pre-Bushveld gabbroic rock which is metamorphosed in the greenschist facies, and the Maruleng type of diabase, a noritic rock, which was originally of Lydenburg type, but had assimilated considerable amount of country rock. Frick (1973) referred also to two phases of magmatic activity before and during

the emplacement of the Bushveld Complex. The first “Sill Phase” indicates a pre-Bushveld calc-alkaline sill suite and the later “Chill Zone”, which comprise the fine-grained chilled margin of the Bushveld Complex and a dolerite sill suite with tholeiitic composition. For diabases in the Lydenburg district, eastern Transvaal, Sharpe (1978) compiled a classification dependent on their stratigraphic position and their location. He suggested that diabases intruded into shales showing a variably high grade of alteration because of the absorbed water from the shales. Instead mafic magmas that intruded into quartzite, which is a relatively dry rock, are more representative for the original magma composition. There also exist metamorphosed variants of the two types.

Sharpe (1981a) compared pre-Bushveld sills from the eastern Transvaal and sills from the region around Middelburg that intruded into the Waterberg Group. Analogue to the previous authors he subdivided the sills into highly altered pre-Bushveld sills with a widely varying composition, and relatively fresh dolerites and gabbro-norites with a comparatively similar mineralogy. Continuing investigations (Sharpe, 1984; Sharpe & Hulbert, 1985) described sills of syn-Bushveld age and assigned them to the corresponding marginal rocks of the Bushveld Complex (fig. 1.3). There are two main suites of marginal rocks, which have analogues in the sill suite beneath the complex. The lower marginal pyroxenitic zone (B1) shows equivalent pyroxenitic and noritic sills, partly possessing quenched textures. The upper marginal gabbroic zone (B2 and B3) has comparable gabbroic to gabbro-noritic sills as well as corresponding quench-textured microgabbroic rocks (N) (Sharpe, 1981b). The magmas of B1 and B2 were of particular importance for the development of the Uitkomst Complex (De Waal & Gauert, 1997; Gauert, 2001).

A sill classification of the western Transvaal was presented by Cawthorn et al. (1981), which proposed four distinct ages of sills. The first and the last are doleritic sill, which conform to the pre- or rather post-Bushveld age. The middle two are generally related to the Bushveld Complex and indicate two major magma injections into the Complex.

A first geological mapping, which includes sills and dykes within the study area was produced by Van Eeden (1936). At this time the Uitkomst Complex was already discovered, but is missing in Van Eeden’s map (fig. 1.4). He described the mapped sills and dykes uniform as diabase. Furthermore it is proposed, that the sills extend parallel to the Mpumalanga Drakensberg Escarpment within the units of the Lower Transvaal Supergroup.

The important investigation by Kenyon et al. (1986) indicated the existence of three major diabase sills and numerous smaller secondary sills with minor amounts of sulphide mineralization, probably as a result of contamination by the ultramafic complex. They suggested a post-Uitkomst age for the intrusive sills, maybe injected by a major fault or fracture zone along the length of the Complex. Furthermore

Kenyon et al. (1986) observed that the diabase intrusions close to the Complex are mainly sills, lesser dykes.

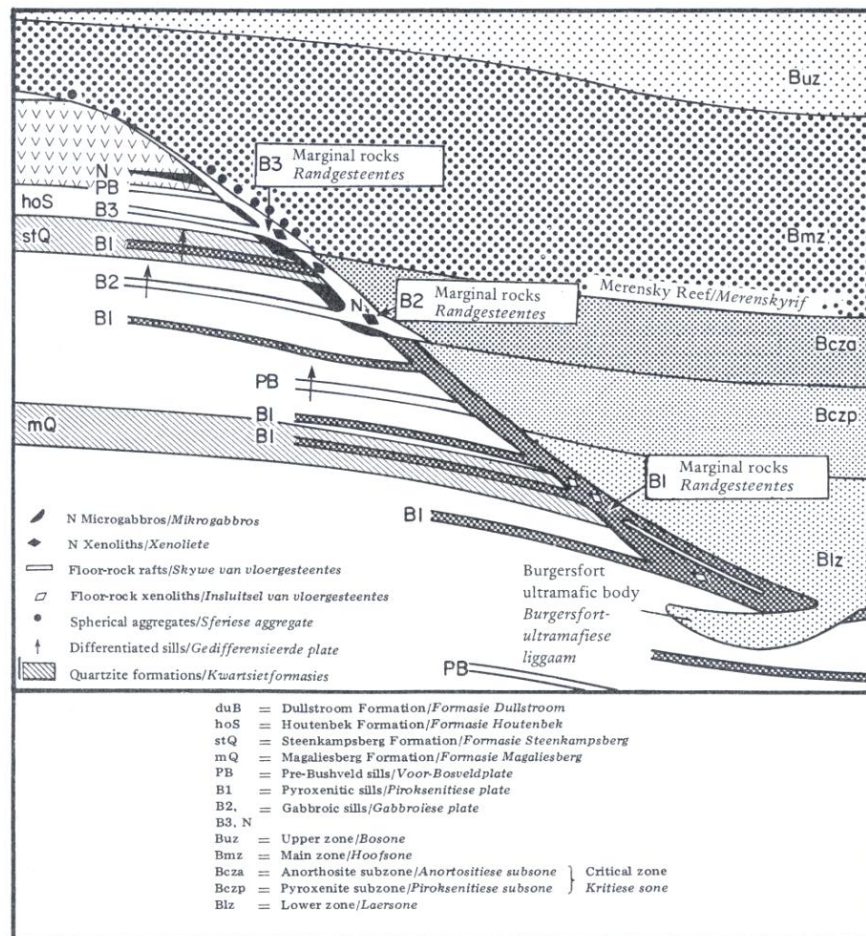


Figure 1.3: Relationship between sills, marginal rocks and the layered sequence of the Bushveld Complex (Sharpe, 1984).

A comprehensive study about mafic dykes and their relationship with major mafic magmatic events on the Kaapvaal Craton was compiled by Uken & Watkeys (1997). According to their study, the Uitkomst Complex was controlled by a northwest-trending fracture system, which was initiated by the Pongola rift system and later re-utilized by the Bushveld Intrusions.



Figure 1.4: Extract of van Eeden's (1936) geological map. Shown are diabase sills and dykes (greenish color) in the eastern Transvaal and also in the vicinity of the farm Uitkomst. The Uitkomst Complex itself is not shown in the original map, but additional marked by the author (UC = Uitkomst Complex, light green).

1.5 Aims of the project

This thesis is an investigation of several mafic to ultramafic sills and dykes in the immediate vicinity of the Uitkomst Complex in the Mpumalanga Province.

The investigation focuses on:

- Geological mapping of sills and dykes in the Mpumalanga escarpment region between Badplaas and Ngodwana, and their stratigraphic classification according to age and intrusive trend.
- Description of emplacement mechanisms, contact to host rocks, indicators of fractionation as well as other macroscopical features such as distribution, thickness and crystal size.
- Petrographic description of the mapped sills and dykes including semi-quantitative volume percentage of rock forming minerals, alteration minerals and sulphide mineralisation, and rock type classification based on modal mineral proportions.
- Mineralogical and geochemical classification of the sills and dykes by using XRF analytics primarily for parental magma lineage determination as well as norm calculations.
- Comparison of the compositions of the mapped sills and dykes to the intrusive rocks of the Uitkomst Complex and similar regional events (Bushveld related sills).
- Estimation of the Ni-Cu-PGE sulphide bearing potential of the mapped intrusive rocks based on several mineralogical and geochemical criteria.
- Development of a geochemical fingerprint using multivariate geostatistical methods for distinction between barren and fertile igneous rocks.

2. Geological Setting

2.1 Regional Geology

The following provides a geochronological overview of the evolution of north eastern South Africa with main focus on mafic sills and dykes in the Mpumalanga district in the area between Barberton, Nelspruit, Machadodorp and Badplaas belonging to the Mpumalanga Drakensberg Escarpment.

Granitoid-Greenstone Terrane and related dykes

The oldest rock units underlying the area are of Archaean age and constitute the Kaapvaal Craton on which younger sedimentary rocks were deposited. This basement consists of a succession of volcanic and sedimentary rocks with oceanic as well as continental affinity, termed as Barberton Greenstone Belt, a classical greenstone belt with a roughly triangular form and cusp-shaped boundaries (Arndt et al., 1997; Ward, 2002). The strong deformation and metamorphism that affected the rocks of the Greenstone Belt was the result of the intrusion of numerous granite bodies. Several stages of intrusive granitoids and migmatites restrict the Barberton Greenstone Belt; beginning with 3.5 to 3.2 Ga old tonalite-trondhjemite Granodiorite plutonism, followed by potassic magmatism (3.1 Ga), which formed large batholiths, and a final stage of smaller potassium-rich granite and syenite plutons from 3.1 to 2.7 Ga in age. Due to the interaction of the granites with the earlier-formed greenstones a variety of metavolcanic and metasedimentary rock types were produced (Anhaeusser, 2001; Viljoen & Reimold, 1999; Ward, 2002).

Furthermore the granitoid-greenstone terrain of the Archaean basement in the eastern and northern Kaapvaal Craton host prominent mafic dyke swarms of three different orientation trends (fig. 2.1). The granitic rocks surrounding the Barberton Sequence contain a northwest-trending swarm of mafic dykes. The age of the swarm is unknown, but it is assumed that the dykes could be similar in age to the mafic intrusives of the 2.8 Ga Usushwana Complex because of the parallel alignment of the swarm to these intrusives (Uken & Watkeys, 1997). According to Burke et al. (1985) the orientation of the Usushwana Complex is determined by the Pongola structure, a preserved northwest-trending continental rift system, in which the Pongola Supergroup (age 3.0 Ga) was deposited. The resulting fracture system was re-utilized during the emplacement of the Bushveld Complex and controlled the intrusive direction of the Uitkomst Complex (fig. 2.2) at the base of the Transvaal Supergroup (Uken & Watkeys, 1997). Another northeast-trending dyke swarm occurs in the northeastern Kaapvaal Craton (fig. 2.1), which is conforming in orientation and age with the 2.7 Ga old Ventersdorp rift system. A third east-west trending dyke swarm is observed in the central part of the eastern Kaapvaal Craton. However, this swarm coincides with the long axis of the Bushveld Complex, so that a Bushveld related age of the east-west trending dyke is suggested (Uken & Watkeys, 1997).

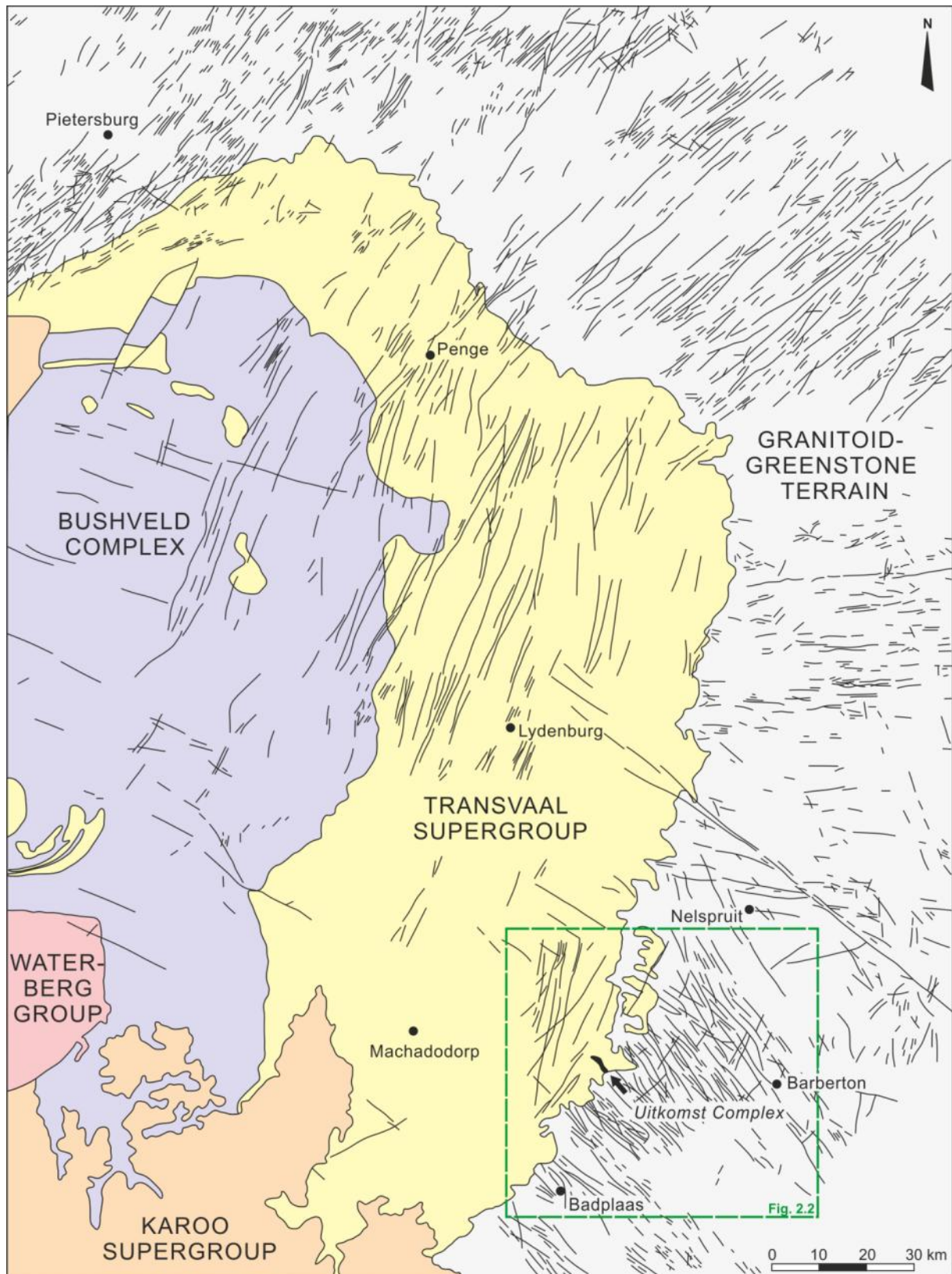


Figure 2.1: Regional geological map of the eastern Kaapvaal Craton showing the distribution of mafic dykes within the granitoid-greenstone basement and cover sequences in relation to the eastern part of the Bushveld Complex (modified after Uken & Watkeys, 1997). The Mpumalanga Drakensberg Escarpment forms the border between Transvaal Supergroup and the granitoids-greenstone terrain.

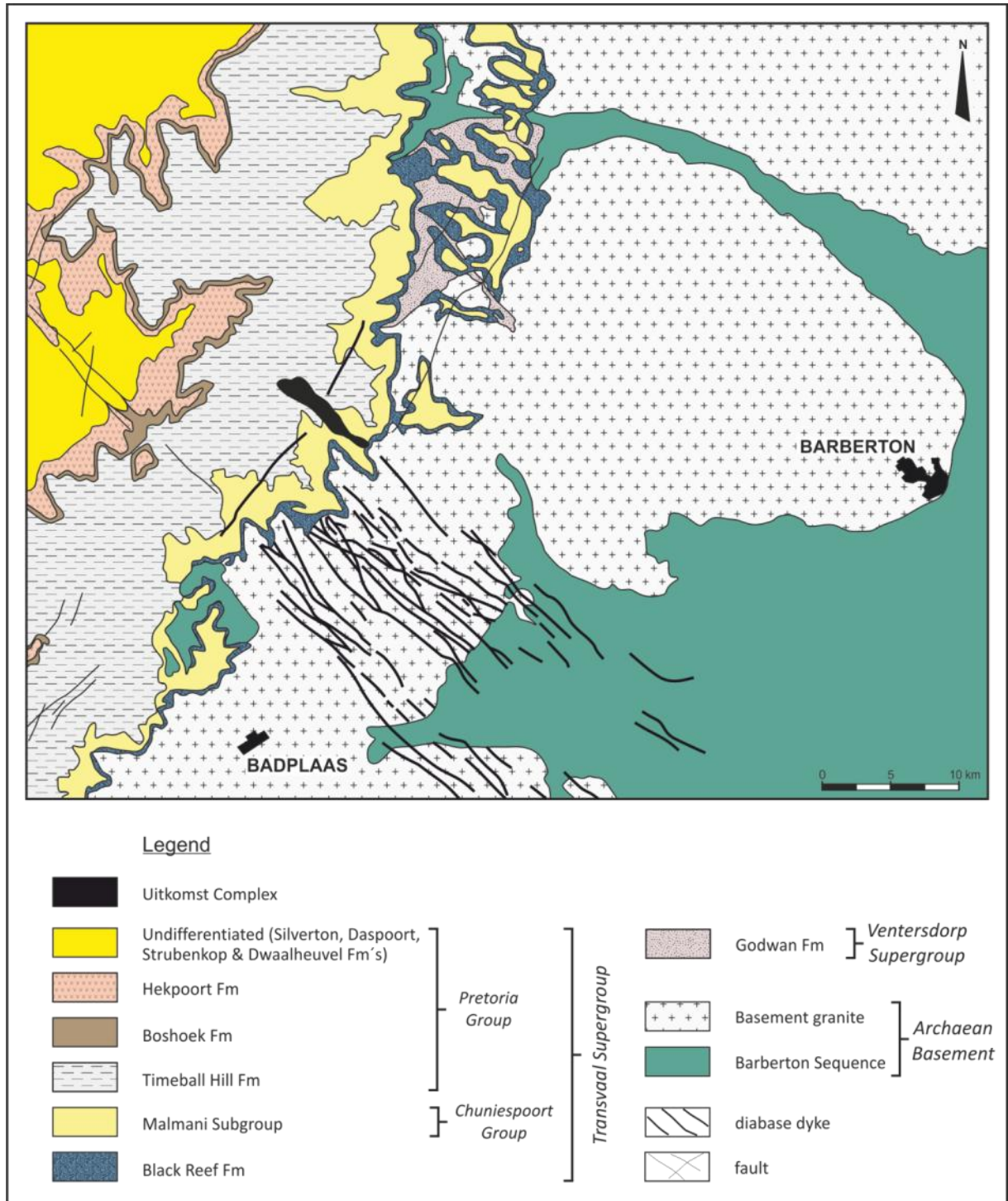


Figure 2.2: Regional geology of the area surrounding the Uitkomst Complex illustrating the major lithological units and structural features (modified after Hornsey, 1999). The NW-trending diabase dykes follow the orientation of the Pongola rift structure. Other dykes are excluded for clarity.

Transvaal Supergroup

Northwest of the Archaean basement early Proterozoic sediments and volcanics of the Transvaal Supergroup are deposited. The boundary is marked by the prominent Mpumalanga Drakensberg Escarpment (fig. 2.1 and 2.2). The Transvaal Supergroup, which covered the Kaapvaal craton during a period from 2.6 Ga to about 2.2 Ga, belongs to a number of almost unmetamorphosed sedimentary-volcanic sequences like the Archaean Pongola, Witwatersrand, Ventersdorp Supergroups and the younger Waterberg Supergroup (Cahen et al., 1984). Due to the fact that rocks of the Transvaal Supergroup host most of the mafic sills and dykes of the study area, it deserves a more detailed description (see chapter 2.3).

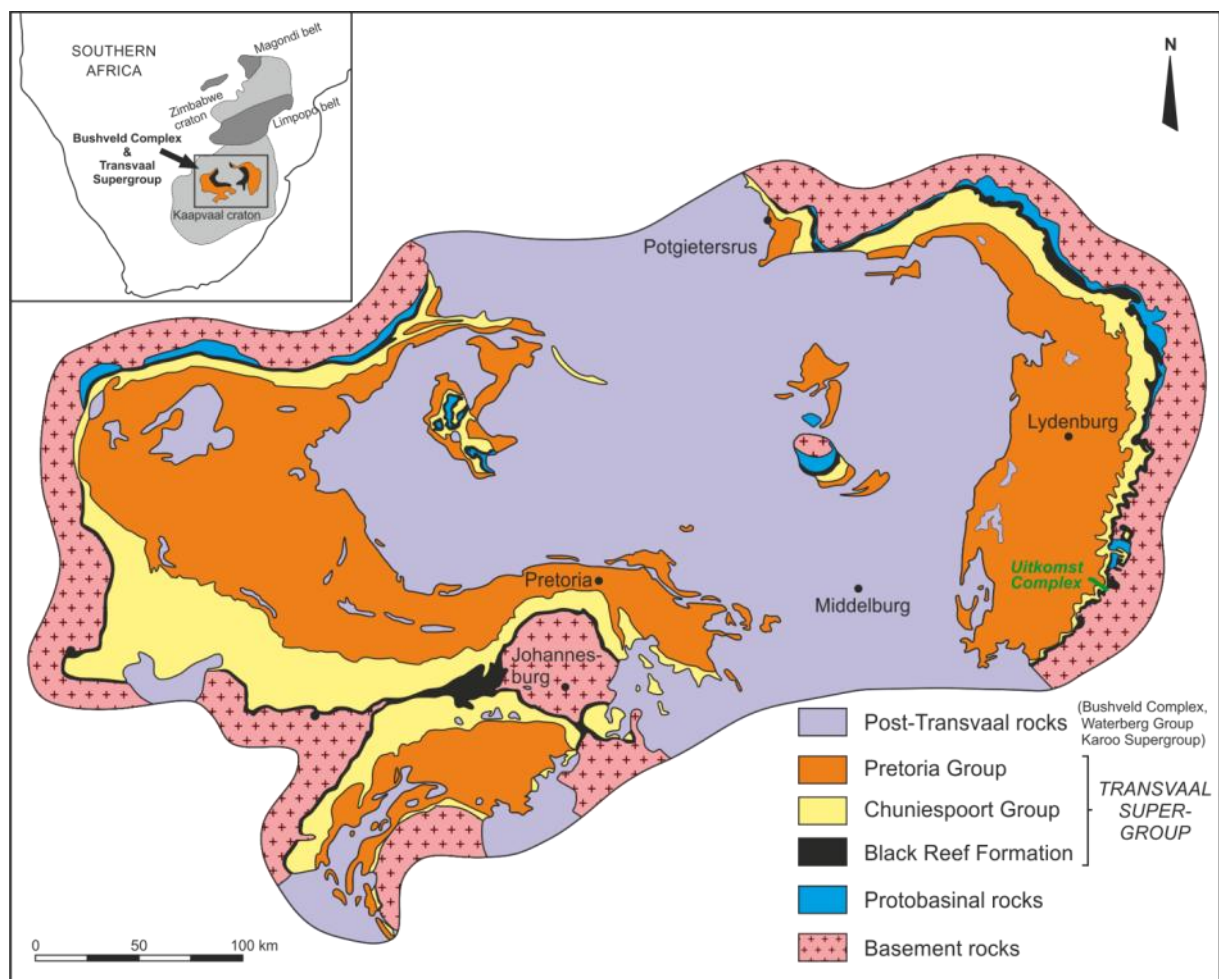


Figure 2.3: General geological map of the Transvaal Supergroup within the Transvaal-Bushveld basin showing the distribution of the principal stratigraphic units. The inset map illustrates the location of the Transvaal-Bushveld succession within the Kaapvaal craton (modified after Clarke et al., 2009).

The deposition of the Transvaal Sequence commenced at about 2.6 Ga when more stable crustal conditions established while the Kaapvaal craton was inundated by an extensive epeiric sea (Visser, 1970).

Generally the Transvaal Supergroup is preserved within three structural basins in southern Africa, whereas the Transvaal basin (fig. 2.3) is the largest with an approximate thickness of 15000 m and contains the most complete sequence of Neoarchaeon to Palaeoproterozoic rocks (Button, 1986; Eriksson et al., 2001). It comprises protobasinal successions, overlain by the Black Reef Formation, Chuniespoort Group and the uppermost Pretoria Group (fig. 2.3). According to Eriksson & Reczko (1995) the protobasinal sequences were deposited in separate strike slip or small extensional basins, which formed by a series of rifting events and south-easterly directed tectonic escape accompanied by the collision of the Kaapvaal and the Zimbabwe craton during Ventersdorp times (about 2.7 Ga). The Buffelsfontein Group shows an evidenced age of 2657 - 2659 Ma (Eriksson & Reczko, 1995) for the protobasinal rocks. The Godwan Group as one of these successions crops out along the escarpment around Kaapsehoop, northeast outside the study area (fig. 2.2).

The overlying undated Black Reef Formation consisting of thin arenaceous lithologies represents a fluvial sedimentation as reflecting initial thermal subsidence of the late Ventersdorp rift systems (Eriksson et al., 1995). Due to further thermal subsidence a transgressive marine environment led to the deposition of the Chuniespoort Group carbonate-BIF platform succession. This group includes abundant dolomite strata with interbedded chert-layers of the Malmani Subgroup and the predominant micro- to macro-banded iron formations of the Penge Formation. The basal unit of the Malmani sequence is determined at 2550 ± 3 Ma by Walraven & Martini (1995). After the epeiric platform sedimentation, an estimated 80 Ma hiatus followed with slow uplift and karstic weathering of the Chuniespoort dolomites. The uppermost Pretoria Group, which covers large areas in the centre of the Transvaal basin, was deposited in varied environments. Two-thirds of the total thickness of the Pretoria Group is composed by shales and mudstones of the Timeball Hill and Silverton Formation, induced by slow thermal subsidence in an intracratonic sag basin. The extensive volcanic units (Hekpoort Formation and Machadodorp Volcanic Member) as well as the inferred alluvial-fluvial sandstone series (Boshoek, Daspoort, Magaliesberg, Lakenvlei and Steenkampsberg Formations) of the Pretoria Group represent a fan-delta environment controlled by plate tectonically induced rifting, which effected volcanic activity (Eriksson, 1999; Eriksson et al., 1995 & 2001; Eriksson & Reczko, 1995; Ward, 2002).

Bushveld Complex and related sills and dykes

After sedimentation of the Pretoria Group the intrusion of the 2055 Ma old Bushveld Complex took place in the Upper Transvaal Supergroup (fig. 2.3). Large volumes of mafic magma were also injected into and parallel to the bedding of quartzites and shales of the Silverton and Magaliesberg Formations (Viljoen & Reimold, 1999). Post-Magaliesberg sedimentation continued in separate eastern and western sub-basins.

The top of the Bushveld Intrusion is formed by the mafic and felsitic volcanics of the uppermost Rooiberg Group of the Transvaal Sequence, which are sporadically developed within the Transvaal basin (Eriksson & Reczko, 1995). The emplacement mechanisms of the Bushveld Complex are still poorly understood and numerous intrusive models (see Clarke et al. (2009) for further information) exist. Generally the Bushveld Igneous Complex is known as the world's largest layered intrusion because of an extension of approximately 61000 km². The complex is formally subdivided in three units. The lower mafic to ultramafic Rustenburg Layered Suite forms four lobes and can be divided into a number of zones. The following two suites of felsic rocks, Lebowa Granite and Rashedoop Granophyre, are located in the central part (Eriksson et al., 1995; Ward, 2002). A detailed description of the Bushveld Complex is beyond the scope of this study.

Also a wide variety of mafic sills (Table 2.1) intruded also into the Transvaal Sequence, but shows a general increase in frequency upwards and towards the discordant contact between the Bushveld Complex and the sedimentary floor rocks (Sharpe, 1984). Syn-Bushveld sills corresponding marginal rocks of the Bushveld Intrusion intruded above the Machadodorp Volcanic Member up to the base of the Dullstroom Formation and consequently on a higher stratigraphical level as the sills in the vicinity of the Uitkomst Complex.

Table 2.1: Stratigraphic framework of the Kaapvaal Craton and cover sequences in relation to intrusive events and associated mafic dykes and sills (modified after Uken & Watkeys, 1997).

Age	Stratigraphic framework/intrusive event	Associated mafic dykes/sills
~180 Ma	Karoo Supergroup/Karoo mafic volcanism Re-activation of the Ventersdorp rift	WNW trending dykes NE-NNE trending dykes
~1.4 - 1.7 Ga	Waterberg Group	Post-Waterberg diabase dykes and sills, NW trending dykes
~2.0 Ga	Bushveld Complex Uitkomst Complex	Bushveld ultramafic/mafic sills Uitkomst mafic sills EW trending dykes
~2.6 - 2.2 Ga	Transvaal Supergroup	No dykes or sills
~2.7 Ga	Ventersdorp Supergroup/Ventersdorp rifting Godwan Formation	NE trending dykes
~2.8 Ga	Usushwana Complex	NW trending dykes
~3.0 Ga	Pongola Supergroup/Pongola rifting	NW trending dykes
~3.5 Ga	Establishment of the Granite-Greenstone terrain	No mafic dykes or sills

The Uitkomst Intrusion itself presents a potential satellite intrusion to the Bushveld Complex based on age, composition, intrusive direction and distance (Gauert et al., 1995; Kenyon et al., 1986; Sharpe et al., 1981). Contrary to pre-Bushveld sills, which are truncated in places by the Bushveld Complex, are distributed bimodal in the Silvertown and Magaliesberg Formations of the Lower Pretoria Group as well as in the Upper Pretoria Group (Harmer & Von Gruenewaldt, 1991; Sharpe, 1984).

As mentioned above, Uken & Watkeys (1997) correlated an east-west-trending dyke swarm (fig. 2.1) in the central part of the eastern Kaapvaal Craton with the main axis of the Bushveld Complex. It is significant to notice that only mafic sills intruding at the base of the Transvaal Supergroup, such as the sills in the study area, are coincident with the east-west-trending dyke swarm and accordingly are of Bushveld age. Northwards and southwards of this dyke swarm relevant diabase sills occur higher up in the Transvaal Stratigraphy (Uken & Watkeys, 1997).

Karoo volcanism and related sills and dykes

The last dyke emplacement event on the eastern Kaapvaal Craton was initiated by Karoo mafic volcanism (about 182 Ma) during the final stage of depositing the Karoo Supergroup, which covers two-thirds of South Africa (Viljoen & Reimold, 1999). Various trends of dykes are formed by activating a plume-generated triple junction as well as re-utilizing the Ventersdorp rift structure (Table 2.1). The latter occur as prominent NE to NNE trending dyke swarms in the study area. According to Uken & Watkeys (1997) the direction of the dykes change from a NE trend in the granitoid basement to a NNE trend in the Transvaal Supergroup (fig. 2.1). Karoo volcanics and Karoo dolerite sills do not appear in the study area.

2.2 Local Stratigraphy

The investigated mafic sills and dykes of the study area as well as the Uitkomst Complex are hosted in sediments of the Lower Transvaal Supergroup and in Archaean basement rocks, which are described below. Therefore a more detailed description of the local stratigraphy is given in this chapter.

2.2.1 Nelshoogte Pluton

The Archaean basement in the southeast of the study area is formed by the Nelshoogte Pluton, one of several plutons of tonalitic-trondhjemitic composition which surrounded the Barberton Greenstone Belt. It has been dated at 3236 ± 1 Ma using U-Pb isotope ratios from zircon and titanite dating technique (De Ronde & Kamo, 2000).

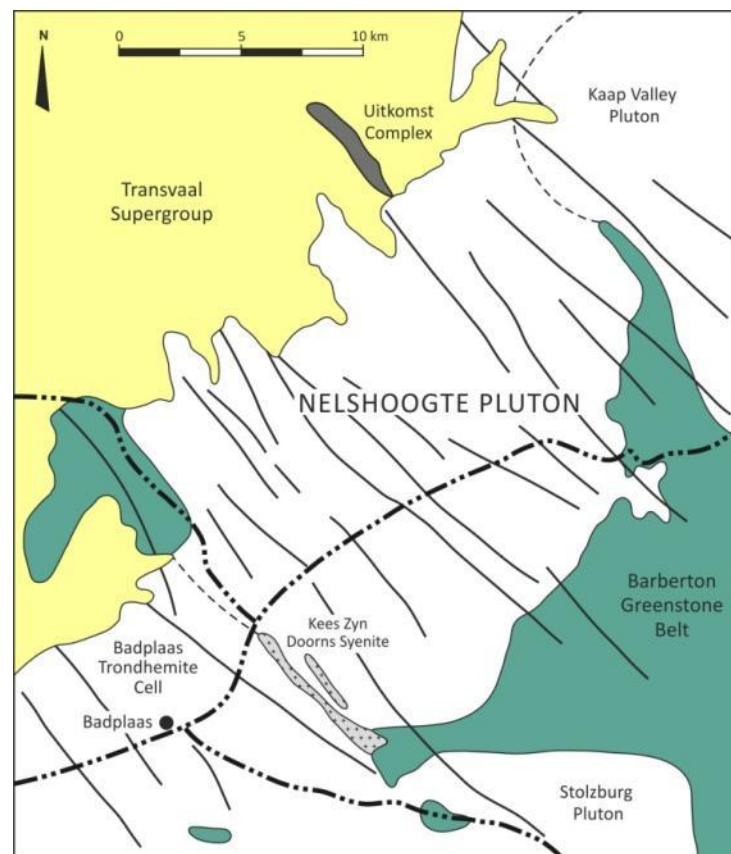


Figure 2.4: Location of the Nelshoogte Pluton between sediments of the Transvaal Supergroup and rocks of the Barberton Greenstone Belt (modified after Layer et al., 1998).

The Pluton is exposed as semicircular body with a diameter of approximately 20 km (fig. 2.4), whereas the probably western half is covered by the Transvaal Supergroup. The schists of the Barberton Greenstone Belt mark the eastern border and on the north and south the Nelshoogte Pluton abutted on congenerous plutons (Anhaeusser, 2001; Layer et al., 1998).

According to Anhaeusser (2001) the Pluton is generally a biotite trondhjemite gneiss, which is composed mainly of quartz, plagioclase, microcline, biotite and minor minerals. Towards the centre of the pluton the granite gneiss is homogeneous and has a poorly developed foliation. Close to the contacts with the Greenstone Belt the granite gneiss is strongly foliated and shows variation in composition, from feldspar- and quartz-rich to biotite- or hornblende-rich subtypes. The Nelshoogte Pluton is intruded by a northwest-southeast trending mafic dyke swarm (fig. 2.4), recognizable in the form of prominent ridges in the otherwise plain valley of the biotite trondhjemite gneiss (Anhaeusser, 2001; Hunter & Halls, 1992). On the basis of cross-cutting relationships Hunter & Reid (1987) presumed an early Proterozoic age for the dyke swarm.

2.2.2 Lower Transvaal Supergroup

Within the study area the lower succession of the Transvaal Supergroup overlies unconformably the Nelshoogte Gneiss. The whole Transvaal Sequence in this area amounts to a maximum of about 8000 m in comparison to the 15000 m in the centre of the Transvaal basin (Button 1986; Ward 2002). Generally the sediments dip in northwest direction at angles between 5° and 10°, but increase towards the Uitkomst Complex and related intrusives (Eriksson et al., 1995). Close to the Complex and the surrounding sills and dykes the Transvaal sediments are partly metamorphosed (Kirste, 2009).

Black Reef Formation

The Black Reef Formation, which represents a topographic high in the area, forms the basal unit of the Transvaal Supergroup (fig. 2.5). It overlies directly the Archaean basement as undulating basal contact due to the absence of stratigraphical lower Ventersdorp Supergroup. The Formation thickens northwards, from less than 1 m west of Badplaas to more than 30 m near Kaapsehoop (Eriksson et al., 1993; Ward, 2002). In the eastern Transvaal basin the formation consists of an eroding and a depositing series. The first is characterized by robust conglomerate series with incised channels and tendencies to fill irregularities in the basement palaeotopography, whereas the latter is marked by coarse quartz arenites and unconfined channels. It is interpreted to be a braided fluvial sedimentation or a braid-delta deposition or a combination of these settings (Eriksson & Reczko, 1995; Henry et al., 1990).

Age (Ma)	Sequence & Groups	Formation	Lithology	Depositional environment	Tectonic setting				
Bushveld Igneous Complex									
PROTEROZOIC	TRANSVAAL SUPERGROUP	Pretoria Group	Houtenbek Steenkampsberg Nederhorst Lakenvlei Vermont	Rayton/ Woodlands	Mudrocks/sandstones/lavas/ pyroclastic rocks/carbonates	alluvial fan & shallow basins	pre-rift doming (uplift)		
			Magaliesberg Silverton Daspoort		Sandstones Mudrocks/volcanics/carbonates Sandstones	regressive shoreline shallow to deep marine fluvial/marine in the east	tectonic stability: intracratonic sag basin		
			Strubenkop Dwaalheuwel Hekpoort Boshhoek		Mudrocks/sandstones Sandstones/conglomerates Basaltic andesites Conglomerates/sandstones	shallow lacustrine alluvial fan & braided stream volcanics alluvial fan & braided stream	syn-rift tectonics, extensional subsidence		
			Timeball Hill		Shales/mudrocks/minor quartzites	shallow to deep marine	tectonic stability: intracratonic sag basin		
			Rooihoochte		Conglomerates/quartzites/sandstones	alluvial & lake deposits	syn-rift tectonics, extensional subsidence		
		ARCHAEOAN	CHUNIESPOORT GROUP	Duitschland		Dolomites/shales/limestones	lacustrine sedimentation	pre-rift uplift ± glacio-eustatic fall	
					Penge		Iron formation	marine environment	tectonic stability: intracratonic sag basin
				Malmmani Subgroup	Frisco Eccles Lyttelton Monte Cristo Oaktree		Dolomites/ interbedded chert layers	marine environment large carbonate platform	tectonic stability: intracratonic sag basin
					Black Reef		Quartzites/conglomerates	braid-delta & braided fluvial	tectonic stability: intracratonic sag basin
					Protobasinal rocks (Ventersdorp age) (Buffelsfontein Group/Tshwene-Tshwene belt/ Godwan Group/Wolkberg Group/Bloempoot Group/Wachteenbeetje Fm./Mogobane Fm.)		Sandstones/mudrocks/carbonates Mafic & felsic volcanics/ Metamorphic rocks	subaqueous facies deltaic, alluvial facies volcanics	extensional setting: pull-apart or rift basins
2050 ⁽¹⁾									
2224 ⁽¹⁾ ± 21									
2432 ⁽¹⁾ ± 31									
2500									
2550 ⁽¹⁾ ± 3									
2642 ⁽²⁾ ± 2,3									
2658 ⁽¹⁾ ± 1									

Figure 2.5: Stratigraphy of the Transvaal Supergroup including geochronology, depositional environments and tectonic settings (modified after Catuneanu & Eriksson, 1999; Eriksson et al., 1993). Wavy lines suggest unconformable contacts. Age data: (1) Eriksson & Reczko (1995); (2) - (5) Walraven & Martini (1995); (6) Harmer & Von Gruenewaldt (1991).

Chuniespoort Group

The Malmmani Subgroup is the only member of the Chuniespoort Group around the Uitkomst Complex, furthermore only the lower Oaktree and Monte Christo Formation are developed from a total of five formations of the Malmmani Subgroup (fig. 2.5). After the submarine chemical sedimentation of the Malmmani dolomites resulting in a widespread carbonate platform, a period of uplift, extensive weathering and erosion followed, in which the upper formations of the Chuniespoort Group were removed and accordingly the remnant lower formations of the Malmmani Subgroup were reduced (Button, 1986; Ward, 2002). The lithologies consist of mainly compact dolomites with numerous thin chert bands, fine interlayered quartzites and minor mudrocks. Along the escarpment the thickness varies from about 700 m in the Sabie area to less than 200 m around Badplaas. Within the study area the Malmmani Subgroup thickens in northwest direction from 145 to 300 m.

The basal Oaktree Formation comprises of a 2-3 m thick well bedded dolomite overlain by the approximately 3 m thick coarse grained Oaktree quartzite (Hornsey, 1999). The Oaktree dolomite is referred to as the Basal Shear Zone and has been interpreted to be a major bedding plane thrust zone that predates the Uitkomst intrusion (De Waal & Gauert, 1997). Gauert et al. (1995) supposed that the floor of the intrusion is either the Black Reef quartzite on the Uitkomst Farm or the Oaktree quartzite at Slaaihoek.

Pretoria Group

Within the study area the units of the Lower Pretoria Group (fig. 2.5) were deposited over the weathered palaeokarst surface of the Malmani dolomites and consist basically of shales, siltstones and mudstones, which were separated by resistant quartzite bands as prominent marker horizons of the Lower Pretoria Group. This alternation is inserted by significant volcanic, largely basaltic units (Eriksson et al., 1993; Ward, 2002). The first of these marker horizons at the base of the Pretoria Group is the Bevets Conglomerate Member, the only unit of the Rooihogte Formation in the study area (Button, 1986). The Bevets Conglomerate Member is sharply overlain by the Timeball Hill Formation, which represents the major portion of the country rocks with a thickness of about 1200 m in the vicinity of the Uitkomst Complex. It is composed of predominantly laminated shales and mudrocks with minor beds of quartzite and oolitic ironstone. One of these quartzite beds is the Klapperkop Quartzite Member, also a resistant quartzite band that goes through the study area from southwest to northeast. A deep marine environment caused the succession of the laminated shales, but the appearance of varved shales and turbiditic mudrocks in the Upper Timeball Hill succession proved periglacial influences (Eriksson & Reczko, 1995). In the contact zone to the Uitkomst Complex the Timeball Hill shales are metamorphosed to hornfels.

In the northeastern part of the study area the Timeball Hill Formation is overlain by the Boshhoek Formation, which largely comprises sandstones and conglomerates. It is best preserved in the eastern Transvaal basin with a thickness of about 100 m. Eriksson et al. (2001) interpreted the Boshhoek lithologies as periglacial deposits that laid down by alluvial fans and braided streams.

The uppermost depositions of the Pretoria Group within this area are the subaerial basaltic andesites of the Hekpoort Formation, which thicken southwards from about 200 m in the Sabie area to some 400 m in the Komati River Valley (Ward, 2002). The good outcrop conditions show no evidence for fault controlling of these extensive eruptive rocks, so Eriksson and Reczko (1995) supposed many fissure eruptions as source for the Hekpoort volcanism. The relative lack of pyroclastics suggests also quiet fissure eruptions.

2.2.3 Uitkomst Complex

The Uitkomst Complex, with a model age of 2025 Ma (Kenyon et al. 1986) and a U-Pb age on zircon of 2044 ± 9 Ma (De Waal et al., 2001), is a tubular shaped layered mafic-ultramafic intrusion, which crops out on the farms Slaaihoek 540 JT, Uitkomst 541 JT and Vaalkop 608 JT, on the Mpumalanga Drakensberg Escarpment, about 20 km north of Badplaas. The elongated body forms a narrow, fault-controlled, northwest-striking trough in host rocks of the Transvaal Supergroup. It is exposed over a distance of approximately 9 km. In cross section, the complex has an anvil-shape and becomes more laterally extensive (fig. 2.6), from an 800 m wide basal part to a maximum extent of about 2500 m close to the top (Gauert et al., 1995; Gauert, 1998; Hornsey, 1999; Ward, 2002).

Gauert et al. (1998) identified six lithological units, which are, from bottom to top: Basal Gabbro, Lower Harzburgite, Chromitiferous Harzburgite, Main Harzburgite, Pyroxenite and Gabbronorite. Hornsey (1999) and Maier et al. (2004) split the Gabbronorite unit into a Main Gabbronorite and an Upper Gabbronorite unit, combined here as one. Based on the lithological composition, the Uitkomst Intrusion is briefly described below.

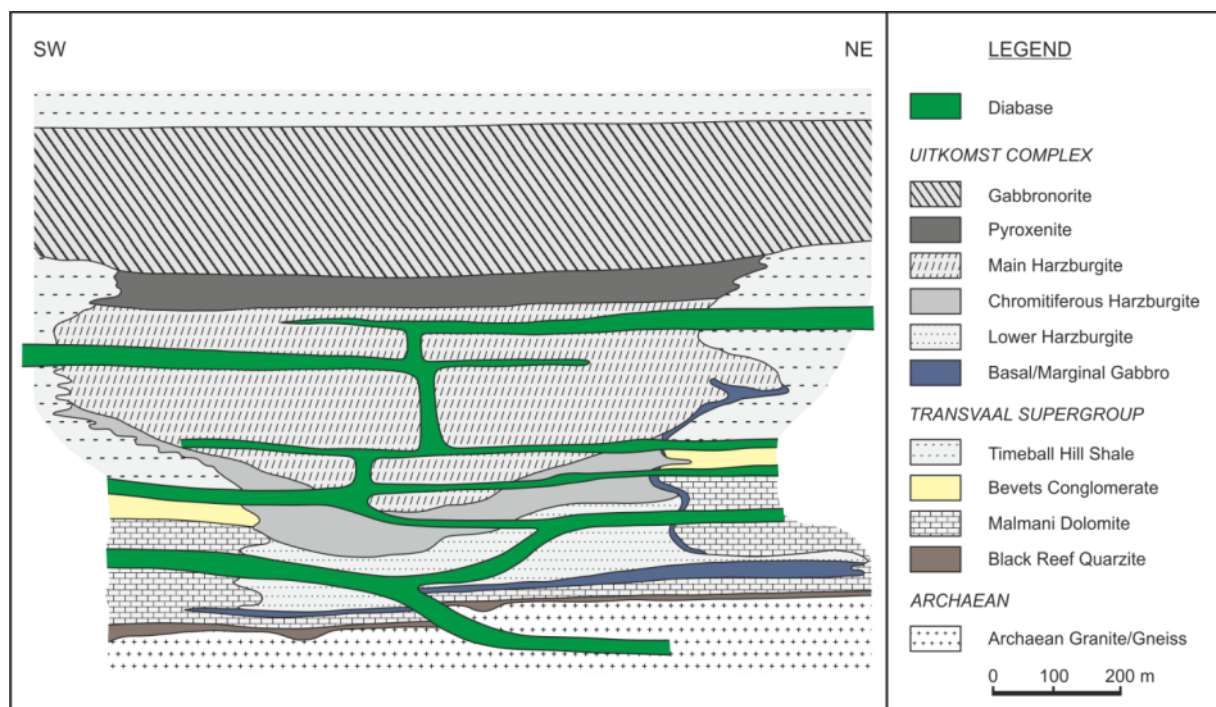


Figure 2.6: schematic section through the Uitkomst Complex and its host rocks based on borehole information from the farm boundary Slaaihoek-Little Mamre (modified after De Waal & Gauert et al., 1997). Notice the network of sill and dykes, which intersect the four lower units of the Complex.

The base of the Complex is formed by the *Basal Gabbro Unit (BGAB)* with an average thickness of 5.6 m ranging between zero and 15 m. In contact to the quartzitic country rocks the BGAB is defined by a strongly sheared talc-chlorite-carbonate rock with a chilled margin of up to 1.5 m (Gauert, 1998).

Otherwise it is a relatively homogeneous, medium-grained plagioclase-clinopyroxene-orthopyroxene rock containing minor amounts of olivine, quartz, titanian magnetite and sulphides (mainly chalcopyrite, pyrrhotite, pentlandite and pyrite) (De Waal et al., 2001). The BGAB is largely altered, showing intense saussuritization and uralitization. Compared to overlying units, the Basal Gabbro extends more laterally into the country rocks following the shear zone at the base at the Uitkomst Complex (Gauert, 1998). Scheibler et al. (1995) explained the offshoots of the BGAB as an earlier sill. In fact the drilling of the Complex revealed a network of diabase sills interconnected by diabase dykes (fig. 2.6, see also in chapter 2.2.4), but these are not limited to the Basal Gabbro (Gauert et al., 1995; Gauert, 1998).

The *Lower Harzburgite Unit (LHZBG)* with an average thickness of 50 m crops out sparsely in the southeastern end towards the middle of the farm Uitkomst (Gauert et al., 1995). The heterogeneous LHZBG contains a variety of ultramafic lithologies, including harzburgite, lherzolite, websterite and wehrlite. These rocks are highly altered through serpentization, saussuritization and uralitization. Additionally the Lower Harzburgite Unit comprises abundant xenoliths of country rocks which appear to have reacted with the intruding magma (Hulley, 2005).

The *Chromitiferous Harzburgite Unit (PCR)* ranges in thickness between 30 m in the downdip area of Slaaihoek and about 60 m on Uitkomst. Olivine and chromite are the predominant cumulus phases, while orthopyroxene is the main intercumulus phase, poikilitically enclosing olivine and chromite. Lenses and schlieren of chromitite are embedded within the medium-grained Harzburgite that is highly altered to a serpentine-talc-chlorite-carbonate rock. The top of the bowl-shaped unit is defined by a 3 to 4 m massive chromitite layer (Gauert et al., 1995; Gauert, 1998; De Waal et al., 2001).

The *Main Harzburgite Unit (MHZBG)* forms the bulk of the Uitkomst Complex with an average thickness of 330 m, more than one third of the total thickness. It is composed of poikilitic harzburgite grading locally into dunite. The main magmatic phases are olivine, chromite and orthopyroxene, lesser plagioclase and clinopyroxene (De Waal et al. 2001). In contrast to the units below the Main Harzburgite shows only serpentization as dominant alteration type (Gauert, 1998).

The 60 to 70 m thick *Pyroxenite Unit (PXT)* is relatively unaltered and forms a distinct marker horizon recognizable in drilling cores. Gauert et al. (1995) subdivided the PXT into three sub-units: a lower olivine-orthopyroxenite, a homogeneous orthopyroxenite with minor accessory chromite and sulphide, and an upper norite to gabbronorite. The succession of rocks within this unit represents a transition between the lower ultramafic units and the overlying Gabbronorite Unit, observable by a generally increase in SiO₂ (Gauert, 1998; De Waal et al., 2001).

The overlying Gabbronorite Units, which can be subdivided into a *Main Gabbronorite Unit (MGN)* and an *Upper Gabbronorite unit (UGN)*, have a total thickness of about 330 m. The heterogeneous MGN ranges in composition from unaltered noritic and gabbroic rocks to altered diorites. The contact between MGN and UGN is marked by a 5.5 m thick magmatic breccia of diorite. The Upper Gabbronorite rocks are highly altered, including saussuritized plagioclase, tremolite, chlorite and biotite (Gauert, 1998; De Waal et al., 2001; Maier et al., 2004). The roof contact of the complex to the overlying Timeball Hill Formation is commonly marked by a well-defined aphanitic chilled margin (Gauert et al., 1995). Scheibler et al. (1995) indicate also sill-like extensions of the Gabbronorite Unit, but the total width of these extensions is unknown as well as the possibility of a lateral transition from the Gabbronorite into a regional sill.

The sulphide mineralization occurs according to Gauert et al. (1995) and Gauert (1998) as disseminated grains, local concentrations in pegmatoidal pyroxenite, net-textured sulphides enclosing olivine and orthopyroxene, and as massive ore. The mineralization is concentrated in the Basal Gabbro and in the Lower Harzburgite, mostly close to xenoliths of country rocks. The massive ore, termed as “massive sulphide body”, appear in a number of associated lenses, which are presently mined. Stratigraphically, the massive sulphides are situated in the footwall rocks of the intrusion. The dominant minerals are pyrrhotite, pentlandite, chalcopyrite, magnetite, chromite and a range of PGE-bearing minerals (Hornsey, 1999).

2.2.4 Diabase intrusions

Previous authors observed diabase intrusions interconnected with the layered rock sequence of the Uitkomst Complex. Borehole information exposed a network of diabase sills and dykes (fig. 2.6), which are cross cutting the floor sequence of country rocks as well as the lower four lithological units of the Complex (Gauert et al., 1995; Gauert, 1998; De Waal & Gauert, 1997). Kenyon et al. 1986 defined precisely three major intrusive sills at the farm Uitkomst, which generated numerous smaller, secondary sills. The diabase sills near the Uitkomst Intrusion show chilled margins towards the host rock boundaries and ranges in thickness from less than 1 m up to 30 m. The sills are of gabbroic composition with mainly pyroxene, plagioclase, hornblende, biotite and opaque minerals (Gauert, 1998; Kenyon et al., 1986).

The vertical dilation of the diabase intrusions is known from borehole information and ranges from tens of meters to maximal 100 m (Gauert, 1998). Structural features complicated the comparison of drilling data recognizable in the abrupt absence of some sills between different boreholes (fig. 2.7). Generally two structural directions dominate the study area, along which also prominent diabase dyke swarms are orientated (Uken & Watkeys, 1997). The NW-SE trending dykes follow the direction of the Uitkomst lineament that belongs to a major fracture system re-utilized by the intrusion of the Bushveld Complex.

The second NE-SW trending dyke swarm coincides with the orientation of the Ventersdorp rift structure, which was re-utilized by Karoo age dykes (Uken & Watkeys, 1997). The former implies syn-Bushveld age, whereas the latter is post-Bushveld in age.

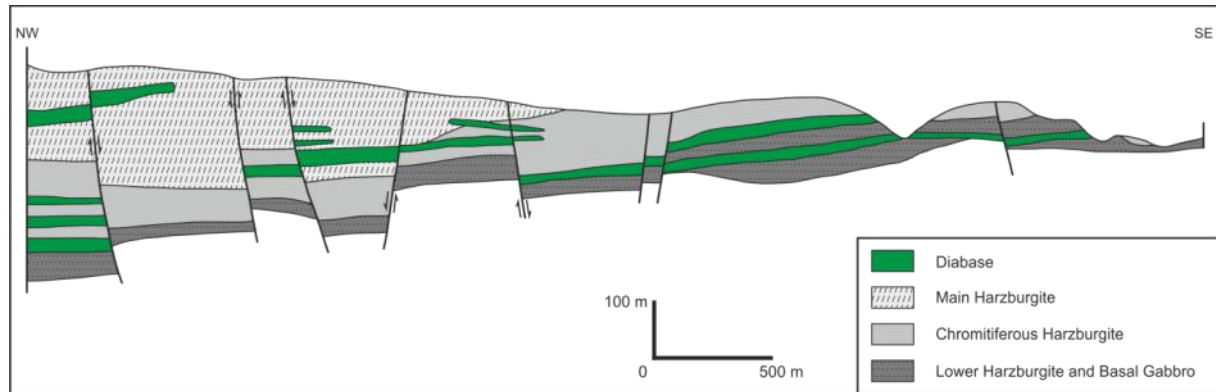


Fig. 2.7: Longitudinal profile through the Uitkomst Complex on the farm Uitkomst. The profile follows the main axis of the body in NW-SE direction and is crosscutted by NE-SW trending faults, so that giving rise to horst and graben structures. Note the different horizontal and vertical scales (modified after Gauert et al., 1995).

Various indices argue for respective different chronological classification of the diabase intrusions in relation to the magmatic events (Bushveld and Uitkomst intrusion). Hornsey (1999) indicated a pre- to syn-Bushveld age for the sills due to the presence of diabase xenoliths in the marginal rocks. Whereas borehole information supported a post-Bushveld age (≈ 2059 Ma) due to the occurrence of sills in the lower lithological rock units (2044 ± 9 Ma, De Waal et al., 2001) of the Uitkomst Complex as well as the NW-SE dilation of sills close to the Complex following the intrusive direction of the Complex (fig. 2.7), known as Uitkomst lineament. Kenyon et al. 1986 proposed major faulting or fracture zones in NW-SE direction along which the diabase was injected. Afterwards NE-SW trending faults and dykes, probably caused by younger Karoo volcanism, disjointed the Uitkomst body and the sills into horst and graben structures (fig. 2.7) (Gauert et al., 1995).

A further aspect for a syn-Bushveld age is the mineralogical composition and the low degree of alteration of sills close to the Complex. These sills show mostly hydrothermal alteration of pyroxenes and plagioclase, but no evidence for a strong metamorphic overprinting like the pre-Bushveld amphibolite sills, which are described by Sharpe (1984). However, they are more altered than the sills of post-Bushveld age, also characterized by Sharpe (1984). On the other hand the network of diabase sills and dykes permeated the layered rock sequence of Uitkomst postulates a post-Bushveld age for the diabase intrusions. Minor sulphide mineralization in the sills could be a result of contamination with material from the complex itself and could point also towards a post-magmatic intrusion of the sills (Kenyon et al. 1986, Hornsey, 1999). An argument for a pre-Bushveld age is the wide stratigraphic range, from Archaean basement to Hekpoort Formation, in which the diabase sills and dykes intruded. Sharpe (1984) suggests a similar wide distribution for the pre-Bushveld sills.

Detailed field observations and geochemical investigation of the sills and dykes nearby the Uitkomst Complex have not been the main focus of previous research. Therefore this study is concerned with these mafic sills and dykes.

3. Methods of investigation

3.1 Mapping

One of the objectives of this thesis was to map the mafic intrusives in the vicinity of the Uitkomst Complex. The mapping was concentrated within the license area of the Nkomati Nickel Mine and carried out over a period of eight weeks, from 2 June until 24 July 2009.

The geographical information system software *ESRI ArcGIS 9.2* was used to generate geological maps of the mafic sills and dykes related to the Uitkomst Complex. A topographical map and a geological base map were provided as digital files by the Council of Geoscience, Pretoria. Additionally, aerial pictures from *GOOGLE EARTH* were taken to identify possible surface related geomorphological structures as well as tracks, which weren't visible in the provided topographical map. In order to define the exact position of the mafic intrusives a GPS from *Garmin (eTrex Summit)* was utilized, mainly to mark the extension of the different sills and dykes and to mark borders to adjacent country rocks. During the field work, which was done by foot as well as by car due to the long distances within the study area, about 1500 waypoints were taken with the GPS. After converting the GPS coordinates into a conformable file format with the software *Garmin MapSource* the waypoints were imported as shape file into *ArcGIS 9.2*. Every single waypoint was classified through attributes, such as rock type, sampling, rock form, grain size, mineralogical composition, alteration, etc. Therefore a comprehensive database was created of the mapped intrusive rocks. The coordinates are represented in *ArcGIS 9.2* by the geodetic reference system *World Geodetic System 1984 (WGS 84)*, which is already used by the GPS.

The result of the mapping is a geological overview map on a scale of 1:25.000, which shows the significant mafic intrusives around the Nkomati Mine in contrast to the surrounding rocks. Furthermore detailed maps on a scale of 1:10.000 and cross sections are generated in order to illustrate extension, form, as well as thickness of selected sills. In chapter four the results of the mapping are presented, including a structural description and a tectonic interpretation of the intrusives rocks.

3.2 Sampling

Rock sampling

The sampling of rocks was carried out during the field work. Altogether 309 samples were taken from the field; some of these were rejected due to strong weathering. About 295 rock samples reached the laboratories of the Department of Geology at the University of the Free State, Bloemfontein. The majority of the rocks are mafic intrusives and where possible, the chill zones as well as central zones of the dykes and sills were sampled. Also some samples from every country rock lithology were collected for the later description. The field outcrops were selected after in-situ and relatively fresh conditions for

sampling. Most outcrops showed a strong weathering on the surface, so that rocks had to be broken apart with a large sledge in order to get fresh samples. All samples were taken with the help of two mine workers (fig. 3.1) and afterwards reduced into proper pieces for analytical procedures. All hand specimens were labeled with the name of the farm, at which the sampling took place, the date and the outcrop number. Additionally, the waypoints from the GPS were assigned to the sample name.



Figure 3.1: A mine worker picked up a dolerite boulder from a weathered outcrop.

Palaeomagnetic sampling

The locations for palaeomagnetic sampling were provided after unambiguous in situ conditions for geographic orientation of each sample. For palaeomagnetic investigations core samples were collected by using a water-cooled portable rock drill (fig. 3.2). After drilling one core with a diameter of 2.5 cm and a length of 15 to 20 cm, the upper side and the lower side are marked at the sample while it is still attached to the outcrop at its base. A geological compass combined with a wooden extension was used to determine the orientation of the core (fig. 3.3), because a sun compass was not available. After breaking the core from the outcrop, the wooden extension with exactly the same diameter as the core was put into the borehole to avoid the close contact between rock and geological compass. In fact the magnetic effect of the rocks is still low, but the method was a hedge against measuring mistakes. The sample orientation was identified by measuring the azimuth as well as the inclination (dip) of the core axis. The dipping direction was marked by arrows on the cores (fig. 3.4). Altogether 8 sites were sampled with 3 to 4 core samples at each site (tab. 3.1). The palaeomagnetic analyses were carried out at the University of Johannesburg and are described separately in chapter 7.



Figure 3.2: All cores for palaeomagnetic investigations were drilled in the field with a water-cooled portable rock drill. The sample sites were selected after in situ conditions for geographic orientation.



Figure 3.3: For orientation a geological compass combined with a wooden extension was used to exclude any measuring mistakes due to magnetization of the outcrop.



Figure 3.4: After orientation every core was labeled. The arrows marked the dipping direction.

Table 3.1: Summary of totally 8 sampling sites with GPS coordinates and in situ orientation. A location map of the palaeomagnetic sampling sites is shown in chapter 7.1.

Site	GPS		Sample name	Azimuth/ direction of drilling	Dip of drilling
	Y	X			
PM-1	-25,7311	30,5543	W_19-7_1/1	14	72
			W_19-7_1/2	310	62
			W_19-7_1/3	359	69
PM-2	-25.7667	30,5783	HM_19-7_2/1	328	71
			HM_19-7_2/2	287	71
			HM_19-7_2/3	308	71
			HM_19-7_2/4	303	78
PM-3	-25,7611	30,6763	VK_20-7_1/1	195	41
			VK_20-7_1/2	230	35
			VK_20-7_1/3	33	26
PM-4	-25,6563	30,5834	HB_20-7_2/1	352	39
			HB_20-7_2/2	96	50
			HB_20-7_2/3	265	60
PM-5	-25,6933	30,5886	HB_22-7_1/1	262	10
			HB_22-7_1/2	274	1
			HB_22-7_1/3	180	32
PM-6	-25,7129	30,6047	UZ_22-7_2/1	200	71
			UZ_22-7_2/2	218	44
			UZ_22-7_2/3	68	60
PM-7	-25,7713	30,5905	U_23-7_1/1	336	88
			U_23-7_1/2	352	75
			U_23-7_1/3	278	50
PM-8	-25,7674	30,6736	VK_23-7_2/1	330	55
			VK_23-7_2/2	88	60
			VK_23-7_2/3	126	45

3.3 XRF Analysis

Sample preparation

After field sampling the hand specimens were prepared in the laboratories of the Department of Geology at the UFS Bloemfontein. The first step was to remove weathering crusts and to cut samples into smaller pieces (fig. 3.6). The remaining pieces were stored for reference purposes. For XRF analysis the whole set of samples were prepared, at first by crushing with a Osborn Massco (4" x 6") Laboratory Jaw Crusher and then by milling for 2-3 minutes in a Siebtechnik Labor-Scheibenschwingmühle (type 250 with 1000 revolutions per minute) with a tungsten carbide grinding set to get a homogenized powder. The milled powders were weighed, dried at 110°C for 24 hours and reweighed to determine the amount of adhesive water. To release the volatile content the powders were roasted for another four hours at 1000°C in a muffle furnace and weighed again to detect the loss on ignition (LOI). The roasted material formed the basis for the production of fusion disks and pellets for the XRF analysis. The powders of the samples were prepared as fusion disks to detect the major element concentration and as pressed powder pellets, used for the trace element analyses. To fabricate the fusion disks 0.28 g of the roasted powder was mixed with 1.52 g of lithium-meta- and lithium-tetraborate, afterwards the mixture was smelted for 20 minutes at 1200°C. Whereas the pellets were made of 8 g roasted powder and 3 g Hoechst Wax that were formed to pellets in a hydraulic press.

Sample analysis

The X-ray fluorescence spectroscopy was used to determine the whole rock chemistry in samples of unknown composition. The major and trace element analyses were arranged with a PANanalytical WD-XRF Axios spectrometer (fig. 3.5) at the Department of Geology, UFS Bloemfontein. The spectrometer operated with SuperQ Software (Version 4) with the two analytical options IQ+ for semi quantitative analysis and Pro-trace mode for quantitative analysis. For the analyses of this study the anode is operated with:

- Accelerator voltage: max. 60 kV
- Current: max. 66 mA
- Power level: 4 kW

The standards used for calibration include about 100 international certified reference materials as well as in-house standards.

Altogether the major elements of 214 samples were determined as oxides in wt % (SiO₂, Al₂O₃, Fe₂O₃, MnO, MgO, CaO, K₂O, TiO₂, P₂O₅) by the Super Q application of PANanalytical "Major Beads 2". For

analyzing the trace elements the application "Traces" was used, which detected the traces Ca, Sc, Ti, V, Cr, Fe, Co, Ni, Cu, Zn, As, Br, Rb, Sr, Y, Zr, Nb, Mo, Ag, Cd, Sn, Sb, Ba, Tl, Pb, Th and U in ppm from 237 samples. The concentration of sodium was measured separately as oxide Na₂O with the application "Sodium only" on the pressed powder pellets, because of the presence of sodium in the fusion disks flux.



Figure 3.5: PANalytical WD-XRF Axios spectrometer

3.4 Microscopy

Altogether 88 representative samples of diabase, ultramafic rocks and country rocks were selected to prepare polished uncovered thin sections, which were studied under transmitted and reflected light. The sample preparation scheme is given in figure 3.6. The laboratories of the Department of Geology at the UFS Bloemfontein produced 20 thin sections during the stay. The remaining thin sections were prepared by the laboratory of the Department of Geosciences at the MLU Halle-Wittenberg. For investigations a ZEISS JENALAB polarisation microscope was used. Photographs of the thin sections were made using a ZEISS AXIOPHOT microscope and a coupled digital camera NIKON XL 3t.

The aim of the microscopic observation was to determine the mineralogical composition as well as to distinguish individual mineral grains in their habitus, size and intergrowths with other minerals. The rock texture and the alteration of primary minerals gave information about the magmatic origin. Based on the petrographic description of the thin sections specific samples were chosen for further analyses to clarify uncertainties (fig. 3.6).

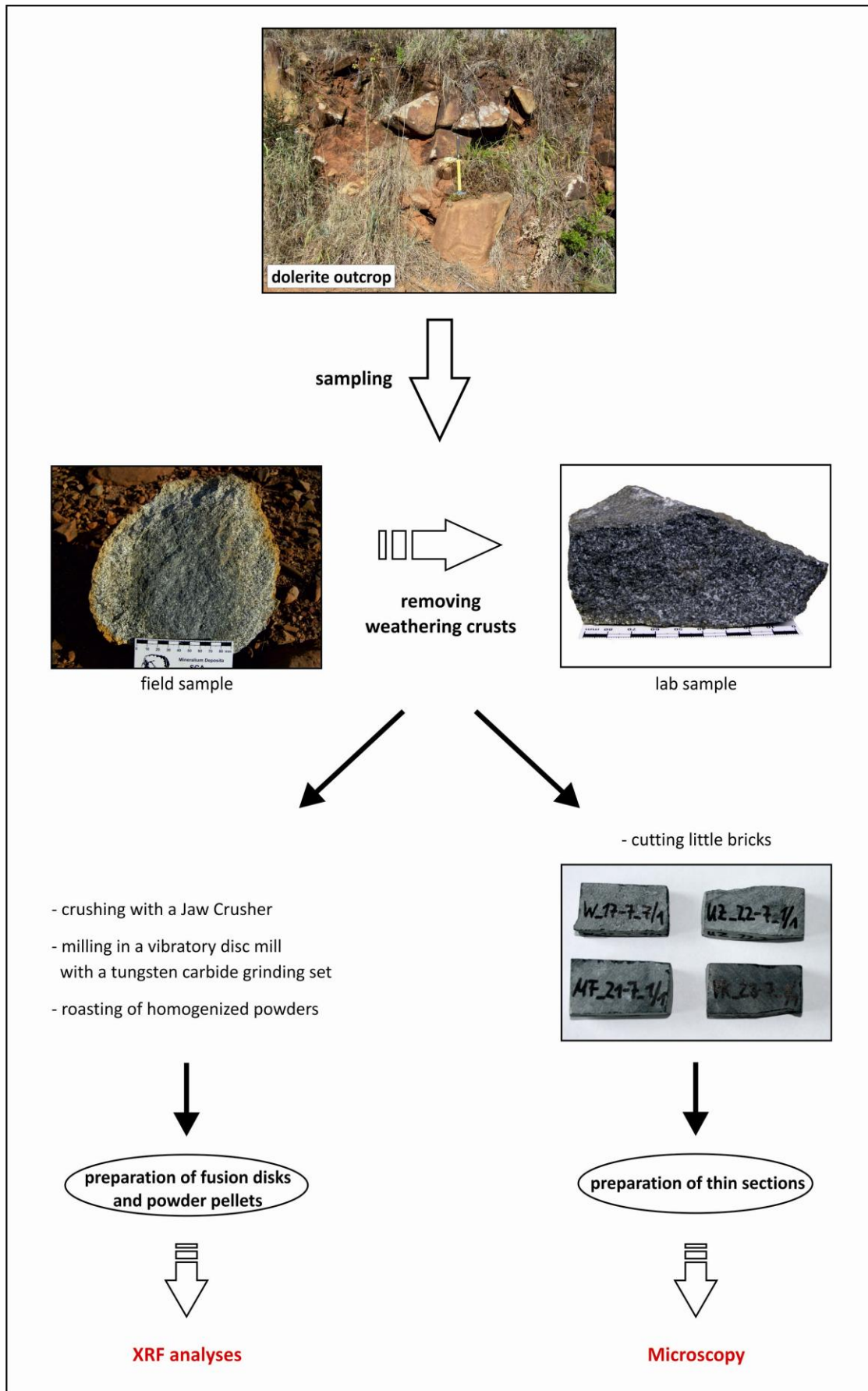


Figure 3.6: Illustration of the preparation cycle; from field outcrop to finish supplement for further investigations.

4. Geological mapping

4.1 Working area

The study region is situated in the Mpumalanga Province in the northeastern part of South Africa, bordered by Mozambique and Swaziland. The mapping area is within the license territory of the Nkomati Mine, which is located in the area between Barberton, Machadodorp, Badplaas and the provincial capital Nelspruit (fig. 4.1). These towns are connected by highway N4 in the north, regional roads R541 in the southwest, R38 in the southeast and R40 in the east.

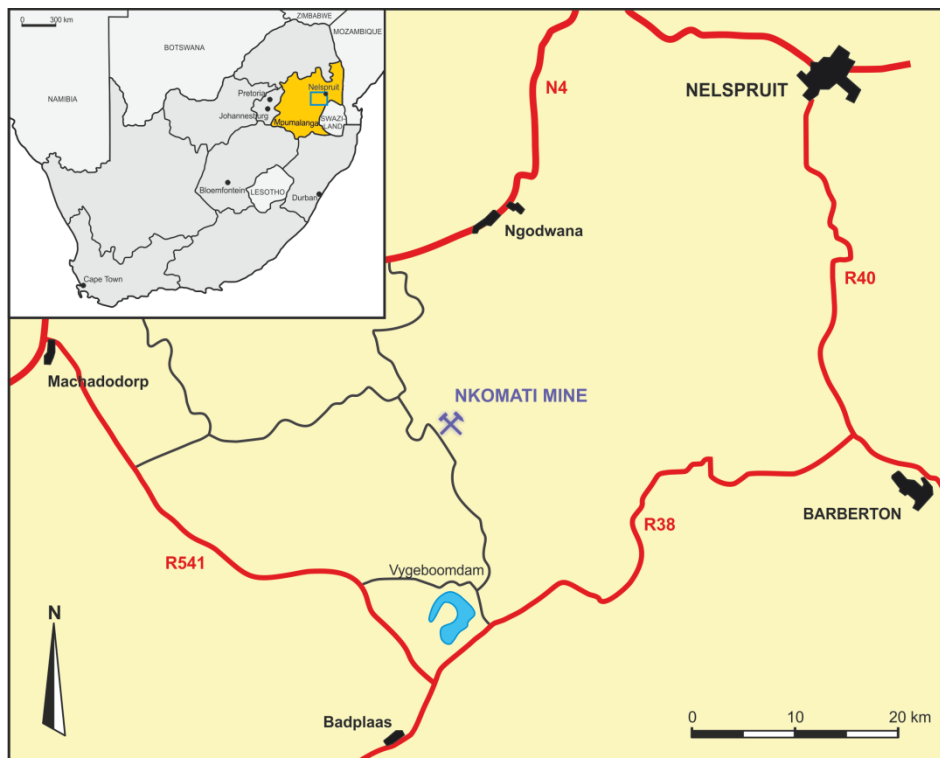


Figure 4.1: The study area belongs to the license area of Nkomati Mine, which is surrounded by the cities Nelspruit, Barberton, Badplaas and Machadodorp.

Every province in South Africa is divided into farm sections of variable size resulting from the agricultural used land. The 275 km² large license area of Nkomati Mine includes 14 of these farms (fig. 4.2), which are mainly used by the forestry industry as well as cattle pastures. The Mine has the approbation for exploration within the area. The Uitkomst Complex itself extends from the farm Slaaihoek in the northwest over the Uitkomst farm to the Vaalkop area in the southeast. These three farms include also the production area of Nkomati Mine. The farms Weltevreden, Doornhoek, Hofmeyr and Engelschedraai are located in the southwest of the elongate Uitkomst Complex. In the northeast the farms Mooifontein, Krige and Uitzicht are situated. In northwest distance to the Uitkomst Complex the farms Houtboschloop, Mamre, Little Mamre and Elandshoek are located.

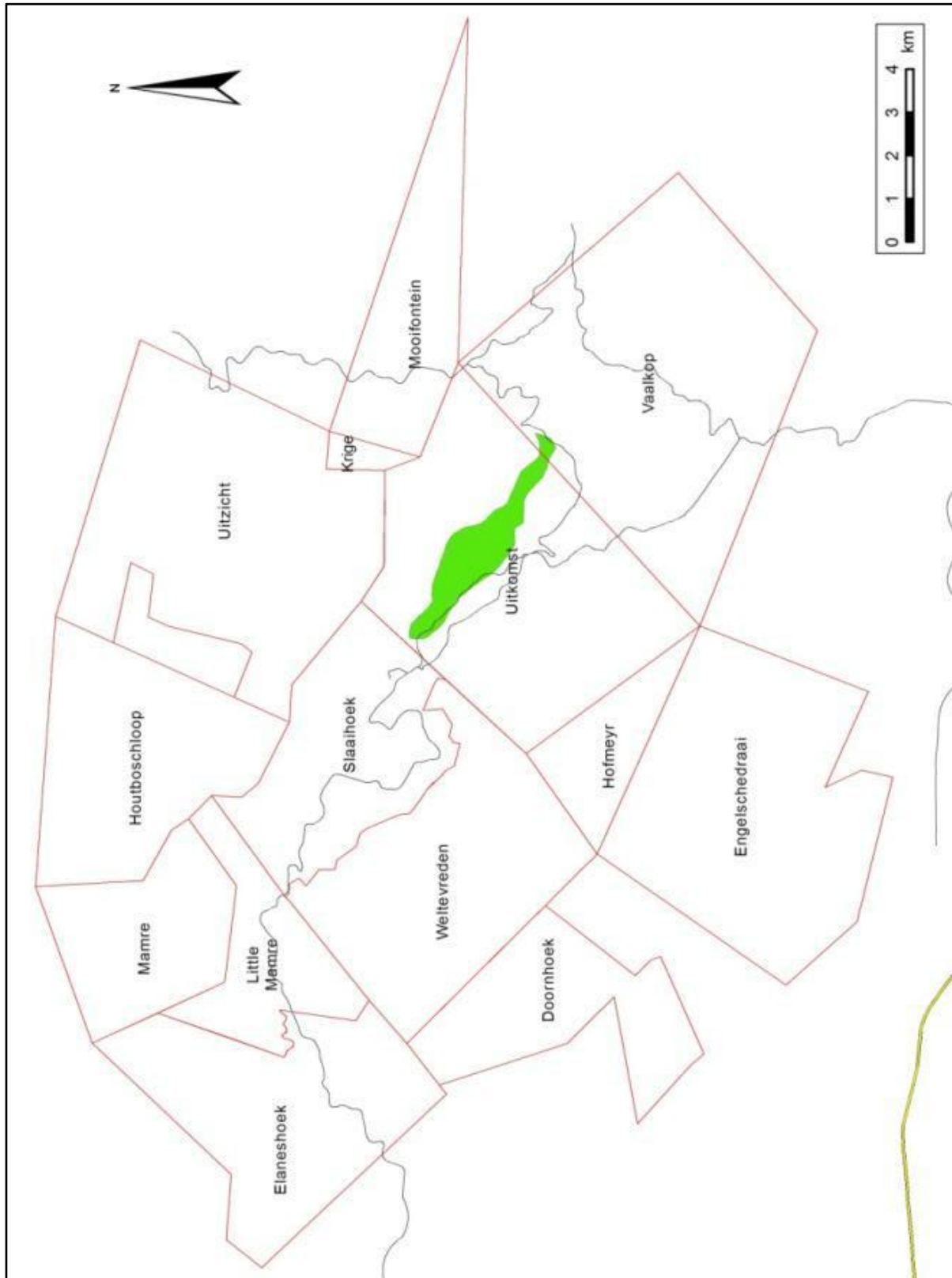


Figure 4.2: The study area is subdivided into 14 farms, which are situated around the Uitkomst Complex (green color: wasting asset of Nkomati Mine). Seven farms were of special interest for the mapping: Vaalkop, Uitkomst, Slaaihoek, Hofmeyr, Weltevreden, Doornhoek, and Houtboschloop.

4.2 Lithology of the country rocks

The mafic sills and dykes as well as the Uitkomst Complex itself are hosted within sediments of Lower Transvaal Supergroup and within the granite gneisses of the Archaean basement terrain.

The focus of the given work was a selective local mapping of the country rocks around intrusive rocks in order to identify contact zones to the intrusive rocks and to understand the behavior of the country rocks at intrusion conditions. Where necessary the geology of the base map, which was provided as digital file by the Council of Geoscience, Pretoria, was changed due to field observations. Since the main focus of this thesis was laid on the mapped sills and dykes, only an overview over the lithology of the country rocks including macroscopic descriptions of outcrops, contact zones and samples is given in the following subchapters. Detailed results on the mapped sills and dykes are given in chapter five.

4.2.1 Nelshoogte granite gneiss/Archaean basement

The Archaean basement is represented by the granite gneiss of the Nelshoogte Pluton within the southeastern part of the study area on the farm Vaalkop. The Nelshoogte Pluton forms a plain valley outside of the study area, where the basement dykes occur as prominent ridges. Within the farm Vaalkop the geomorphology increases through the Mpumalanga Drakensberg escarpment, so that the Archaean basement is covered by the Lower Transvaal Succession. In outcrops the granite gneiss is strongly weathered to brittle rocks with distinctive joints (fig. 4.3). The soft hills forming the Nelshoogte Pluton are covered by an orange to light red weathering soil which is the result of granite gneiss erosion. Compared to the mafic intrusive rocks fresh hand specimen of the granite gneiss, which are sparse due to the strong weathering, are clearly harder because of their higher SiO₂ content.



Figure 4.3: In outcrop the granite gneiss occurs as weathered orange blocky rocks, which are structured by many joints of different orientation (left picture, close up view from a big block of granite gneiss). In contrast the fresh hand specimen on the right shows a grey coloration interspersed with black biotite and hornblende. Compared to the mafic sills and dykes it is distinctively harder due to the high quartz content. The weakly foliation is defined by the planar alignment of biotite and hornblende components.

In hand specimens the coarse grained Nelshoogte granite gneiss shows a grey to beige speckled coloration interspersed with dark green or black components (fig. 4.3). The major mineral phases are feldspar (> 45 %), quartz (25 %), mica (≤ 10 %) and hornblende (8-10 %). The feldspar component can be distinguished into dominant light grey to greenish white plagioclase and minor reddish white potassium feldspar. The former occurs as strongly saussuritized granular masses as well as rather scarce long prismatic crystals (up to 6 mm) with a well-developed cleavage. The potassium feldspars form anhedral to euhedral prismatic crystals. Quartz appears as colorless grains (up to 2 mm) with conchoidal fractures, which are arranged together in clusters between the feldspars. The mica component is dominated by bronzy brown to black biotite, which forms flaky to platy crystals up to 3 mm. Transparent white platy muscovite is rare in macroscopic scale. The micas often show intergrowth with elongated crystals (up to 5 mm) of dark green to black hornblende. The minor mafic mineral phases (biotite and hornblende) define a noticeable developed foliation.



Figure 4.4: The best preserved contact zones show the intrusions of gabbroic basement dykes. On the left the intruded dyke (VK_10-6_1/2) is surrounded by orange granular granite gneiss, which is produced by intensive weathering and erosion. On the right the vertical contact to a dyke (VK_11-6_9/1) is marked by a zone of very brittle granite gneiss intersected by many vertical joints. Outside of the contact zone the granite gneiss shows a greater hardness and resistance.

The gabbroic basement dykes (chapter 5.4, p.91) as well as the microgabbro Vaalkop Sill 1 and 2 (chapter 5.2.3, p.63) intruded into the Nelshoogte granite gneiss. The direct contact to the microgabbro sills is weakly developed. The Vaalkop Sill 2 forms a central sill body, which is overlying the granite gneiss. The lateral contacts are marked by soft valley cuttings caused by small scale faults, but a distinctive color change is observable from the red brown weathered sills to the orange weathered granite gneisses. This color change occurs also in the contact zone to the smaller sized outcrops of Vaalkop Sill 1. The best contact zones to the granite gneisses are defined by the intrusion of the basement dykes. At the contact the rocks are very brittle and intersected by vertical joints (fig. 4.4). The color of the granite gneiss is also clearly light orange to white grey. In contrast the gabbroic dykes appear as robust blocky boulders (fig. 4.4) with a greater hardness.

4.2.2 Lower Transvaal Supergroup

The succession of the Lower Transvaal Supergroup within the study area comprises the Black Reef Quartzite, the Malmani Dolomite, the Rooihogte Quartzites & Conglomerates, the Timeball Hill Shale and the Klapperkop Quartzite.

4.2.2.1 Black Reef Quartzite

The Black Reef Formation occurs as some meters thick band in the southeastern part of the study area on the farm Vaalkop. Together with the Malmani Dolomites, which directly covered the Black Reef, it forms the prominent Mpumalanga Drakensberg Escarpment. The formation is very inhomogenic and becomes more calcareous and argillaceous when grading upwards into the overlying Malmani dolomites (Clendenin et al., 1991; Hornsey, 1999). The quartzite layers are mostly mixed with pebbly layers (fig. 4.5), which have a conglomerate like appearance in contact with dolomite. Outcrops of Black Reef Quartzite are sparse. The quartzites occur as small rock pieces on the surface or they are mixed with other rocks as scree, which covered sill outcrops. In hand specimen the fine grained quartzites have a creamy to light greenish grey coloration (fig. 4.5), whereas the conglomerate like layers are mostly white to pink colored and interspersed with dark grey quartz pebbles.



Figure 4.5: In contact with the overlying Malmani Dolomite the Black Reef Quartzites occurs as pebbly layers with a conglomerate like appearance (outcrop on the left is located on the farm Vaalkop). In hand specimen the fine grained quartzite has a creamy color with a slight greenish color cast (right).

The Black Reef Quartzite hosted sections of the Vaalkop Sill 1 (chapter 5.2.3, p.63) as well as one of the basement dykes (chapter 5.4, p.91). Direct contact with mafic intrusive rocks was not observed in the field. The high amount of loose rock pieces within scree, covering the mafic sill, suggested the occurrence of Black Reef Formation. The Black Reef Quartzite forms the footwall zone of the Uitkomst Complex at the farm Vaalkop and Uitkomst. Near to the Uitkomst Complex on the farm Vaalkop the

quartzites are fritted by the thermal conditions of the Uitkomst Intrusion. They show boxwork structures due to the weathering of sulphides as well as a coating of iron oxides (fig. 4.6).



Figure 4.6: The Black Reef Quartzites occur in the footwall zone of the Uitkomst Complex on the farm Vaalkop and Uitkomst. Fritted quartzites (left) indicate the high thermal conditions due to the Intrusion. The hand specimens show boxwork structures caused by the weathering of the sulphides (right, VK_11-6_1/1). These boxes are covered by a coat of light brown iron oxides.

4.2.2.2 Malmani Dolomite

The dolomites of the Malmani Subgroup are the most distributed country rocks within the southeastern part of the study area. In field outcrops the inhomogeneous Malmani Subgroup comprises mainly of compact and poorly bedded dolomites, especially in contact with the overlying Bevets Conglomerate (fig. 4.9). Numerous thin chert layers up to 20 cm are contemporarily integrated in the dolomites. Furthermore carbonaceous mudrocks and thin interlayered quartzites are located at the base of the formation, which make it rather difficult to distinguish them from the underlying Black Reef Quartzite.



Figure 4.7: Both outcrops appear on the farm Vaalkop close to the mining area of Nkomati Mine. The outcrop on the left shows compact blocks of dolomite with weakly developed bedding. The outcrop is intersected by a network of joints caused by the emplacement of the Uitkomst Complex. The strongly weathered dolomite outcrop on the right is also intersected by vertical and lateral joints, which are refilled with white quartz. The dolomite appears as granulated material similar to soil due to weathering and erosion.

Within the contact aureole of the Uitkomst Intrusion at the farm Vaalkop, the Malmani Dolomites show distinctive signs of metamorphic conditions. The dolomites form talc on the surface as well as elongated aggregates of transparent amphibole, probably tremolite. The outcrops near the Uitkomst Complex show a network of joints, which are infilled with white chert or weathered soil (fig. 4.7). These joints were not observed in outcrops farther away from the Uitkomst Complex, they are probably the result of the emplacement of the Uitkomst Complex.

The dolomites host the gabbroic Uitkomst Sill 3, the microgabbroic Uitkomst Sill 1 & Vaalkop Sill 1 as well as one of the gabbroic basement dykes. Therefore the Malmani Dolomites are the only unit, which hosted all three types of the mapped sills and dykes within the study area.

In field outcrops the contact to the sills are mostly horizontal conformable. Resistant mafic boulders overlie the Malmani Dolomite (fig. 4.8). The lithologies are strongly weathered, but the weathering color is a good indicator for differentiation. The mafic intrusive rocks weathered to a red brown soil interspersed with robust rock boulders, whereas highly weathered dolomites have a light red orange to violet color. Noticeable is the fact that the dolomites are mostly stronger altered in contact to the mafic sills, whereas single outcrops of dolomite appear not as much weathered in comparison.

The direct contact with the basement dyke is sparse, because the dyke is surrounded by the microgabbroic rocks of the Vaalkop Sill 1. The main portion of the dyke is covered by the dolomites due to the post-Transvaal age of the dyke. In a single outcrop the resistant dykes caused an inclined layering of the dolomites, which is noticeable by white chert layers within green gray dolomites (fig. 4.8) affected by the contact metamorphism of the Uitkomst Intrusion.



Figure 4.8: The Malmani Dolomite included numerous thin white chert layers, which are observable in the outcrop on the right. The dark violet colored dolomite is overlain horizontal by a microgabbro sill (Uitkomst Sill 1). Notice the color change to red brown soil as well as the small rock boulders on top of the outcrop. Within the farm Vaalkop the dolomites are modified by the contact metamorphism of the Uitkomst Complex. The dolomites on the left have a green grey color intersected by veins of white chert and show an inclined layering caused by the intrusion of the basement dyke.

4.2.2.3 Rooihoogte Quartzite and Conglomerate

The Rooihoogte Formation occurs as a small layer (10 to 20 m) throughout the area in northeast to southwest direction. The Rooihoogte Formation consists of quartzites and conglomerates, with the latter being mostly the only unit within the study area and known as Bevets Conglomerate Member (Button, 1986). In hand specimen the conglomerate is composed of light grey chert clasts of several cm in size (fig. 4.9), which are remnants from karst weathering of the underlying Malmani Dolomite, enclosed in a dark grey quartzitic matrix. Some of the clasts have a more angular form that suggests more breccia like character. The components show a chaotic texture. The best outcrop of Bevets Conglomerate is a large pot hole formed by the Gladdespruit River.

The Rooihoogte Quartzites and Conglomerates hosted only small sections of the Weltevreden-Slaaihoek Sill1 and the Uitkomst Sill 1 to 3. A direct contact with the sills was not observable due to the strong weathering of the conglomerates. However fragments of the conglomerates and quartzites are among the scree, which covered the mafic sills.



Figure 4.9: The left outcrop of light grey quartzitic conglomerate of the Rooihoogte Formation is directly over the underlying yellow to light brown Malmani Dolomite. The picture was taken from the riverside of the Gladdespruit River (Uitkomst farm), which formed large pot holes within the Rooihoogte Quartzites and Malmani Dolomites. The right picture shows the Bevets Conglomerate from the riverside. Notice the chaotic arrangement of the chert and dolomite clasts within the dark quartzitic matrix.

4.2.2.4 Timeball Hill Shale

The shales belong to the Timeball Hill Formation, which occupies over half of the study area and reach a thickness of about 1200 m in the vicinity of the Uitkomst Complex (Eriksson & Reczko, 1995). The Timeball Hill Shale occurs in outcrops as well as in small debris or scree of loose rock fragments. In field outcrops the fine grained shales show an intensive red brown color (fig. 4.10) caused by iron hydration due to weathering. From fresh borehole specimens a dark grey color with well-developed lamination is known. In field outcrops the visible lamination is weakly developed, but a defined well-bedding is clearly observable. The shales are interlayered with occasional quartzite layers of variable size.

The Klapperkop Quartzite Member (see 4.2.2.5, p.42) is the most consistent of these quartzite layers throughout the Timeball Hill Shale and divides the formation into the Upper and Lower Timeball Hill Shales (Eriksson & Reczko 1995). Within the Upper Shales small beds of bluish black ironstone occur as heavy single rocks with a distinct magnetism and banded textures (fig. 4.10).



Figure 4.10: The left picture shows a huge shale outcrop on a road cut within the farm Slaaihoek. The bedding of the shale is clearly visible, which is cross cut by lateral and vertical joints. Also the layers of shale become more massive, but a direct contact to a mafic sill is not observed. The ironstone rock on the right (Hofmeyr farm) belongs to the small beds of ironstone, which are intersected within the Upper Timeball Hill Shale. Notice the fine banded texture within this bluish black rock.

The Timeball Hill Shales are intruded by the gabbro-noritic sills (chapter 5.3, p.69): Hofmeyr Sill 1, Weltevreden Sill 1, Uitkomst Sill 4 and Houtboschloop Sill 1 & 3, as well as by the microgabbro sills (chapter 5.2, p.55): Doornhoek Sill 1, Houtboschloop Sill 2, Uitkomst 1 & 2 and Weltevreden-Slaaihoek Sill 1.

Close to the intrusive rocks the bedding of the shales becomes more massive and is interrupted by a network of vertical and lateral joints. In contact to the mafic sills as well as within the contact aureole of the Uitkomst Complex, hornfels is formed due to contact metamorphism. The very fine compact hornfels rocks are observable by their quartzitic composition, light to dark grey color and their extreme hardness. Within the contact aureole of the Uitkomst Complex the hornfels include layers of corundum (chapter 4.3, p.44). The occurrence of such clear contact metamorphism indicators are not developed in the contact zone to the mafic sills. The formation of hornfels or massive banks of shale of thin thickness are mostly present at the sill contacts due to heat generation from the sill intrusion (fig. 4.11).

It is observed that the dipping angle within the shales near the contact zone increases slightly towards the contact, which is changing from flat dipping (5 to 10°) into inclined layers with an average dipping angle varying from 15° to 25°. In smaller sills this dip increase is not clearly developed.



Figure 4.11: Both pictures present shale outcrops at the contact to a mafic sill. On the left the contact is irregular wavy and the weathered shales show a more massive layering (Uitkomst farm). The shales on the right are altered to hornfels blocks, which show only poorly remained bedding after contact metamorphism. The contact with the overlying sill is conformable horizontal (Doornhoek farm). In both cases the shales or hornfelses are clearly more resistant against weathering than the mafic sills.

4.2.2.5 Klapperkop Quartzite

The quartzites of the Klapperkop Quartzite Member divide the shales of the Timeball Hill Formation into an Upper and Lower portion and expressed in the study area as a northeast to southwest running corridor. The Klapperkop Quartzite Member is composed of several highly quartzitic sandstone layers, which occur as prominent escarpment (fig. 4.12) throughout the Uitkomst valley and reach a thickness of about 100 m (Eriksson et al., 1993).

In hand specimen the light beige colored quartzites are of fine to medium grain size and seem to be relative homogeneous. In outcrops also argillaceous parts were observed within the quartzites as well as sedimentary structures like ripple marks (fig. 4.12) indicating a marine depositional environment.

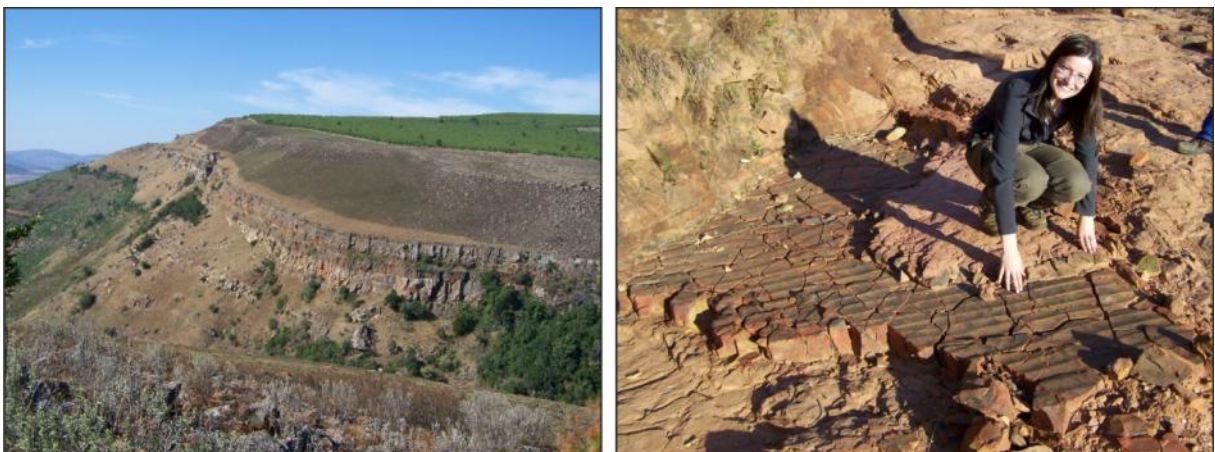


Figure 4.12: The Klapperkop Quartzite Member forms a prominent escarpment within the study area consisting of two obvious quartzitic layers (left, view in southern direction to Hofmeyr Sill 1). In some areas the Hofmeyr Sill 1 overlies the quartzites directly, but an outcrop of the contact zone was not observed. The right picture shows nice ripple marks within the quartzites, which are overlying by a fine argillaceous layer (at the hand of the author).

The Klapperkop Quartzite hosts parts of the gabbro-noritic Hofmeyr Sill 1, Weltevreden Sill 1, Uitkomst Sill 4 and Houtboschloop Sill 1 & 3. It appears that the gabbro-noritic sills form a cord like distribution on top of the Klapperkop Quartzite Member, which could indicate its function as some sort of barrier. The mafic sills lie above the quartzites, so a direct contact with the quartzites was not observed.

4.3 Metamorphism

Within the study area metamorphic effects are observed mostly in country rocks adjacent to the Uitkomst Complex as well as to the mafic sill intrusions.

The emplacement of the large ultramafic Uitkomst body caused a thermal contact aureole, which has strongly affected the surrounding country rocks. According to Kirste (2009) there are different zones of metamorphism within the shales and dolomites depending on the distance to the contact (table 4.1). Field observations supported the investigations of Kirste (2009). Within the contact aureole hornfels is formed as a result of the contact metamorphism of the Timeball Hill Shale. Also layers of corundum can be identified within a distance of about 300 to 400 m to the Uitkomst Complex on the farm Slaaihoek (fig. 4.13). In outcrops of the Malmani Dolomites a mineral assemblage of tremolite, talc and mica verify the contact metamorphism.

Table 4.1: Zones of mineralization within the country rocks in distance to the Uitkomst Intrusion (after Kirste, 2009)

Distance to contact	Timeball Hill Shale	Distance to contact	Malmani Dolomite
0 - 50 m	Silimanite zone [1100°C]	0 - 50 m	Wollastonite zone [1100°C]
50 - 100 m	Augite-antigorite zone	50 - 150 m	Diopside-serpentine-hornblende zone [650°C]
100 - 200 m	Sanidine zone [750°C]	150 - 300 m	Hornblende zone [500°C]
200 - 250 m	Almandine zone [500°C]	300 - 500 m	Quartz-diopside-mica zone [400°C]
250 - 300 m	Corundum zone [400°C]	500 - 800 m	Quartz-hornblende-mica zone

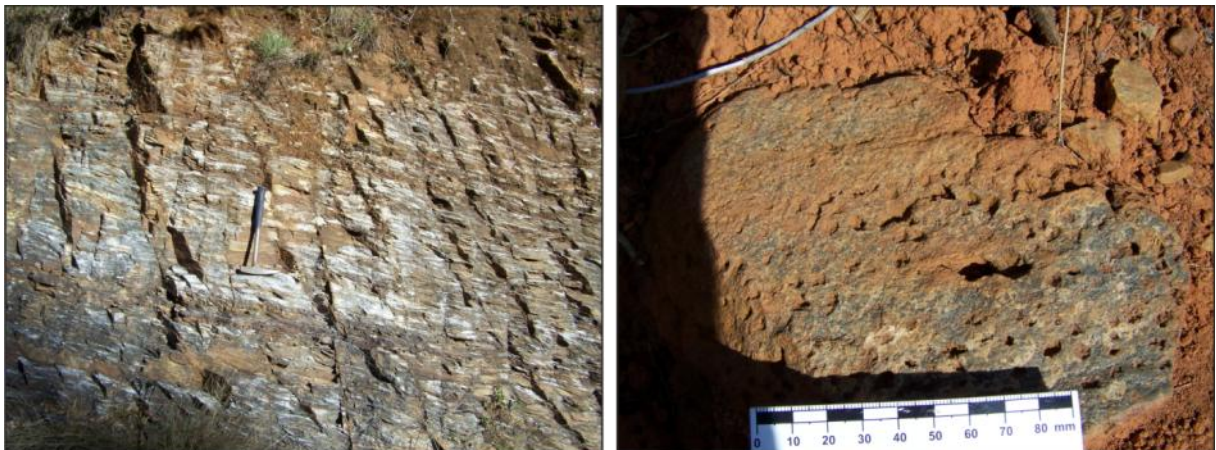


Figure 4.13: Both pictures show Timeball Hill Shales, which are affected by contact metamorphism varying in distance to the Uitkomst Complex. On the left the surface of the shales is coated by light mica, which reflects the sunlight. The outcrop is located on the farm Mooifontein north of the Uitkomst Complex. The right picture shows tiny holes arranged in layers within the shales, which were refilled by weathered out corundum blasts. The formation of corundum suggests a distance to contact of the Uitkomst Intrusion at 250 to 300 m.

The mafic magma of the sills possibly reached temperatures similar to the Uitkomst magma (about 1100°C for basaltic magma Okrusch & Matthes, 2005), but the low thickness and small magma volume compared to the larger layered intrusions (e.g. Bushveld Complex or Uitkomst Complex) caused only small scale contact metamorphic zones. In contact with nearly every sill that intruded into shaly country rocks, hard splintery hornfels was formed, but corundum as indicator mineral for even higher temperatures were not observed.

A series of secondary mineral assemblages within the mafic sills indicate low grade metamorphism. The occurrence of albite, epidote, chlorite and actinolite as well as reaction rims around primary minerals support a lower greenschist facies metamorphism (Schweitzer & Kröner, 1985). The petrographic investigation of the sills revealed a high content of these secondary minerals within the investigated sills and dykes.

The microgabbro sills intruded mainly in shaly and dolomitic country rocks, whereas the gabbronorite sills mostly hosted by quartzites and shales. Sharpe (1978) suggests a stronger contact metasomatic effect for mafic magmas that intruded into hydrous shales due to the absorption of water from these shales. Whereas mafic magmas intruded into dry quartzites or dolomites show only minor metasomatic effects. The lack of chilled margins in the contact zone with the country rocks provides relative high temperatures for the country rocks (Cawthorn et al., 1981), so that either the country rocks were already heated by other intrusions (e.g. Uitkomst Intrusion) or the heat was generated by thermal subsidence (Sharpe, 1984).

The basement dykes show also moderate to high grades of alteration up to lower greenschist facies represented by similar mineral assemblages such as found in the sills. Additionally, the basement dykes are distinctively older than the sill groups and are hosted in hydrous granite gneiss, which could also supply hydrous fluids for alteration processes. The granite gneiss pluton itself has experienced low regional metamorph condition, which is indicated by a rather weak developed foliation.

4.4 Tectonic and structural features

The structural evolution of the study area was not the focus of this thesis and is documented elsewhere (see Hornsey, 1999). However for the acknowledgement of sill intrusions the detection of structural outcrop features is important in order to understand the emplacement mechanism of these intrusions.

Geometry and emplacement mechanisms

In general, a sill or flat-lying sheet describes a body ranging in size from a few meters up to hundreds of square kilometers, which is concordant with the intruded country rocks (Hall, 1996). Within the study area the shape of the sills varies from oval to circular for the central sill bodies of the gabbronorite sill group to wavy elongated shapes for the microgabbro sills, which indicates different emplacement mechanisms as well as feeding systems for the sill magma. Table 4.2 gives a short summary of the geometrical features of the investigated sills and dykes.

Table 4.2: Summary of structural features of the sills and dykes within the study area

sill/dyke	Geometry	Long axis (m)	Short axis (m)	Main orientation
GABBRONORITE SILLS				
Hofmeyr Sill 1	ovoid sill body, one tentacular offshoot	6675	1550	WNW-ESE
Houtboschloop Sill 1	ovoid sill body, two tentacular offshoots	3250	1375	WNW-ESE
Houtboschloop Sill 3	wavy elongated	1250	575	E-W
Weltevreden Sill 1	ovoid sill body, two tentacular offshoots	3550	1220	NW-SE
Uitkomst Sill 3	wavy elongated	3100	750	NW-SE
Uitkomst Sill 4	ovoid to circular	1650	400	NW-SE
MICROGABBRO SILLS				
Uitkomst Sill 1	wavy elongated, with slubs	4600	1625	NW-SE
Uitkomst Sill 2	wavy elongated, with slubs	2250	800	WSW-ENE
Vaalkop Sill 1	elongated in two directions	1: 2000 2: 1750	1: 750 2: 150	1: NE-SW 2: NW-SE
Vaalkop Sill 2	ovoid sill body	1025	750	(NW-SE)
Weltevreden-Slaaihoek Sill 1	wavy elongated	2625	1125	NW-SE
Houtboschloop Sill 2	wavy elongated	4500	875	WNW-ESE
Doornhoek Sill 1	wavy elongated	2000	950	NW-SE
BASEMENT DYKES				
swarm of 7 NW-trending dykes	linear slope	max: 4450 min: 600	max:125 min: 50	NW-SE
single NE-trending dyke	linear slope	2150	75	NE-SW

The gabbronorite sills form huge outcrops within the study area and covered mostly underlying shales and quartzites (see profile BB' in appendix). The oval geometry of the gabbronorite sill bodies suggest a single vertical feeder pipe as feeding system, where the magma spread out in a radial way. Furthermore the main distribution of the gabbronorite sills along the lithological contrast zone between Upper Timeball Hill shale and Klapperkop quartzite indicates a magma emplacement parallel to the compensation surface, where magma and lithostatic pressure are identical (Meyboom & Wallace, 1978; Hall, 1996) and the magma is “cought” in this position. The tentacular offshoots of these sills represent magma, which extend away along bedding planes or lines of weakness at stable pressure conditions. One gabbronorite sill (Uitkomst Sill 3) is located on a lower stratigraphic position within the Malmani dolomites. This could be an indication for a change of the lithostatic pressure due to fractures and faults.

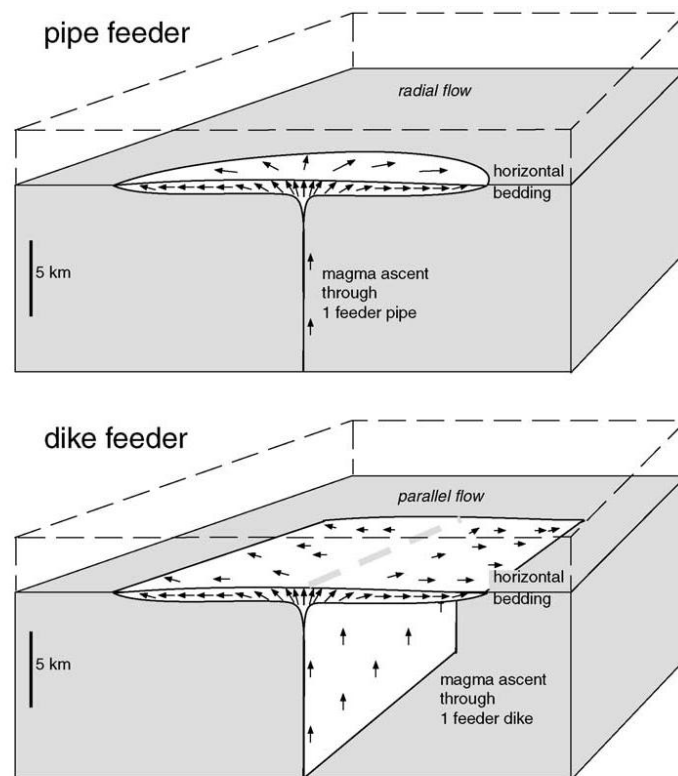


Figure 4.14: Theoretical models for feeding systems according to Ferré et al (2002). Radial magma flow is mostly the result of a single feeder pipe, whereas parallel magma flow indicate a feeder dyke as feeding system for magma emplacement

For the wavy elongated microgabbro sills a dyke feeder system is obvious (fig. 4.14), where the magma extended parallel to each side. Field observations indicate a more or less northwest-southeast arrangement for the microgabbro sills, which are intruded into the Transvaal sediments, on similar height levels on each side of the Uitkomst Complex. So it could be assumed that the magma used already existing fracture and fault systems for the emplacement.

The basement dykes (see profile AA' in appendix), which occur as prominent ridges within the Archaean Nelshoogte granite gneiss, show two main orientations (NW-SE and NE-SW). Characteristic is the linear slope extension and the small width of the dykes. The emplacement of the basement dykes is caused by different rifting events. The northwest-trending dykes within the study area belong to a dyke swarm of the same orientation. According to Uken & Watkeys (1997) the northwest orientation is determined by the 3.0 Ga Pongola rift system, which was re-utilized again by the emplacement of the Bushveld Complex and the Uitkomst Complex. The single northeast-trending dyke within the farm Vaalkop follows the orientation of the 2.7 Ga Ventersdorp rifting event (Uken & Watkeys, 1997).

The sedimentary country rocks within the study area were deposited within the Transvaal basin and show a flat dipping angle (5-10°) in northwest direction towards the centre of this basin. Due to the intrusion of the sills the dipping of the country rocks becomes more inclined, which is most obvious by the slopy dipping angle of shaly layers (see outcrop profile Uitkomst Sill 2).

Stereograms in figure 4.15 show the change from nearly horizontal slightly dipping layering to inclined dipping of the country rocks. Observable was a steeper dipping of dolomites and conglomerates (50° to 75°) in contact with the sills, whereas shales and quartzite show moderate changing of dipping (20° to 40°).

Furthermore outcrop profiles (see fig. 4.16, 4.17 & 4.18, p.50-52) are given in order to show the behavior of the country rocks during the sill intrusions as well as to show the geometry of typical sill outcrops within the study area. In field outcrops the strong weathered sills show mostly a horizontal layering above or below the country rocks.

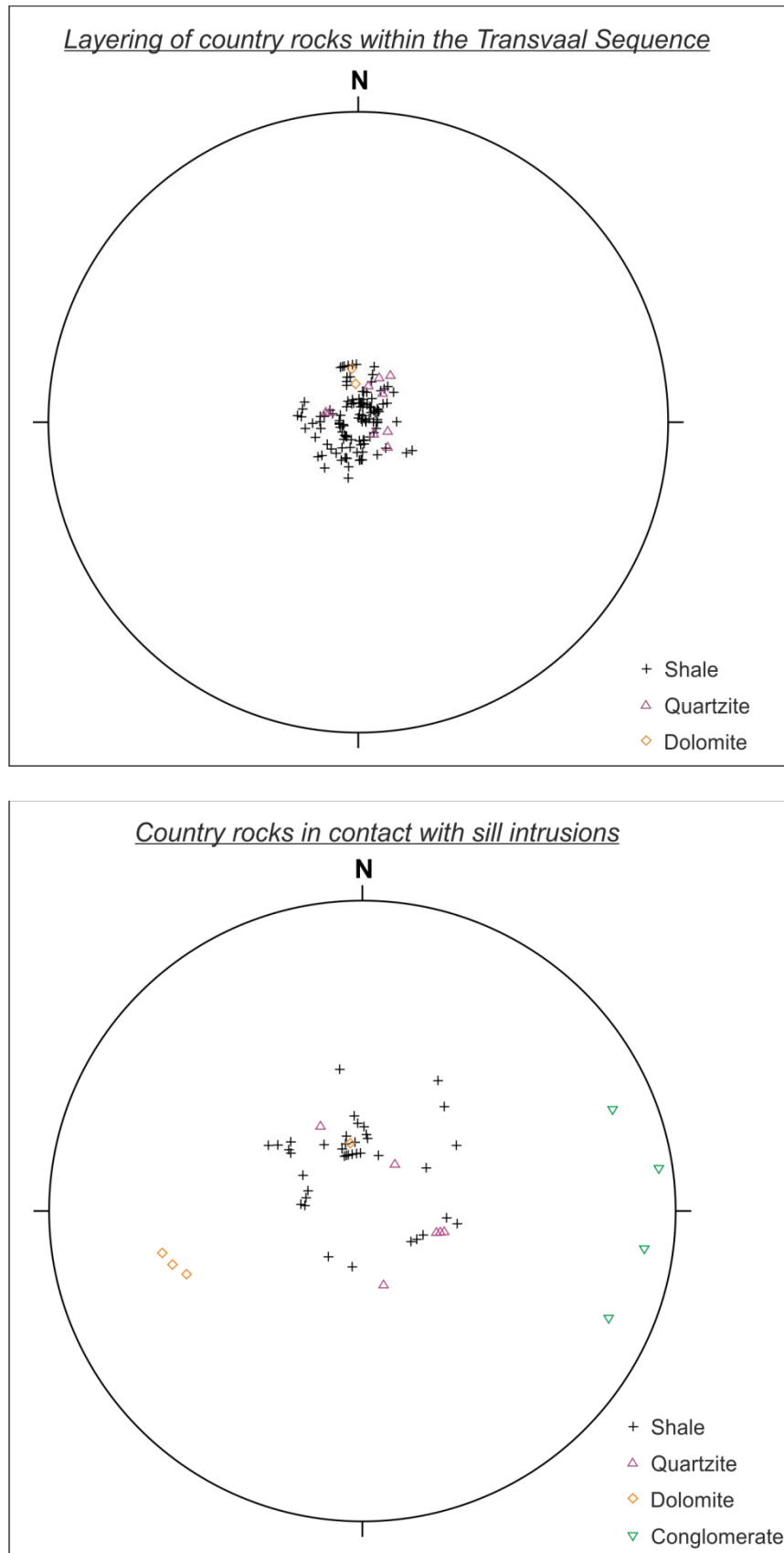


Figure 4.15: Comparison of the both stereograms shows a significant change in dipping angle for country rocks in contact with the sill intrusion. Furthermore conglomerates and dolomites exhibit a steeper inclination (50°-75°) than shales and quartzites (20°-40°).

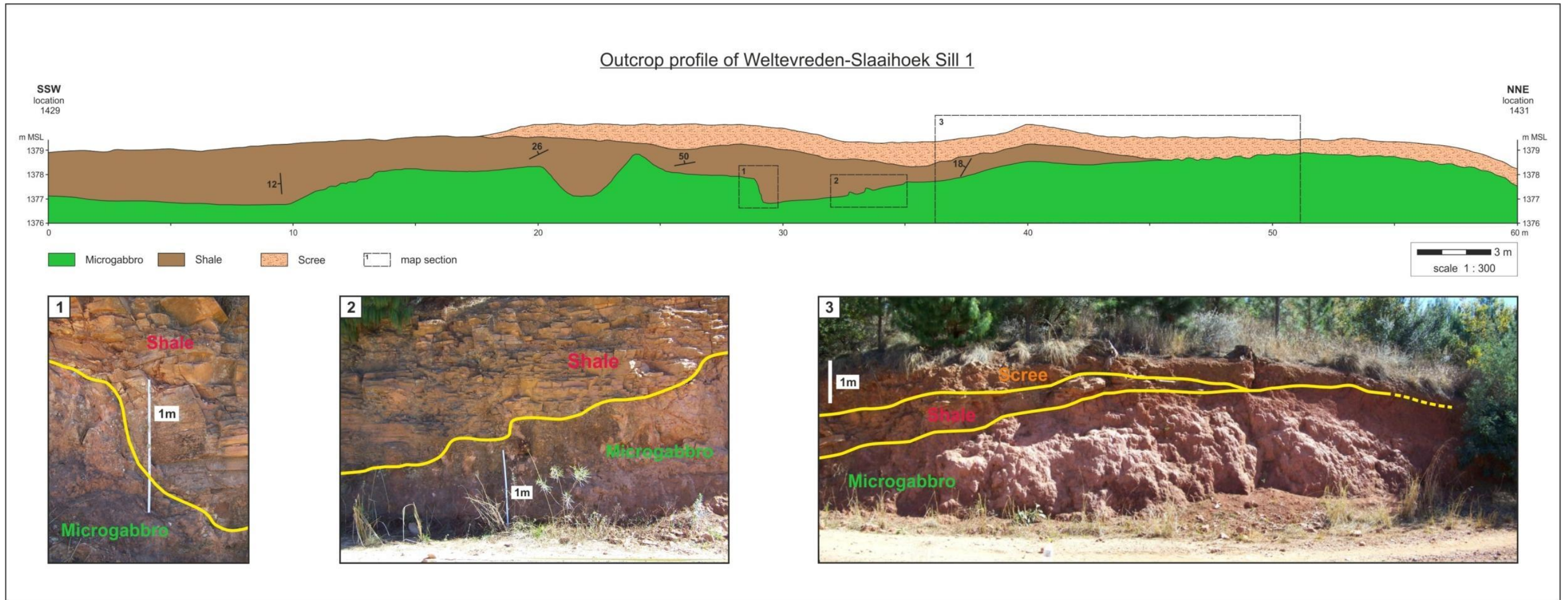


Figure 4.16: The outcrop profile of the Weltevreden-Slaaihoek Sill 1 shows a microgabbro sill, which is covered by shale. The contact zone to the shale is wavy developed and the shale are steeper inclined. The outcrop is overlain by scree and soil, and also the microgabbro is strongly weathered to reddish brown soil interspersed with resistant rock boulders.

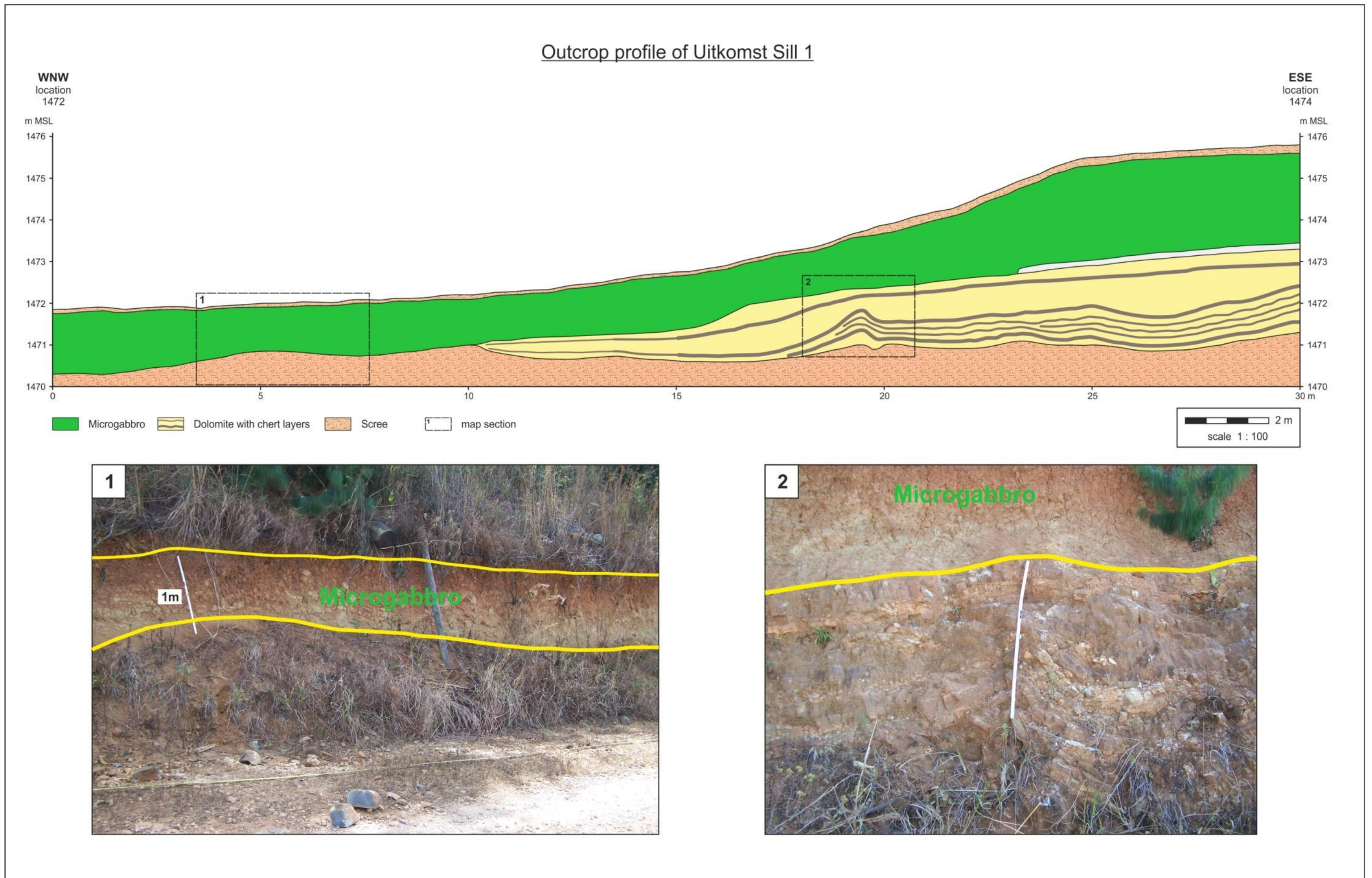


Figure 4.17: In the outcrop profile of the Uitkomst Sill 1 the microgabbro sill overlies the Malmani dolomites. In contact to the dolomites the microgabbro sill developed a chilled margin due to the fast cooling by the intrusion.

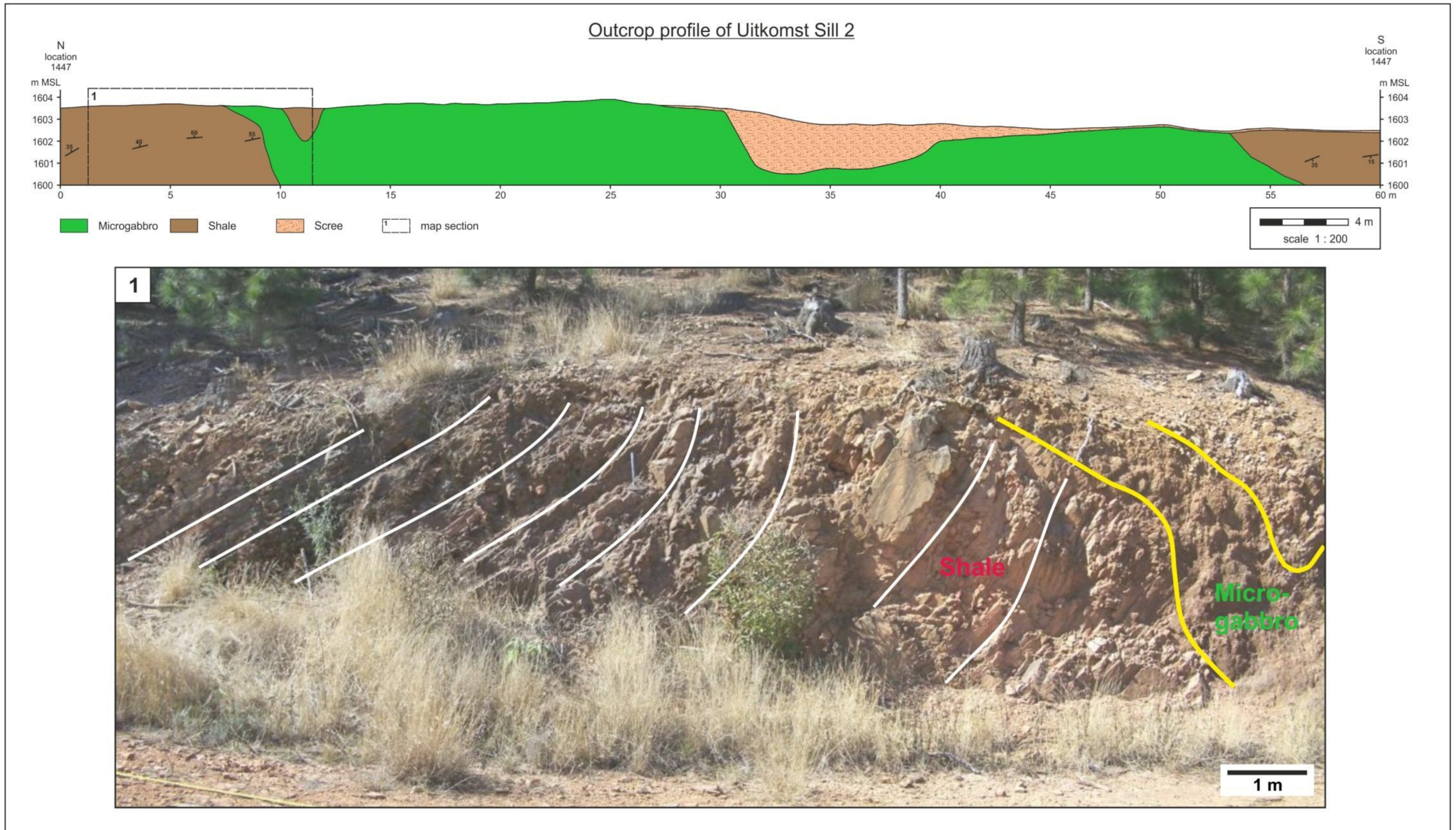


Figure 4.18: Within this microgabbro outcrop of the Uitkomst Sill 2 the shale is obvious inclined by the intrusion of the sill. In the centre of the sill outcrop a large part of the microgabbro is weathered to scree.

5. Petrography

5.1 Rock classification

The following petrographic description is based on the IUGS-classification for igneous rocks after Le Maitre (2002) and Streckeisen (1976) using the modal mineralogical composition (fig. 5.1). According to this classification all sampled and mapped sills and dykes are of gabbroic to noritic composition. The main primary mineral phases are plagioclase (commonly labradorite or bytownite), clinopyroxene, orthopyroxene, amphibole, minor biotite and quartz. Gabbro (sensu stricto) consists primarily of plagioclase and clinopyroxene, whereas norite consists of plagioclase and orthopyroxene. Gabbro-norite contains clinopyroxene as well as orthopyroxene (both > 5 %). Orthopyroxene gabbro has more clinopyroxene than orthopyroxene, whereas clinopyroxene norite contains more orthopyroxene than clinopyroxene next to plagioclase.

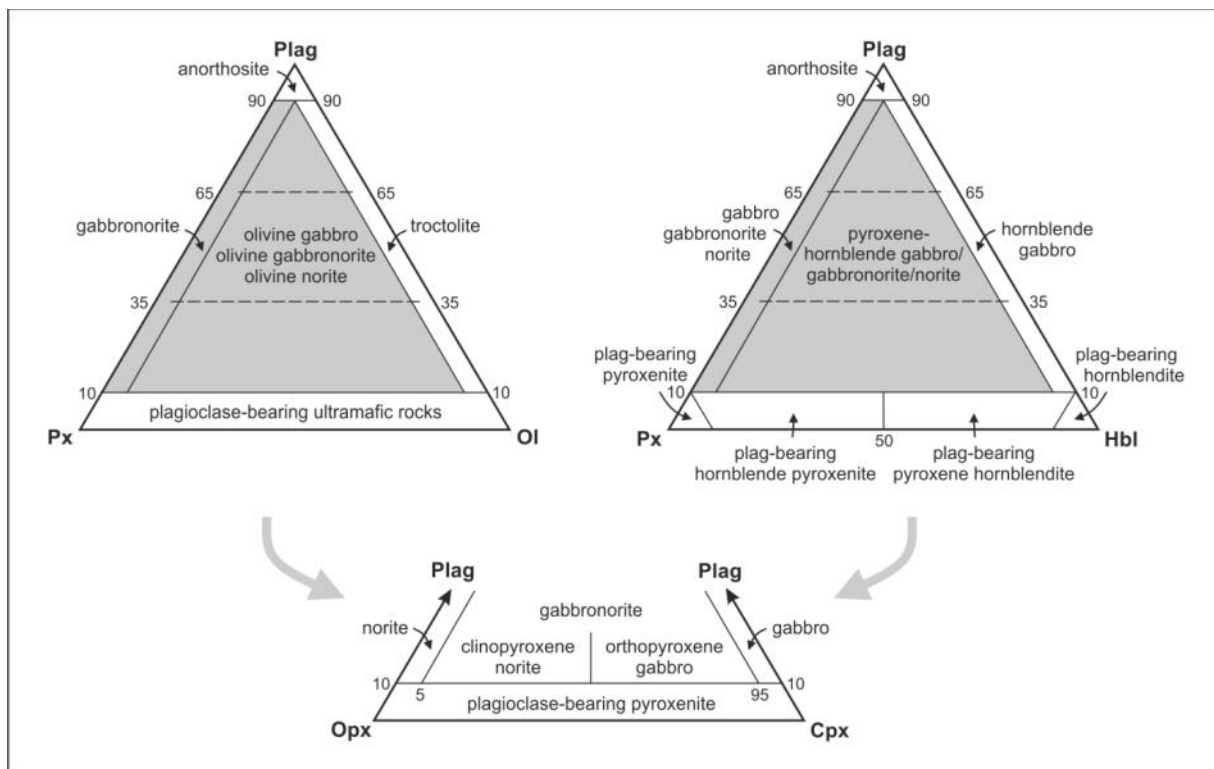


Figure 5.1: Classification and nomenclature of gabbroic rocks based on the proportions of plagioclase (Plag), pyroxene (Px), Olivine (Ol), orthopyroxene (Opx), clinopyroxene (Cpx), and hornblende (Hbl). Rocks within the shaded area of either triangular diagram may be further subdivided according to the middle diagram. (modified after Streckeisen, 1976; Le Maitre, 2002)

The use of the terms diabase and dolerite, which are common to describe dyke rocks are quite problematic. The significant differences between a gabbroic rock and diabase or dolerite are grain size and texture.

According to Le Maitre (2002) diabase or rather dolerite describes fine to medium-grained rocks of gabbroic composition, essentially made of plagioclase (labradorite), pyroxene and opaque minerals. The term dolerite implies a characteristic ophitic texture, but within the South African geology the term dolerite is strongly associated with dolerites of the Karoo Supergroup. However, these are considerably younger (Jurassic age) and show no relationship to the Uitkomst or Bushveld Intrusions. In the following petrographic description the term dolerite is therefore disregarded.

The term diabase is currently regarded “as being synonymous with dolerite and an approved synonym for microgabbro” (Le Maitre, 2002) based on the QAPF modal classification of plutonic rocks after *Streckeisen*. Also diabase is the conventional term used at the Nkomati Mine for sills and dykes that intruded in the vicinity of the Uitkomst Complex, but the use of the term diabase implies an identical mineralogical composition and texture for all of the occurring sill and dykes. However, that is not the case.

The characterization of the mapped sills and dykes given below is based on mineralogical composition, texture, grade of alteration and morphologic field observations. Based on this information three different groups of mafic rocks (sills & dykes) were identified. These are: **Microgabbro sills, Gabbronorite sills and Basement dykes**. In table 5.1 all mapped sills and dykes are listed together with the corresponding subchapter number.

Table 5.1: All mapped sills and dykes listed below including the corresponding subchapter number.

SILLS				DYKES	
Microgabbro sills	5.2	Gabbronorite sills	5.3	Basement dykes	5.4
Characteristics	5.2.1	Characteristics	5.3.1	Characteristics of all sampled & mapped gabbronoritic basement dykes	5.4.1
Uitkomst Sill 1	5.2.2	Hofmeyr Sill 1	5.3.2		
Vaalkop Sill 1	5.2.3	Houtboschloop Sill 1	5.3.3		
Vaalkop Sill 2	5.2.3	Houtboschloop Sill 3	5.3.4		
Uitkomst Sill 2	5.2.4	Uitkomst Sill 4	5.3.5		
Doornhoek Sill 1	5.2.4	Weltevreden Sill 1	5.3.6		
Houtboschloop Sill 2	5.2.4	Uitkomst Sill 3	5.3.7		
Weltevreden-Slaaihoek Sill 1	5.2.4				

5.2 Microgabbro

5.2.1 Characteristics

The microgabbro group comprises seven of the mapped sills, which are the **Uitkomst Sill 1 (US-1)**, the **Vaalkop Sill 1 (VKS-1)**, the **Vaalkop Sill 2 (VKS-2)**, the **Uitkomst Sill 2 (US-2)**, the **Doornhoek Sill 1 (DS-1)**, the **Houtboschloop Sill 2 (HBS-2)** and the **Weltevreden-Slaaihoek Sill 1 (WSHS-1)**. This group of sills shows a widespread spatial as well as stratigraphic distribution within the study area. These mostly small to medium sized sills intruded into the Archaean Basement and also into the Transvaal Sequence ranging from Black Reef Formation to Timeball Hill Formation.

Basic outcrop features

Generally, all microgabbro sills show distinctive signs of weathering. The outcrops in-between the shaly or quartzitic country rocks consist of red-brown to red-beige soil interspersed with resistant rock boulders of various size (fig. 5.2.a). These robust boulders are surrounded by a brittle weathering crust (fig. 5.2.c). In outcrops with direct contact to the shales, quartzites or dolomites the sills show a clear horizontal or slightly inclined layering. Microgabbro sills that intruded into the Archaean basement appear as widespread unshaped rock dumps, which cover the more weathered granite gneisses. The reddish soil resulting from weathering has already been eroded or underlies the huge boulders (fig. 5.2.d).

Basic macroscopic features

In spite of the stratigraphic range the microgabbro sills are relative homogeneous in their mineralogical composition. The microgabbro is a fine to medium grained rock of typical gabbroic composition and texture. Hand specimens show an obvious speckled grey-black and white coloration (fig. 5.2.b,c) with a dominance of the grey to black components. Nearly every hand specimen is magnetic and reacts with hydrochloric acid due to alteration processes.

The major minerals phases in the epigranular appearing samples are feldspar, pyroxene, amphibole and more or less biotite and quartz. Feldspar occurs as small grey transparent elongated crystals as well as granular masses showing first hints of alteration processes. The pyroxene component shows also granular masses of dark grey color. Single matt black pyroxene crystals are sparse. In strongly altered hand specimens amphibole is the dominant mafic mineral visible by a dark green color cast. Accessory minerals are epidote and fine disseminated pyrite or chalcopyrite.

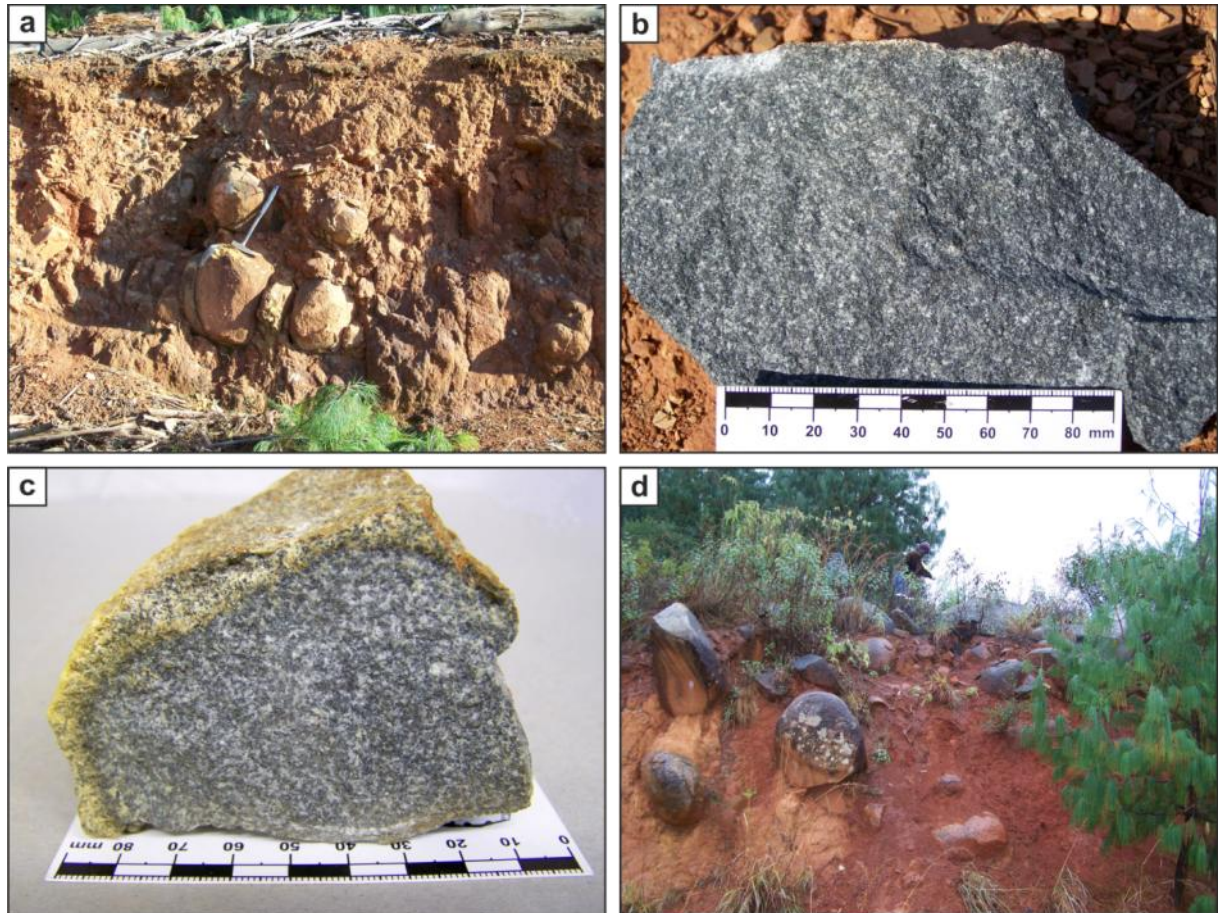


Figure 5.2: Microgabbro outcrops are strong weathered to a mixture of reddish beige soil and resistant rock boulders in between (a: US-1, d: VKS-1). These rock boulders are mostly surrounded by a weathering crust (c: WSHS-1), whereas the core of larger boulders occurs as relative fresh for sampling (b: HBS-2). Notice the speckled grey-black and white colouration of the hand specimens.

Basic microscopic features

Plagioclase occurs as euhedral to subhedral lath-shaped or prismatic crystals, with an average anorthite content of An_{55-60} as well as fine anhedral interstitial fillings between other minerals. Most of the plagioclase is affected by sericitisation and saussuritisation starting from the centre of the crystal. Characteristic for the microgabbro lithology is the subophitic to ophitic texture (fig. 5.3.a,b), which shows small plagioclase crystals completely or partly enclosed in larger grains of pyroxene or amphibole. Anhedral grains of quartz appear mostly as interstitial patches, but usually do not exceed 5 %.

The contents of pyroxene and amphibole are variable depending on the grade of alteration. Euhedral to subhedral clinopyroxene (mainly augite) forms short prismatic to elongated crystals. Orthopyroxene is either absent or appears as subhedral stubby prismatic grains. All pyroxenes are strongly altered; especially the margins are replaced by amphibole.

Two forms of mainly secondary amphibole are developed. Pale green actinolite occurs as fibrous to small columnar alteration mineral, whereas green or brown hornblende appears as replacement product of pyroxene (uralitisation) with fine inclusions of magnetite as well as primary mineral, which is also altered to actinolite. Next to actinolite (fig. 5.3.c) and hornblende a series of further alteration minerals are definable. This includes varying mineral assemblages of biotite, sericite, epidote, zoisite, calcite, talc and clay minerals, probably initiated by alteration and minor weathering. Biotite (amounts up to 8 %) occurs mostly as anhedral flaky crystals in intergrowth with amphibole, chlorite or other alteration minerals. Euhedral tabular crystals of biotite, which indicates a primary origin, are scarce. Generally the smaller sills like Weltevreden-Slaaihoek Sill 1 or Doornhoek Sill 1 are more affected by alteration than the larger sills (Vaalkop Sill 1, Uitkomst Sill 1) of the microgabbro group.

Another characteristic feature of the microgabbro sills is the relative high amount of Fe-Ti-oxides, which are mainly magnetite, ilmenite and hematite as well as their skeletal to hackly shapes (fig. 5.3.d).

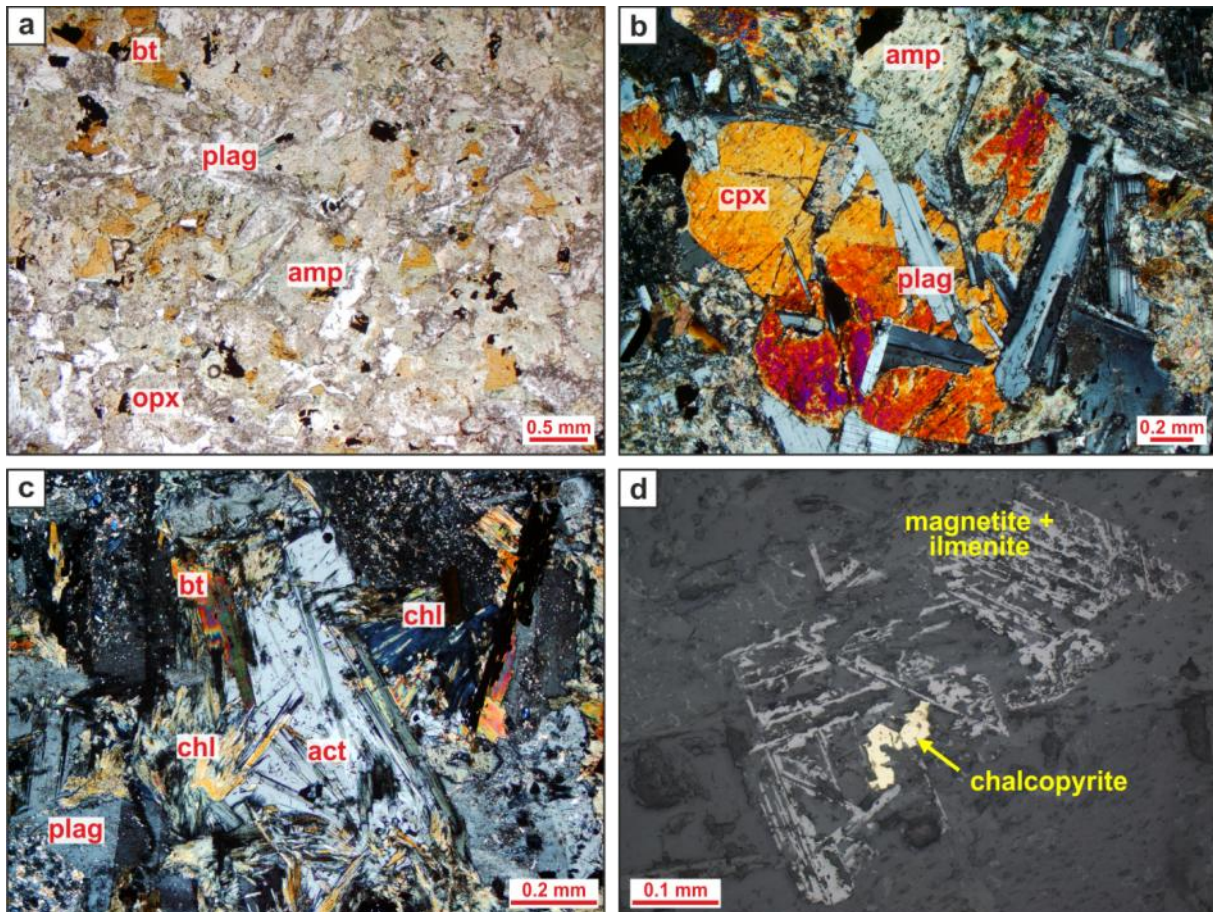


Figure 5.3: Typical for microgabbro rocks is the subophitic to ophitic texture, which shows prismatic to lath-shaped plagioclase crystals enclosed in pyroxene or amphibole (a: VKS-1, under PP view; b: US-1, under XP view), as well as intergranular pyroxene, amphibole or biotite between plagioclase laths (pic.a). A series of alteration minerals occur as individual crystals or in intergrowth with primary minerals. Picture c (US-1, under XP view) shows actinolite needles in intergrowth with chlorite and biotite, also sericitic plagioclase. Within the microgabbros Fe-Ti-oxides form distinct skeletal shapes of magnetite and ilmenite, often intergrown with pyrite or chalcopyrite (d: HBS-2, under PP view reflected light)

In the following sub chapters (5.2.2-5.2.4, p.59) the seven sills of the microgabbro group are either described separately or combined as one subgroup to characterize individual features.

5.2.2 Uitkomst Sill 1

The Uitkomst Sill 1 (US-1) is one of the most sampled sills because of the good accessibility over the whole extension of 7.35 km². The Uitkomst Sill 1 intruded into different country rocks including Timeball Hill Shale, Rooihoogte Quartzite, Malmani Dolomite and Black Reef Quartzite (see geological map, appendix). Considering this and the large length of the sill, the US-1 shows more heterogeneity in mineralogical composition compared to the smaller microgabbro sills described above.

Macroscopic description

Macroscopically, all microgabbro hand specimens of US-1 have the typical grey-black and white speckled coloration and are mainly of fine to medium grain size (fig. 5.4). In hand specimens the texture seems to be epigranular, only some single elongated feldspar individuals stand out, such as in sample VK_13-6_3/1 or U_11-7_15/1. The major mineral phases are feldspar, pyroxene, amphibole, biotite and minor quartz, with accessory epidote, pyrite and magnetite. The dominant feldspar component occurs as light grey transparent elongated crystals as well as white granular masses with green discolorations due to saussuritisation. In between the feldspar phase some small colorless quartz grains are observable with typical conchoidal fractures. The mafic minerals amphibole and biotite form distinct crystals of prismatic to fibrous or flaky habit. The dark green amphibole causes a greenish color cast in samples with higher amphibole content and appears sometimes as arcuated crystals (U_11-7_9/1). Generally, the microgabbro hand specimens from the middle part of the sill occur more finely grained. Also a higher content of mafic minerals is noticeable.

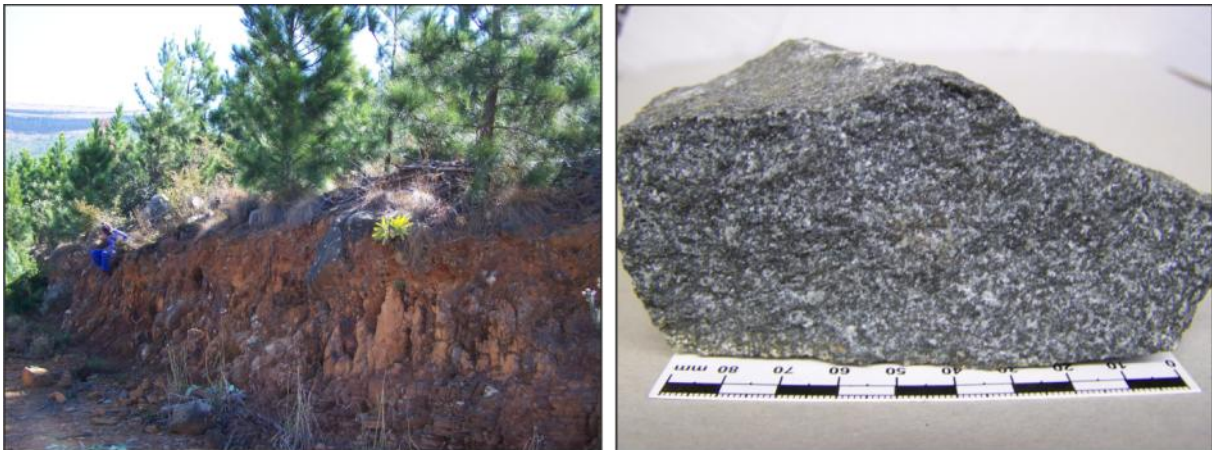


Figure 5.4: The hand specimen (U_11-7_13/1) on the right is medium grained with a grey-black and white speckled coloration and seems to be epigranular in texture. The left picture shows a strong weathered outcrop of US-1, where sampling was not possible. Notice the horizontal layering of the microgabbro sill over dark-brown shale in the front of the picture.

Microscopic description

At microscopic scale, the samples from different outcrops show more inhomogeneity in mineralogical composition within the US-1, whereas the typical microgabbro texture of subophitic to ophitic plagioclase crystals enclosed in pyroxene or amphibole is still preserved. The primary mineral phases are plagioclase (30-35 %), quartz (3-6 %), orthopyroxene (0-10 %), clinopyroxene (12-20%) and biotite (8-10 %). Their content varies due to different alteration grades within the sill. A detailed petrographic description of the samples U_11-7-3/1, VK_13-6-3/1, W_17-7_7/1 and VK_23-7_1/1 are listed in appendix p.150 – 153.

Plagioclase occurs still as euhedral to subhedral, prismatic to lath-shaped crystals (up to 3.2 mm in VK_13-6_3/1). They appear also as fine granular interstitial filling together with quartz and alteration minerals. The plagioclase has an anorthite component of An_{55-60} , which suggests labradorite as the dominant plagioclase. The alteration grade varies from fresh (e.g. U_11-7_3/1) to strongly altered (e.g. W_17-7_7/1) plagioclase. The latter forms a mixture of saussurite and sericite. Quartz appears as interstitial patches often together with plagioclase as well as single grains up to 0.5 mm.

The occurrence of pyroxene is directly dependent on the grade of alteration. In fresh samples ortho- and clinopyroxene are the dominant mafic minerals. Subhedral pale green to brown orthopyroxene forms stubby prismatic crystals (up to 1 mm), which are altered to amphibole on the margins (fig. 5.5). Short to long prismatic clinopyroxene shows also signs of uralitisation at the margins. An inclined extinction of 43° suggests augite as preferred clinopyroxene. Both pyroxenes occur also as intergranular fillings between lath shaped plagioclase crystals.

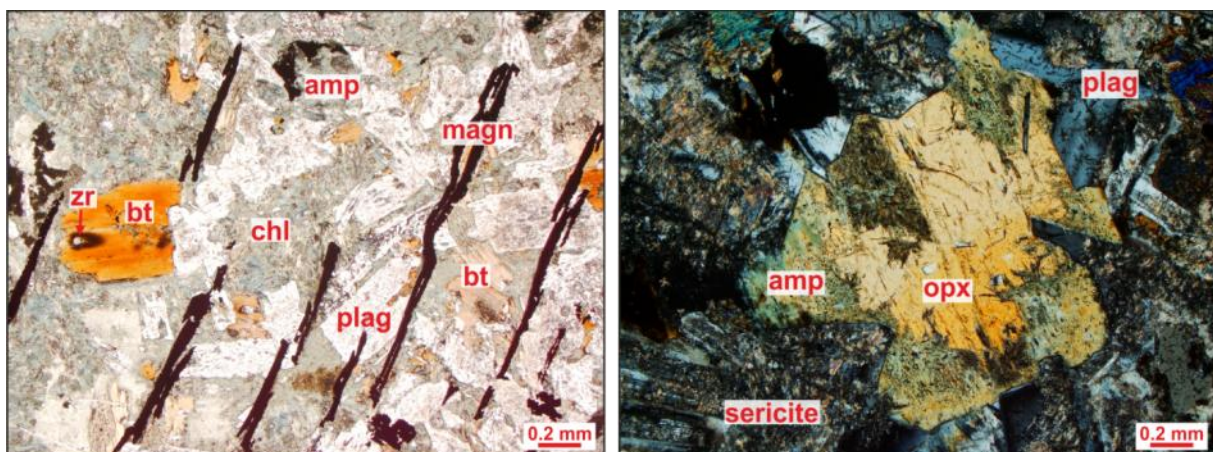


Figure 5.5: The left picture (under PP view) shows magnetite laths parallel arranged in groups as well as a big anhedral biotite crystal with pleochroic halo around a zirconium crystal. In the background prismatic plagioclase crystals are surrounded and penetrated by chlorite, biotite, amphibole and Fe-Ti-oxides. In the right picture (under XP view) a subhedral orthopyroxene crystal is altered to green amphibole on the margins.

The content of amphibole in unaltered sections like U_11-7_3/1 is relatively low and is also restricted to short columnar green brown hornblende with fine inclusions of magnetite.

In thin section of W_17-7_7/1, which was taken from the other side of the Uikomst Sill 1, pyroxene is supposedly completely altered to amphibole. This is indicated by the pseudomorphic replacement after pyroxene. Secondary amphibole occurs as stubby prismatic to columnar hornblende as well as fibrous pale green actinolite. Both are intergrown with biotite and Fe-Ti-oxides (fig. 5.5). Biotite and other alteration minerals like epidote, chlorite, calcite and sericite are found within the whole sill, but are well developed especially in the strongest altered samples.

Fe-Ti-oxides are distributed within all thin sections of US-1 and form mainly skeletal to multilateral shaped magnetite in intergrowth with titanomagnetite, ilmenite and hematite. A special feature of magnetite is found in W_17-7_7/1. Magnetite forms long laths up to 2.4 mm, which are parallel arranged in groups (fig. 5.5) and penetrate the surrounding minerals. So it seems to be a secondary forming texture.

A specific feature of US-1 is a well-defined chill margin in the contact zone between microgabbro sill and dolomitic country rocks. The outcrop occurs in the southeastern part of US-1. The dark grey-black hand specimen (VK_23-7_1/1; fig. 5.6) shows a very fine groundmass interspersed with small white-grey needles (up to 5 mm) of probably feldspar. In the outcrop the chilled margin zone occurs as small white layer with a thickness of 15 cm. The white color resulted from a film of clay minerals surrounding the chilled microgabbro rocks.



Figure 5.6: The hand specimen of the chilled margin of US-1 has a fine dark grey groundmass interspersed with fine light grey needles of feldspar. Notice the white film surrounding the sample on the left. Microscopically, the groundmass consists of variolitic plagioclase, quartz, alteration minerals and glass. Lath-shaped plagioclase and stubby prismatic orthopyroxene occur as phenocrysts within the groundmass (right picture, under XP view).

Microscopically, the groundmass of the chilled margin consists of fine variolitic arranged plagioclase crystals together with quartz, alteration minerals and glass. Euhedral to subhedral plagioclase (12 %) laths as well as elongated to stubby prismatic orthopyroxene (18 %) occur as phenocrysts (fig. 5.6) within the groundmass.

The orthopyroxene crystals are often altered to amphibole and clay minerals along the crystal margins. Generally the chilled margin of the microgabbro is more noritic in composition compared to the microgabbro rocks itself.

The inhomogeneity in composition is effectively an inhomogeneity in grade of alteration, from which some areas of the sill are more affected than others. Generally the northwestern part of US-1 shows more effects of alteration in hand specimens and thin sections. That excluded a directly contact metamorphism overprinting, initiated by the intrusion of the Uitkomst Complex, but supported an alteration initiated by the intrusion of the sill itself. Possible reasons for the heterogenic alteration could be the varying thickness of the sill, so that small segments of the sill are stronger influenced by alteration processes than thicker one, as well as the varying host rocks lithologies, whereas the sill segments, which intruded into shales, are more affected by alteration.

5.2.3 Vaalkop Sill 1 & 2

This subgroup contains the only two sills, which intruded partly or completely into the Archaean basement. Vaalkop Sill 1 is also hosted and partly covered by the Black Reef Quartzite and the Malmani Dolomite, whereas Vaalkop Sill 2 is completely surrounded by the Archaean basement and not covered by any other country rocks. Both sills are more or less unshaped and compared to other sills they are not restricted on a certain height level. The spatial distribution of both sills is bound to the position of three basement dykes. They probably used the structural weakness for their intrusion caused by the basement dykes.

Macroscopic description

The fine to mainly medium grained hand specimens show feldspar, pyroxene, amphibole and biotite as major mineral phases. Comparable to the other microgabbro sills is the dark grey and white speckled coloration and an epigranular texture in hand samples.

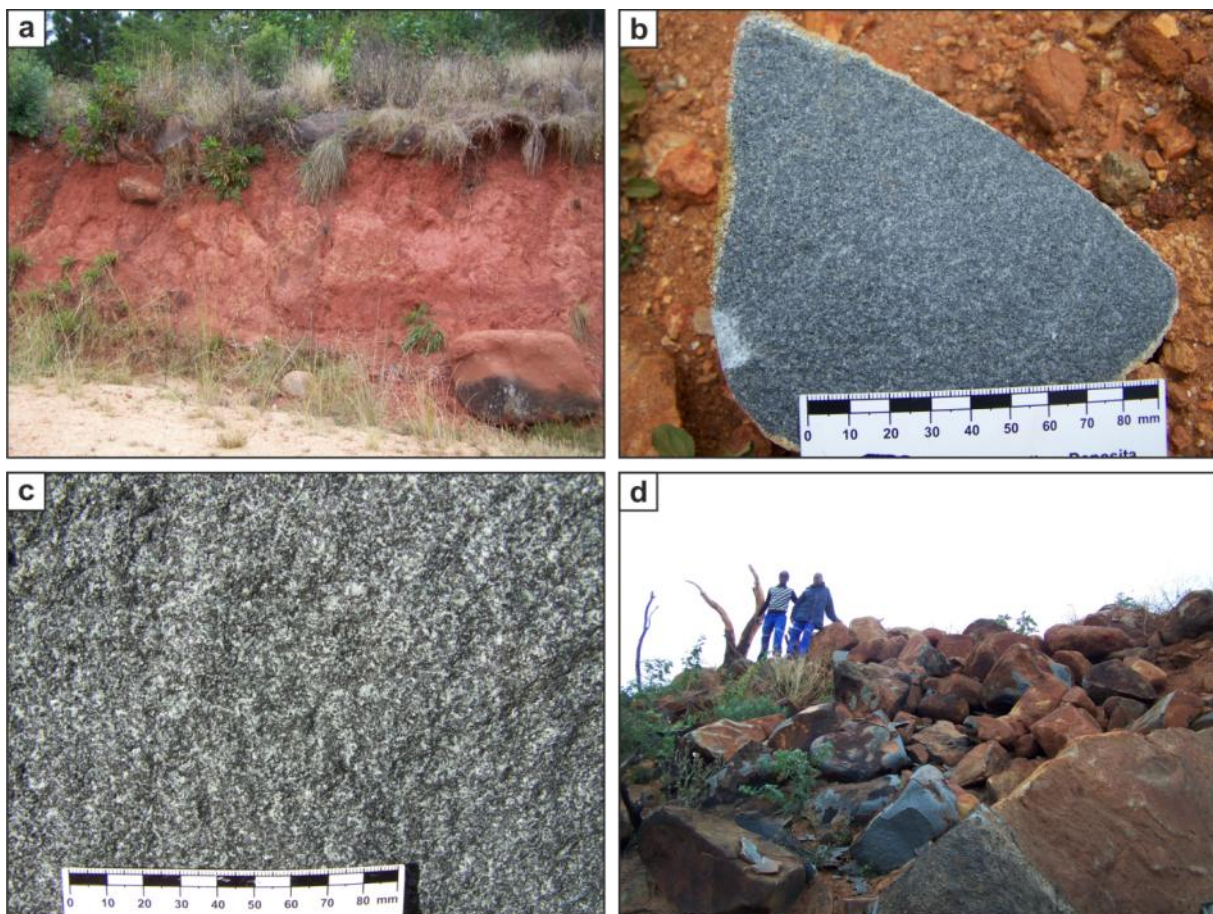


Figure 5.6: The Vaalkop Sills appear as highly weathered outcrops with large rock boulders on top (a: VKS-1) or form wide ranging rock dumps overlying the Archaean basement (d: VKS-2). In hand specimens these microgabbros occur as epigranular dark grey and white speckled rocks (b: VKS-1, c: VKS-2). Notice the white coloration of altered feldspar in picture c.

The white color of feldspar (fig. 5.6.c) indicates a strong alteration grade supported by partly intergrowth with pistachio green epidote patches (e.g. VK_11-6_5/1). In spite of the saussuritisation the feldspar crystals form small tabular shapes (up to 2 mm) with well developed cleavage planes. Single quartz grains also appear between the feldspar, but do not exceed 5 %. On macroscopic scale the pyroxene component is the dominant mafic mineral and mostly occurs as black granular masses surrounded by feldspar. Among these masses dark green to black elongated crystals of amphibole appear, which sometimes show a fibrous surface on developed cleavage planes.

Half of the samples show a distinctive magnetism suggesting the occurrence of magnetite. Hand specimen VK_8-6_7/1 exhibits small grains of bronzy yellow pyrrhotite that are weakly magnetic. In sample VK_9-6_13/1 very small cubes of black hematite are observable, which could be a pseudomorphose after pyrite.

Microscopic description

A detailed petrographic description of the representative sample VK_8-6_5/2 is given in appendix, p.154. On microscopic scale the main constituents are plagioclase (25-30 %), quartz (3-5 %), clinopyroxene (15-18 %), amphibole (20 %) and biotite (4-6 %). Euhedral to subhedral plagioclase crystals are distinctively bigger in size than the remaining mineral phases, but also occur as small crystals and form interstitial fillings between other minerals. The typical microgabbro texture of subophitic to ophitic enclosed plagioclase in pyroxene or amphibole is clearly visible (fig. 5.7.a,b). Prismatic clinopyroxene is mostly altered, but shows also euhedral larger individual crystals (fig. 5.7.c).

Microscopic investigations indicate a relative high amount of primary hornblende (8-10 %) in both sills, thus the sills can be termed as hornblende bearing microgabbro. Additionally, secondary amphibole occurs in intergrowth with biotite, chlorite and little magnetite cubes. Further alteration minerals are sericite, calcite and epidote.

The amount of accessory Fe-Ti-oxides reach up to 4 % and include mainly four-sided or skeletal shapes of magnetite in intergrowth with ilmenite and hematite (fig. 5.7.d).

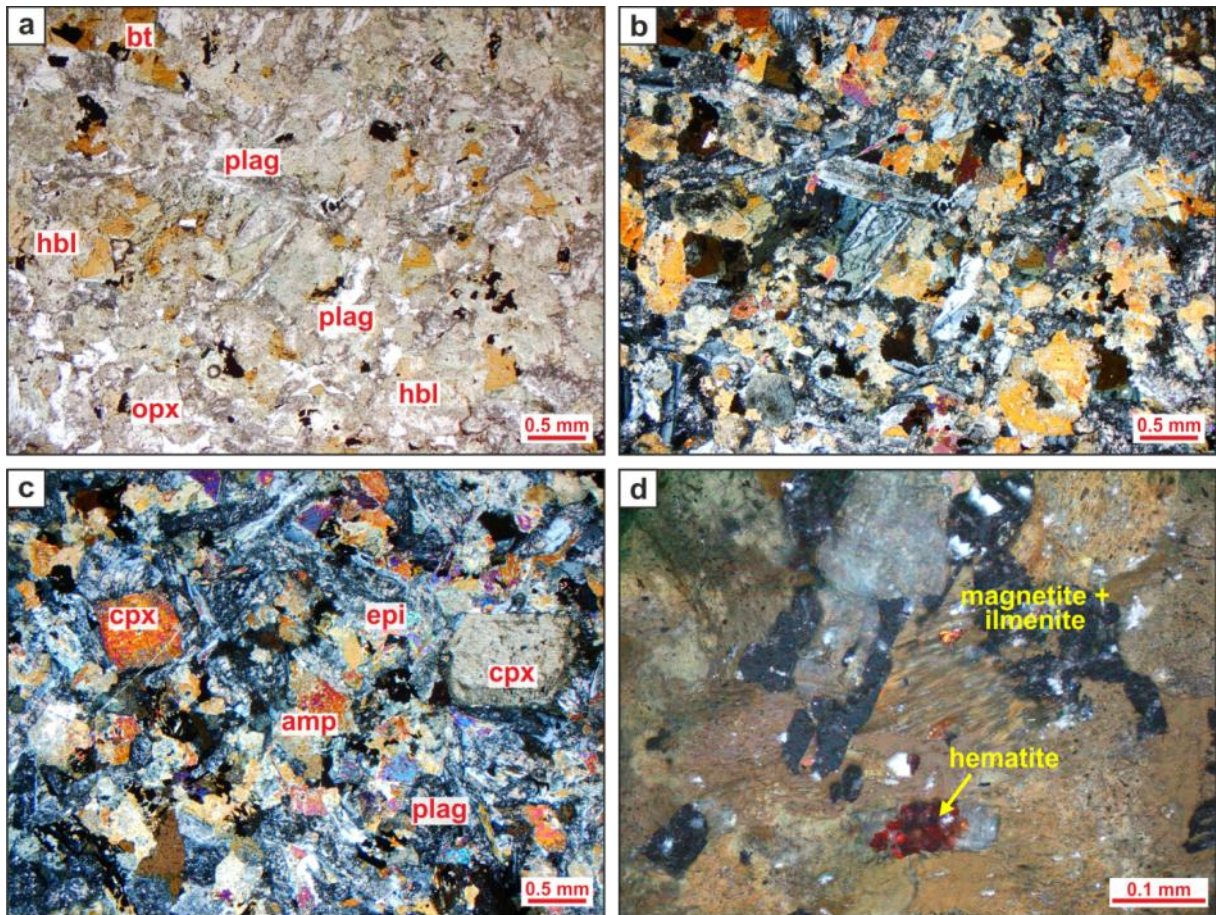


Figure 5.7: All pictures are taken from the thin section of sample VK_8-6_5/2, which combined all representative features of this subgroup. Both pictures above show subhedral plagioclase laths subophitic enclosed in anhedral hornblende (a under PP view; b under XP view). In picture c (XP view) two larger euhedral crystals of clinopyroxene are embedded within the otherwise epigranular texture. Fe-Ti-oxides occur as magnetite in intergrowth with ilmenite and hematite, which show distinctively red reflections (d under PP view, reflected light).

5.2.4 Subgroup of small microgabbro sills

This subgroup includes the relative small **Uitkomst Sill 2 (US-2)**, **Doornhoek Sill 1 (DS-1)**, **Weltevreden-Slaaihoek Sill 1 (WSHS-1)** and **Houtboschloop Sill 2 (HBS-2)**, which all intruded into the Timeball Hill Shale. Common to all of them is their low thickness (varying from a few meters to about 150 m), their stratigraphic position and their petrographic homogeneity throughout the complete extension of every sill.

Macroscopic description

In hand specimens, a distinct grey-black and white speckled coloration is visible caused by the strong grade of alteration, which affected all sills of this subgroup. The primary mineral phases are feldspar, pyroxene and amphibole. The feldspar component occurs as white granular masses (fig. 5.8) with a green discoloration (saussuritisation) starting from the centre of the crystal. Single euhedral prismatic to short lath-shaped crystals (up to 4 mm) show a noticeable bluish luster on the cleavage planes, which is typical for labradoritic plagioclase (e.g. HB_8-7_3/1 from Houtboschloop Sill 2). The quartz content is very low, only small single anhedral grains are macroscopically observable. Amphiboles are the dominant mafic minerals, recognizable on the varnish-like brilliance, green grey color and columnar to acicular habit. In contrast the pyroxenes form small black stubby prismatic crystals as well as granular masses. Biotite appears as minor phase and is definable by the flaky appearance and low hardness. Accessory minerals are pistachio-green epidote, small grains of light yellow pyrite and magnetite, which is identifiable by magnetism of the majority of samples.

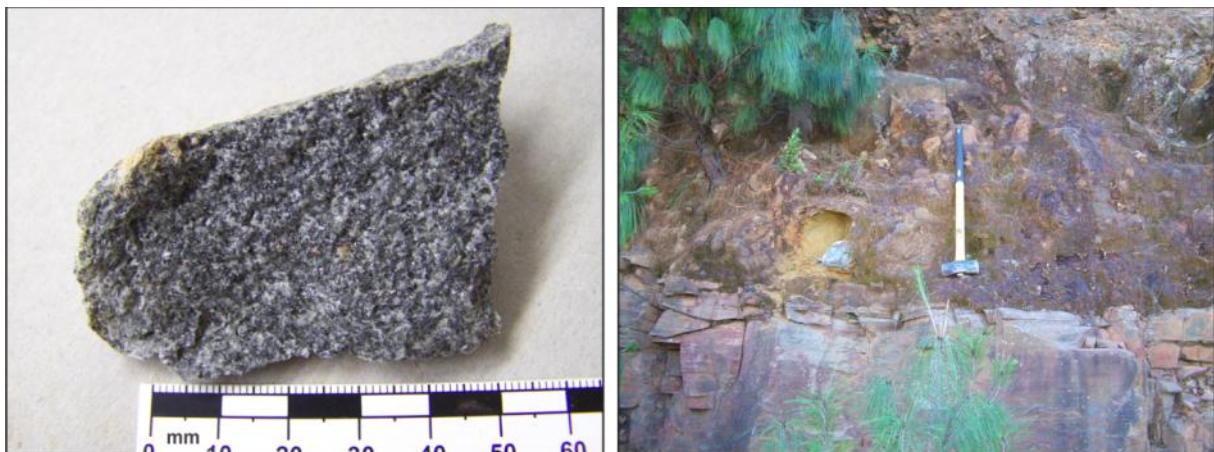


Figure 5.8: Both pictures are from Uitkomst Sill 2. The hand specimen (left) shows the typical microgabbro grey-black and white speckled coloration caused by altered feldspar (white to light grey) and granular amphibole-pyroxene masses. The sample is taken from the outcrop on the right side. Notice the horizontal layering of the microgabbro sill over the shale of the Timeball Hill Formation as well as the strong weathering to red brown soil including resistant rock boulders of microgabbro.

Microscopic description

Detailed petrographic descriptions of the samples U_19-6_7/1, UZ_8-7_6/1, U_22-6_3/1 and D_20-6_6/1 are given in appendix p. 155 – 158. On microscopic scale the fine to medium grained microgabbro sills are mainly composed of plagioclase (30-35 %), pyroxene (≤ 7 %), amphibole (20-30 %), biotite (3-8 %) and minor quartz (4-7 %). Plagioclase occurs as euhedral to subhedral lath shaped (up to 3 mm, U_22-6_3/1) to prismatic crystals and as an interstitial phase. The anorthite component ranges from An₄₀₋₅₀ (US-2 & WSHS-1) to An₆₀ (HBS-2). Generally the crystal centers are strongly altered to sericite and other alteration minerals. Subordinate pyroxene appears as anhedral pale brown fragments of crystals, which are nearly completely replaced by amphibole. A subdivision into clino- or orthopyroxene is difficult due to lack of optical properties. The microscopic investigations prove the dominance of amphibole, which occurs as secondary actinolite and hornblende resulting from alteration processes (uralitisation of pyroxenes) as well as primary hornblende of magmatic origin. In the sills US-2 and WSHS-1 more primary hornblende (up to 12 %) is observable, so these sills can be described as hornblende bearing microgabbros. Magmatic subhedral hornblende (fig. 5.9) shows alteration to actinolite on the margins, similar to pyroxene. In contrast the secondary amphibole component forms pale green fibrous to acicular actinolite and green-brown prismatic hornblende, which is pseudomorph after pyroxene and included tiny magnetite grains. Another characteristic for the microgabbro rocks is the relative high content of biotite compared to other lithologies. Anhedral biotite occurs as platy to flaky brown grains with the typical birdseyes extinction and pleochroic halos around zirconium inclusions. In U_22-6_3/1 (US-2) euhedral biotite crystals with hexagonal basal sections that indicate a magmatic origin are observable.

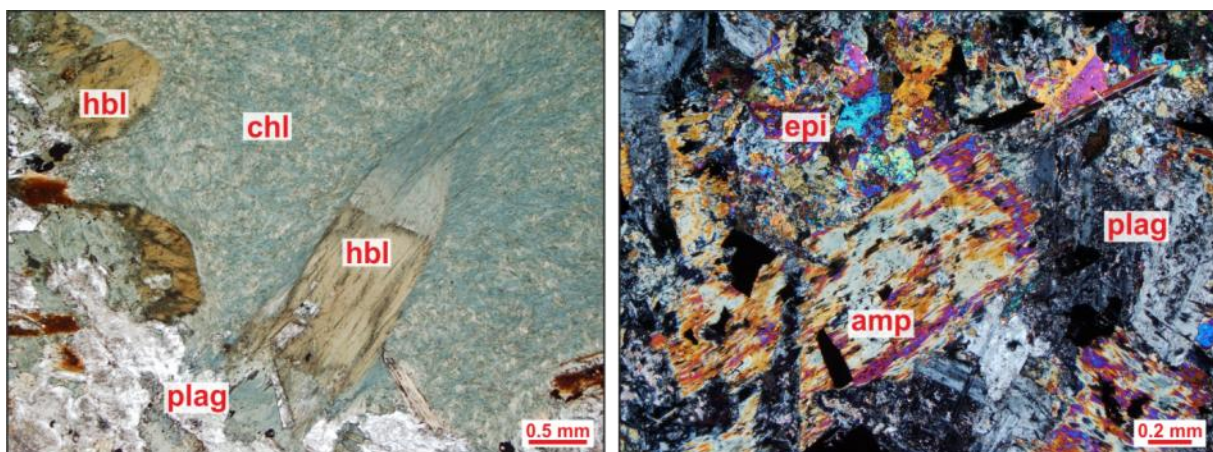


Figure 5.9: Both pictures show predominant alteration minerals with a preserved gabbroic texture of subophitic to ophitic enclosed plagioclase laths in amphibole. In the left picture (U_19-6_7/1, under PP view) fibrous chlorite crystals arranged in a bubble-like cluster encompass hornblende crystals (brown, cleavage angles 60°/120°), which are pseudomorph after pyroxene (octagonal basal sections). The prismatic hornblende crystal in the middle is replaced by chlorite on the margins. In the right picture (UZ_8-7_6/1, under XP view) an anhedron hornblende crystal has enclosed plagioclase and magnetite grains. Also granular epidote with shiny interference colors in intergrowth with amphibole is observable.

The formation of biotite as a result of contamination with shaly country rock together with alteration processes is also conceivable. The amount of further alteration minerals like chlorite, epidote (fig. 5.9), calcite, sericite and clay minerals confirm the high grade of alteration. In spite of that the gabbroic texture is still preserved. Plagioclase crystals are subophitic to ophitic enclosed in amphibole or pyroxene, which also occur intergranular between plagioclase laths.

The two hornblende bearing microgabbro sills (US-2 and WSHS-1) have the highest biotite content as well as the lowest anorthite content of 40-50 % that suggests a more dioritic composition for both. Compared to DS-1 and HBS-2 they are located closer to the Uitkomst Complex and stratigraphically intruded into the lower Timeball Hill Formation, whereas DS-1 and HBS-2 intruded into the upper Timeball Hill Formation. Based on similarities like alteration grade and texture as well as field observations these four sills are combined in one subgroup.

5.3 Gabbronorite

5.3.1 Characteristics

The gabbronorite group consists of seven sills, which were all mapped within the study area. These include the **Hofmeyr Sill 1 (HMS-1)**, **Houtboschloop Sill 1 (HBS-1)**, **Houtboschloop Sill 3 (HBS-3)**, **Weltevreden Sill 1 (WS-1)**, **Uitkomst Sill 3 (US-3)** and **Uitkomst Sill 4 (US-4)**.

The main distribution of the gabbronorite group is mainly restricted to the northwestern part of the study area with a cord-like extension in northeast to southwest direction (see geological map, appendix). The stratigraphic distribution is limited to the Transvaal Sequence ranging from the Malmani Dolomite to the Timeball Hill Shale. Six of the seven mapped gabbronorite sills are strictly located within the Upper Timeball Hill Shale and closely associated with the Klapperkop Quartzite Member, which divides the Upper and Lower Timeball Hill Shale. Only the Uitkomst Sill 3 is situated on a lower stratigraphic position and intruded into the Malmani Dolomites, the Rooihogte Quartzite as well as into the Lower Timeball Hill Shale

Basic outcrop features

Characteristic for the larger gabbronorite sills (HMS-1, HBS-1 and WS-1) is a wide-spread central sill body, which is overlying the country rocks and dominant in the field as big boulders (fig. 5.10.a,d). The sill body changes into small offshoots, which are located in between the layers of shaly or quartzitic country rocks. A direct contact of the sill body with the country rocks was not observable, but the gradual change of mafic rock boulders into country rock boulders marks the border of the larger sills. The smaller gabbronorite sills (HBS-3, US-3 and SHS-1) are similar in outcrop to the microgabbro sills. They appear as resistant rock boulders of various sizes within weathered red brown soil. Direct contacts, if observable, with country rocks show mostly a lateral layering of the sills. The Uitkomst Sill 4 forms ring shaped outcrops, whereas the central part of the sill is obviously covered by shaly country rocks.

Basic macroscopic features

Compared to the microgabbro sill group, the gabbronoritic sills are more heterogeneous in their mineralogical composition and texture despite the narrow stratigraphical range of their occurrence. The gabbronorites have an average medium to coarse grain size. The inequigranular hand specimens (fig. 5.10.c) show a dark grey to grey black coloration, sometimes associated with a light green to white weathering crust. Strongly altered specimens have a dark green color cast. Magnetism of hand samples or reaction with hydrochloric acid is rare to absent. The main mineral phases are feldspar, pyroxene, amphibole and minor quartz.

In a few hand specimens the black pyroxene component forms extremely long laths, sometimes with a greenish color cast suggesting uralitisation to amphibole (fig. 5.10.b). The long pyroxene needles are surrounded by granular masses as well as small prismatic crystals of feldspar. This quenched texture, which is mostly observable within the weathering zone of big gabbronorite boulders, is a cooling effect of hot mafic magma in contact with the colder country rocks.

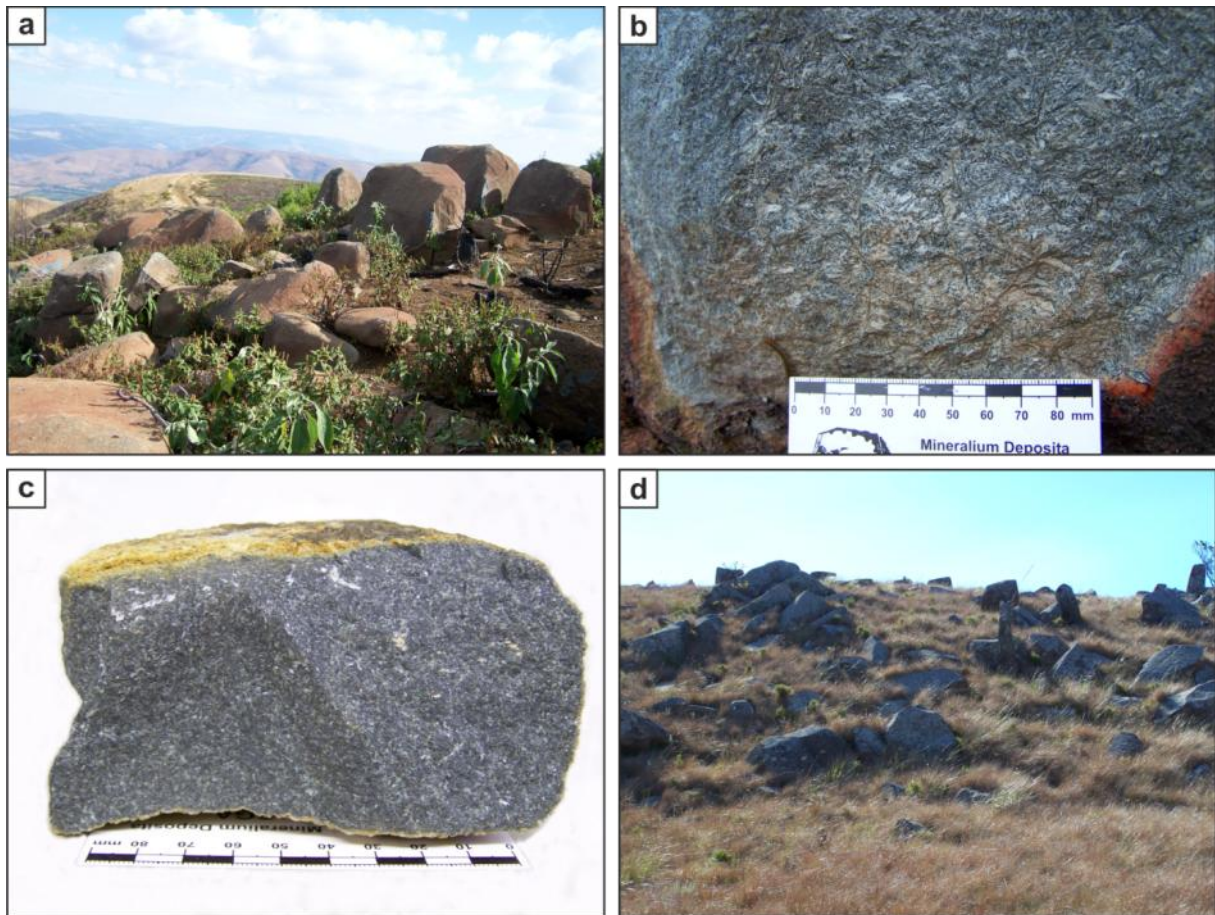


Figure. 5.10: The widespread gabbronorite sills are often located on top of hills or mountains, free of any country rock cover (pic.a: HMS-1; pic.d: US-4). Weathering leaves only resistant boulders, partly as huge erratic blocks. Picture c shows a typical inepigranular gabbronorite sample (from HBS-3) of dark grey color and medium grain size. In a few hand specimens a quenched texture consisting of long laths of pyroxene is observable, which is quite prominent in the weathered zone of big boulders due to color differences (pic.b: WS-1).

Basic microscopic features

The primary mineral components at microscopic scale are plagioclase, clino- and orthopyroxene, amphibole and more or less quartz. Euhedral to subhedral plagioclase crystals occur often as very long laths (up to 8 mm), but also as small prismatic crystals. The long plagioclase laths are sometimes arranged as spherulites or variolites (fig. 5.11.a) and the space between the single crystals is filled with pyroxenes, amphibole or various other alteration minerals. In nearly every sill plagioclase crystals also form a fine interstitial phase, sometimes variolitic or spherulitic (fig. 5.11.d).

The average content of anorthite (An₇₅₋₈₅) is higher than in the microgabbro sills (see chapter 5.2.1, p.55). Most of the plagioclase is strongly affected by sericitisation and saussuritisation, whereas the long plagioclase laths appear relatively fresh. A subophitic to ophitic texture is rather inconspicuous in the gabbronorite sills. The content of quartz is higher than in the microgabbros, but lower than in the quartz-bearing basement dykes. Anhedral quartz crystals appear as single grains or as interstitial patches with typical undulose extinction.

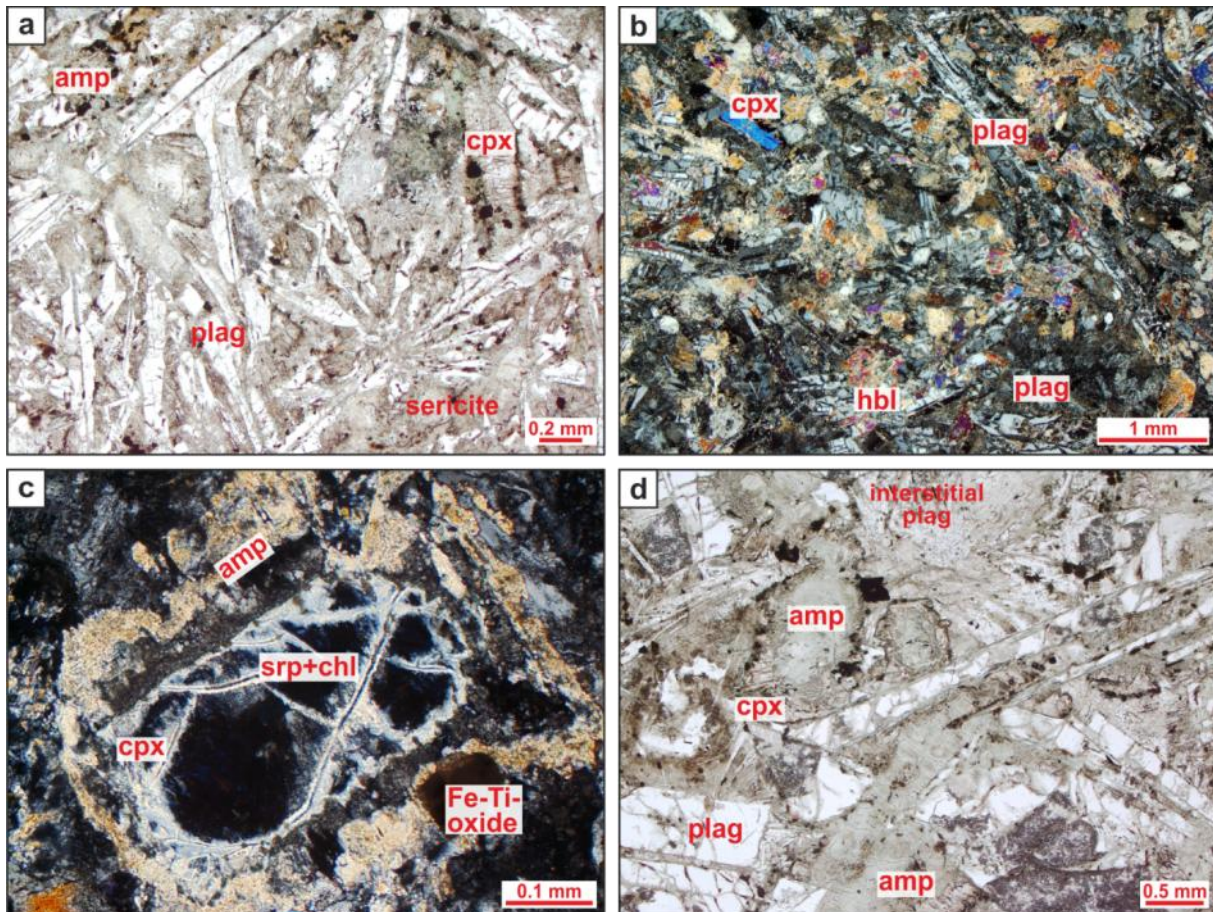


Figure 5.11: Picture a (under PP view, US-3) shows long plagioclase laths arranged as spherulites. The interstitial space is filled with prismatic crystals of clinopyroxene as well as secondary amphibole or other alteration minerals. The spherulitic arrangement of plagioclase occurs also as interstitial phase (pic.d under PP view, HMS-1). A weakly developed subophitic texture of plagioclase laths enclosed in amphibole is also observable in d. Some of the sills are described as hornblende bearing like the Weltevreden Sill 1. In picture b clinopyroxene as well as hornblende appear as small crystals between the elongated plagioclase crystals (under XP view, WS-1). The gabbronorite sills in the northern part of the study area are dominated by a higher content of orthopyroxene, which is often strongly altered to a mixture of serpentine and chlorite as well as surrounded by a rim of secondary amphibole (pic.c under XP view, HBS-1)

The dominant mafic minerals are clino- and orthopyroxene in various proportions. The subhedral to anhedral pyroxenes occur as stubby prismatic to long lath shaped crystals (up to 13 mm) similar to the identified plagioclase. Small pyroxene crystals form also as intergranular filling between plagioclase laths.

Generally a change in amount of orthopyroxene to clinopyroxene is observable within the study area from northeast to southwest direction. Elongated orthopyroxene crystals are rather dominant in HBS-1 and HBS-3, which are identifiable by the alteration to chlorite and serpentine within the crystal centre (fig. 5.11.c). Clinopyroxene is predominantly in WS-1 and HMS-1 as lath-shaped crystals, which show centric alteration to amphibole (uralitisation) and chlorite. Secondary amphibole occurs basically as pale green fibrous actinolite and brown to green hornblende. Both amphiboles form subhedral single crystals in an assemblage with other alteration minerals as well as anhedral aggregates on the margins or in the centre of pyroxene crystals. In a few sills brown hornblende appears as a primary mineral phase, which identifies these gabbronorites as hornblende bearing rocks (fig. 5.11.b). Apart from secondary amphibole, other alteration minerals identified include sericite, chlorite, calcite, talc, clay minerals, minor biotite and serpentine. Epidote and zoisite are nearly absent. Compared to the microgabbro sills, the gabbronorites do not show the diversity of alteration minerals.

Another characteristic for the gabbronorite sills is the relative low amount of Fe-Ti-oxides, which show mainly four-sided to multilateral shapes of magnetite or tiny inclusions of magnetite in intergrowth with amphibole. Exsolution lamellae of ilmenite in magnetite are rare and skeletal to hackly shapes are totally absent.

5.3.2 Hofmeyr Sill 1

The Hofmeyr Sill 1 (HMS-1) occurs in the middle of the southwestern part of the study area. The stratigraphical distribution is restricted to the Upper Timeball Hill Shale and the Klapperkop Quartzite Member. The Hofmeyr Sill 1 is the largest of the mapped sills and extends over the three farms, Hofmeyr, Weltevreden and Doornhoek (see geological map, appendix). The central body (fig. 5.12) of the sill is located on the farm Hofmeyr, whereas the very long offshoot extends up to the farm Doornhoek.



Figure 5.12: The landscape picture above shows the central body of the HMS-1 (view in SSE direction). The yellow dashed line marks the contact with the Timeball Hill Shale. Notice the different Klapperkop Quartzite layers below the Timeball Hill Shale.

Macroscopic description

The predominantly coarse grained hand specimens of HMS-1 have a grey black coloration with a dark green color cast (fig. 5.13.d). Some samples are of medium grain size (e.g. HM_16-6_6/1 or HM_15-6_1/1). Macroscopically, the main mineral phases are feldspar, quartz, pyroxene and amphibole. The quartz component is observable in every sample as single colorless grains with typical chonchoidal fractures. Transparent grey feldspar crystals form elongated individuals up to 2 mm (e.g. W_12-6_4/1). Feldspar appears also as white to grey granular masses without any cleavage plains, which is an indication for alteration processes (saussuritisation). In samples amphibole is the dominant mafic mineral phase. It occurs as small prismatic or elongated black crystals with a varnish-like brilliance as well as light green fibrous laths up to 1.2 cm (W_12-6_4/1). The pyroxene component forms matt-glossy black stubby crystals or grey black granular masses. The hand specimens of HMS-1 indicate a difference in the mineralogical composition. In samples from the central sill body the content of feldspar is distinctively higher than in samples from the offshoot at the southwestern end of the sill.

An opposite trend applies to the mafic mineral phases. The highest content of amphibole and pyroxene was observed in samples from the end of the HMS-1 on the farm Doornhoek. Furthermore some

samples of the tentacular offshoot are magnetic (e.g. HM_15-6_10/1, EN_16-6_10/1) and therefore contain magnetite as additional mafic mineral, which probably supported the differentiation trend.

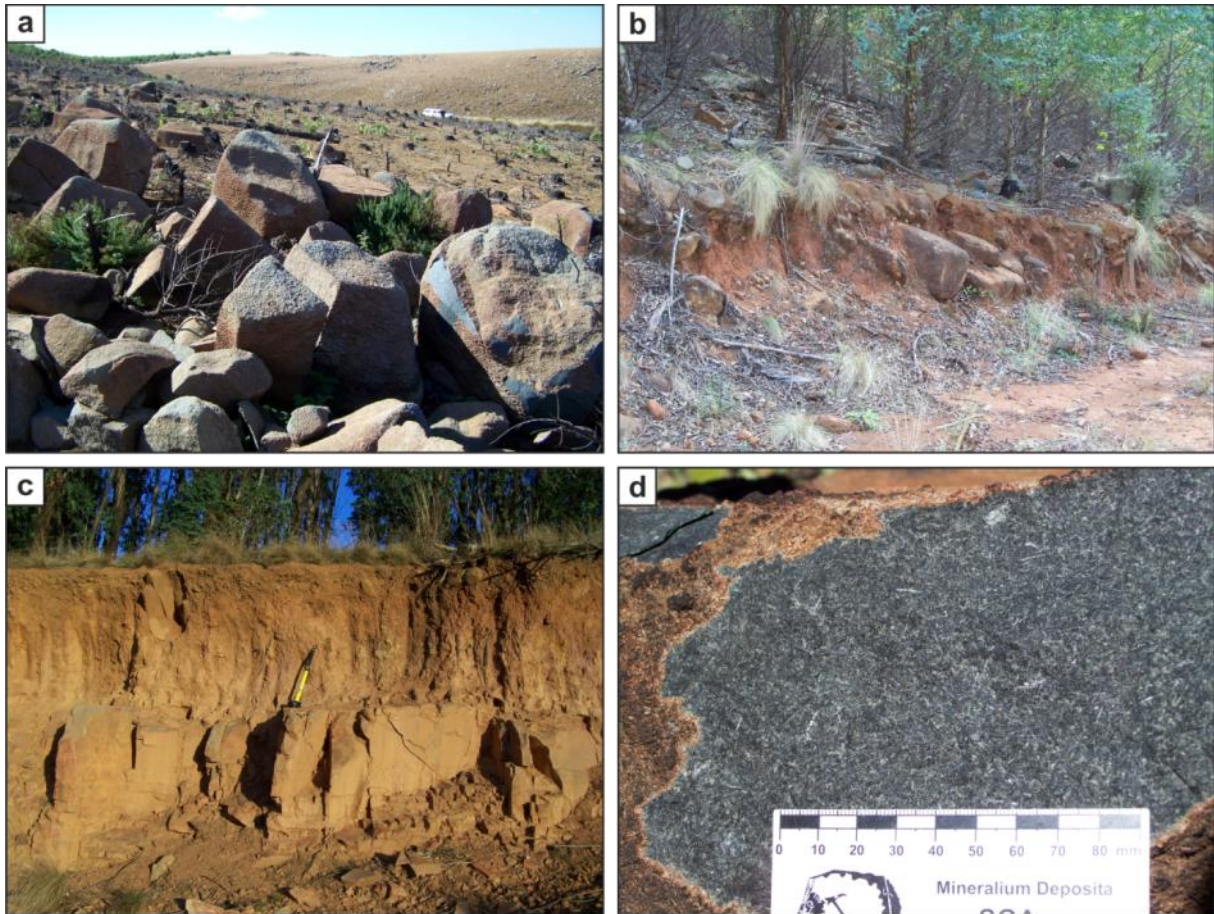


Figure 5.13: A particular order of outcrop conditions is demonstrated in picture a till c: Large gabbro-norite boulders from the central part of the sill, followed by an outcrop from the sill offshoot and at last (pic.c) a heavy weathered sill outcrop over shale at the end of HMS-1 on the farm Doornhoek. The hand specimen (pic.d) has a dark grey color interspersed by transparent feldspar laths, which reflected the sunlight. The weathering crust of the sample were not cut off with the hammer, but blasted by the heat of forest fires.

Microscopic description

On a microscopic scale, the main mineral phases are plagioclase (25-35 %), quartz (3-6 %), orthopyroxene (8-12 %), clinopyroxene (15-18 %) and amphibole (20-25 %). There are microscopical differences between the rocks from the centre of the sill and the edge of HMS-1.

One of these differences is the grain size varying from coarse grained within the sill body to medium grained at the end of the sill, which can be explained by the faster cooling in areas of minor thickness.

Within the centre of the sill body euhedral to subhedral plagioclase laths (up to 4 mm) are the dominant components together with small interstitial plagioclase crystals, which show well developed variolitic or spherulitic textures (fig. 5.14.a,b). The crystals of the lath-shaped plagioclase are often penetrated by fractures, along which the plagioclase is altered to sericite. Otherwise the euhedral plagioclase crystals

appear relatively fresh and show distinct polysynthetic twinning. Subophitic to ophitic textures are weakly developed. Within the offshoots of the sill the plagioclase component forms also small single prismatic to lath-shaped crystals (up to 1.8 mm), but occurs predominantly as interstitial mixture of plagioclase together with quartz and alteration minerals. Anhedral quartz occurs in both types as anhedral single grains as well as interstitial patches with undulatory extinction.

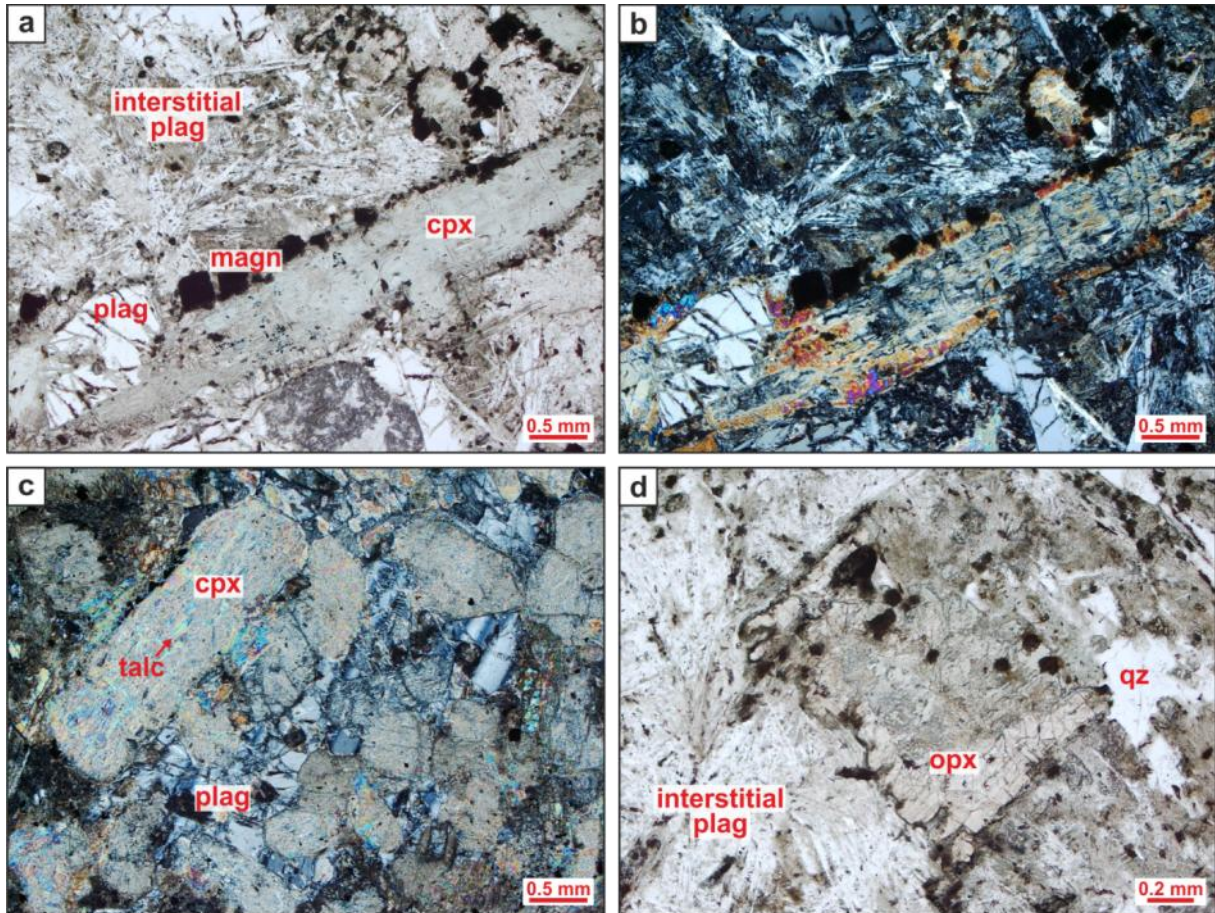


Figure 5.14: Picture a (PP view) and picture b (XP view) from the sill body (HM_15-6_6/1) show a lath-shaped clinopyroxene crystal, which is highly altered to amphibole, clay minerals and chlorite within the crystal centre. Cubes of magnetite are accumulated at the cpx margins. Plagioclase occurs as variolitic interstitial filling, but also as relative fresh anhedral crystals penetrated by fractures. A subhedral altered orthopyroxene crystal (pic.d, sample HM_15-6_6/1) is also surrounded by interstitial plagioclase as well as quartz. Picture c is from the offshoot of HMS-1 (sample EN_16-6_12/1). It shows elongated to stubby prismatic clinopyroxene crystals, which are altered to talc and amphibole, subophitic enclosed in an anhedral plagioclase crystal.

Compared to the northernmost gabbro-norite Houtboschloop Sill 1, clinopyroxene is the dominant pyroxene in the Hofmeyr Sill 1. Pale brown euhedral clinopyroxene appears as short prismatic to long lath-shaped, long columnar crystals, which reach up to 13 mm in length (HM_15-6_6/1) within the sill centre and a maximum of 2.2 mm at the edge of HMS-1 (EN_16-6_12/1). The inclined extinction angle suggested augite or diopside. A special feature is subophitic enclosed clinopyroxene in larger plagioclase crystals (fig. 5.14.c). Subhedral colorless to pale brown orthopyroxene forms mostly stubby prismatic to tabular crystals, recognizable by the parallel extinction and low order interference colors. Also fine exsolution lamellae of orthopyroxene in clinopyroxene crystals can be observed in some cases. However, the clinopyroxene as well as the orthopyroxene crystals are strongly affected by alteration (uralitisation) throughout the whole sill. The clinopyroxene laths show centric alteration to amphibole, chlorite and clay minerals, so that partly clinopyroxene forms a rim around these alteration minerals (fig. 5.14.a,b). Orthopyroxenes show mostly a marginal alteration to amphibole and clay minerals, sometimes only fragments of the primary crystal remained. Secondary amphibole is the major alteration mineral with contents up to 25 %. It occurs as subhedral to anhedral pale green actinolite with a fibrous habit, intergrown with chlorite and magnetite grains. Sometimes brown subhedral hornblende crystals are observable (e.g. HM_15-6_6/1), which could be of primary origin. The amphibole forms pseudomorphs after clinopyroxene, which explains the similar grain size and habit. Other than amphibole and chlorite, alteration minerals noticeable include sericite, calcite, talc and clay minerals. Isotropic magnetite with rare exsolution lamellae of ilmenite is the only evidence for Fe-Ti-oxides. The dark grey magnetite crystals have a four-sided shape and are paragenetically related to amphibole and chlorite.

5.3.3 Houtboschloop Sill 1

The HBS-1 is the northernmost sill of the study area and stratigraphically located in the Upper Timeball Hill Shale. Like other gabbronoritic sills, the HBS-1 consists of a wide central sill body with decreasing offshoots in between the shales. This gabbronoritic sill is close to a microgabbro sill (HBS-2), but HBS-2 is located at a deeper stratigraphic level as compared to HBS-1.

Macroscopic description

The hand specimens are dark grey to dark green colored with light green to white weathering crusts. The grain size varies between fine (e.g. HB_8-7_17/1) to coarse (e.g. HB_6-7_5/2) grained, but is medium in average. Feldspar, pyroxene and amphibole can be identified as main components in the coarser specimens. Feldspar is macroscopically the most frequently mineral phase, which occurs in form of small laths up to 0.5 mm as well as granular bodies. In places the feldspar crystals show greenish white discoloration, which indicates a saussuritic alteration. Amphibole forms long dark green laths with a varnish-like brilliance (e.g. HB_6-7_5/2), whereas the pyroxenes appear as matt black small crystals or granular masses. In sawn hand specimens an ophitic texture is observable with small white feldspar laths enclosed in a mafic mineral component. Accessory epidote occurs as pistachio green coating in some samples (e.g. HB_6-7_8/1).



Figure 5.15: The outcrop on the left shows a strong weathered gabbronorite outcrop with typical round boulders in a creamy red brown soil. Notice the big boulder right from the hammer, which is strongly fractured, such that it seems to be block-like weathering. The typical dark grey color could be observed in the medium grained hand specimen (HB_6-7_5/1) on the right.

Microscopic description

A detailed petrographic description of sample HB_8-7_4/1 is listed as petrographic data sheet in the appendix p.159.

Main constituents of the sill are plagioclase (20-30 %), quartz (5-8 %), orthopyroxene (15-20 %), clinopyroxene (5-8 %) and amphibole (8-10 %). The lath-shaped plagioclase is strongly altered to chlorite, epidote as well as sericite and only the plagioclase contour is visible. In interstices plagioclase forms small variolitic to spherulitic bodies and appears together with quartz, sericite and other alteration minerals. In thin section of HB_8-7_1/1 well-developed spherulites of small plagioclase laths are observable. Microscopically, the subophitic to ophitic texture of the rocks is verified by euhedral plagioclase enclosed by anhedral clinopyroxene (fig. 5.16). The quartz component seems to be relatively high (up to 8 % in HB_8-7_4/1). Quartz crystals occur as single anhedral grains or are arranged in rapidly crystallised patches with typical undulose extinction. It is also mixed as very small grains with mini plagioclase laths and alteration minerals.

Typical for the HBS-1 is the relative high amount of orthopyroxene compared to other sills. Euhedral to anhedral orthopyroxene forms short prismatic to long lath-shaped crystals, which show typical properties of orthopyroxene like parallel extinction, low order of interference colors or colorless to pale green brown coloration. The centre of the orthopyroxene crystals (fig. 5.16) is strongly altered to serpentine, chlorite and carbonate in form of small calcite crystals. The pseudomorphic replacement by serpentine within the centre and along fractures is named as bastite. Some orthopyroxenes have a rim of amphibole, which surrounded the whole pyroxene crystal as a corona texture. This could be an indication for unstable conditions for the orthopyroxene component, such that the crystals begin to react with its surrounding crystals. Compared to other sills the amount of clinopyroxene is relative low in this sill. The subhedral to anhedral prismatic clinopyroxene crystals are strongly altered to amphibole, especially at the margins. Generally, the HBS-1 is characterized by a relative strong grade of alteration. Almost every primary mineral except quartz is affected by alteration processes. Secondary amphibole appears as pleochroic green rim on pyroxenes as well as small pale green needles. The former is hornblende, which shows often pseudomorphs after clinopyroxene. Sometimes the rims surrounding orthopyroxenes are strongly developed, so that it is difficult to define the primary orthopyroxene. The latter small columnar amphiboles, which are actinolite crystals, are located interstitial in a mixture with other alteration minerals. The alteration of plagioclase has produce most of the secondary minerals. Sericite and saussurite occur as micro- to cryptocrystalline aggregates at the expense of plagioclase. Saussurite describes a not differentiable mixture of epidote, chlorite, calcite, actinolite and sericite that is formed due to dissolution of the anorthite component.

Chlorite is also an alteration product of orthopyroxene together with pale yellow serpentine. The anomalous blue interference colors of chlorite indicate a high Fe content.

Accessory Fe-Ti-oxides appear as unshaped or three to four-sided bodies, which surround pyroxenes or amphiboles. This includes mainly magnetite with exsolution lamellae of ilmenite and leucoxene (fig. 5.16.d), an alteration product of Ti-containing minerals like ilmenite, rutile and titanomagnetite.

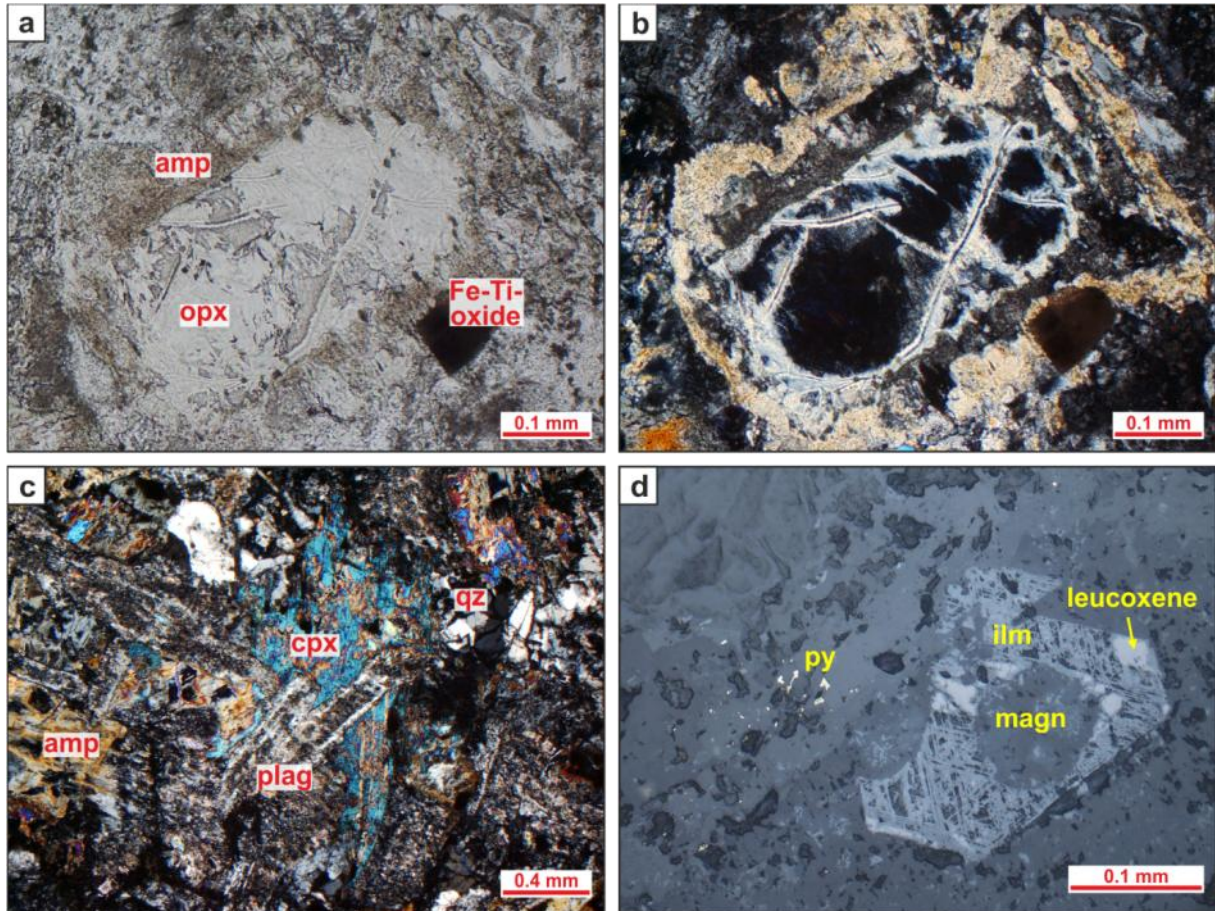


Figure 5.16: A highly altered orthopyroxene is surrounded by a rim of green to light brown amphibole (pic.a, PP view & pic.b, XP view). The centre of this orthopyroxene is completely replaced by chlorite and serpentine, which form a pseudomorphose after opx (bastite). Picture c (XP view) shows sericitic plagioclase laths subophitic enclosed in clinopyroxene. A nice example of multilateral Fe-Ti-oxides is given in the last picture (d). A network of ilmenite (light grey) is segregated from a magnetite crystal, which is only preserved as round aggregate within the centre. Further progressive alteration transforms the ilmenite lamellae into white leucoxene. All pictures were taken from sample HB_8-7_4/1.

5.3.4 Houtboschloop Sill 3

The HBS-3 is a small sill located on the southeastern border of the farm Houtboschloop with a small extension to the adjacent farm Uitzicht. The surrounding country rocks comprise of shales and quartzites of the Timeball Hill Formation. In outcrop this gabbronorite sill appears as small to huge boulders surrounded by typical red brown weathering soil and by scree, which is a mixture of various sized rock fragments of mainly country rocks and remaining soil from the weathered mafic igneous rocks.

Macroscopic description

The dark grey colored hand specimens of HBS-3 vary in grain size between medium (e.g. HB_1-7_3/1) and coarse (e.g. HB_1-7_7/1) grained. The main minerals, which can be distinguished in macroscopic scale, are feldspar, pyroxenes and amphibole. Feldspar forms elongated laths up to 0.5 cm as well as unshaped bodies of white to green discoloration due to saussuritic alteration. In hand specimens the content of amphibole seems to be higher than the pyroxene content. Sample HB_1-7_5/1 shows long greenish amphibole laths (up to 1.3 cm), but the microscopic description presents primary pyroxene, which is altered to amphibole along the margins. The pyroxenes form small black crystals as well as granular masses. Especially the hand specimens (e.g. HB_1-7_5/1, HB_1-7_6/1 & HB_1-7_7/1) from outcrops, which are surrounded by quartzite instead of the shaly country rock, offer black matt clusters (average length of 1 cm) of pyroxenes.



Figure 5.17: The outcrop on the left consists of big boulders of gabbronorite, which is intruded into the Klapperkop Quartzite (sample HB_1-7_5/1 is taken from here). The medium grained hand specimen (HB_1-7_3/1) on the right shows the typical grey color and contains mainly feldspar, pyroxene and amphibole.

Microscopic description

A detailed petrographic description of sample HB_1-7_6/1 is listed as petrographic data sheet in the appendix p. 160.

The medium to coarse grained gabbronorite sill is mainly composed of plagioclase (35 %), orthopyroxene (10 %), clinopyroxene (15 %) and amphibole (15 %). Plagioclase occurs as euhedral and subhedral, lath shaped (up to 5.2 mm), poorly twinned crystals and as an interstitial phase. The elongate crystals could be arranged as spherulites, the space between the individual plagioclase crystals is occupied by pyroxene, other plagioclase laths or alteration minerals. Some plagioclase individuals are subophitic enclosed by altered pyroxene crystals. The alteration of plagioclase is restricted to the centre (fig. 5.18) of the elongated crystals, but the interstitial phase is composed of a mixture of alteration minerals as sericite, calcite, zoisite, epidote, clay minerals and chlorite.

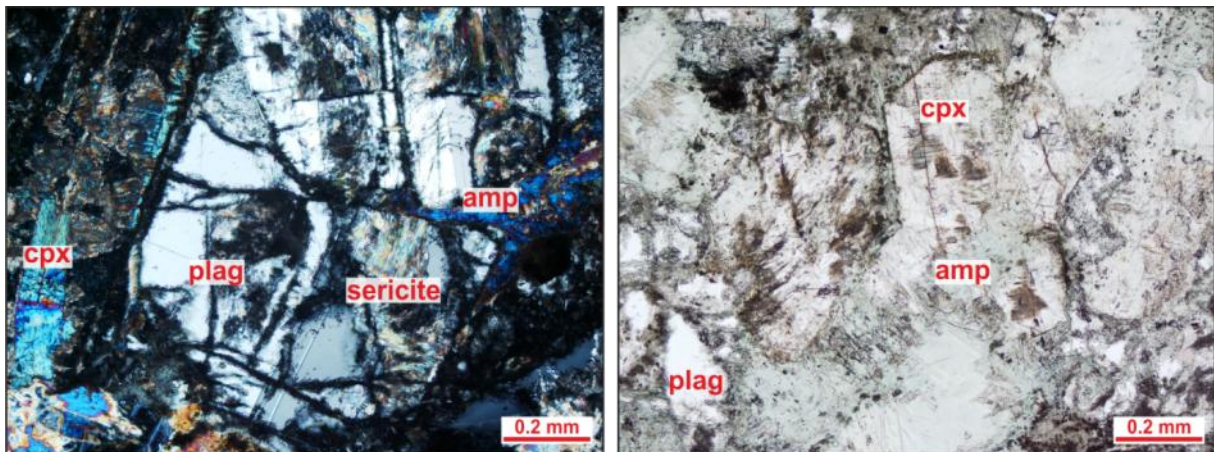


Figure 5.18: Both pictures are from sample HB_1-7_6/1, but do not show the same detail. On the left a part from a lath shaped plagioclase crystal is presented, which is altered to sericite along the fractures and within the crystal centre. The euhedral plagioclase is surrounded by clinopyroxene (light blue) and amphibole (blue), which seems to be concentrated along a big fracture within the plagioclase crystal. On the right a subhedral pale brown clinopyroxene, notice the adumbrated octagonal shape, is penetrated by green amphibole and clay minerals. Anhedral aggregates of plagioclase are also visible.

The proportion of orthopyroxenes is approximately similar to the slightly dominant clinopyroxene. Both are altered to amphibole, especially at the grain margins. Frequently the pyroxenes occupy the space between the plagioclase laths, termed as intergranular texture. Sometimes the interstitial pyroxenes are so intensively developed that it is macroscopically visible in form of black matt clusters (e.g. HB_1-7_5/1 and HB_1-7_6/1). The light brown clinopyroxene crystals form subhedral short prismatic grains (fig. 5.18). Basal sections show perpendicular cleavage planes. Inclined extinction angles at 38° signify diopside as the common clinopyroxene. The subhedral and anhedral orthopyroxene crystals appear as prismatic crystals or elongated laths (up to 2 mm). Along the margins and fractures, which resulted from deformation and alteration, the orthopyroxenes are replaced by amphibole. The centre is replaced by serpentine in form of the pseudomorph bastite.

Mostly only relicts of orthopyroxene are recognizable. The subhedral to anhedral amphibole crystals are results from the intensive uralitisation of the pyroxenes. The intensive green colored amphiboles have inclined extinction angles between 10° and 20°, so it could be actinolite and hornblende. They are arranged along the pyroxene margins or appear pseudomorphic after them.

Accessory Fe-Ti-oxides appear as very small hackly-shaped or three to four sided bodies, mainly at the amphibole or pyroxene margins. Primarily it is magnetite with exsolution lamellae of ilmenite. Insignificant low content of sulphides occur in form of small pale yellow pyrite grains, which are finely disseminated through the sample.

In general this sill is petrographically similar to sill Houtboschloop 1 and the two are macroscopically identical, too. Minimal differences are observable in contents of minerals.

5.3.5 Uitkomst Sill 4

This sill is a relative small gabbronorite sill similar to HBS-3. The basic part of the sill intrudes into the Upper Timeball Hill Shale, while the southeastern end is surrounded by quartzite of the Klapperkop Quartzite Member. A specific feature of US-4 is its circular shape, probably caused by the also circular formation of the Klapperkop Quartzite at this location. A main part of the sill is still covered by shale, so that the central body of the sill is still covered by shale (fig. 5.19).

Macroscopic description

The hand specimens show the typical characteristics for the gabbronoritic group. All samples are coarse grained with distinctively dark grey color. When the rocks are strongly altered, they have a greenish color cast. Feldspar as main component forms small elongated crystals with a very well developed cleavage, but also light grey granular masses as a result of saussuritic alteration. Macroscopically, quartz is not identifiable. In hand specimens dark grey amphibole occurs as fibrous lath shaped crystals. Later microscopic investigations identify them as pyroxene crystals, which are highly altered to amphibole. At macroscopic scale the pyroxene component appears as dark grey granular masses. In some samples small patches of pistachio green epidote are observable.

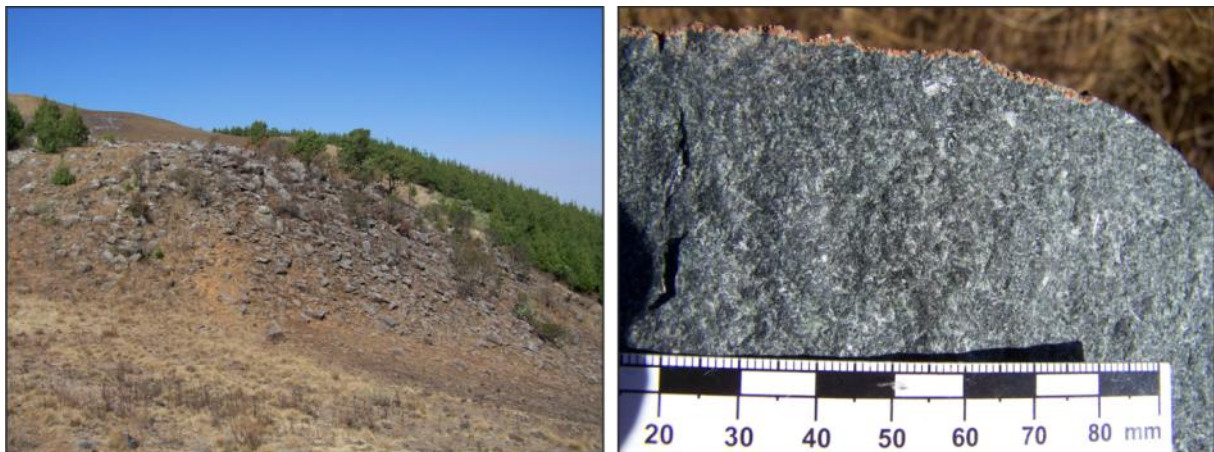


Figure 5.19: The picture (view in SE direction) on the left shows big boulders of gabbronoritic rocks (sample UZ_22-7_1/1) at one of the highest mountains within the study area. The outcrop belongs to the circular shaped US-4 and is overlain by shale. The sample (U_23-6_7/2) on the right contain elongated feldspar laths, which appear white in the sunlight, and amphibole & pyroxene, which form dark grey patches within the hand specimen.

Microscopic description

As described in the gabbronorite sills before, plagioclase (30-35 %), quartz (< 5 %), clinopyroxene (20 %), orthopyroxene (7 %) and amphibole (10 %) are also the main constituents. Subhedral to euhedral plagioclase laths reach up to 8 mm.

Larger prismatic plagioclase crystals appear as intercumulus phase because they are interspersed with smaller ophitic pyroxene crystals. Variolitically arranged plagioclase needles form an interstitial phase together with quartz and alteration minerals.

A special feature is the rim-like shape of the clinopyroxene, which occur as short prismatic to lath shaped crystals. Nearly the whole crystal is replaced by amphibole, chlorite or clay minerals and also the octagonal or four-sided shape is still preserved by the secondary minerals (fig. 5.20). The rim of primary clinopyroxene is more amorphous than its alteration products, but clearly definable by the inclined extinction and perpendicular cleavage. Orthopyroxene is minor in content and forms pale brown stubby prismatic crystals of small size, which are also commonly altered. Both pyroxenes appear also as anhedral intergranular crystals between plagioclase laths. Actinolite as amphibole is the dominant alteration mineral recognizable by its pale green color and fibrous to columnar habit (fig. 5.20). Other secondary components are sericite, chlorite, calcite, talc and clay minerals.

The rare opaque phase is formed by small multilateral magnetite crystals with exsolution lamellae of ilmenite as well as fine disseminated grains of pyrite and chalcopyrite.

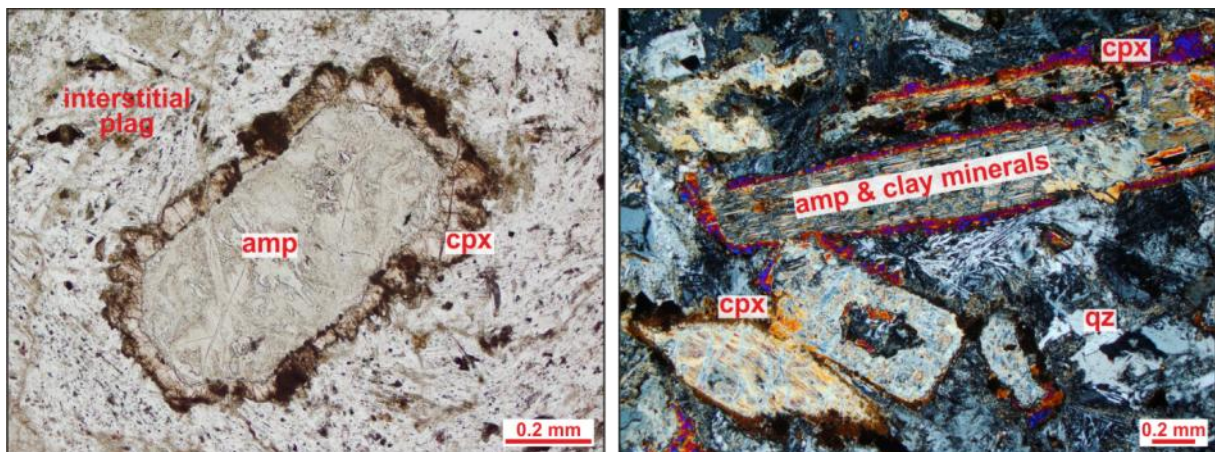


Figure 5.20: Both pictures are from sample U_23-6_7/2, but do not show the same detail. On the left under PP view, a long prismatic clinopyroxene crystal is replaced by amphibole within the centre, such that it seems to be a rim of brown clinopyroxene around an octagonal shaped grain. An accumulation of cpx crystals occur on the right picture (XP view). In spite of alteration, the cpx retain its optical properties like the middle order interference colors and the inclined extinction. In both pictures, small plagioclase crystals appear as interstitial filling.

5.3.6 Weltevreden Sill 1

This gabbronorite sill is located on the farm Weltevreden in the central to northwestern part of the study area and belongs to the more extensive mapped sills (fig. 5.21). The basic body of WS-1 intruded into the quartzites of the Klapperkop Quartzite Member, whereas the marginal offshoots occur within the Upper Timeball Hill Shale. Generally the sill has a crescent shape and extends from northwest to southeast direction. This suggests that the main sill body is still covered by the Upper Timeball Hill Shale.

Macroscopic description

The mainly medium grained hand specimens appear relatively inhomogeneous caused by different alteration grades, most visible at the feldspar component. Fresh to low altered feldspar (e.g. in W_15-7_3/1) occurs as transparent grey laths with a distinctive cleavage as well as minor granular masses with a slightly red-grey coloration as indication for initiating sericitisation. Strong altered feldspar (e.g. in W_14-7_5/1 & W_15-7_2/2) forms only dimmish white granular masses, at which the centre is greenish discolored as hint for saussuritisation. The quartz component is minor in content, but appears as single small grains with conchoidal fracture throughout the samples.



Figure 5.21: The WS-1 appears often as big blocks in field outcrops (left picture). Notice the waved surface on the right side of the gabbronorite block resulting from the weathering. After cutting the weathering crust some of the huge boulders show a coarse grained texture with long laths of probably amphibole (right picture) surrounded by white intergranular feldspar.

The mafic mineral phase is dominated by amphibole, which shows elongated black crystals with varnish-like brilliance as well as blue grey to green grey laths (up to 8 mm in W_15-7_2/2) with fibrous surface. These laths are well developed in hand specimens on areas of strong weathering (fig. 5.21). Minor pyroxene occurs as matt black stubby prismatic to elongated crystals.

Accessory minerals in hand samples are pistachio green epidote, tiny flake-like black biotite crystals and fine yellow grains of pyrite.

Microscopic description

The different alteration stages in the samples are reflected in microscopic scale. The primary mineral phases are plagioclase (20-40 %), quartz (3-5 %) clinopyroxene (10-15 %), hornblende (8-18 %). Euhedral to subhedral short prismatic and lath shaped crystals of plagioclase up to 4.2 mm are observable within the low altered specimen (W_15-7_3/1). The highly altered gabbro-norites show mostly subhedral short prismatic crystals as well as anhedral unshaped intercumulus plagioclase between the mafic minerals. Sericitisation and saussuritisation are common (fig. 5.22).

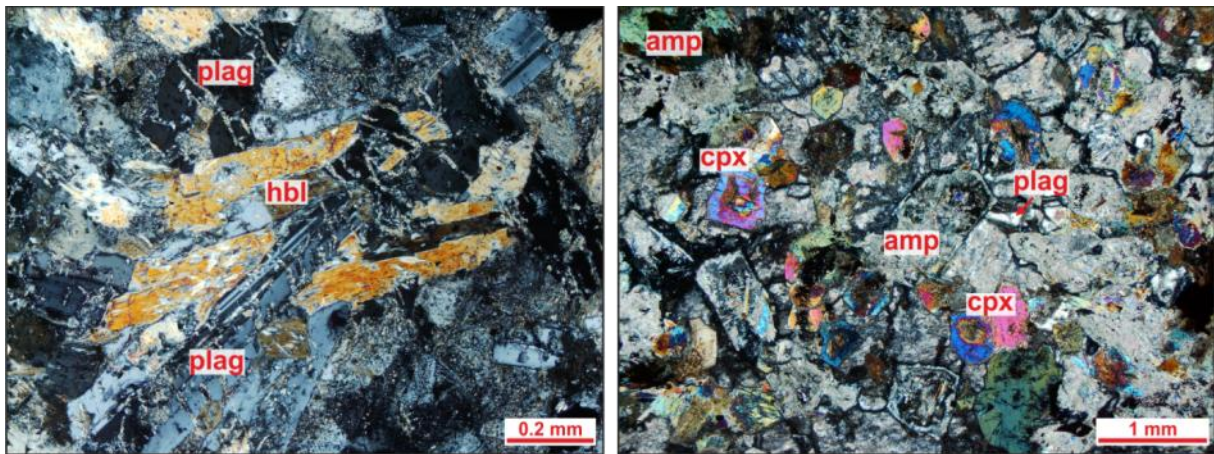


Figure 5.22: On the left a primary hornblende crystal is penetrated by a twinned plagioclase lath. Both are surrounded by other plagioclase crystals and an interstitial phase consisting of plagioclase, quartz and sericite (sample W_15-7_3/1, XP view). The right picture shows stubby prismatic clinopyroxene crystals. Some of them appear relatively fresh with pink to blue interference colors. Notice the change in color from the centre of the clinopyroxene crystal (dark violet) to the margin (light blue) that could indicate zoning within the crystal. The main part of the clinopyroxene is altered to a mixture of amphibole, chlorite and clay minerals. The amphibole component occurs as pseudomorphs after cpx. (sample W_14-7_5/1, XP view)

The amphibole component can be subdivided into primary green hornblende and secondary actinolite and hornblende. The former occurs as subhedral long prismatic to short columnar crystals with an inclined extinction of 20° to 24°. In fresh samples the hornblende reach up to 20 % in content, which identifies the WS-1 as hornblende bearing sill. Secondary hornblende forms pseudomorphoses after clinopyroxene as well as subhedral to anhedral crystals with 60° cleavage angles and hexagonal basal sections. Pale green actinolite appears as fibrous needles or as intergrowth with clinopyroxene.

The pyroxene component is restricted at clinopyroxene in WS-1. Especially in the thin sections of the strong altered samples, the clinopyroxene shows stubby prismatic crystals with centric alteration to amphibole and clay minerals.

Noticeable is a zoning of interference colors (e.g. W_14-7_5/1) from crystal centre to the margin (fig. 5.22), probably due to depletion or enrichment of certain elements (Mg, Fe). Orthopyroxene could not be clearly identified or is not present. The amount of alteration minerals next to amphibole includes sericite, chlorite, calcite and clay minerals. The occurrence of Fe-Ti-oxides is limited to multilateral

shapes of magnetite, ilmenite or hematite as well as to fine inclusions of magnetite within amphibole. Exsolution lamellae or skeletal shapes are absent.

The lack of orthopyroxene suggests a gabbroic composition instead of a gabbronorite. Together with the high content of hornblende the Weltevreden Sill 1 is a hornblende bearing gabbro according to the nomenclature of *Streckeisen*. In correlation to the stratigraphic position, field observations and compared to the other gabbronorite sills, WS-1 can be assigned to the gabbronorite group.

5.3.7 Uitkomst Sill 3

The US-3 is located on the farm Uitkomst, northeastern from the Uitkomst Complex. This sill is the only mapped gabbronorite sill occurring on a lower stratigraphically position. The US-3 intruded into the Malmani Dolomites of the Chuniespoort Group, whereas the northwestern end of the sill is surrounded by quartzites of the Rooihogte Formation (fig. 5.23). In spite of the stratigraphical as well as spatial distance to the rest of the gabbronorite sill group, similar macroscopic and microscopic features classify US-3 into a gabbronorite sill. Close to this sill the microgabbro sill US-2 is located, which intrudes into the Timeball Hill Shales on a slightly higher stratigraphic position.

Macroscopic description

The grey to black hand specimen show a variable grain size ranging from fine (e.g. U_23-6_8/1) to coarse (e.g. U_22-6_7/1) grained. Major mineral phases at macroscopic scale are feldspar, pyroxene and amphibole. The former show well developed light grey transparent elongated crystals up to 5 mm (e.g. U_22-6_9/1) as well as granular masses with signs of sericitisation. The elongated feldspar crystals are embedded in granular masses of dark grey pyroxene. The pyroxene component forms matt black stubby crystals. Relative fresh samples (e.g. U_22-6_6/2) suggest a high amount of pyroxene, whereas altered specimens have more amphibole in composition. The fibrous habit of the dark green elongated amphibole crystals indicates a secondary formation. A special feature is the unique occurrence of a sulphidic aggregate (fig. 5.23) within the sample U_24-6_2/1. The 5 mm large round aggregate consists of clearly distinguishable core and marginal zone. The core is composed of greenish yellow chalcopryrite surrounded by bronzy yellow pyrrhotite, which is distinctively magnetic.

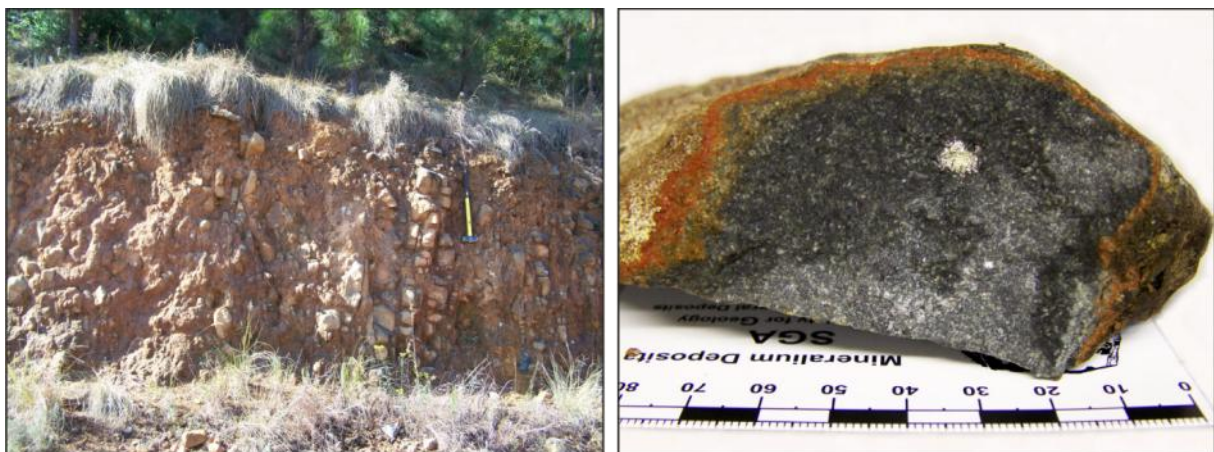


Figure 5.23: The left picture shows an outcrop from US-3. The left side is strongly weathered soil, whereas some in situ boulders of gabbronorite remain on the right (close to the hammer). Hand specimen (U_24-6_2/1) on the right picture shows the unique sulphidic aggregate, which consists of chalcopryrite in the centre with a rim of magnetic pyrrhotite.

Microscopic description

Petrographic data sheets from the samples U_22-6_7/1 and U_24-6_2/1 are given in the appendix p. 161-162. Microscopically, the main mineral phases are plagioclase (25-40 %), quartz (3-5 %), orthopyroxene (8-10 %), clinopyroxene (18-25 %) and amphibole (15-18 %). Characteristic for US-3 is the spherulitic to variolitic texture of arranged plagioclase laths (up to 4 mm) occurring in fresh and low altered samples. The interstitial space as well as the centres of the spherulites are filled with smaller plagioclase individuals, quartz grains, pyroxene, amphibole or alteration minerals. These textures are rare to absent in strongly altered specimen of US-3, where the plagioclase component forms only an interstitial phase together with other minerals. Furthermore, small plagioclase crystals are partly optically enclosed in larger pyroxene individuals (fig. 5.24). The clinopyroxene and minor orthopyroxene components appear as long to stubby prismatic crystals, which are more or less replaced by amphibole. Exsolution lamellae of orthopyroxene in clinopyroxene are unusually common.

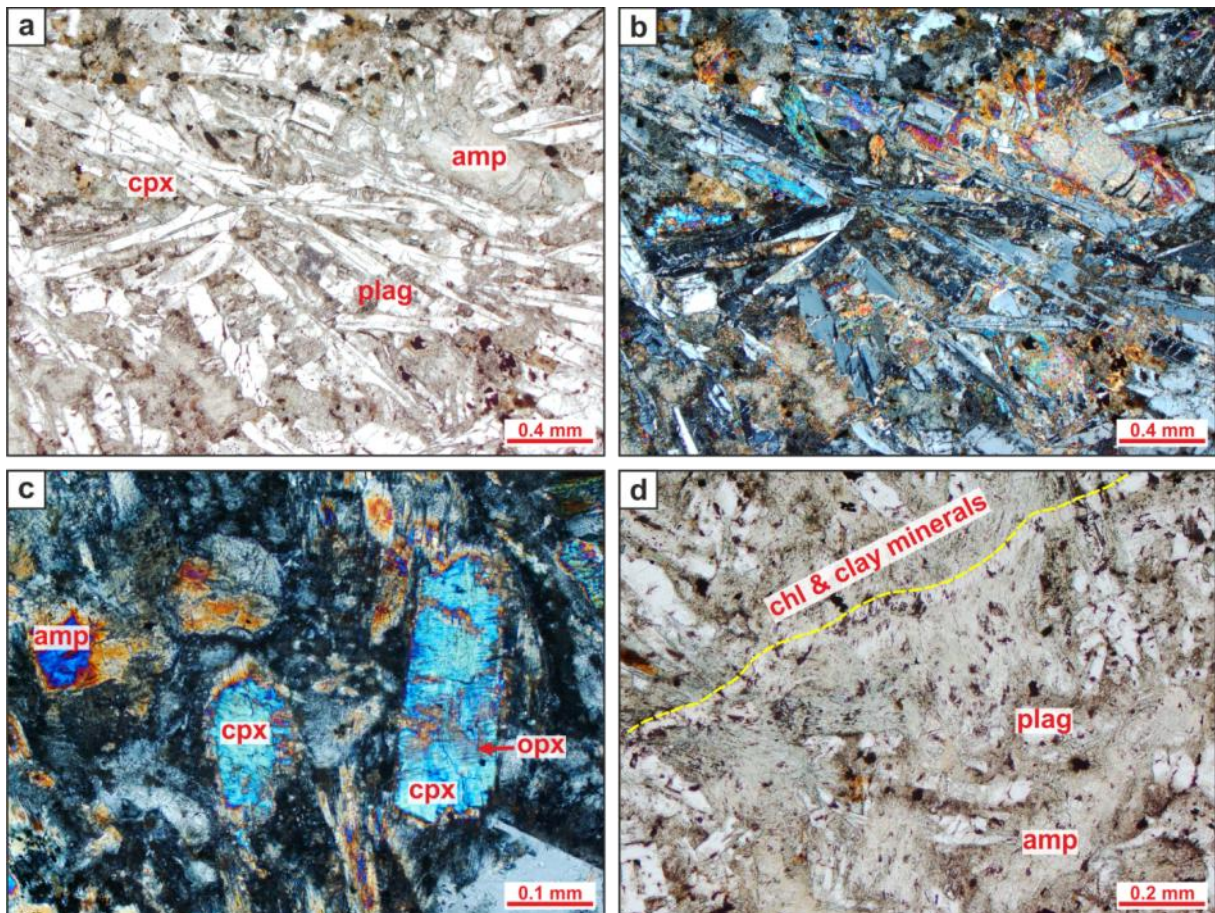


Figure 5.24: Both pictures above (U_22-6_7/1; pic.a: PP view, pic.b: XP view) show spherulitic arranged plagioclase laths. The interstitial space is filled with pyroxene, amphibole and further alteration minerals. Fine exsolution lamellae of orthopyroxene are observable in subhedral to anhedral clinopyroxene (U_24-6_2/1, pic.c: XP view). In picture 4 (U_22-6_7/1; XP view) a small fracture goes through the whole thin section. The fracture (see yellow dashed line) is infilled with clay minerals and chlorite. Primary minerals are more altered along this fracture as compared to other parts of the section.

Next to secondary amphibole (actinolite and hornblende) a series of further alteration minerals including chlorite, sericite, epidote and clay minerals are observable. Their amount is depending on the grade of alteration.

The microscopic investigation of US-3 shows no further indications for the occurrence of sulphides, which are observed in hand specimen. The content of sulphides or Fe-Ti-oxides is insignificant.

5.4 Basement dykes

5.4.1 Characteristics

The spatial distribution of basement dykes within the study area is limited to the farm Vaalkop (see geological map, appendix). As the name suggests, the dykes intruded into the Archaean basement and belong to a group of mafic dyke swarms, which cover the Archaean granite-greenstone terrain in the eastern Transvaal. Altogether 10 basement dykes were sampled, but only four of them are located within the study area (see geological map, appendix). The other six were sampled in order to expand the geochemical data basis for the basement dyke group.

Basic outcrop features

Compared to the mafic sills, the basement dykes form prominent ridges (fig. 5.25) in the plain area of the Archaean basement terrain. Within the farm Vaalkop the geomorphology increases through the Mpumalanga Drakensberg escarpment, so it becomes more and more difficult to identify them as individual dykes. Field characteristics are the higher hardness, the block-like weathering and of course the sharply pronounced contacts with the country rocks (fig. 5.26).



Figure 5.25: The upper landscape picture shows basement dykes in the front, which form prominent ridges in the otherwise plain terrain of Archaean granitic rocks outside of the study area. Samples from that dyke (BD_6-6_1/1, BD_6-6_1/2, BD_6-6_2/1 and BD_6-6_2/2) belong to the quartz-bearing gabbro-noritic variety of basement dykes.

Generally the group of basement dykes is rather heterogeneous in hand specimens as well as in thin sections. Two main subgroups can be distinguished based on their SiO_2 content. But due to their otherwise very similar mineralogical composition, no further separation will be done. So besides a gabbro-noritic variety a quartz-bearing gabbro-noritic variety (fig. 5.26) of basement dykes was identified.

Basic macroscopic features

The intrusive rocks are medium to coarse grained with a fine grained margin, which is not always exposed due to the weathering of these chill zones. The hand specimens show middle to dark grey coloration with a green color cast which is dependent on alteration grade and SiO₂ content (fig. 5.26b). Major mineral phases are feldspar, quartz, pyroxene and amphibole. Feldspar occurs as elongated crystals up to 5 mm (e.g. VK_11-6_8/1) as well as granular masses of white and green discoloration, which implies saussuritic alteration. The content of quartz varies clearly between the two named subgroups. In the gabbronoritic samples quartz is not observable at macroscopic scale, whereas the quartz-bearing gabbronoritic hand specimens show single quartz grains or interstitial patches up to 8 mm (e.g. BD_6-6_3/1). Round xenocrysts of quartz (up to 2 cm) as well as small quartz veins appear in two samples (BD_6-6_1/2 and BD_6-6_3/1). The pyroxene component forms mostly granular dark grey masses between the feldspar, but occurs also as matt black stubby prismatic crystals. In sample VK_8-6_11/1 the pyroxene is lath-shaped (up to 1.3 cm) with a distinct cleavage and marginal intergrowth with amphibole.

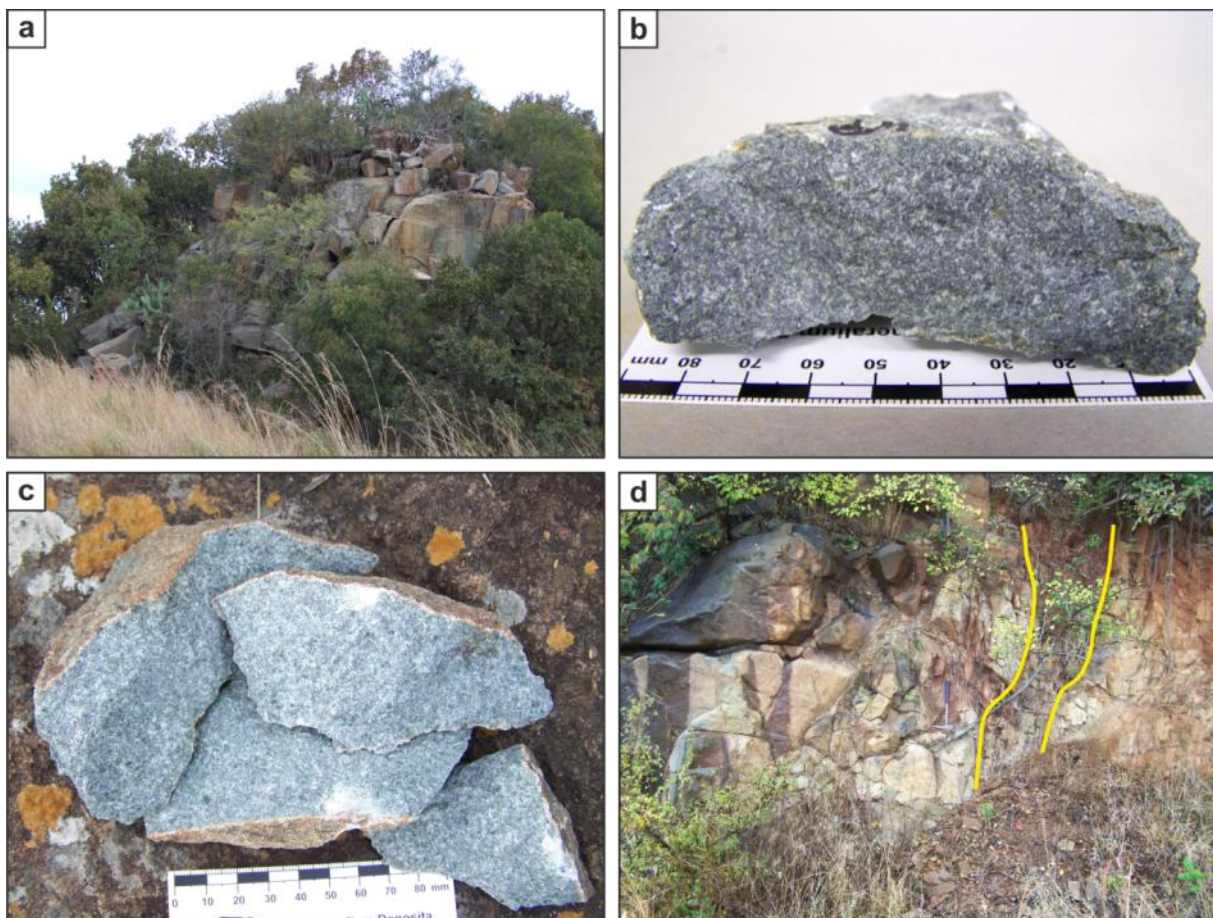


Figure 5.26: Picture a shows a cross section of a dyke within the plain gneiss-granite terrain outside the study area. On the farm Vaalkop, where the terrain increases through the Mpumalanga Drakensberg Escarpment, the dykes penetrate sharply the country rocks (pic.d, the contact zone is marked by yellow lines). The hand specimens (BD_6-6_1/1) in pic.c show the quartz-bearing variety of basement dykes, whereas the sample in pic.b belongs to the gabbronoritic variety (VK_10-6_1/2).

Dark green amphibole occurs as small elongated crystals with a fibrous character, but its content is distinctively lower than that of the pyroxene. Fine grains of light yellow pyrite appear as accessories in some medium grained samples.

Basic microscopic features

A petrographic data sheet for the sample BD_13-7_1-1 is given appendix p. 163. Microscopically, the predominantly medium grained dykes consist of plagioclase (25-35 %), clinopyroxene (15-20 %), orthopyroxene (7-14 %), amphibole (5-12 %) and more or less quartz (2-10 %). Euhedral to subhedral plagioclase laths or prisms are mainly altered to sericite in the centre of the crystals. Plagioclase occurs also as interstitial filling together with alteration minerals and quartz between the mafic mineral phases. Characteristic for the basement dykes are micrographic or granophyric intergrowths between quartz and plagioclase (fig. 5.27.c), observable on their radiate arrangement along the crystal margins. Some small plagioclase crystals are also subophitic to ophitic enclosed in pyroxene, but this texture is rather rare. As mentioned above, there are two subgroups of basement dykes due to their SiO₂ content. The thin section description shows a slightly higher content of plagioclase, but a relative considerable increase in quartz content from the gabbro-noritic to the quartz-bearing gabbro-noritic variety. Anhedral quartz crystals appear as single grains as well as interstitial patches (up to 1 mm, VK_10-6_4/1), often in micrographic intergrowth with plagioclase. Clino- and orthopyroxenes are the dominant mafic minerals. Pale brown subhedral clinopyroxene forms lath-shaped (up to 9.5 mm) to short prismatic crystals with an inclined extinction of 44°, which suggests augite as preferred clinopyroxene. Some crystals or aggregates of clinopyroxene show a twinning like field division under crossed polarisers as a result from deformation processes (fig. 5.27.a,b). Colorless to pale brown orthopyroxene occurs as stubby prismatic crystals with parallel extinction, but also as fine exsolution lamellae in clinopyroxene. Both pyroxenes are affected by alteration to amphibole (uralitisation), especially at the crystal margins. Compared to the microgabbro and gabbro-norite sills the average content of amphibole is low. In addition to amphibole the basement dykes also show numerous alteration mineral phases like sericite, epidote, chlorite, calcite and clay minerals. Subhedral calcite forms relative big single crystals (up to 1 mm, BD_13-7_1/1) with the typical parallel twins, speckled extinction as well as their typical interference pastel colors (fig. 5.27.d). Skeletal to multilateral shapes of Fe-Ti-oxides are also present with mainly magnetite, ilmenite, hematite (fig. 5.27.f) and rutile. The latter can be observed under transmitted light and occurs as tiny red-brown grains with a distinct high relief (fig. 5.27.e). Compared to the microgabbro sills and gabbro-norite sills, the basement dykes show also rutile as Fe-Ti-oxide. In general the basement dykes outside of the study area have a higher content of quartz. This suggests an increase of quartz in southeastern direction. That could imply a slightly increase of SiO₂ towards the centre of the Archaean basement terrain, but the few existing data could not verify this theory.

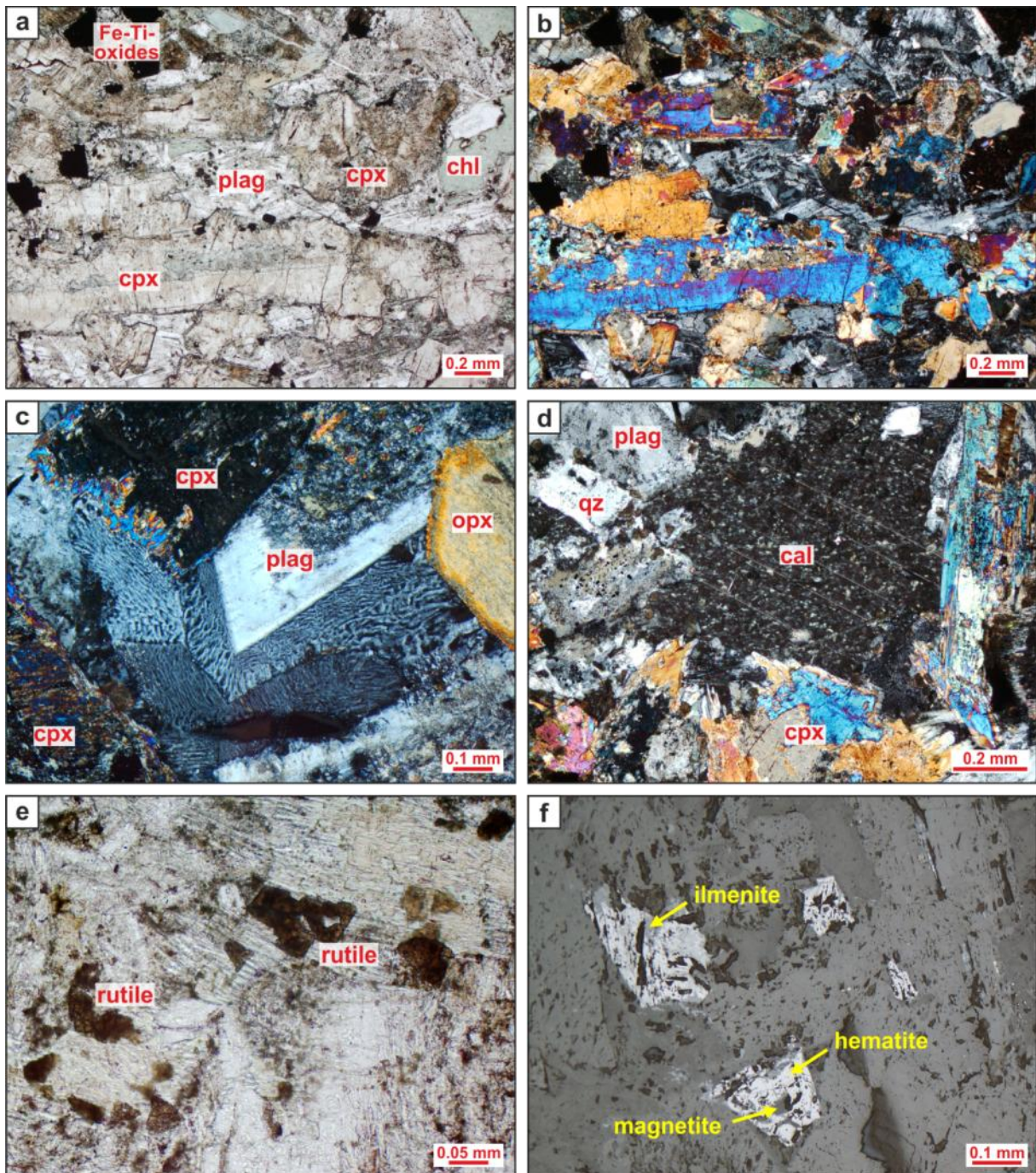


Figure 5.27: Picture a (under PP view) and picture b (under XP view) are from sample BD_13-7_1/1. They show a pale brown clinopyroxene lath and a cpx aggregate, which is divided into single fields looking like twinning. Both are surrounded by interstitial plagioclase and chlorite. Characteristic features for the gabbronoritic basement dykes are the micrographic intergrowth between plagioclase and quartz (c: VK_8-6_11/1, under XP view), and large patches of calcite resulting from the alteration of plagioclase (d: BD_13-7_1/1, under XP view). Notice the marginal intergrowth of calcite, plagioclase, quartz and clinopyroxene, which underline the secondary formation of the anhedral calcite crystal. Under reflected light the multilateral shapes of Fe-Ti-oxides (a) were identified as magnetite, ilmenite and hematite, which are strongly intergrown (f: BD_13-7_1/1, under PP view). Additional to magnetite, ilmenite and hematite as Fe-Ti-oxides, small anhedral grains of rutile occur within the thin sections of the basement dykes (e: VK_10-6_1/2, under PP view). Rutile can be observed under transmitted light and forms unshaped red-brown crystals with a distinctively high relief.

5.5 Summary of petrography

The following subchapters give a short tabulate summary of the basic petrographic features of the investigated sills and dykes and their modal composition.

5.5.1 Basic petrographic features

Table 5.2. Basic petrographic features

Feature	Microgabbro Sills	Gabbronorite Sills	Basement Dykes
Grain size	fine to medium	medium to coarse	medium to coarse
Primary minerals	plagioclase, clinopyroxene, hornblende, biotite, lesser quartz	plagioclase, ortho- pyroxene, clino- pyroxene, quartz, hornblende	plagioclase, ortho- pyroxene, clino- pyroxene, quartz, biotite, hornblende
Alteration minerals	actinolite, hornblende, sericite, epidote, chlorite, calcite, zoisite, clay minerals	actinolite, hornblende, sericite, chlorite, calcite, clay minerals	amphibole, sericite, chlorite, epidote, calcite, clay minerals
Fe-Ti-oxides	many skeletal magnetite, ilmenite, hematite	less multilateral magnetite, ilmenite, hematite	many skeletal magnetite, ilmenite, hematite, rutile
Texture	ophitic to subophitic, Intergranular, epigranular	intergranular, spherulitic to variolitic, corona rims, subophitic	ophitic to subophitic, micrographic inter- growths, intergranular

5.5.2 Modal composition**Table 5.3.** Modal composition

Sill/dyke	Plagioclase (modal %)	Orthopyroxene (modal %)	Clinopyroxene (modal %)	Hornblende (primary) (modal %)	Minor mineral phases (≥ 5 modal %)
MICROGABBRO SILLS					
Uitkomst Sill 1	30-35	0-10	12-20	-	amphibole, sericite, biotite, quartz, chlorite, epidote, Fe-Ti-oxides
Chilled margin (Uitkomst Sill 1)	12	18	-	-	amphibole
Vaalkop Sill 1	30	4	15	8-10	amphibole, biotite, epidote
Vaalkop Sill 2	25-30	-	18	5	amphibole, biotite, quartz
Uitkomst Sill 2	35	-	6	12	amphibole, biotite, quartz, sericite, chlorite
Doornhoek Sill 1	30	-	6		amphibole, chlorite, epidote, biotite, quartz
Houtboschloop Sill 2	35	-	7	-	amphibole, Fe-Ti-oxides, sericite, chlorite, epidote
Weltevreden- Slaaihoek Sill 1	40	-	-	12	amphibole, biotite, quartz, chlorite
GABBRONORITE SILLS					
Hofmeyr Sill 1	25-35	8-12	15-18	-	amphibole, quartz, sericite
Houtboschloop Sill 1	20-30	15-20	5-8	-	amphibole, quartz, sericite, epidote
Houtboschloop Sill 3	35	12	18	-	amphibole, quartz, sericite, chlorite
Weltevreden Sill 1	20-40	-	10-15	8-18	amphibole, quartz, biotite, sericite, chlorite
Uitkomst Sill 4	30-35	7	20	-	amphibole
Uitkomst Sill 3	25-40	8-10	18-25	-	amphibole, quartz, sericite
GABBRONORITIC BASEMENT DYKES					
Variety 1: Gabbronorite	35	8-10	15-18	-	amphibole, sericite
Variety 2: quartz-bearing Gabbronorite	25-30	7-13	18-20	-	quartz-bearing (7-10%), amphibole, biotite, sericite, chlorite

5.5.3 Semi-quantitative rock classification

The investigated sills and dykes are classified after the nomenclature of gabbroic rocks according to Streckeisen (1976) and Le Maitre (2002) (see subchapter 5.1, p.53). Therefore the modal composition is used, which is determined by semi-quantitative microscopically identification (see 5.5.2, p.96). The classification is based on the primary components: plagioclase, clinopyroxene and orthopyroxene. 50% of total determined amphibole content is added as pyroxene for the calculation due to the moderate to highly alteration grade, which affected all samples. It can be assumed from microscopy that a great part of the amphibole amounts represent former pyroxene. Neglecting this would imply higher amounts of plagioclase for the sills and dykes than usual. With this assumption the sills and dykes show the expected distribution within the triangular diagram of plag, cpx and opx (fig. 5.28). The gabbronorite sills and gabbronoritic basement dykes plot within the gabbronorite field, whereas the microgabbro sills are of gabbroic composition. The chilled margin of the microgabbroic Uitkomst-Sill 1 is classified as noritic rock.

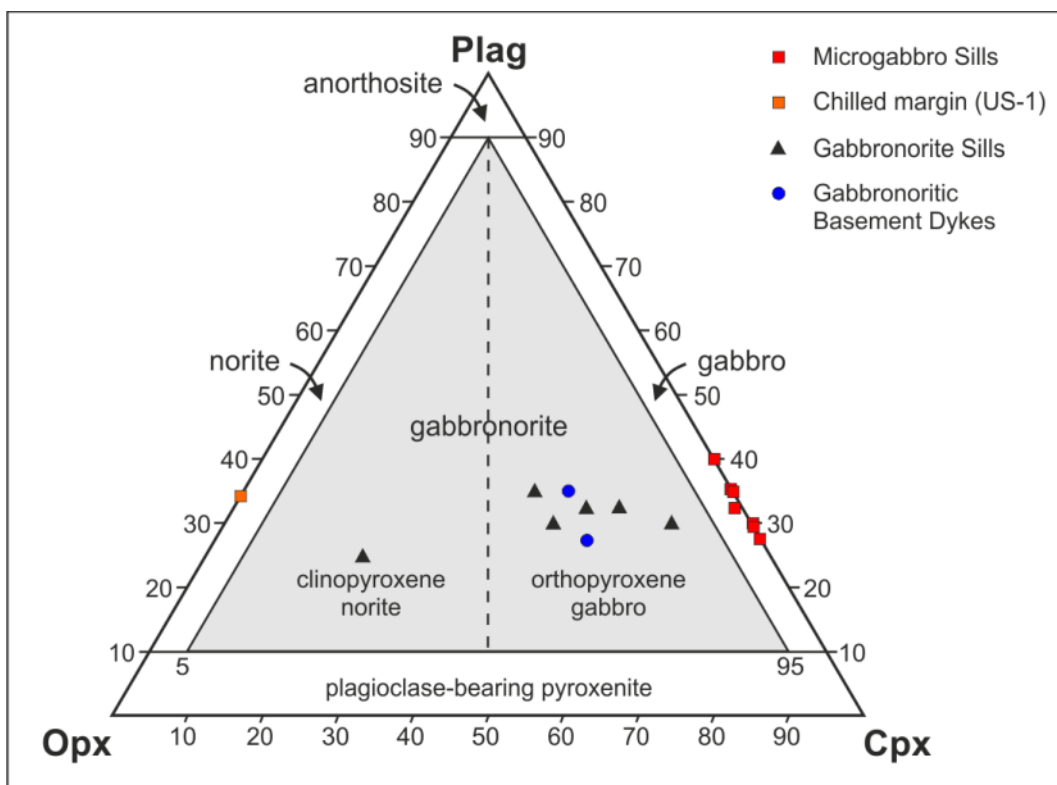


Figure 5.28: Due to the semi-quantitative microscopic identification of the modal composition the investigated sills and dykes can be classified as gabbronorites and gabbros. Notice that the triangular diagram shows an ascending order of plagioclase on the y-axis, whereas the x-axis gives the content of clinopyroxene and orthopyroxene (modified after Streckeisen, 1976).

6. Geochemistry

The presented geochemical data in this thesis are from XRF analyses, which were carried out in the laboratories of the Department of Geology at the University of the Free State Bloemfontein (see chapter 3, p.26). A disc with all XRF data of the analysed samples is attached within the appendix.

6.1 Rock classification

In general plutonic igneous rocks are classified by the QAPF modal classification scheme (Q = Quartz, A = Alkali feldspar, P = Plagioclase and F = Feldspathoid) after *Streckeisen* (Le Maitre, 2002) (see chapter 5.1, p.53). The CIPW norm, which converts the rock chemistry into the molecular proportions is commonly used for the calculation of the modal mineral phases. Due to the strong alteration of most of the investigated samples the CIPW norm is unsuitable, especially that hydrous minerals such as biotite or hornblende, which are common in the analysed mafic sills and dykes, are not permitted (Rollinson, 1993). Calculations of the CIPW norm for all samples show a distinctive Si oversaturation, so that the analysed mafic sills and dykes plotted mostly within the granodiorite and tonalite fields. Such compositions are not verified by the petrographic investigations (see chapter 5, p.53), but could be due to non-consideration of alteration minerals within the calculation. The tendency to Si oversaturation could also be an indication of crustal contamination.

If the modal proportions are not determinable, the total alkali-silica diagram (TAS) is used to classify igneous rocks. Primary conceived for volcanic rocks by Cox et al. (1979) and Le Maitre (1989), the TAS diagram was modified by Middlemost (1985) for plutonic rocks. In the plot of the total alkalis versus silica (fig. 6.1) the analysed sills and dykes cover a restricted area within the fields of gabbro, gabbroic diorite and diorite. Also a clear subdivision between the three groups of sills and dykes (microgabbro sills, gabbronorite sills and gabbronoritic basement dykes) is noticeable. The microgabbro sills with an average SiO₂ content of 50.43 wt.% are classified as gabbros, whereas the gabbronorite sills (average SiO₂ of 55.25 wt.%) are distributed within the gabbroic diorite and diorite field. The basement dykes plot between both sill groups with an average SiO₂ content of 53.63 wt.%. The TAS diagram shows a more intermediate composition, especially for the gabbronorite sills and basement dykes. The increased amounts of SiO₂ as well as K₂O and Na₂O could be an indication for crustal contamination during the magma rising. The undistinguishable difference in alkali content is explainable by the high mobility of the elements K and Na during alteration and metamorphic processes. Therefore other classifications use additionally lesser mobile elements as such Fe and Mg or preclude the very mobile alkali elements.

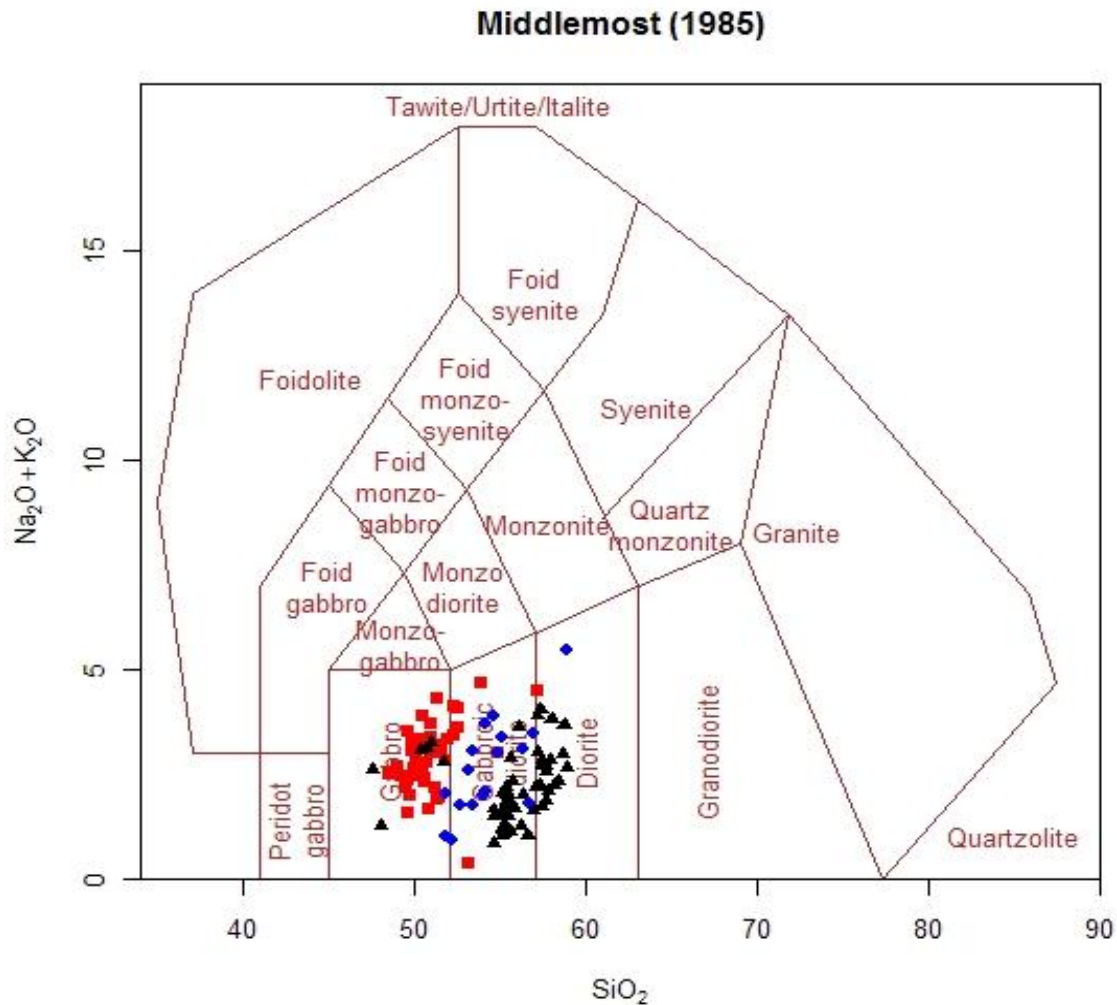


Figure 6.1: Total alkali-silica (TAS) diagram modified by Middlemost (1985) classify a gabbroic to dioritic composition for all investigated rocks. The microgabbro sills plotted mainly within the gabbro field, whereas the gabbronorite sills and gabbronoritic basement dykes show a more intermediate composition. However, the alkalis ($\text{Na}_2\text{O}+\text{K}_2\text{O}$) are very mobile during secondary processes like alteration and low grade metamorphism, which affected all three investigated groups. The primary composition, especially for the gabbronorite sills and basement dykes, has to be more mafic as the TAS diagram suggested. (Symbols: Microgabbro sills = red, Gabbronorite sills = black, Basement dykes = blue)

The AFM ($A = \text{Na}_2\text{O}+\text{K}_2\text{O}$, $F = \text{FeO}_{\text{tot}}$ and $M = \text{MgO}$) diagram according to Irvine and Baragar (1971) comprises Fe and Mg to divide sub-alkaline igneous rocks into tholeiitic and calc-alkaline magma suites. The plotting of the investigated three groups of mafic sills and dykes shows a general tholeiitic trend (fig. 6.2). The microgabbro sills give a more or less central cluster of data points within the AFM diagram. Their average Fe/Mg ratio is higher than in the two other groups due to enrichment of iron, which could be a function of their higher content of Fe-Ti-oxides compared to the other groups. The gabbronorite sills show a lower Fe/Mg ratio, which is because of their higher content of magnesium end members (orthopyroxene). Also this group possesses a more pronounced trend of iron enrichment compared to the microgabbro sills. The flattened trend of the basement dykes could also suggest a calc-alkaline magma suite formed by the early separation of Fe rich minerals.

The $\text{FeO}_{\text{tot}}/\text{MgO}$ versus SiO_2 diagram (fig. 6.2) according to Miyashiro (1974) verifies a distinctive tholeiitic characteristic for the microgabbro sills, which imply high degree partial melts and an enrichment of Fe compared to calc-alkaline rocks. However, the gabbronorite sills as well as the basement dykes plotted within the calc-alkaline series (fig. 6.2). For the calc-alkaline trend of the gabbronorite sills argued the absence of clearly skeletal Fe-Ti-oxides due to the depletion of Fe in early stage of magma evolution, which is typical for calc-alkaline magma suites (Okrusch & Matthes, 2005). Both groups show a few outlier values plotted in the field of the tholeiitic series. The outlier values of the gabbronorite sill group belong to the Weltevreden Sill 1 and plot also in the following diagrams among the microgabbro sills, which will be discussed later.

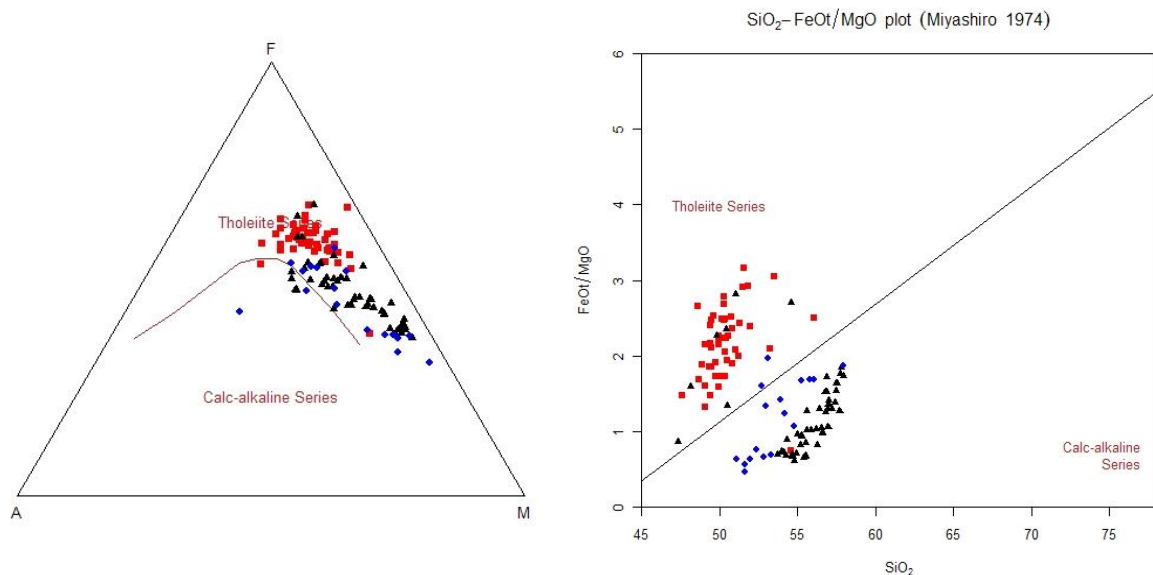


Figure 6.2: According to Irvine and Baragar (1971) all three groups of investigated sills and dykes plotted within the field tholeiitic magma series within the AFM diagram (left). Noticeable is the lower Fe enrichment of gabbronorite sills and basement dykes compared to the microgabbro sills suggesting a rather calc-alkaline trend. A calc-alkaline magma suite for the main part of gabbronorite sills and basement dykes is verified by the $\text{FeO}_{\text{tot}}/\text{MgO}$ versus SiO_2 diagram (right) according to Miyashiro (1974), whereas the microgabbro sills show a distinctive tholeiitic composition. (Symbols: Microgabbro sills = red, Gabbronorite sills = black, Basement dykes = blue).

6.2 Alteration

The petrographic investigations (see chapter 5, p.53) prove a moderate to high grade of alteration of primary minerals, whereas the primary texture is mostly preserved indicating very low grade metamorphism (lower greenschist facies). Alteration could affect the distribution of major elements (e.g. K_2O , Na_2O), which is mostly observable by erratic distributed values (Schweitzer & Kröner 1985). The ternary CaO/Al_2O_3 - $MgO/10$ - $SiO_2/100$ diagram after Schweitzer and Kröner (1985) is used to distinguish between altered and unaltered rocks (fig. 6.3). The majority of the samples including nearly all microgabbro samples plot in the field of unaltered basalts (fig. 6.3). Half of the gabbronorite sills as well as basement dyke samples seem to be altered. This is contrary to field observations, where all samples show more or less hints of alteration. At this point the ternary CaO/Al_2O_3 - $MgO/10$ - $SiO_2/100$ diagram is used to point up different grades of alteration within the investigated sills and dykes.

According to Rollinson (1993) high values (> 3 wt.%) of LOI (loss of ignition) determine also strong altered samples. The analyses, which was used for geochemical characterisation, show values of LOI < 3 wt.%.

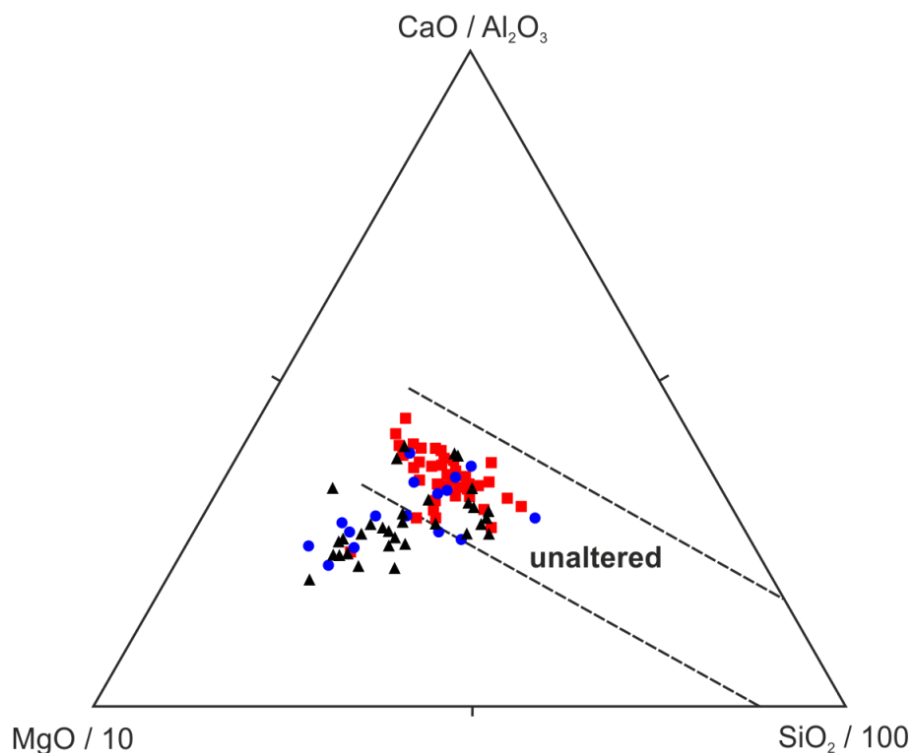


Figure 6.3: Ternary system for basalts after Schweitzer and Kröner (1985) to recognise alteration on the basis of major element data. At this point the diagram is used to identify highly and less altered samples. (Symbols: Microgabbro sills = red, Gabbronorite sills = black, Basement dykes = blue)

In spite of that, elements that are less to moderately mobile during low-temperature alteration and low-grade metamorphism were chosen for the following geochemical investigations. This includes major element oxides such as MgO, Fe₂O₃, CaO and SiO₂, as well as trace elements such as Zr, Sc, Ti, Nb, V, Co, Cr and Ni belonging to the High Field Strength Elements (HFSE), which show a great ionic potential at small ionic radius. Whereas Low Field Strength Elements (LFSE) with low ionic potential at large ionic radius such as Ba, Rb, K, Sr, Th and U tend to be very mobile during secondary processes (Pearce & Norry, 1979; Rollinson, 1993; Shervais, 1982).

Igneous trends for various major elements versus MgO in the Harker plots (fig. 6.3) indicate that among the major elements all the elements, except for Na₂O and K₂O, are not perturbed by post-magmatic processes.

6.3 Geochemical characterisation of the mafic sills and dykes

In order to verify the results of the petrographic investigations of the mafic sills and dykes in the vicinity of the Uitkomst Complex, geochemical characteristics using XRF are presented below. A more detailed classification of the three groups of mafic sills and dykes is possible by using bivariate diagrams (fig. 6.4) to illustrate the analysed data.

Major element data

The major elements data have already been used for rock classification (see 6.1 and data disc in appendix), but furthermore they are a helpful instrument to indicate trends of AFC processes (assimilation and fractional crystallisation). Commonly for mafic rocks is the use of MgO or the Mg number (Mg#) as fractionation index, which are plotted against other major elements in oxide form (Rollinson, 1993).

MgO content itself shows a strong variation in all three individual groups. The microgabbro sills form a rather tight cluster with an average MgO content of 6.38 wt.%. The other two groups show more variability. The gabbronorite sills have an average MgO content of 9.7 wt.%, but ranging between 4.61 and 17.5 wt.%. A similar behaviour is observable for the basement dykes (average MgO content of 9.65 wt.%), which show also a wide variation from 3.49 to 18.32 wt.% MgO. The wide range within the MgO content of gabbronorite sills and basement dykes suggests a higher grade of differentiation compared to the microgabbro sill group. According to Best (2003) a content of MgO > 8 wt.% together with 400 ppm Ni and 1000 ppm Cr as well as a Mg number > 68 marked the lower limit for composition of primary melts. The Mg number ($Mg\# = 100 \times MgO / (MgO + FeO_{tot})$) is a Mg/Fe ratio, which is also commonly used as fractionation index for basaltic liquids (Rollinson, 1993). The investigated sills and dykes show a clearly lower Mg#.

The microgabbro sills have an average Mg# of 32.4, whereas the gabbronorite sills and the basement dykes show similar average amounts of Mg# with 47.7 or rather 48.7 with the exception of one of the basement dykes revealing a Mg# of 68.3. That suggests a distinctive fractionation for all three groups of mafic rocks. The MgO content plotted against SiO₂ (fig. 6.4) supports this trend. The decreasing of MgO affects an increase of SiO₂, so that the rocks become more intermediate in composition.

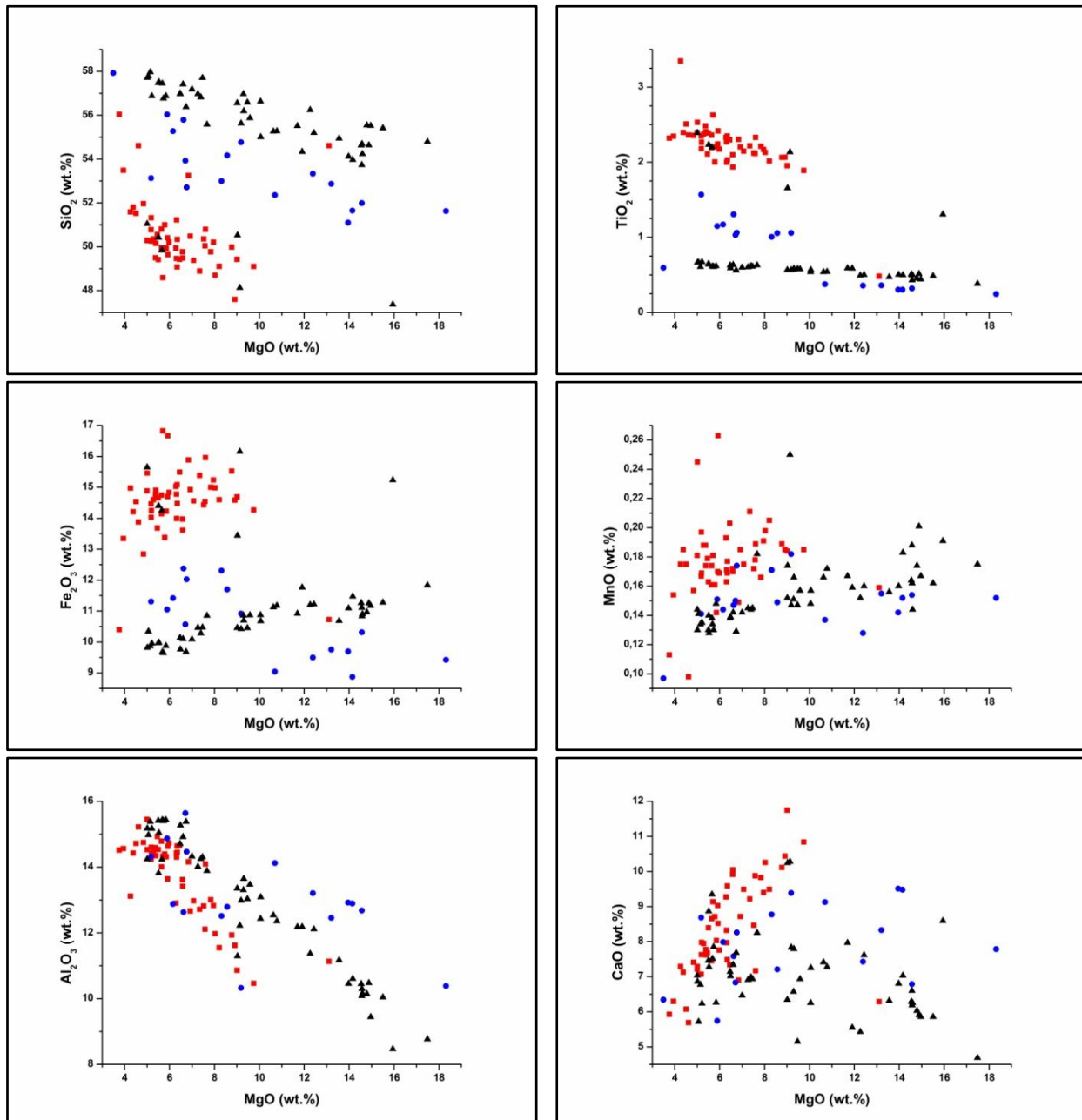


Figure 6.4: Bivariate diagrams of major elements plotted with MgO (wt.%) as fractionation index. Notice the increasing of fractionation with decreasing in MgO content. Further explanation see text. (Symbols: Microgabbro sills = red, Gabbronorite sills = black, Basement dykes = blue)

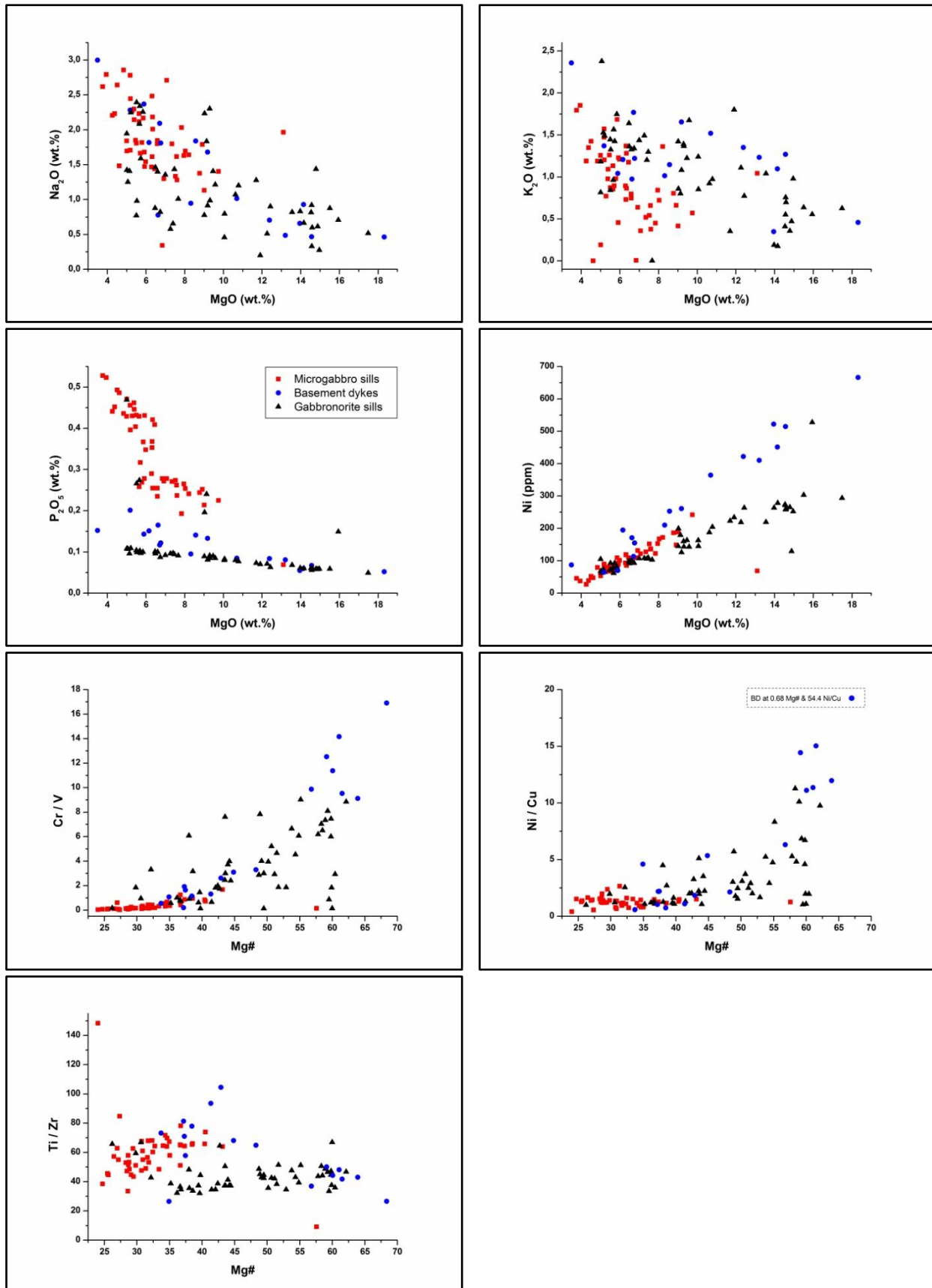


Figure 6.4 (continuation): Bivariate diagrams of major and trace elements as well as trace element ratios plotted with MgO or Mg number ($\text{Mg\#} = 100 \times \text{MgO}/(\text{MgO} + \text{FeO}_{\text{tot}})$). FeO_{tot} is recalculated from Fe_2O_3 . (Symbols: Microgabbro sills = red, Gabbronorite sills = black, Basement dykes = blue)

The classification into three mafic rock groups is verified by their very distinct levels of TiO_2 contents (fig. 6.4). The sills can be further distinguished into a low Ti (gabbronorite sills < 0.68 wt.%) and high Ti (microgabbro sills > 1.88 wt.%) group. The TiO_2 values of the gabbronorite sills stay at a relative constant level with decreasing MgO. The gabbronorite sills show five outlier values with higher TiO_2 amounts, which are all from the Weltevreden Sill 1 and suggest a second trend within this group.

The microgabbro sills form a relative tight cluster in a distinctive interval to the gabbronorite sill group, which could indicate different magma derivations. Also a slightly negative correlation of increasing in TiO_2 content with a decrease in MgO is observable. This is explained by the enrichment of incompatible Ti in residual melts, whereas high contents of Mg are an indication for primitive melts. Only one sample (from Uitkomst Sill 1) of the microgabbro sill group has a lower TiO_2 content and plotted within the gabbronorite sill cluster. In relation to the cluster of microgabbro sill values this could indicate a similar magma source. The TiO_2 amounts of the basement dykes show a more variable distribution, but in spite of those also two subgroups, a low Ti (basement dykes < 0.6 wt.%) and a high Ti (basement dykes > 1.0 wt.%) subgroup, are noticeable.

The values of P_2O_5 against MgO reflect similar trends, which can be correlated to the determined TiO_2 contents. The amounts of P_2O_5 subdivided the microgabbro sills into a low P_2O_5 (< 0.3 wt.%) and high P_2O_5 (> 0.3 wt.%) subgroup with slightly decreasing MgO content.

The microgabbro sills as well as the gabbronorite sills show more or less linear trends with regards to CaO and Al_2O_3 content (fig. 6.4). The microgabbro sills present a synchronic decreasing of CaO and MgO content, which indicates the depletion of Ca during fractionation processes resulting from plagioclase and clinopyroxene crystallisation. The enrichment of Al with decreasing MgO suggests the forming of Al layer-silicates and secondary amphibole due to alteration processes. The gabbronorite sills and basement dykes show the enrichment of Al with decreasing MgO content as a result of secondary processes, whereas the content of CaO is relatively constant.

There are also two trends within the basement dyke group going by Al_2O_3 content. One group of basement dykes follows the trend of the microgabbro sills, whereas the other basement dyke group indicates a lower increase of Al_2O_3 with decreasing MgO.

The subdivision into three groups of mafic sills and dykes is additionally supported by the contents of Fe and Mn (fig. 6.4), but a trend by depletion or enrichment of one of these elements with decreasing MgO is not clearly noticeable. The amounts of Fe within the basement dykes show yet again a subdivision into two basement dyke subgroups.

The alkalis Na_2O and K_2O display no regular trends when plotted against MgO (fig. 6.4).

When considering all rock samples together there is an increase of Na_2O with decreasing MgO, whereas the K_2O values are constant. Nevertheless the alkali elements seem to be more affected by post-magmatic processes like alteration than the other major oxides.

Trace element data

For further classification of the three groups trace elements as well as trace element ratios are used to plot against the fractionation index MgO or Mg#.

The transitional metals Ni, Cr and Co show similar trends within the three groups due to their similar compatible behaviour. The increase in contents of Ni, Cr and Co with increasing MgO, meaning an increasing fractionation, suggests an early fractionation of olivine and its separation from the melt. The similar linear trend with increasing of Ni and MgO is observable in all three groups, but the increase of Ni is steeper within the basement dyke group, followed by the microgabbro sills and most gently within the gabbronorite sills (fig. 6.4). Only a few samples from gabbronorite sills and basement dykes show amounts of Ni > 400 ppm and Cr > 1000 ppm, which could suggest together with high Mg# a primary melt composition (Best 2003). In spite of that, the basement dykes and gabbronorite sills seem to be more primitive than the microgabbro sills.

The Cr/V ratio plotted against the Mg# proved this assumption (fig. 6.4). The content of Cr increases with increasing fractionated crystallisation, whereas the amount of V rises. The element V is also a transitional metal like Cr, Ni and Co, but remains in early-liquidus mafic phases during crystallisation (Shervais 1982). Cr is therefore highly compatible in both pyroxenes and magnetite, whereas V is more compatible in magnetite and hornblende (partition coefficients for basaltic liquids after Rollinson 1993). Obviously the higher content of V in the microgabbro sills is a result of the mineral composition, and indicates later stage of magma, whereas gabbronorite sills and basement dykes are already crystallised.

A similar curved trend is observable at Ni/Cu ratios plotted against Mg# (fig. 6.4). The more fractionated microgabbros show higher amounts of Cu and lower contents of Ni compared to the gabbronorite sills and basement dykes, which consist of the Ni compatible minerals like orthopyroxene and clinopyroxene. Both trace element ratios Cr/V and Ni/Cu indicate a similar magma derivation for microgabbro sills, gabbronorite sills and basement dykes due to their continuous transition.

Another feature to compare the three groups is the choice of ratios of trace elements, which incompatible in mafic liquids. The Ti/Zr ratio plotted against Mg# (fig. 6.4) shows distinctive variations between the two sill groups, whereas the values of the basement dykes are erratically distributed.

The microgabbro sills presents a decrease of Ti/Zr with decreasing Mg# resulting from the crystallisation of Fe-Ti-oxides such that the melt becomes higher in Zr content. The gabbronorite sills show a more continuous Ti/Zr ratio during fractionation, but below the Ti/Zr ratio of the microgabbro sills, which supports a calc-alkaline trend for the gabbronorite sills (see 6.1, fig. 6.2), indicating an earlier separation of Fe-Ti-oxides from the melt.

In summary, the geochemical trends of the investigated three groups indicate fractionated melts of different sub-alkaline magma derivations. The microgabbro sills are of high-Ti tholeiitic composition, whereas the gabbronorite sills represent a low-Ti calc-alkaline magma suite. Furthermore the gabbronorite sills could be indicated as more primitive in composition compared to the microgabbro sills. The basement dykes are divided into two subgroups, which seem to be related to each sill group. One of these subgroups shows more affinity to the gabbronorite sills than the other subgroup to the microgabbro sills.

6.4 Geotectonic environment and magma derivation

As mentioned above, two different magma suites are distinguished based on the given data. Furthermore trace elements and trace element ratios can be used to determine tectonic environments basing on statistical discriminant analyses.

The most common tectonic discrimination diagram after Pearce & Norry (1979) based on the ratio of Zr/Y-Zr. Both trace elements are relatively immobile during alteration and up to medium metamorphic grades.

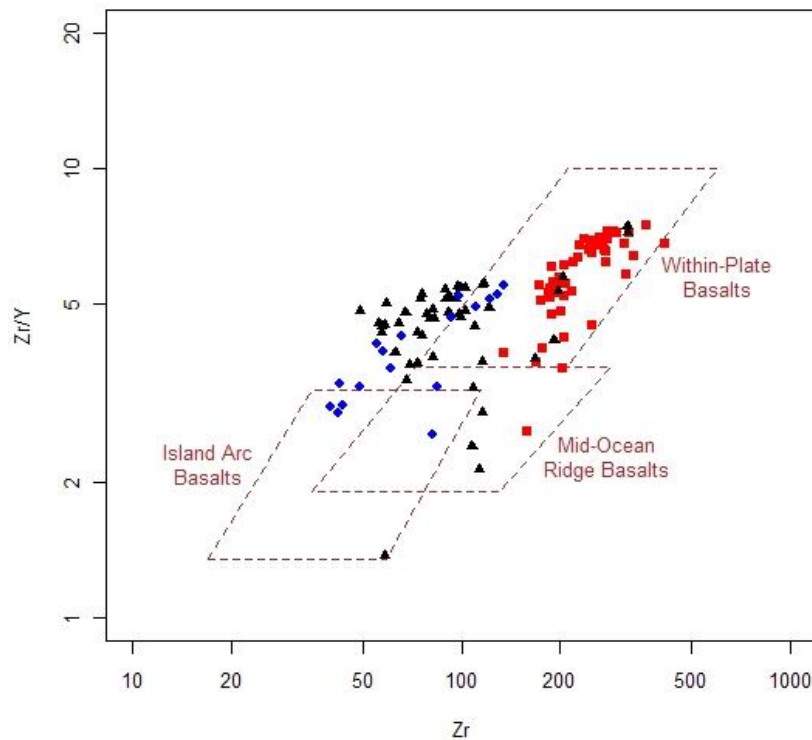


Figure 6.5: Zr/Y vs. Zr tectonic discrimination diagram after Pearce and Norry (1979). The microgabbro sills plot in the field of continental within-plate basalts, whereas the main part of gabbronorite sills and basement dykes cannot be related to one of the specified tectonic settings. This could be the effect of crustal contamination, which is not considered in this diagram. (Symbols: Microgabbro sills = red, Gabbronorite sills = black, Basement dykes = blue)

The microgabbro sills plotted within the field of continental within-plate basalts (oceanic within-plate basalts have a < 3 Zr/Y ratio) derived from an enriched mantle source, whereas mid-ocean ridge basalts (MORB) originated from a depleted mantle source. The main part of gabbronorite sills and basement dykes plotted outside of any field, but the Zr/Y ratio is nearly the same as for the microgabbro sills. This nonlinear trend suggests a rather different magma derivation for microgabbro sills and gabbronorite sills or contamination with continental crust.

It should be noted that crustal contamination is mostly not considered for such classifications, which could result in misclassifications for basalts from transitional settings (Pearce, 1996).

The tectonic discrimination diagram for volcanic rocks according to Shervais (1982) uses the trace elements Ti and V to distinguish between arc settings (VAB) and non arc settings (MORB and OIB). Both elements show a similar immobile geochemical behaviour under conditions of alteration and metamorphism (Rollinson, 1993). V is compatible in minerals such as orthopyroxene, clinopyroxene, hornblende and magnetite, whereas Ti is basically compatible in magnetite and hornblende.

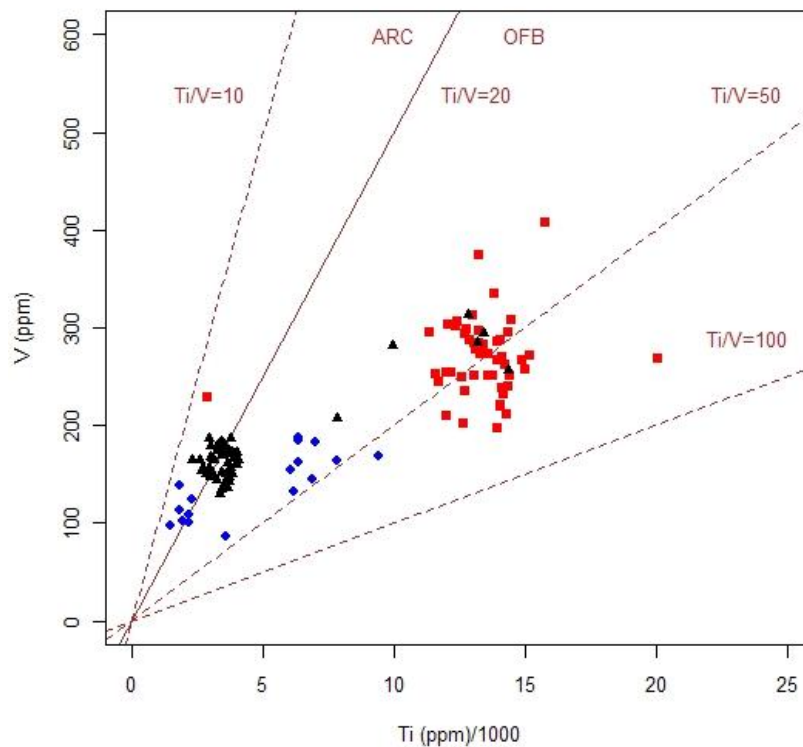


Figure 6.6: The Ti/V diagram according to Shervais (1982) identifies lower Ti/V ratios for the gabbronorite sills as well as a few of the basement dykes, which indicates an arc setting for these. The higher Ti/V ratios of the microgabbro sills and the remaining basement dykes suggest a non arc setting like MORB or OIB. (Symbols: Microgabbro sills = red, Gabbronorite sills = black, Basement dykes = blue)

The gabbronorite sills and a part of the basement dykes show a low Ti/V ratio of 20, which is typical for volcanic arc settings (fig. 6.6). The high V content is the result of the predominant amounts of orthopyroxene and clinopyroxene within the gabbronorite sills. Additionally the arc setting indicates a calc-alkaline magma suite (i.e. gabbronorite sills), which is depleted in Fe or rather Ti-bearing magnetite (Shervais, 1982). The microgabbro sills and the other part of the basement dykes offer a higher Ti/V ratio of 50 and plot within the non arc setting (fig.6.6). Furthermore the microgabbro sills are situated within the transition zone of MORB and OIB. Both of the non-arc settings are dominated by tholeiitic magma series (i.e. microgabbro sills), which show an enrichment of Fe and Ti-bearing magnetite.

Another possibility to classify derivations of different magma suites is adapted from Hatton and Sharpe (1988), who investigated quench-textured micro-orthopyroxenites from syn-Bushveld sills in order to determine the parental magma derivation of the lower zone of the Bushveld Complex. They presented a tectonic environment diagram on the basis of Ti and Zr contents with the argument that the earth mantle is initially formed with a constant Ti/Zr ratio comprehensible by meteorite compositions.

The Ti/Zr diagram after Hatton and Sharpe (1988) seems to be useful for the investigated mafic sills and dykes because of the assumed correlation to marginal rocks of the Bushveld Complex. The diagram (fig. 6.7) shows the Ti/Zr ratios for rocks from the lithosphere below the Kaapvaal Craton (Ti/Zr = 25) as well as for rocks related to mantle processes (Ti/Zr = 100). The latter imply the extraction of MORB (high Ti and Zr contents) from primitive mantle which leaves depleted mantle (low Ti and Zr contents). Furthermore, mantle associated rocks are komatiites (yellow stars in fig. 6.7), which represented the most similar mantle composition due to their high degree partial melting origin. The Ti/Zr ratios of the komatiites can be influenced by mixing with upper crust (thin solid lines, fig. 6.7 left) and also by assimilation of upper crust (dashed lines, fig. 6.7 left). Also shown are the Ti/Zr ratios of upper and lower continental crust as well as their mixing curve (dash-dot line, fig. 6.7 left)

The Ti/Zr ratios of the mafic sills and dykes plot between mantle derived rocks and rocks from the sub-continental lithosphere and form a nearly linear trend at Ti/Zr = 52. This indicates a strong fractionation for all three groups, but also suggests that the sills and dykes resulted from the upper crust assimilation by mantle rocks. The gabbro sills and part of the basement dykes are nearly situated on the AFC curve for assimilation of upper crust by komatiites (orange line, fig. 6.7 right). This could propose an originally primitive magma composition. The microgabbro sills and the remaining basement dykes have a distinctively higher content of Ti and Zr, so that they have to be more fractionated. A few samples of the basement dykes plot within the MORB field, whereas the microgabbro sills follow in a curved trend (orange lines, fig. 6.7 right). This suggested the derivation from MORB contaminated by upper crust for the microgabbro sills. The basement dykes show a precursor position in front of the microgabbro sills as well as the gabbro sills and can be indicative of an early stage of each magma suite.

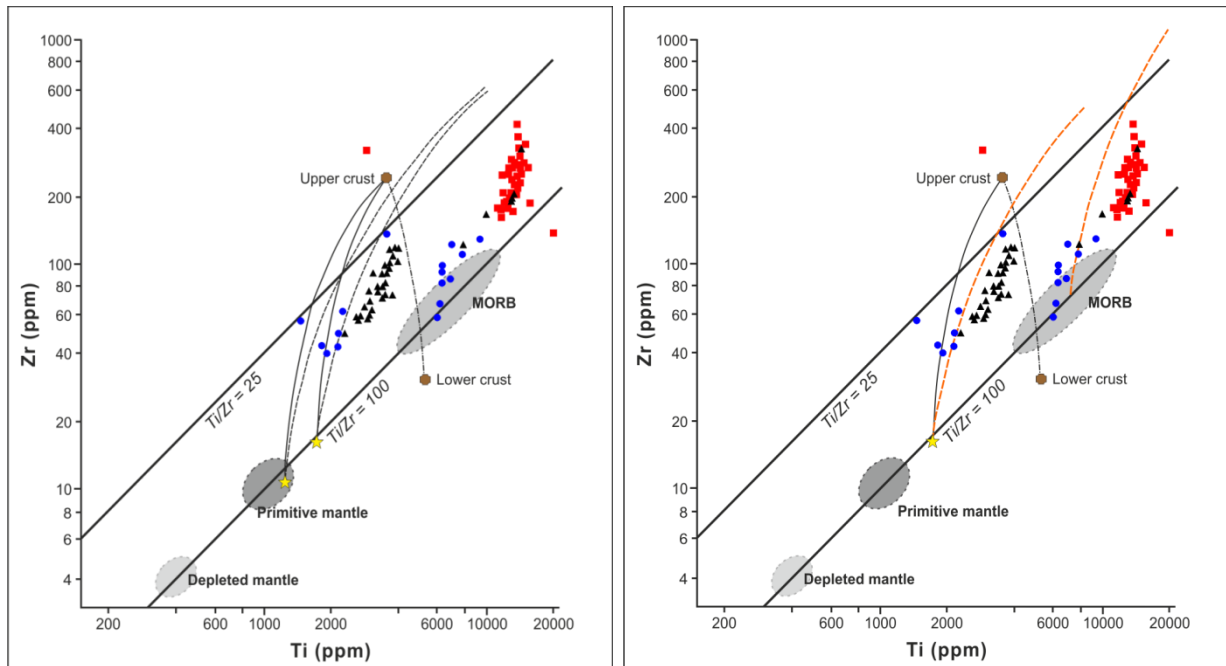


Figure 6.7: On the left the analysed samples are plotted within the Ti/Zr diagram after Hatton and Sharpe (1988). It suggests different magma derivation for the microgabbro sills (red squares) and for the gabbronorite sills (black triangle). Own assumption for magma derivation of the sills and dykes are presented in the Ti/Zr diagram *modified* after Hatton and Sharpe (1988) on the right. The gabbronorite sills seem to be the result of mixing and assimilation of upper crust material by a relative primitive magma (e.g. komatiites: yellow stars). The microgabbro sills could be derived from a fractionated MORB, which has assimilated crustal material. Orange lines are supposed assimilation curves. The basement dykes (blue circles) are divided into two subgroups, which occupy a precursor position in front of each sill group. Further explanations of symbols see text.

6.5 Comparison with Bushveld marginal rocks

According to Harmer and Sharpe (1984), Hatton and Sharpe (1988), Harmer and Von Gruenewaldt (1991), the nature of the parental magma of the different zones of the Bushveld Complex is reflected by syn-Bushveld sills. The boninitic B1 group, which is formed by quenched textured micropyxenites, represent the parental magma of the lower critical zone. The gabbronorite sills of the B2 and B3 group are representatives of tholeiitic magmas of the upper critical zone or rather main zone, which injected the Bushveld magma chamber in a later stage. The comparison of the sills and dykes with the marginal rocks as well as sills of the Bushveld Complex seems to be useful to make inferences about the origin of the mapped rocks.

Therefore incompatible as well as compatible trace elements and ratios are normalised against B1, B2 and B3 composition (fig. 6.8). The gabbronorite sills and the basement dykes show a similar trend in all three plots, a similar composition of trace element contents can therefore be assumed. The microgabbro sills show a more distinguishable trend. The composition of the gabbronorite sills and basement dykes comes closest to the composition of the B1 magma.

A low enrichment of incompatible elements (Zr, Y, Sr, Rb, K₂O) and a depletion of compatible elements (Ni, Cr, V, MgO) and incompatible element ratios (Zr/Rb, Zr/Y) is observable. This suggests a more evolved magma composition for the gabbronorite sills and basement dykes compared to the B1 magma, whereas the basement dykes seem to be most similar to the B1 norm composition. The microgabbro sills follow partly this trend, but higher peaks of incompatible elements and lower peaks of compatible elements indicate a stronger differentiation trend in comparison to gabbronorite sills and basement dykes.

Table 6.1: Average whole-rock composition of the investigated mafic sills and dykes as well as of average composition of B1 quenched textured microproxenites (Sharpe and Hulbert, 1985), B2 & B3 gabbroic sills (Hatton and Sharpe, 1988) and Basal Gabbro chilled margins at Uitkomst 541 JT and Slaaihoek 540 JT (Gauert, 1998).

	Gabbro-norite sills	Micro-gabbro sills	Basement dykes	B1	B2	B3	Uitkomst chill margin	Slaaihoek chill margin
Major elements (in wt.%)								
SiO ₂	55,26	50,51	53,63	56,07	51,60	51,70	51,37	55,16
TiO ₂	0,73	2,23	0,78	0,34	0,59	0,19	1,62	1,65
Al ₂ O ₃	12,86	13,71	13,31	11,47	15,80	16,80	15,61	15,12
Fe ₂ O ₃	11,14	14,51	10,44	10,59	2,09	1,69	14,04	10,00
FeO	10,02	13,06	9,40	9,53	8,85	5,56	12,64	9,00
MnO	0,16	0,18	0,15	0,18	0,20	0,15	0,15	0,16
MgO	9,70	6,38	9,65	12,96	7,74	7,94	6,72	5,12
CaO	7,01	8,33	7,96	6,68	11,20	11,80	7,60	8,2
Na ₂ O	1,15	1,88	1,37	1,68	2,41	2,31	2,79	4,07
K ₂ O	1,06	0,93	1,24	0,80	0,19	0,24	0,90	1,23
P ₂ O ₅	0,10	0,34	0,11	0,07	0,11	0,02	0,15	0,19
Mg#	49,20	32,83	50,67	57,63	46,65	58,81	34,71	36,26
Trace elements (in ppm) and trace element ratios (dimensionless)								
Co	52,77	54,00	50,88	90	99	81	57	37
Cr	588,13	101,63	699,66	1240	317	547	73	41
V	174,98	269,69	138,46	167	198	130	223	228
Zn	65,27	104,38	72,30	78	109	56	70	56
Cu	61,02	85,12	71,46	56	121	11	148	115
Ni	166,75	101,25	290,01	295	122	126	109	87
Nb	5,03	9,66	3,64	3,6	3	-	7	11
Zr	98,53	239,53	77,14	77	28	26	87	147
Y	25,22	41,01	19,08	13	18	11	19	29
Sr	119,58	273,03	280,40	158	324	329	301	364
Rb	55,63	33,87	43,65	30	3	4	24	40
Zr/Rb	1,77	7,07	1,77	2,57	9,33	6,50	3,63	3,68
Zr/Y	3,91	5,84	4,04	5,92	1,56	2,36	4,58	5,07

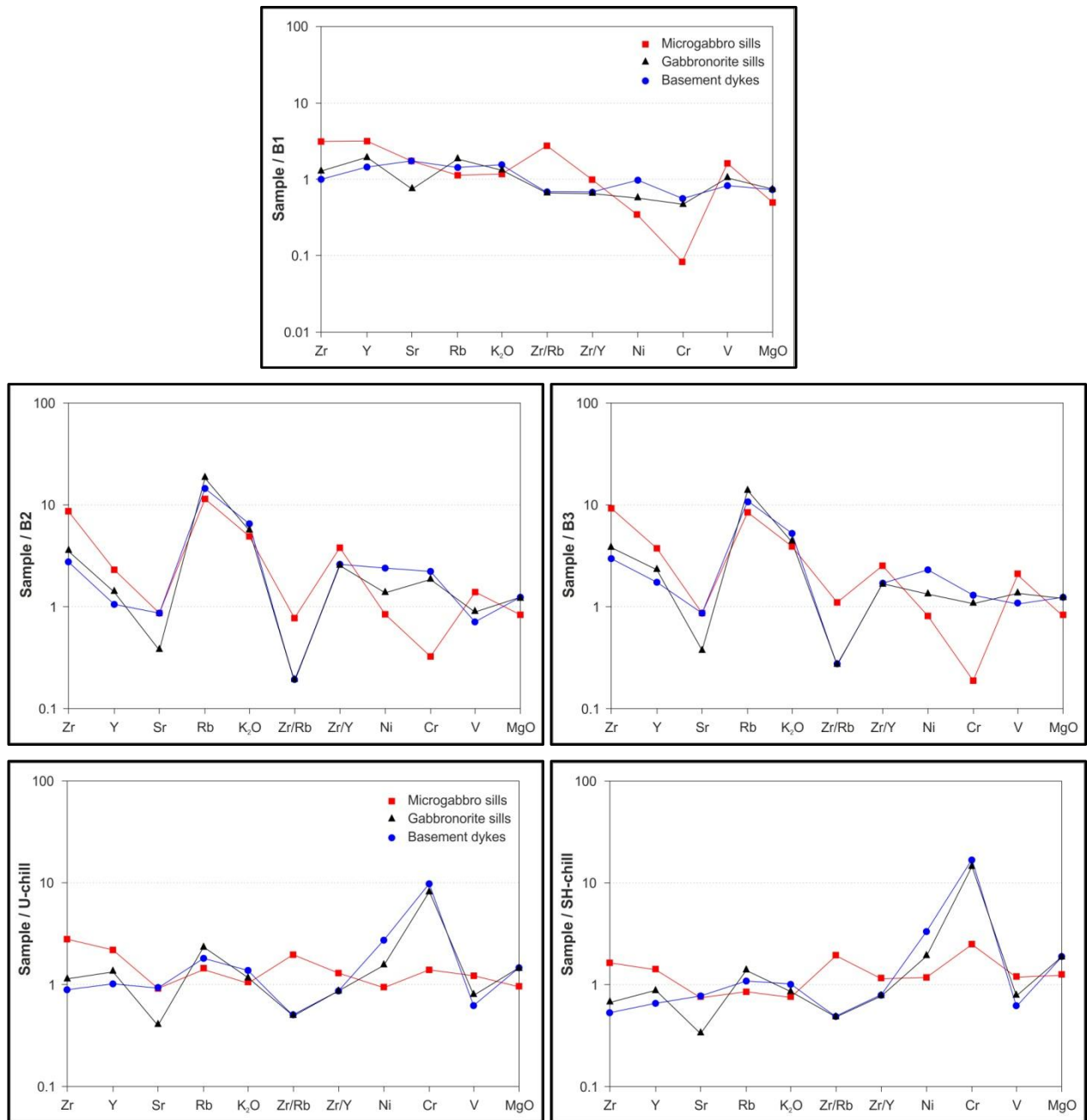


Figure 6.8: The spider diagrams showing the investigated sills and dykes normalised against magma composition of B1, B2 and B3 marginal Bushveld rocks as well as against the average composition of the Basal Gabbro chilled margins of Uitkomst and Slaaihoek. The basement dykes (blue line) come closest to the B1 norm, followed by the gabbronorite sills (black line), whereas the microgabbro sills (red line) show more variation. All three groups deviate from the B2 and B3 norm composition. The gabbronorite sills as well as the basement dykes show a more primitive composition compared to B2 and B3, whereas the microgabbro sills seem to be more evolved in composition. Compared to the chilled margins from Uitkomst and Slaaihoek, the gabbronorite sills and basement dykes show a similar trend, slightly enriched in Cr and Rb, but depleted in Sr and Zr/Rb. The microgabbro sills are nearly conformable with the composition of the Basal Gabbro chilled margins, but tend to be enriched in all trace elements. Symbols are the same as in fig. 6.1. Norm composition adapted from B1: Sharpe and Hulbert (1985), B2 & B3: Hatton and Sharpe (1988), U-chill & SH-chill: Gauert (1998).

Distinctive differences exist between the magma composition of the B2 and B3 group and the investigated sills and dykes. A high enrichment of incompatible elements, with the exception of Sr, in all three groups compared to B2 and B3 can be observed. Furthermore the gabbro sills and the basement dykes also show enrichment in compatible elements, which indicates a more primitive composition compared to the B2 and B3 magmas. The microgabbro sills are depleted of compatible elements, with the exception of V. That suggests an evolved trend of the microgabbro magma in comparison to B2 and B3.

Therefore the gabbro sills as well as the basement dykes are closest to the B1 norm composition, but more primary in magma composition than the B2 and B3 norm. The microgabbro sills tend to be more evolved than the magmas of the B2 and B3 group.

The average whole-rock composition of the investigated sills and dykes compared to the average composition of Basal Gabbro chilled margins at Uitkomst and Slaaihoek (fig. 6.8) also show similar trends for gabbro sills and basement dykes. Cr and Rb are enriched within the gabbro sills and basement dykes, whereas the incompatible element Sr and the ratio of Zr/Rb are slightly depleted against the chill margin composition of the Basal Gabbro Unit. That supported a more primitive lineage for gabbro sills and basement dykes compared to the Basal Gabbro chilled margin composition.

The composition of the microgabbro sills is similar to that of the Uitkomst and Slaaihoek chill margins. However, the microgabbro sills are slightly more enriched in nearly all the trace elements. This could be due to the fact that the microgabbro sills were derived from a more evolved magma as opposed to Uitkomst and Slaaihoek Basal Gabbro, which was derived from a more primitive magma.

7. Palaeomagnetic investigations

For palaeomagnetic investigations 10 to 15 cm long rock cores were drilled at various sills and dykes of the study area during the field work (see chapter 3.2). Measurements were carried out at the palaeomagnetic laboratories of the University of Johannesburg with the help of Dr. Michiel De Kock and Tumelo Mokgatle.

The main objective of the palaeomagnetic study was to characterise the palaeomagnetic signatures of the mapped sills and dykes. In addition, the palaeomagnetic analyses were undertaken to constrain the relative ages of the sills and dykes with respect to the Kaapvaal Craton, the Uitkomst Complex, marginal Bushveld rocks and the Bushveld Igneous Complex.

7.1 Sample sites

In total 25 samples from 8 sites were collected from each identified sill lithology as well as from the basement dykes (fig. 7.1). The gabbro sills (five sample sites) were preferred for palaeomagnetic sampling due to the good in-situ outcrops. In-situ exposures of microgabbro sills and basement dykes are restricted to three sample sites. The sampling method used for the palaeomagnetic study is described in chapter 3.2, p.26.

7.2 Palaeomagnetic methods

After preparation of the core samples into marked cubic pellets a demagnetisation procedure was carried out for every sample from each site in a magnetic-field-free room. The demagnetisation sequence started with measuring the natural remanent magnetisation (NRM), followed by a pre-treatment in a low field-strength alternating-field in four steps up to 10 mT. The following step included either a main alternating-field treatment starting at higher field-strength up to 100 mT or the thermal demagnetisation of the samples at decreasing intervals until specimen intensity dropped below noise level (De Kock, 2007).

The natural remanence was measured on a cryogenic magnetometer (fig. 7.2) using a SQUID magnetic field sensor, which is superconducting at liquid helium temperatures. The SQUID (Superconducting Quantum Interference Device) determined the magnetic moment of the sample. Together with the orientation data of the individual samples, the software application Paleomag 3 (Jones, 2002) calculated the best-fit direction of NRM in sample coordinates and in geographic coordinates (Butler, 1998).

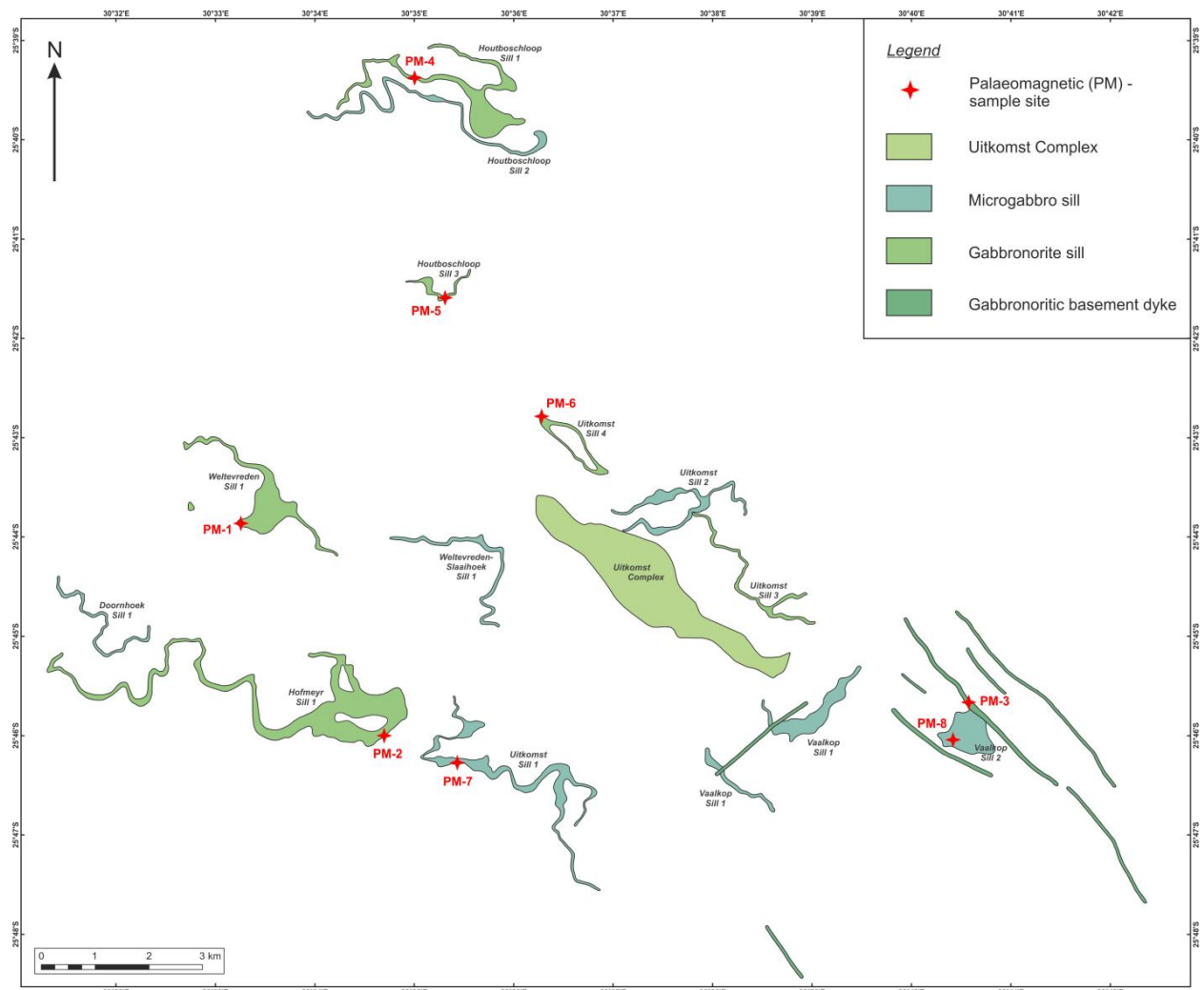


Figure 7.1: Location map of the 8 palaeomagnetic sample sites from this study. The gabbronorite sills were sampled at 5 locations (PM-1, PM-2, PM-4, PM-5, PM-6), the microgabbro sills at 2 sites (PM-7, PM-8) and the gabbronoritic basement dykes at PM-3.

The following alternating-field (AF) demagnetisation was carried out on a Molspin two-axis tumbling AF-demagnetiser (fig. 7.2), which generates an alternating magnetic field by rotating the sample in tumbler apparatus. The field strength was increased continuously at intervals of 5 to 10 mT up to a maximum of 100 mT. In addition, the samples were also thermally demagnetised in a shielded furnace. At first the specimen was heated at 100°C, then cooled down and the NRM was measured again on the cryogenic magnetometer. The sample was then heated to elevated temperatures below the Curie temperature at decreasing temperature intervals until the sample lost its magnetisation. The specimens approached a temperature of approximately 580°C before they got demagnetised.

The magnetic components were calculated via least-squares principal component analysis after Kirschvink (1980), which is used by the software applications Paleomag 3 (Jones, 2002) and PaleoMac (Cogné, 2003). All calculations of virtual geomagnetic poles and palaeomagnetic poles are provided for

an axial-geocentric dipolar magnetic field and a palaeoradius of the earth equal to the present earth radius (De Kock, 2007).



Figure 7.2: On the left the cryogenic magnetometer is shown, which measured the natural remanent magnetisation (NRM) of the samples. The following demagnetisation procedure was carried out on a Molspin two-axis tumbling Alternating-field (AF) - demagnetiser (right) (pictures by courtesy of Tumelo Mokgatle).

7.3 Palaeomagnetic results

Thermal demagnetisation up to 580°C has a strong effect on the remanence of the samples. The demagnetisation at this temperature indicates a Curie-Temperature $T_c = 580^\circ\text{C}$ and specifies magnetite as principle ferromagnetic mineral (Butler, 1998), which is in agreement with the petrographical determined opaque minerals. It is noticed that magnetite is also the result of alteration processes (exsolution of titanomagnetite to magnetite and ilmenite) affecting all described mafic sills and dykes thus possibly changing the information of magnetic direction.

As previously described, the measured magnetic components were determined via least-squares principal component analysis after Kirschvink (1980) by using software applications. The results are summarised in table 7.1. To display the results of the progressive demagnetisation graphically, NRM vector components and directions are used. The behaviour of the samples during the different demagnetisation levels is visualised in orthogonal projection diagrams which show directional as well as intensity information in a single diagram by projecting the vector component onto two orthogonal planes (Butler, 1998). The direction of the NRM vector, which is described through inclination ('Inc', with respect to horizontal at the sample site) and declination ('Dec', with respect to geographic north), as well as the geocentric axial dipole is also presented in equal area projections of each sample site.

Five of the sample sites (PM-1, PM-4, PM-5, PM-7 and PM-8) responded well to demagnetisation, whereas the other three sites (PM-2, PM-3, PM-6) offer no specific characteristics to the AF demagnetisation sequence. Unfortunately, the calculation for PM-4 to PM-8 yielded no components and thus were grouped together, so that the parameters (T, Dec, Inc, α_{95} , k, see tab. 7.1) are an average of PM-4, PM-5, PM-6, PM-7 and PM-8. Furthermore the calculation of PM-3 identified components, but no parameters. The results of the individual sample sites are presented in table 7.1.

Table 7.1: Summary of component direction and component mean, which are calculated via least-squares principal component analysis after Kirschvink (1980) using software applications.

sample site	n/N	T	Dec	Inc	α_{95}	k	components identified
PM-1	1/3	NRM-100	7,90	-27,90	-	-	PLF
	2/3	NRM-250	-	-	-	-	SFT
	3/3	250-580	176,80	-0,80	39,05		SH
PM-2	3/4	NRM-250	-	-	-	-	SFT
	2/4	250-580	358,00	-30,60	-	-	PLF
	2/4	NRM-580	NRM-580	-	-	-	LNG
PM-3	1/3	-	-	-	-	-	SFT
	1/3	-	-	-	-	-	PLF
	1/3	-	-	-	-	-	LNG
PM-4	1/3	100-580	59,50	66,10	27,32	6,97	ND?
PM-5	2/3	100-580	59,50	66,10	27,32	6,97	ND?
PM-6	0/3	-	-	-	-	-	-
PM-7	3/3	100-580	59,50	66,10	27,32	6,97	ND?
PM-8	1/3	100-580	59,50	66,10	27,32	6,97	ND?

n/N number of samples included/
Number analysed

α_{95} Radius of 95% confidence cone about
mean

Inc Inclination (°)

T Temperature (°C)

Dec Declination (°)

k Fisher's precision parameter

PLF Present local field (Earth's magnetic field at the sample locality)

SFT Soft components (such components are regarded as noise, they are removed by low temperature demagnetisation steps or even low field AF demagnetisation)

LNG Lightning induced components

SH Southerly horizontal directed components

ND Northerly downward directed components (Bushveld related direction)

Site PM-1 (Weltevreden Sill 1)

For sample site PM-1 within the Weltevreden Sill 1 three magnetic components (tab. 7.1) are identified during the demagnetisation procedure. After removing low-stability components of NRM (SFT) as well as the occasional present local Earth-field component (PLF) at low AF demagnetisation levels, a high AF component remains with a positive declination (176.8°) in southern direction and a low negative or nearly horizontal inclination (-0.8). This highly stable component is indicated as a SH (southerly horizontal) component, which represented an Umkondo age (ca. 1106 - 1112 Ma; Hanson et al., 2004) for the Weltevreden Sill 1 (see subchapter 7.4).

The orthogonal plot as well as the equal area projection of sample number 3 of site PM-1 is shown in figure 7.3. The linear trend after removing SFT and PLF components is clearly noticeable on the orthogonal plot. The remaining high stable component has a southerly horizontal direction displayed by the light blue and blue squares in the equal area projection.

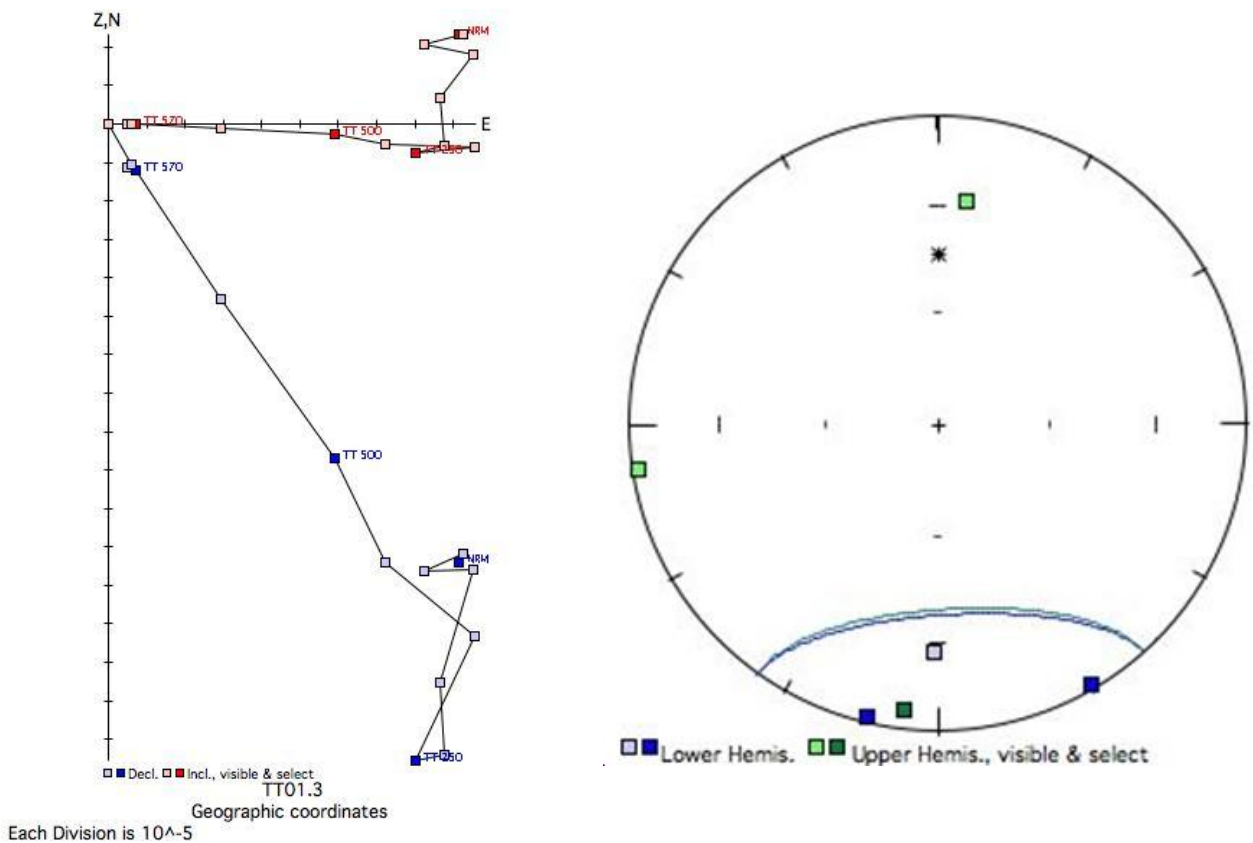


Figure 7.3: The orthogonal plot of sample number 3 of PM-1 (left) shows a linear trend after removing SFT and PLF components at low AF. The demagnetisation levels define a trajectory towards the origin with no significant change in direction at higher AF representing the SH component. The points moved towards the origin, which suggests a good reaction to the demagnetisation and no secondary NRM. The equal area projection (right) shows also the SFT and PLF components (light green and green squares) as well as the SH component (light blue and blue squares). (Both diagrams were generated by Dr. M. De Kock)

Site PM-2 (Hofmeyr Sill 1)

The demagnetisation sequence shows indistinct results for site PM-2. At low AF demagnetisation levels the SFT and PLF components, which caused a scattered distribution in the orthogonal plot (fig. 7.4), are removed similar to site PM-1. A third magnetic component, identified as lightning induced component (LNG, see table 7.1), displays at high AF demagnetisation levels and disturbs the sequence, so that no certain characteristics for PM-2 were determined.

Within the orthogonal plot for sample number 1 of PM-2 (fig. 7.4) the lines/points exceed the origin, which indicates an incorrect response to demagnetisation. Furthermore the equal area projection (fig. 7.4) shows no accumulation of points and therefore no specific direction for this site. One reason could be the sample site itself, the samples were taken from an in-situ outcrop on top of a prominent hill of the Hofmeyr Sill 1. According to Bates & Jones (1996) palaeomagnetic samples from hill tops or prominent exposures have a higher risk of remagnetisation due to lightning strikes.

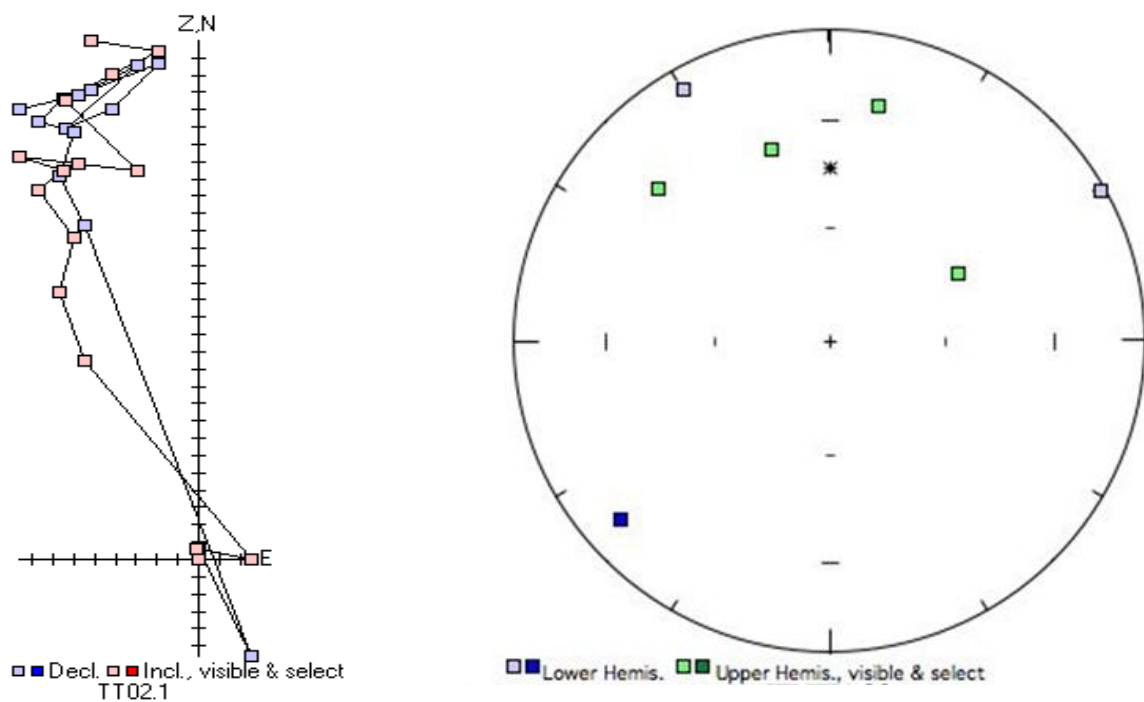


Figure 7.4: The palaeomagnetic signature of PM-2 is overlapped by SFT, PLF and LNG components. The orthogonal plot (left) of sample number 1 of PM-2 shows no linear trend and furthermore the demagnetisation levels (blue and red points) go through the origin, which indicates a bad reaction to AF demagnetisation. That is supported by the equal area projection (right) showing no specific direction for the demagnetisation levels. (Orthogonal plot was generated by T. Mokgatle, the equal area projection by Dr. M. De Kock)

Site PM-3 (Basement Dyke)

The only basement dyke palaeomagnetic sample site PM-3 within this study shows similar demagnetisation behaviour to PM-2. Different magnetic components (SFT, PLF, LNG; see table 7.1) disturb the specific magnetic signature of PM-3. Parameters like Dec, Inc, temperature etc. were not calculated via least-square principal component analysis by the software, but orthogonal plots as well as equal area projections were generated. The orthogonal plot (fig. 7.5) of sample number 2 of PM-3 shows SFT and PLF components at low AF demagnetisation levels, which are removed at higher AF levels. The following linear trend is unreliable because it exceeded the origin indicating no good response to the demagnetisation procedure. Nevertheless, the orthogonal plot as well as equal area projection (fig. 7.5) reflects an easterly downward direction. But this is no identified palaeomagnetic feature for the basement dykes due to the bad demagnetisation response and the lack of samples sites.

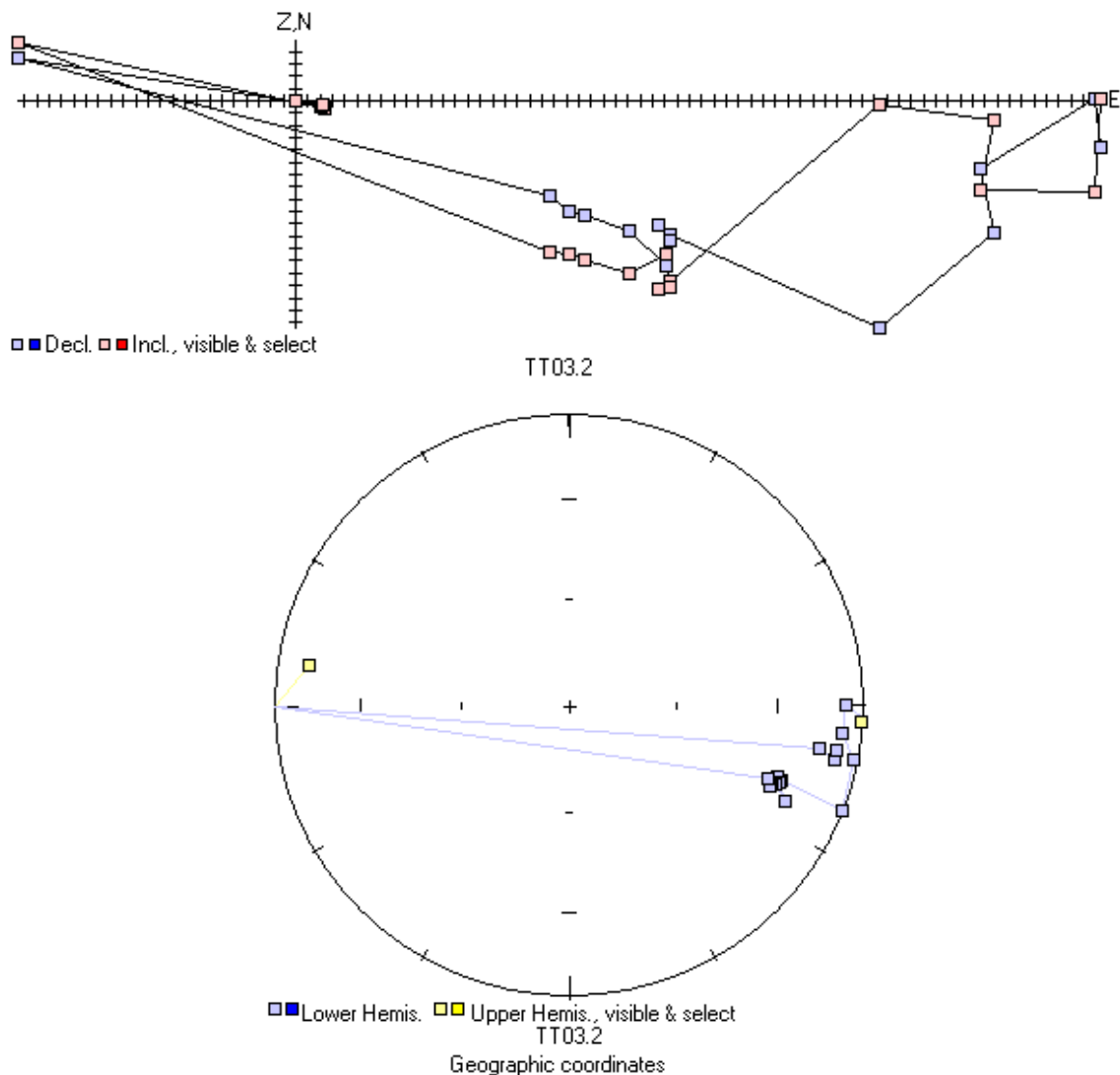


Figure 7.5: The orthogonal plot (above) as well as the equal area projection (below) of sample number 2 of PM-3 indicates an easterly downwards direction, but because of the bad response to the AF demagnetisation sequence this direction is probably caused by disturbing magnetic components (SFT, PLF, LNG). (Both plots were generated by T. Mokgatlé)

Site PM-4 (Houtboschloop Sill 1)

Samples of PM-4 responded well to the demagnetisation, observable within the orthogonal plot of sample number 1 of this site (fig. 7.6). Low-stability magnetic components are eliminated at low AF levels and there are no lightning induced components at higher AF levels, thus the plot at the end of demagnetisation does not exceed the origin. Recognisable is the downward trend of inclination as well as the northerly directed declination within the orthogonal plot (fig. 7.6). The approximately northerly orientation of declination is also shown in the equal area projection (fig. 7.6). The points on the lower hemisphere display the downward trend of inclination within this projection.

The northerly downward component (ND) estimated for PM-4 indicates similarities to the Bushveld direction, which is published by Hattingh (1986), Hattingh (1989) and Hattingh & Pauls (1994) for the main and upper zone of the Bushveld Igneous Complex (see subchapter 7.4).

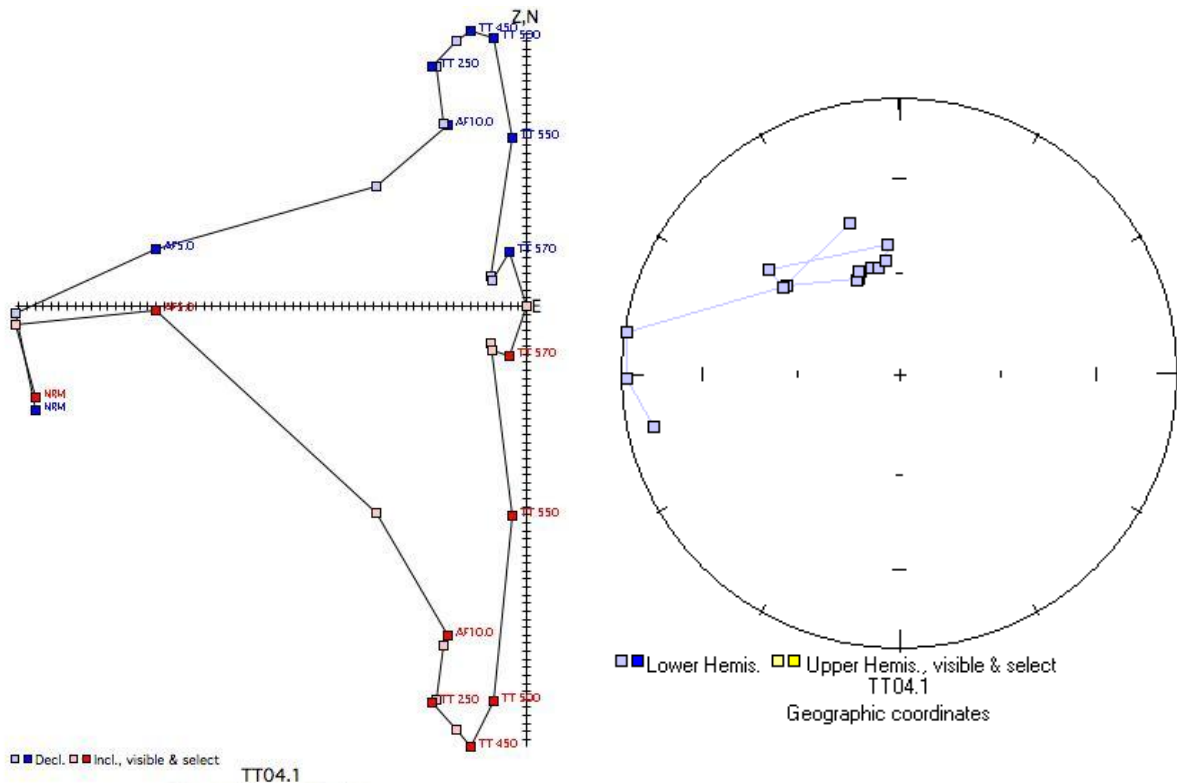


Figure 7.6: The orthogonal plot (left) of sample number 1 of PM-4 shows a well defined northerly downward directed trend of this site resulted by the good response to AF demagnetisation sequence. The points within the plot move in a linear trend fashion to the origin. The equal area projection on the right reflects also this northerly downward orientation trend, which is similar to the Bushveld palaeomagnetic direction. (Orthogonal plot was generated by Dr. M. De Kock, the equal area projection by T. Mokgatle)

Site PM-5 (Houtboschloop Sill 3)

Palaeomagnetic site PM-5 shows a similar magnetic behaviour than PM-4, whereas inclination and declination are not as distinctive within the orthogonal plot (fig. 7.7) of this site. After a linear trending line at lower AF levels disturbing secondary components appear at medium AF levels, which are removed at higher AF levels shown by the points moved towards the origin. The inclination is also downwards directed such as in PM-4, but the declination indicates a more north-western orientation. The same north-western direction can be observed within the equal area projection (fig. 7.7). Nevertheless, sample site PM-5 is grouped together with PM-4, also because of the same lithological description for both as gabbronorite sills. For both, a northerly downward magnetic component is assumed.

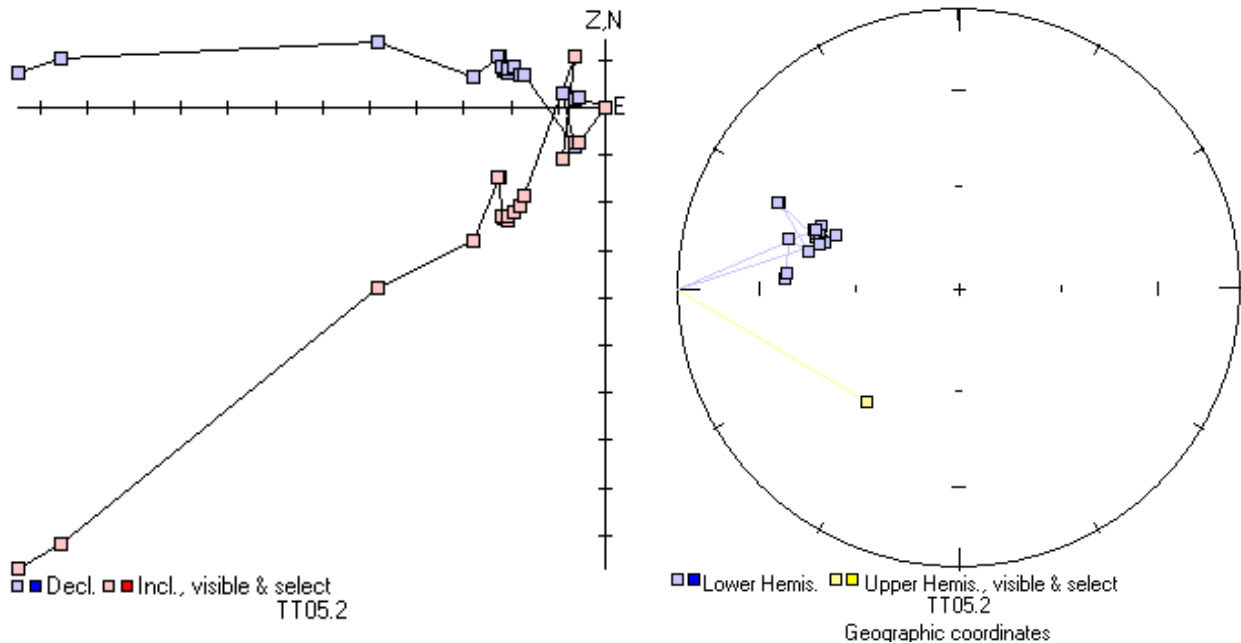


Figure 7.7: Similar to PM-4, the orthogonal plot (left) of sample number 2 of site PM-5 indicates a downward directed inclination as well as a north-western orientated declination. Some disturbing magnetic components at medium AF levels cause a scattered distribution of points within the orthogonal plot, but are removed at higher AF sequence. The equal area projection (right) confirms the north-western direction of declination. However, PM-5 is grouped together with PM-4 as palaeomagnetic sites showing a northerly downwards magnetic component. (Both pictures were generated by T. Mokgatle)

Site PM-6 (Uitkomst Sill 4)

The palaeomagnetic signature of PM-6 is covered by secondary NRM components. Soft magnetic components (SFT) at low AF demagnetisation level are removed, which is displayed as linear trend after a scattered distribution of points within the orthogonal plot (fig. 7.8). The line of demagnetisation steps move beyond the origin of the plot indicating a bad reaction to the demagnetisation sequence, probably

because of alteration effects of the ferromagnetic minerals within the samples or the location of sampling is susceptible to lightning induced magnetic components.

Apart from these secondary NRM components, site PM-6 shows an easterly horizontal directed trend (fig. 7.8). Unfortunately, this is insignificant for further interpretation, because of the reasons mentioned above.

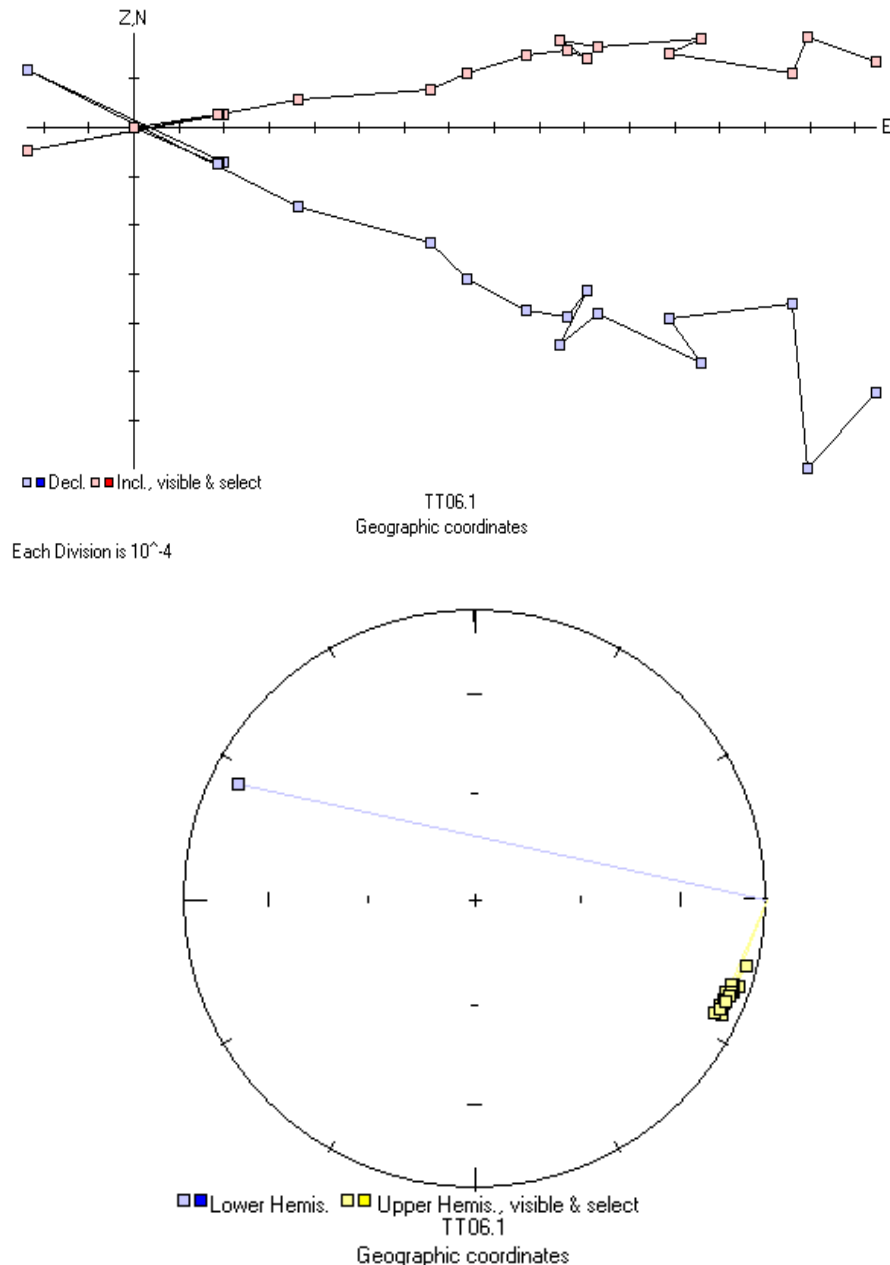


Figure 7.8: The palaeomagnetic signature of PM-6 is covered by secondary NRM components, such as SFT and LNG components causing the move of points beyond the origin within the orthogonal plot (above) of sample number 1 of PM-6. Nevertheless, a trend of horizontal inclination and eastern directed declination (equal area projection below) is slightly recognizable, but insignificant for further interpretation. (Both pictures were generated by T. Mokgatle)

Site PM-7 (Uitkomst Sill 1)

Together with PM-8, this palaeomagnetic site is sampled from microgabbro sills within the study area. The extremely scattered distribution of points at the beginning of the demagnetisation is conspicuous within the orthogonal plot (fig. 7.9), which identifies large secondary NRM components at low AF levels. After removing low-stability components, a nearly linear trend is adjusted towards the origin, which is not really exceeded. The good demagnetisation response estimates a downward trend for inclination as well as a north-easterly directed declination, which is also shown within the equal area projection (fig. 7.9). The mainly downward orientated inclination is displayed as points on the lower hemisphere with the equal area projection. The northerly downward component (ND) is similar to these from PM-4 and PM-5 and could be an indication for Bushveld direction (see subchapter 7.4).

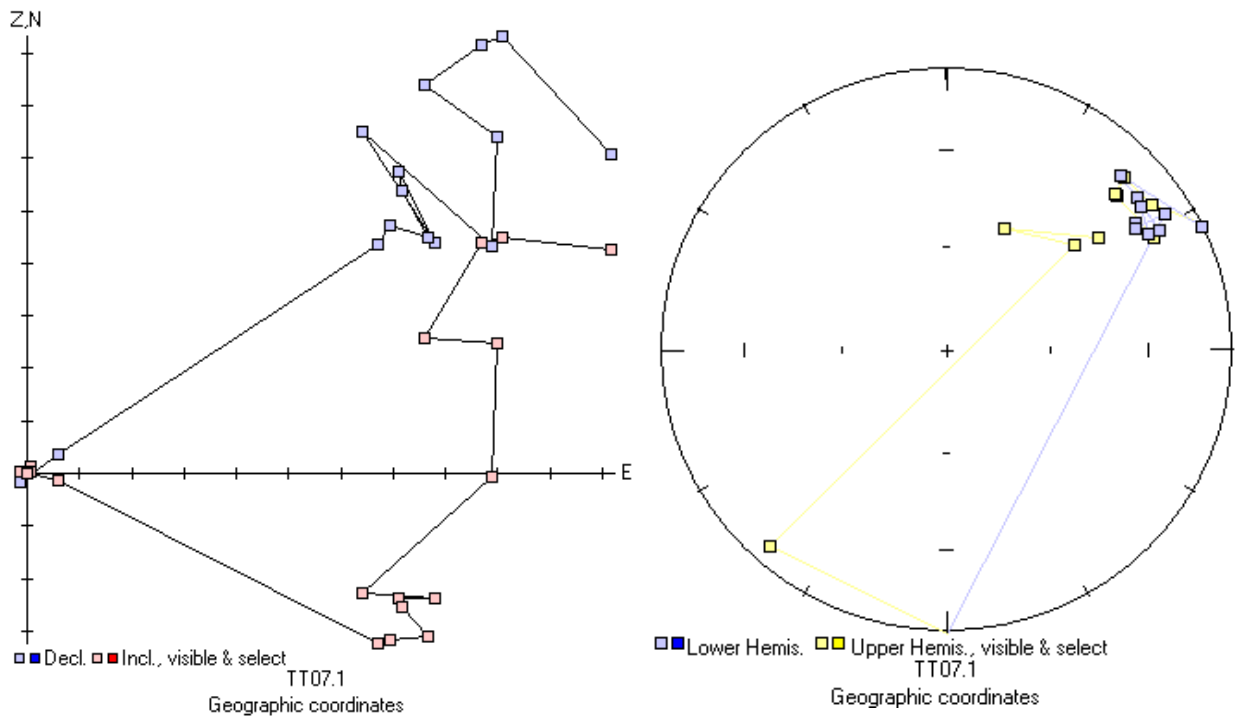


Figure 7.9: Sample number 1 of PM-7 shows a scattered distribution of points at low AF level within the orthogonal plot (left), which identifies large secondary NRM components. The following nearly linear trend indicates a downward directed inclination and a north-easterly orientated declination, which is similar to the ND component of PM-4 and PM-5. (Both diagrams were generated by T. Mokgatle)

Site PM-8 (Vaalkop Sill 2)

As described above for the PM-7, the PM-8 also shows scattered distributed points within the orthogonal plot (fig. 7.10) as a result of secondary NRM components. However, a linear trend is not really recognisable for the whole demagnetisation sequence. Furthermore the points moved beyond the origin of the plot at the end of demagnetisation, which normally expresses a bad response to demagnetisation. However the excess is minimal, so this sample site is accepted for further interpretation. Similar to PM-7, this site shows a north-easterly directed trend in declination (equal area projection, fig. 7.10) as well as a downward orientated inclination. These orientations could be an indication for a trend towards a Bushveld direction.

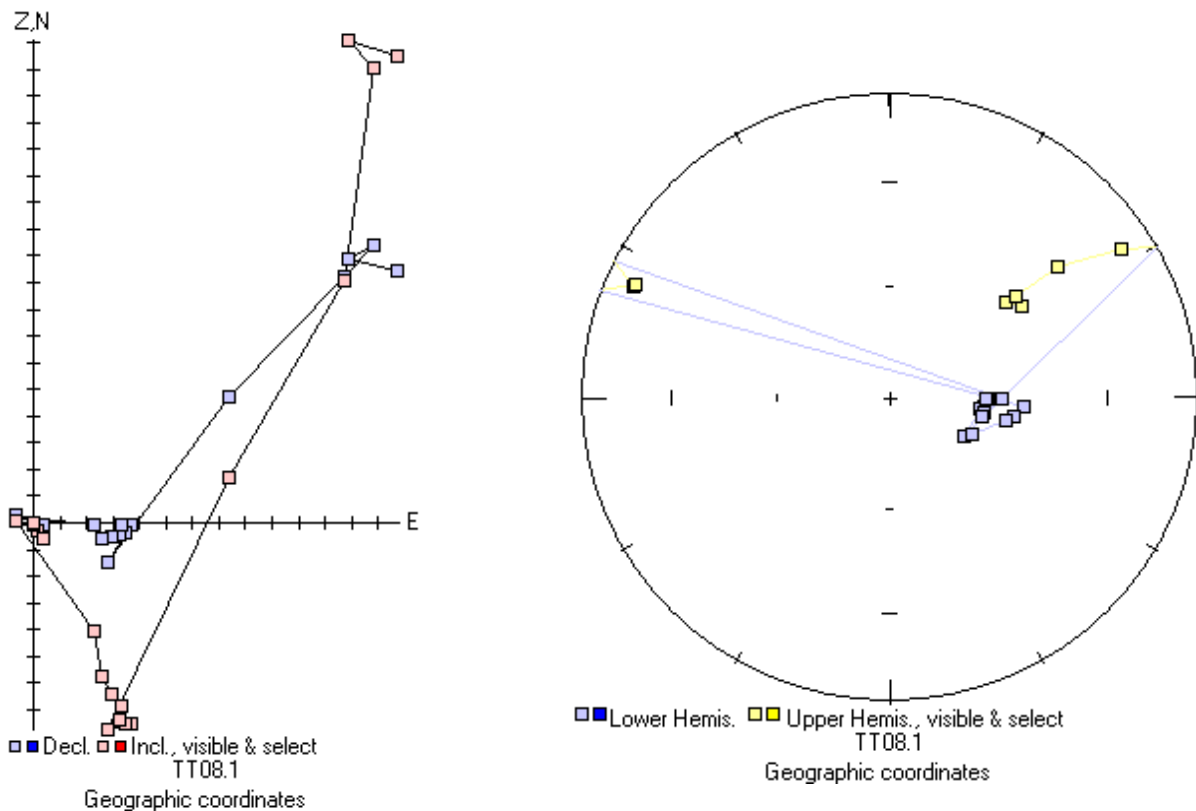


Figure 7.10: The orthogonal plot of sample number 1 of PM-8 displays no good linear trend line after removing soft components at low AF levels. Nevertheless, a north-easterly directed declination as well as a downward inclination could be identified similar to PM-7, which could give a hint for a trend to Bushveld direction. (Both plots were generated by T. Mokgatlé)

7.4 Comparison with other palaeomagnetic poles

The palaeomagnetic signature of the investigated sills and dykes retains secondary NRM components additionally to primary NRM. In case of PM-2, PM-3 and PM-6 the secondary NRM components (SFT, LNG, PLF) disturb the demagnetisation sequence such that an individual characteristic of these sites could not be estimated. The secondary NRM is mainly a result of alteration affected ferromagnetic minerals, sampling sites to nearby lightning strikes or long-term exposure to the geomagnetic field subsequent to rock formation.

The other palaeomagnetic sites responded well to demagnetisation procedures. Two different primary magnetic components are identified for these five sites, which are a southerly horizontal component (SH) for PM-1 and a nearly northerly downward component (ND) for PM-4, PM-5, PM-7 and PM-8. With the help of software applications the palaeomagnetic poles are calculated as shown in table 7.2.

Table 7.2: Palaeomagnetic poles of the identified magnetic components of this study. Dp and dm are semi-axes of the 95% confidence cone about the mean in degree.

Component	Code	Lat (°N)	Long (°E)	dp (°)	dm (°)	Palaeo-latitude
Southerly Horizontal	SH	63.7	23.4	19.5	39.1	-0.4
Northerly Downwards	ND	-1.2	65.5	36.6	44.7	48.5

The palaeomagnetic results do not really support the characterisation of the sills and dykes by petrography and geochemistry, but also do not disprove this division. Estimation of age is possible when the results are compared to palaeomagnetic poles from other events on the Kaapvaal Craton (table 7.3 and figure 7.11).

The palaeomagnetic pole of the southerly horizontal (SH) component of PM-1 is on the same position as the Umkondo palaeomagnetic pole, but wider in range than the Umkondo pole (fig. 7.11). The Umkondo igneous province is named for extensive diabase sills, which intruded into Proterozoic strata of the Umkondo Group in eastern Zimbabwe and parts of Mozambique. It also describes Proterozoic successions of sills in southern Africa including the Waterberg and Soutpansberg Group (Hanson et al., 2004). The Weltevreden sill 1, where sample PM-1 was obtained, is described as gabbronorite sill by petrography and geochemistry. Significant differences were not distinguished, which could verify the younger age of this sill compared to the other gabbronorite sills.

Table 7.3: Virtual geomagnetic poles (VGP) and palaeomagnetic poles from other events on the Kaapvaal Craton. References: (1) Hanson et al. (2004), recalculated by De Kock (2007); (2) Hanson et al. (2004); (3) De Kock (2007); (4) Hart et al. (1995), recalculated by Evans et al. (2002); (5) Morgan & Briden (1981); (6) Hattingh (1986), Hattingh (1989) and Hattingh & Pauls (1994); (7) Evans et al. (1997). Dp & dm are semi-axes of the 95% confidence cone about the mean.

Rock unit	Code	Age (Ma)	Lat (°N)	Long (°E)	dp (°)	dm (°)
Umkondo intrusions ⁽¹⁾	UMKONDO	1112 - 1106	62.7	40.6	5.8	5.8
Post-Waterberg ⁽²⁾	WSD	1872 - 1879	15.6	17.1	8.9	8.9
Waterberg 2 ⁽³⁾	WUBS2	1992 ± 62	-10.5	330.4	274.2	51.4
Vredefort VGP ⁽⁴⁾	VRED	2023 ± 4	22.3	40.7	11.6	15.7
Waterberg 1 ⁽³⁾	WUBS1	2054 ± 4	36.5	51.3	19.1	41.8
Phalaborwa 1 ⁽⁵⁾	PB1	2060.5 ± 0.6	35.9	44.8	6.9	10.5
Bushveld main and upper zones ⁽⁶⁾	BVMU	2061 ± 27	11.5	27.2	4	4
Ongeluk lava ⁽⁷⁾	ONG	2222 ± 13	-0.5	100.7	5.3	5.3
Southerly Horizontal	SH	1112-1106	63.7	23.4	19.5	39.1
Northerly Downwards	ND	?	-1.2	65.5	36.6	44.7

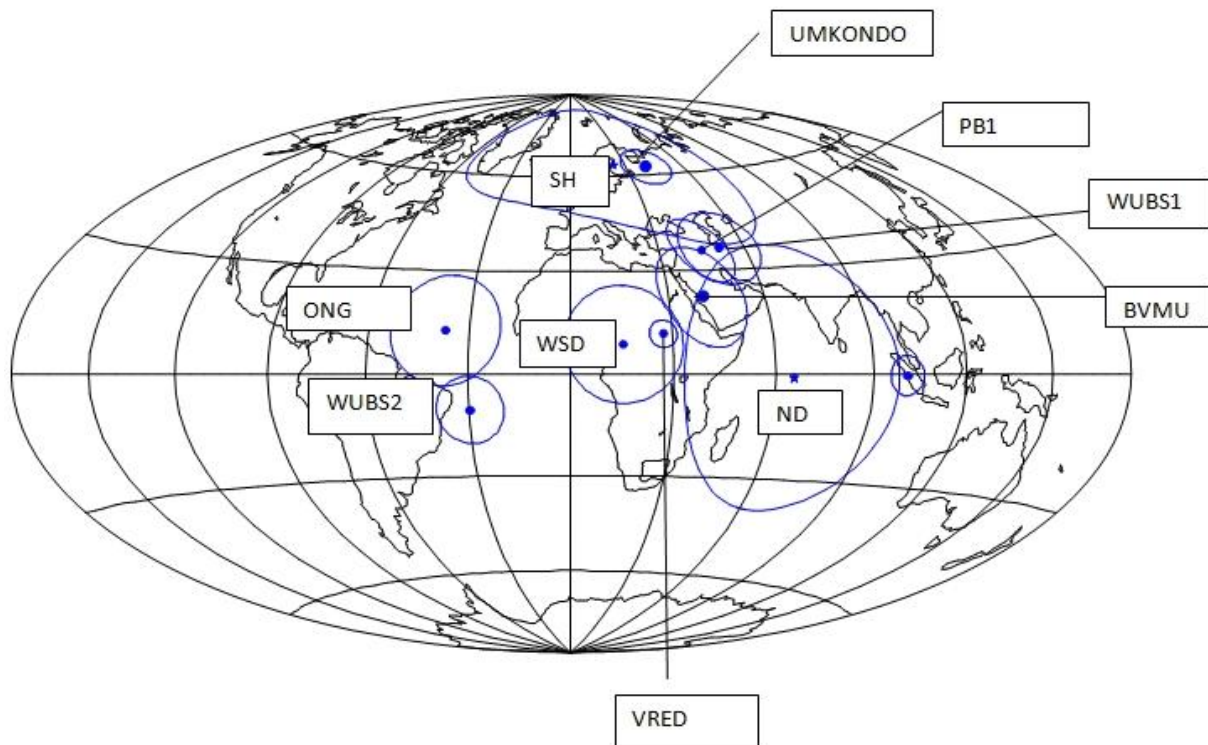


Figure 7.11: Projection of virtual geomagnetic poles (VGP) and palaeomagnetic poles from events on the Kaapvaal Craton, which are listed in table 7.3, as well as palaeomagnetic poles from own identified components (ND, SH). The ND pole overlaps part of the Bushveld main and upper zone pole (BVMU), whereas the SH pole encloses the Umkondo palaeomagnetic pole. (The picture was generated by T. Mogkatle)

The pole of the northerly downwards magnetic component (ND) of PM-4, PM-5, PM-7 and PM-8 overlaps parts of the palaeomagnetic pole of the Bushveld main and upper zone (fig. 7.11). An exactly Bushveld relation for these 4 sites cannot be estimated, because of the wide pole expansion of the ND component resulting from slightly differences in directions of the palaeomagnetic sites (described in 7.3). For a precise statement a representative study with more samples is necessary in order to postulate the age of the sills as Bushveld related.

Finally, the contrast between the palaeomagnetic age differences within the gabbronorite sill group (PM-1 of Umkondo age and PM-4 & PM-5 could be Bushveld related) is not confirmed by the petrographic and geochemical investigations. For further interpretation the classification after petrography and geochemistry is preferred due to the lack of palaeomagnetic samples for a representative palaeomagnetic study. Nevertheless, a Proterozoic age for the palaeomagnetic investigated sills is estimated.

8. Discussion

Based on field observations, petrographical as well as geochemical investigations the mafic sills and dykes are classified into three groups: **microgabbro sills**, **gabbronorite sills** and **gabbronoritic basement dykes**. To start with every single group will be discussed in detail, a theory of magma genesis will then be presented, and in conclusion a prognosis for exploration relevance will be given.

Basement dykes

The gabbronoritic basement dykes represent the oldest group of the investigated rocks within the study area due to their distribution within the Archaean Nelshoogte granite gneiss and their absence in younger stratigraphic positions, with the exception of one dyke (see below). According to Uken & Watkeys (1997) the seven northwest-trending dykes, which are shown on the geological map, belong to a dyke swarm of the same orientation. Following the investigations of Burke et al. (1985) and Uken & Watkeys (1997), the northwest-trending dykes have to be of similar age as the 2.8 Ga Usushwana Complex due to their parallel alignment. The northwest orientation of both is determined by the 3.0 Ga Pongola rift system, which was reactivated again during the emplacement of the Bushveld Complex and the Uitkomst Complex. The emplacement of the northwest-trending dykes is probably caused by northwest-southeast extension conditions of the Pongola rifting event (Burke et al., 1985). The already existing fracture system may have posed an opportunity for the intrusion of further magma (e.g. sill intrusions).

One gabbronoritic basement dyke shows a northeast-trending orientation and is hosted in Archaean granite gneiss as well as younger sediments of the Lower Transvaal Sequence (Black Reef Quartzites and Malmani Dolomites). According to Uken & Watkeys (1997) the orientation as well as stratigraphic position of this dyke suggests the relation to a northeast-trending dyke swarm further north on the Kaapvaal Craton, that was initiated by the 2.7 Ga Ventersdorp rifting event, which was the result of the collision of the Zimbabwe Craton with the Kaapvaal Craton (Burke et al., 1985). Following the rifting event, the emplacement of the single dyke took place within the upper succession of the Godwan formation belonging to the protobasinal rocks of the Transvaal Supergroup (Eriksson et al., 2001). The Godwan Formation is not preserved within the study area in contrast to the basement dykes. It seems that the dyke intruded into sediments of the younger Black Reef Formation.

The two orientations of the investigated basement dykes are attributable to rifting events of different ages, but analogical extension-mechanisms of emplacement.

Petrographic investigations of all basement dykes show similar composition and texture, only a slightly increase in quartz content (e.g. distinctive micrographic intergrowths) is observed for the dykes in southeastern direction towards the centre of the Nelshoogte pluton.

The geochemical analyses also indicate a subdivision into two different dyke groups (high Mg-low Ti and low Mg-high Ti). These are not confirmable neither with the different orientation of the dykes nor with the increasing amount of quartz. A division into a high Mg -low Ti as well as a low Mg-high Ti subgroup was also described by Hunter & Halls (1992), who investigated basement dykes throughout a larger area of the Archaean granitoid terrane. They conclude that the different geochemical trends are the result of a combination of alteration, crustal contamination and crystal fractionation. A fractionation was not observed in the field, but supported by geochemical data (negative correlation of Mg and Ti). The grade of alteration reached up to the lower greenschist facies (epidote, chlorite, calcite). Crustal contamination is inferred from local increase of quartz as distinctive micrographic intergrowths with feldspar. The average trace element composition of the investigated basement dykes is similar to the boninitic B1 magma. Also geochemical conformities in contents of SiO₂, TiO₂ and MgO for one subgroup of basement dykes suggest similar mechanism of magma development (see below), but the huge difference in age obviates any direct correlations to the genesis of the Bushveld or Uitkomst Complex.

Gabbronorite sills

The gabbronorite sills show a cord-like distribution from southwest to northeast direction and are situated in the lithological contrast zone of the Klapperkop Quartzite to the Upper Timeball Hill Shale. It hence is assumed that the quartzites form the footwall zone to the gabbronorite sills. Field observations show that larger gabbronorite sills form oval central sill bodies (up to 1.5 km at Hofmeyr Sill 1) with small tentacular offshoots, which are also restricted by the transition from quartzite to shale. The equal stratigraphic position as well as the undulating nature of the gabbronorite sills suggests a magma emplacement parallel to the compensation surface, where magma and lithostatic pressure are identical (Meyboom & Wallace, 1978; Hall, 1996). The long small offshoots are the result of the propagation of magma along bedding planes or lines of weakness at stable pressure conditions. One gabbronorite sill (Uitkomst Sill 3) is located on a lower stratigraphic position, within the Malmani Dolomites. This could be an indication for a change of the lithostatic pressure due to fractures and faults. The Uitkomst Sill 3 is orientated parallel to the Uitkomst Complex, which could suggest a similar re-utilisation of the northwest trending fracture system for the gabbronorite sill magma.

According to Cawthorn et al. (1981), the lack of chilled margins within the gabbronorite sills are explainable by a high temperature of the host rocks due to heat conduction from early magma impulses. Sharpe (1984) argued for low grade regional metamorphism as well as thermal subsidence, which generated relative warm host rocks. The latter argument seems to be more probable due to the assumption that the gabbronorite sills were not intruded after the emplacement of syn-Bushveld related magmas (e.g. Uitkomst Intrusion).

This is indicated by a higher grade of alteration compared to the relatively fresh syn-Bushveld sills. Furthermore the stratigraphic position of the gabbronorite sills is too low to be syn-Bushveld age sills, which are only intruded above the Machadodorp Formation (Sharpe, 1984).

In contrast to this assumption are similarities in trace element composition to the B1 magma composition, which is represented by quenched textured microproxenites. In some places similar quenched textures within the gabbronorite sills were observed, which are described by Sharpe (1984) for the microproxenites. They consist of elongated needles of altered pyroxene surrounded by a plagioclase intercumulus phase. However, these textures within the gabbronorites are scarce. Otherwise the occurrence of long spherulitic plagioclase laths with intergranular pyroxene indicates a more gabbroic texture and argues against a comparison with B1 microproxenites.

The B1 marginal rocks are characterised by low Ti/Zr ratios (about 25) and high contents of MgO as well as SiO₂ resulting from high crustal contamination. The gabbronorite sills however, show a negative correlation of MgO and SiO₂ at constant low TiO₂ amounts and moderate Ti/Zr ratios (40 to 60), which proposes lower contamination effects as well as a more primitive magma composition compared to the B1 reference magma. The comparisons to B2 and B3 magma compositions show no similarities. A post-Bushveld age for the gabbronorite sills can be excluded because of the stratigraphic correlation as well as the high grade of alteration.

Microgabbro sills

The microgabbro sills are intruded into country rocks of varying stratigraphical distribution, ranging from the Archaean granite gneiss to the Upper Timeball Hill shale. Noticeable is their close vicinity to other intrusions (i.e. basement dykes, gabbronorite sills and Uitkomst Complex). The thickness of the microgabbro sills vary between a few meters up to 250 m and are distinctively thinner in comparison to the huge sill bodies of the gabbronorite sills. Furthermore their distribution is not restricted on lithological contact zones and it seems that the intrusion of the microgabbro sills follows the terrain surface in a northwest-southeast direction. The field observations suggest an emplacement of microgabbroic magma along weak zones, which are induced by the emplacement of other intrusions or other previous events (e.g. Pongola rifting). This means the re-utilisation of existing fracture systems as proposed for the emplacement of the Bushveld or Uitkomst Complex (Uken & Watkeys, 1997). However, a certain direction of intrusion is not comprehensible. Microgabbro sills located within the Archaean granite gneiss terrain (e.g. Vaalkop Sill 1 & 2) are interconnected with the distribution of the different orientated basement dykes, but a parallel alignment is missing. They as such use the fracture regime of the basement dykes for their own intrusion. Similar behaviour is assumed for microgabbro sills near to the Uitkomst Complex. The Uitkomst lineament, which determines the intrusive direction of the Uitkomst Complex, was therefore used for emplacement of the microgabbro sills.

Borehole information exposed a network of gabbroic sills (diabase) cross cutting the lower part of the Uitkomst Complex (De Waal & Gauert, 1997; Gauert et al., 1995). These diabase sills are identical with the investigated microgabbro sills based on petrographical information. The injection of microgabbro magma above the Uitkomst Complex can thus be proposed. This is indicated by the distribution of microgabbro sills at the same height level on each side of the Uitkomst Complex supported by the nearly horizontal layering of the country rocks. Therefore the emplacement of microgabbroic magma is widespread, and transcends stratigraphy, which indicates a post-Bushveld/Uitkomst age of intrusion.

The high grade of alteration up to lower greenschist facies, which is proved by the occurrence of epidote and chlorite, argued against a post-Bushveld age. In general, the smaller microgabbro sills (e.g. Doornhoek Sill 1 and Weltevreden-Slaaihoek Sill 1), which intruded into shaly country rocks, show higher degrees of alteration than the larger microgabbro sills. This could be an effect of the thickness, but also of the host rock chemistry. According to Sharpe (1978), mafic magmas, which intruded into shaly rocks absorbed more water from hydrous shales. This supported the generation of hydrous alteration minerals. For example, parts of the Uitkomst Sill 1 that intruded into the Timeball Hill shale consist mainly of biotite and amphibole, only subordinate to plagioclase, whereas parts of the sill hosted by anhydrous dolomites show clearly more primary clinopyroxene as dominant mafic mineral phase.

The comparison with major and trace element contents of the gabbronorite sills and basement dykes show higher amounts of incompatible elements (Ti, Zr, Y, Sr) and lower contents of compatible elements (Ni, Cr, Mg). The magma of the microgabbro sills as such seem to be more evolved compared to the other two groups. Similar correlations are obvious in comparison with the B1, B2 and B3 magma compositions. In addition, the distinctive differences between microgabbro sills (high TiO_2 , low MgO) and gabbronorite sills as well as basement dykes (low TiO_2 , high MgO) suggest another magma derivation, which is supported by a tholeiitic magma composition for the microgabbro sills in contrast to the calc-alkaline gabbronorite sills.

Chilled margins were also rare within the microgabbro sill group, probably caused by strong weathered outcrop conditions. One distinctive very fine grained chilled margin of the Uitkomst Sill 1 was found, which is mainly composed of plagioclase and orthopyroxene suggesting, due to the fast cooling at the margin, a more noritic composition for the original microgabbro magma. This could be due to crustal contamination with Ca-rich material such as dolomites into the magma to generate Ca-rich clinopyroxene. The contamination by SiO_2 -rich material such as quartzites is low due to the low SiO_2 contents at low MgO amounts compared to the gabbronorite sills (higher SiO_2 at high MgO). A fractionation within the Uitkomst Sill 1 could also explain the different mineral composition between chilled margin and the rest of the sill. The noritic chilled margin (composed of plagioclase and orthopyroxene, fig. 5.28, p.97) could present a more primitive microgabbro melt and after differentiation the remaining microgabbro melt consists of plagioclase and clinopyroxene (fig. 5.28,

p.97). A geochemical analysis of the chilled margin is not readily available. As a matter of fact the contamination with dolomitic material as Ca supplier is relevant to generate clinopyroxene in the microgabbro instead of orthopyroxene in the chilled margin. However, the very fast cooling of chilled margins allows only a low grade of contamination with country rocks.

Magma derivation

Sources of magma were already discussed in chapter 6.4 and 6.5. The gabbronorite sills as well as the main part of the basement dykes seem to be derived from more primitive partial melts than the microgabbro sills. This is indicated by higher contents of incompatible trace elements in the microgabbro sills. Tectonic discrimination diagrams suggest a MORB environment for the microgabbro sills (see chapter 6.4, diagrams of Shervais (1982) and Hatton & Sharpe (1988)), additionally a MORB related melt is synonymous for evolved partial melts. In figure 8.1 a model for possible magma sources and evolution is given, which also gives a relative time correlation of the magma intrusion for the three groups. Based on the average element contents, the basement dykes show the most primitive composition (with highest values of Ni, Cr, MgO, and lowest values of Ti₂O, Y, Zr; see fig. 6.4, p.103), followed by the gabbronorite sills. The microgabbro sills derived from a more evolved partial melt (with highest values of Ti₂O and Fe₂O₃, extremely high P₂O₅ values; see fig. 6.4, p.103), which is developed from the primitive partial melts.

Additionally, crustal contamination is also an important feature during the emplacement of these partial melts. All three groups of investigated sills and dykes are contaminated with crustal material, which is noticeable by lower Ti/Zr ratios (40 to 70) compared to primitive magma source (Ti/Zr = 100, see fig. 6.7, p.111). Furthermore, the geochemical data have shown outlier values of the different groups, especially a few gabbronorite sills plot often within the field of the microgabbro sills. These values belong mainly to the Weltevreden Sill 1, but field observations and petrographic investigations classify them clearly as gabbronorite sill. A possible explanation could be that the gabbronorite sill melt evolves after separation from the primitive partial melt. A similar assumption is applicable for the low Mg-high Ti subgroup of the basement dykes.

The comparison with Bushveld related marginal rocks suggests conformities for the basement dykes and gabbronorite sills with the composition of the B1 magma. But according the Hatton & Sharpe (1988), the B1 magma descended from a depleted mantle source and is more contaminated with crustal material than the investigated groups, which results in high SiO₂ and high MgO contents. So an exact correlation to the B1 magma could be excluded. The source magma for the different sills is probably a less differentiated magma of B1 lineage (fig. 6.8, p.113; sample/B1), but still more evolved than B2 and B3 magma composition (fig. 6.8, p.113; sample/B2 and sample/B3).

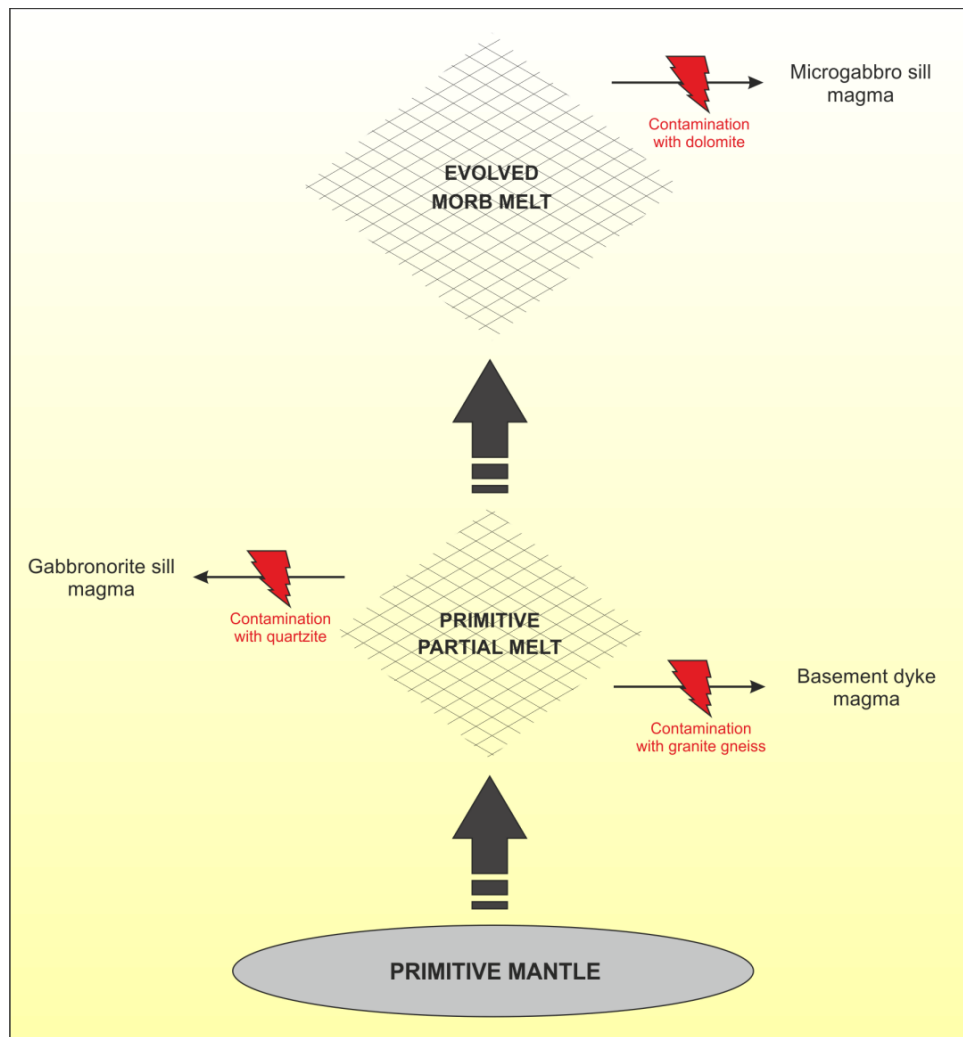


Figure 8.1: The developed schematic model illustrates the magma derivation of the three investigated groups. Gabbronorite sills and basement dykes are descended from a similar primitive partial melt composition, whereas the microgabbro sills show an evolved composition typically for MORB. The magmas of the sills and dykes were contaminated with crustal material. (Figure created by the author).

Compared to the Basal Gabbro chilled margins at Uitkomst and Slaaihoek (fig. 6.8, p.113; sample/U-chill and sample/SH-chill), the gabbronorite sills and basement dykes derived from a more primitive magma source than the Basal Gabbro unit. The composition of the microgabbro sills is conformable to the chilled margin composition or rather slightly more evolved than the magma of the Basal Gabbro chilled margins lineage, which could indicate a similar derivation. The results of the palaeomagnetic investigation (chapter 7, p.115) have identified a possible Bushveld-related direction for two microgabbro sills. This could argue for an age relationship between the Bushveld-related Uitkomst Complex and the microgabbro sills, which are similar in composition to the Basal Gabbro chilled margins. Otherwise the palaeomagnetic results are not significant to establish a possible age relationship (see chapter 7).

Relevance for exploration

Because of the proximity of the investigated mafic sills and dykes to the Uitkomst Complex, the assumption of fertile zones within the sills is obvious.

The comparison of single element contents does not reflect the total geochemical behaviour and would be too comprehensive to explain in detail. A good overview of diverse geochemical fingerprints of intrusive rocks is possible by the use of canonical variance analyses, which is based on the calculation of canonical variables. These algorithms classify all major and trace element data as well as element ratios into two groups of different weighting (fig. 8.2). It is therefore possible to use complete data sets of different intrusions for comparison.

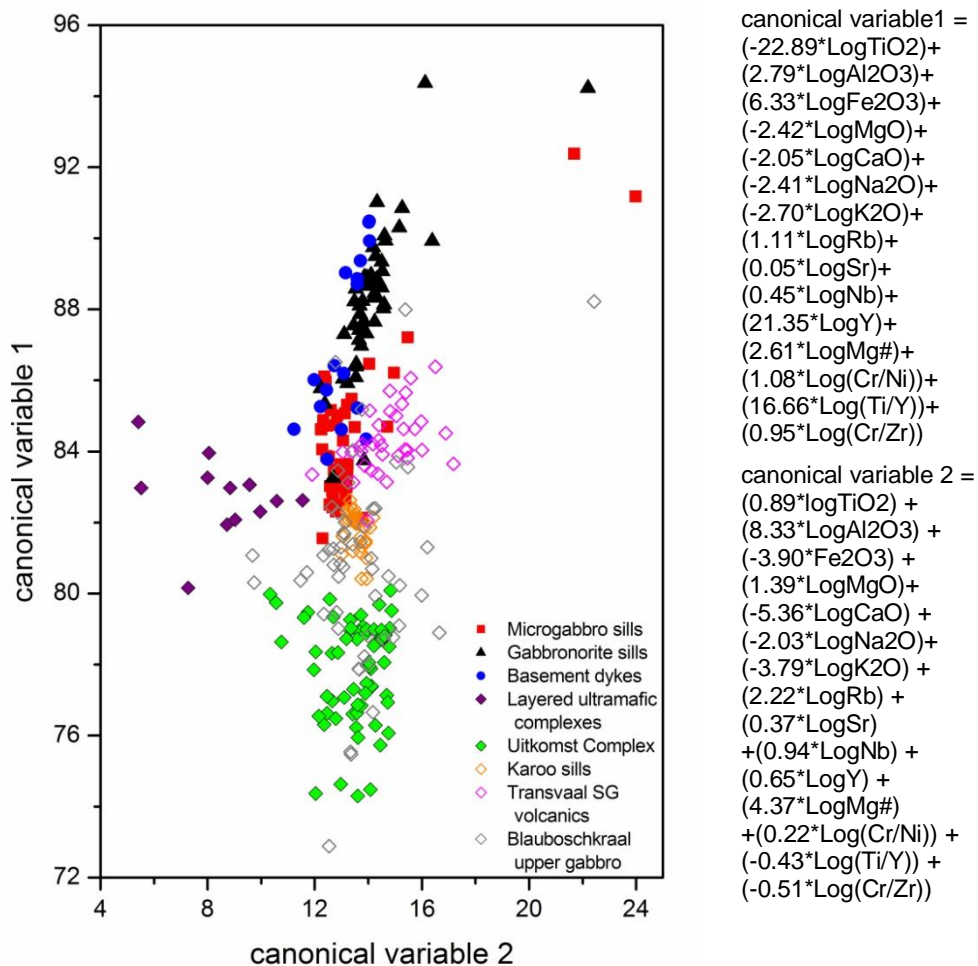


Figure 8.2: Canonical variance analyses of microgabbro sills, gabbronorite sills and basement dykes for comparison with other intrusions or volcanics. The calculation uses a multitude of element contents and ratios, which are divided into two groups of different weighting. Own investigated sills and dykes agree in value of canonical variable 2 with the Uitkomst Complex, but variable 1 is clearly different as a result of higher Ni and Cr contents of the Uitkomst Complex. (Calculation based on an excel-spreadsheet given by C. Gauert)

In figure 8.2 the XRF data of microgabbro and gabbronorite sills as well as basement dykes are correlated with data of the Uitkomst Complex, Karoo age sills, volcanics of the Transvaal Supergroup and diverse layered ultramafic complexes with similar compositions. Canonical variable 1 indicates here a higher weighting of Cr, Ni, Y, Fe, Mg#, whereas canonical variable 2 refers to a higher weighting of Sr, Nb, Rb, MgO, TiO₂. In comparison with the Uitkomst Complex the investigated sills and dykes show similarities in canonical variable 2, but clearly differences in variable 1, which contain a higher significance for the exploration relevant elements Cr and Ni. And in fact, the contents of Cr, Ni and Cu are distinctively low within the microgabbro and gabbronorite sills as well as basement dykes compared to the units of the Uitkomst Complex. Furthermore the diagram shows a close consistence of element compositions between gabbronorite sills and basement dykes, whereas the microgabbro sills are lower in canonical variable 1, which may be as a result of higher Fe amounts.

Exploration potential of the investigated sills and dykes appears to be rather low based on the given geochemical data. This is supported by petrographic investigations, which determined no significant amounts of ore bearing minerals (e.g. pentlandite, pyrrhotite, chromite) and also distinctive indicators for widespread fractionation and layering within the sills were not observed. So the investigated mafic sills and dykes can be classified as barren.

9. Conclusion

The following short list presents the most important results of this thesis:

- Basis for the geochemical investigations was the preparation of a large scale geological map (fig. 9.1), which identified in total 21 mafic sills and dykes in the vicinity of the Uitkomst Complex.

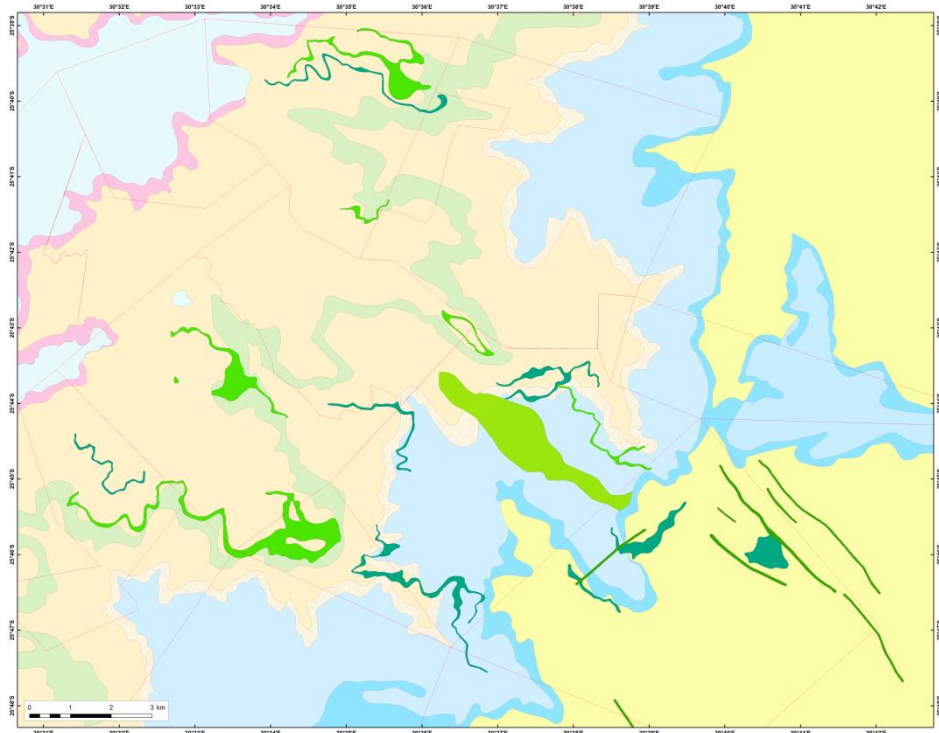


Figure 9.1: One result of this study is a geological map, which contains the three groups of investigated mafic sills and dykes in the vicinity of the Uitkomst Complex (elongated light green body in the center). (A larger geological map of the area with explanations is presented in the appendix.)

- The petrographic description classifies three groups: **microgabbro sills**, **gabbronorite sills** and **gabbronoritic basement dykes** based on modal mineral proportions and microscopical textures (e.g. sub-/ophitic, spherulitic and intergranular textures). A moderate to high grade of alteration is observable within each of the groups due to high amounts of secondary mineral phases.
- Field observations show a widespread spatial as well as stratigraphic distribution of the microgabbro sills, which are mostly of low thickness. The gabbronorite sills form huge sill bodies within a restricted stratigraphic position. The gabbronoritic basement dykes occur as prominent ridges only within the Archaean basement.

- The petrographic classification is verified by geochemical XRF data. The microgabbro sills are characterised by high TiO₂ and low MgO contents, whereas the gabbronorite sills show low TiO₂ and high MgO contents. The basement dykes are split into a high TiO₂/low MgO as well as a low TiO₂/high MgO subgroup, but generally the basement dykes show more affinity to the gabbronorite sills.
- The evaluation of the geochemical results indicate a different magma derivation for the microgabbro sills and gabbronoritic sills as well as basement dykes. The basement dykes and gabbronorites sills are descended from a primitive partial melt, whereas the microgabbro sills show an evolved magma composition. Additional contamination with crustal material changes the magma composition of each group.
- The comparison to Bushveld related marginal rocks show a similar composition of the gabbronorite sills and basement dykes to the B1 quenched textured microproxenites, which are assumed to represent the parental magma composition of the lower zone of the Bushveld Complex. The composition of the microgabbro sills indicates however no correlation to one of the Bushveld marginal rocks.
- The comparison of the geochemical fingerprints of the investigated sills and dykes with the Uitkomst Complex by using multivariate geostatistical methods show significant differences, therefore a direct correlation to the nearby Uitkomst Complex can be excluded.
- All three groups of sills and dykes can be said to be barren igneous rocks due to their low content of relevant elements (Cr, Ni, Cu) and the absence of higher volume percentages of sulphide mineralisations.

10. References

- Anhaeusser, C.R. (2001): The anatomy of an extrusive-intrusive Archaean mafic-ultramafic sequence: the Nelshoogte Schist Belt and Stolzburg Layered Ultramafic Complex, Barberton Greenstone Belt, South Africa. – *South African Journal of Geology*, 104: 167-204.
- Arndt, N.T., Naldrett, A.J. & Hunter, D.R. (1997): Ore deposits associated with mafic magmas in the Kaapvaal craton. – *Mineralium Deposita*, 32: 323-334.
- Bates, M.P. & Jones, D.L. (1996): A palaeomagnetic investigation of the Mashonaland dolerites, north-east Zimbabwe. – *Geophysical Journal International*, 126: 513-524.
- Best, M.G. (2003): *Igneous and metamorphic petrology*. Blackwell Science, Oxford, UK. 729 pp.
- Burke, K., Kidd, W.S.F. & Kusky, T.M. (1985): The Pongola structure of southeastern Africa: the world's oldest preserved rift? – *Journal of Geodynamics*, 2: 35-47.
- Butler, R.F. (1998): *Paleomagnetism: Magnetic domains to geologic terranes*. Blackwell Scientific Publications, Cambridge, USA. 319 pp.
- Button, A (1986): The Transvaal sub-basin of the Transvaal Sequence. – In: Anhaeusser, C.R. & Maske, S. (Eds.): *Mineral Deposits of Southern Africa*, Vol. I: 811-817.
- Cahen, L., Snelling, N.J., Delhal, J. & Vail, J.R. (1984): *The geochronology and evolution of Africa*. Clarendon Press, Oxford. 512 pp.
- Catuneanu, O. & Eriksson, P.G. (1999): The sequence stratigraphic concept and the Precambrian rock record: an example from the 2.3 - 2.1 Ga Pretoria Group, Kaapvaal craton. – *Precambrian Research*, 97: 215-251.
- Cawthorn, R.G., Davies, G., Clubley-Armstrong, A. & McCarthy, T.S. (1981): Sills associated with the Bushveld Complex, South Africa: an estimate of the parental magma composition. – *Lithos*, 14: 1-16.
- Clarke, B., Uken, R. & Reinhardt, J. (2009): Structural and compositional constraints on the emplacement of the Bushveld Complex, South Africa. – *Lithos*, 111: 21-36.

- Clendenin, C.W., Henry, G. & Charlesworth, E.G. (1991): Characteristics of and influences on the Black Reef depositional sequence in the eastern Transvaal. – *South African Journal of Geology*, 94 (4): 321-327.
- Cogné, J.P. (2003): PaleoMac: a Macintosh™ application for reconstructions. – *Geochemistry Geophysics Geosystems*, 4: 1007.
- Cox, K.G., Bell J.D. & Pankhurst R.J. (1979): *The interpretation of igneous rocks*. George, Allen and Unwin, London, UK. 450 pp.
- Davies, G. & Tredoux, M. (1985): The Platinum-Group Element and Gold Contents of the Marginal Rocks and Sills of the Bushveld Complex. – *Economic Geology*, 80: 838-848.
- De Kock, M.O. (2007): *Paleomagnetism of Selected Neoproterozoic Cover Sequences on the Kaapvaal Craton and Implications for Vaalbara*. PhD thesis (unpubl.). University of Johannesburg. 276 pp.
- De Ronde, C.E.J. & Kamo, S.L. (2000): An Archaean arc-arc collisional event: a short-lived (ca 3 Myr) episode, Weltevreden area, Barberton greenstone belt, South Africa. – *Journal of African Earth Sciences*, 30 (2): 219-248.
- De Waal, S.A. & Gauert, C.D.K. (1997): The Basal Gabbro Unit and the identity of the parental magma of the Uitkomst Complex, Badplaas, South Africa. – *South African Journal of Geology*, 100 (4): 349-361.
- De Waal, S.A., Maier, W.D., Armstrong, R.A. & Gauert, C.D.K. (2001): Parental Magma and Emplacement of the stratiform Uitkomst Complex, South Africa. – *The Canadian Mineralogist*, 39: 557-571.
- Eriksson, P.G. & Clendenin, C.W. (1990): A review of the Transvaal Sequence, South Africa. – *Journal of African Earth Sciences*, 10 (1/2): 101-116.
- Eriksson, P.G., Schweitzer, J.K., Bosch, P.J.A., Schreiber, U.M., Van Deventer, J.L. & Hatton, C.J. (1993): The Transvaal Sequence: an overview. – *Journal of African Earth Sciences*, 16 (1/2): 25-51.
- Eriksson, P.G., Hattingh, P.J. & Altermann, W. (1995): An overview of the geology of the Transvaal Sequence and Bushveld Complex, South Africa. – *Mineralium Deposita*, 30: 98-111.

- Eriksson, P.G. & Reczko, B.F.F. (1995): The sedimentary and tectonic setting of the Transvaal Supergroup floor rocks to the Bushveld complex. – *Journal of African Earth Sciences*, 21 (4): 487-504.
- Eriksson, P.G. & Reczko, B.F.F. (1997): Exploration initiatives in South Africa. – *Mineralium Deposita*, 32: 309-311.
- Eriksson, P.G. (1999): Pretoria Group. – In: Johnson, M.R. (Ed.): *Catalogue of South African lithostratigraphic units*, 6:29-32. SA Committee for Stratigraphy, Pretoria.
- Eriksson, P.G., Altermann, W., Catuneanu, O., Van der Merwe, R. & Bumby, A.J. (2001): Major influences on the evolution of the 2.67-2.1 Ga Transvaal basin, Kaapvaal craton. – *Sedimentary Geology*, 141-142: 205-231.
- Evans, D.A.D., Beukes, N.J. & Kirschvink, J.L. (1997): Low-latitude glaciation in the Palaeoproterozoic era. – *Nature*, 386: 262-266.
- Evans, D.A.D., Beukes, N.J. & Kirschvink, J.L. (2002): Palaeomagnetism of a lateritic paleowethering horizon and overlying Paleoproterozoic red beds from South Africa: Implications for the Kaapvaal apparent polar wander path and a confirmation of atmospheric oxygen enrichment. – *Journal of Geophysical Research*, 107 (B12): 2326-2333.
- Ferré, E.C., Bordarier, C. & Marsh, J.S. (2002): Magma flow inferred from AMS fabrics in a layered mafic sill, Insizwa, South Africa. – *Tectonophysics*, 354: 1-23.
- Frick, C. (1973): The “sill phase” and the “chill zone” of the Bushveld Igneous Complex. – *Transactions of the Geological Society of South Africa*, 76: 7-14.
- Gauert, C.D.K., De Waal, S.A. & Wallmach, T. (1995): Geology of the ultrabasic to basic Uitkomst Complex, eastern Transvaal, South Africa: an overview. – *Journal of African Earth Sciences*, 21 (4): 553-570.
- Gauert, C.D.K. (1998): The petrogenesis of the Uitkomst Complex. PhD thesis (unpubl.). University of Pretoria, South Africa. 315 pp.
- Gauert, C.D.K. (2001): Sulphide and oxide mineralization in the Uitkomst Complex, South Africa: origin in a magma conduit. – *Journal of African Earth Sciences*, 32 (2): 149-161.

- Hall, A. (1996): *Igneous petrology*. Longman Group, Essex, UK. 551 pp.
- Hanson, R.E., Crowley, J.L., Bowring, S.A., Ramezani, J., Gose, W.A., Dalziel, I.W., Pancake, J.A., Seidel, E.K., Blenkinsop, T.G. & Mukwakwami, J. (2004): Coeval large-scale magmatism in the Kalahari and Laurentian cratons during Rodinia assembly. – *Science*, 304: 1126-1129.
- Harmer, R.E. & Sharpe, M.R. (1984): Field relations and strontium isotope systematic of the marginal rocks of the Eastern Bushveld Complex. – Research Report, Institute for Geological Research on the Bushveld Complex, University Pretoria, 50. 52 pp.
- Harmer, R.E. & Von Gruenewaldt, G. (1991): Magmatism associated with the Transvaal Basin - Implications for its tectonic setting. – Research Report, Institute for Geological Research on the Bushveld Complex, University Pretoria, 91. 31 pp.
- Hart, R.J., Hargraves, R.B., Andreoli, M.A.G., Tredoux, M. & Doucouré, C.M. (1995): Magnetic anomaly near the center of the Vredefort structure: Implications for impact-related magnetic signatures. – *Geology*, 23: 277-280.
- Hartzer, F.J. (1995): Transvaal Supergroup inliers: geology, tectonic development and relationship with the Bushveld complex, South Africa. – *Journal of African Earth Sciences*, 21: 521-547.
- Hattingh, P.J. (1986): The Palaeomagnetism of the main zone of the eastern Bushveld Complex. – *Tectonophysics*, 124: 271-295.
- Hattingh, P.J. (1989): Palaeomagnetism of the upper zone of the Bushveld Complex. – *Tectonophysics*, 165: 131-142.
- Hattingh, P.J. & Pauls, N.D. (1994): New Palaeomagnetic results from the northern Bushveld Complex of South Africa. – *Precambrian Research*, 69: 229-240.
- Hatton, J & Sharpe, M.R. (1988): Significance and origin of boninite-like rocks associated with the Bushveld Complex. – Research Report, Institute for Geological Research on the Bushveld Complex, University Pretoria, 72. 44 pp.

- Henry, G., Clendenin, C.W. & Charlesworth, E.G. (1990): Depositional facies of the Black Reef Quartzite Formation in the eastern Transvaal. – Geocongress '90, Cape Town, South Africa: Abstracts, 230-233.
- Hornsey, R.A. (1999): The genesis and evolution of the Nkomati Mine Ni-sulphide deposit, Mpumalanga Province, South Africa. MSc. thesis (unpubl.). University of Natal, Durban. 223 pp.
- Hulley, V. (2005): Reactions between country rock xenoliths and the magma of the Uitkomst Complex, with implications for the origin of the sulphide mineralization. MSc. thesis (unpubl.). University of Pretoria, Pretoria. 117 pp.
- Hunter, D.R. & Reid, D.L. (1987): Mafic dyke swarms in Southern Africa. – In: Halls, H.C. & Fahrig, W.F. (Eds.): Mafic dyke swarms. Geological Association of Canada Special Paper 34: 445-456.
- Hunter, D.R. & Halls, H.C. (1992): A geochemical study of a Precambrian mafic dyke swarm, Eastern Transvaal, South Africa. – *Journal of African Earth Sciences*, 15: 153-168.
- Irvine, T.N. & Baragar, W.R.A. (1971): A guide to the chemical classification of the common volcanic rocks. – *Canadian Journal of Earth Science*, 8: 523-548.
- Jones, C.H. (2002): User-driven integrated software lives: "Paleomag" Paleomagnetic analysis on the Macintosh™. – *Computer and Geosciences*, 28: 1145-1151.
- Kenyon, A.K., Attridge, R.L. & Coetzee, G.L. (1986): The Uitkomst Nickel-Copper Deposit, Eastern Transvaal. – In: Anhaeusser, C.R. & Maske, S. (Eds.): *Mineral Deposits of Southern Africa*, Vol. I: 1009-1017.
- Kirschvink, J.L. (1980): The least squares line and plane and the analysis of palaeomagnetic data. – *Geophysics Journal of the Royal Astronomical Society*, 62: 699-718.
- Kirste, J. (2008): Reconstruction of the contact metamorphic aureole around the Ni-Cu-PGE-bearing Uitkomst Complex, near Badplaas, Mpumalanga Province, South Africa. Dipl. Thesis (unpubl.), University of Leipzig, 156 pp.

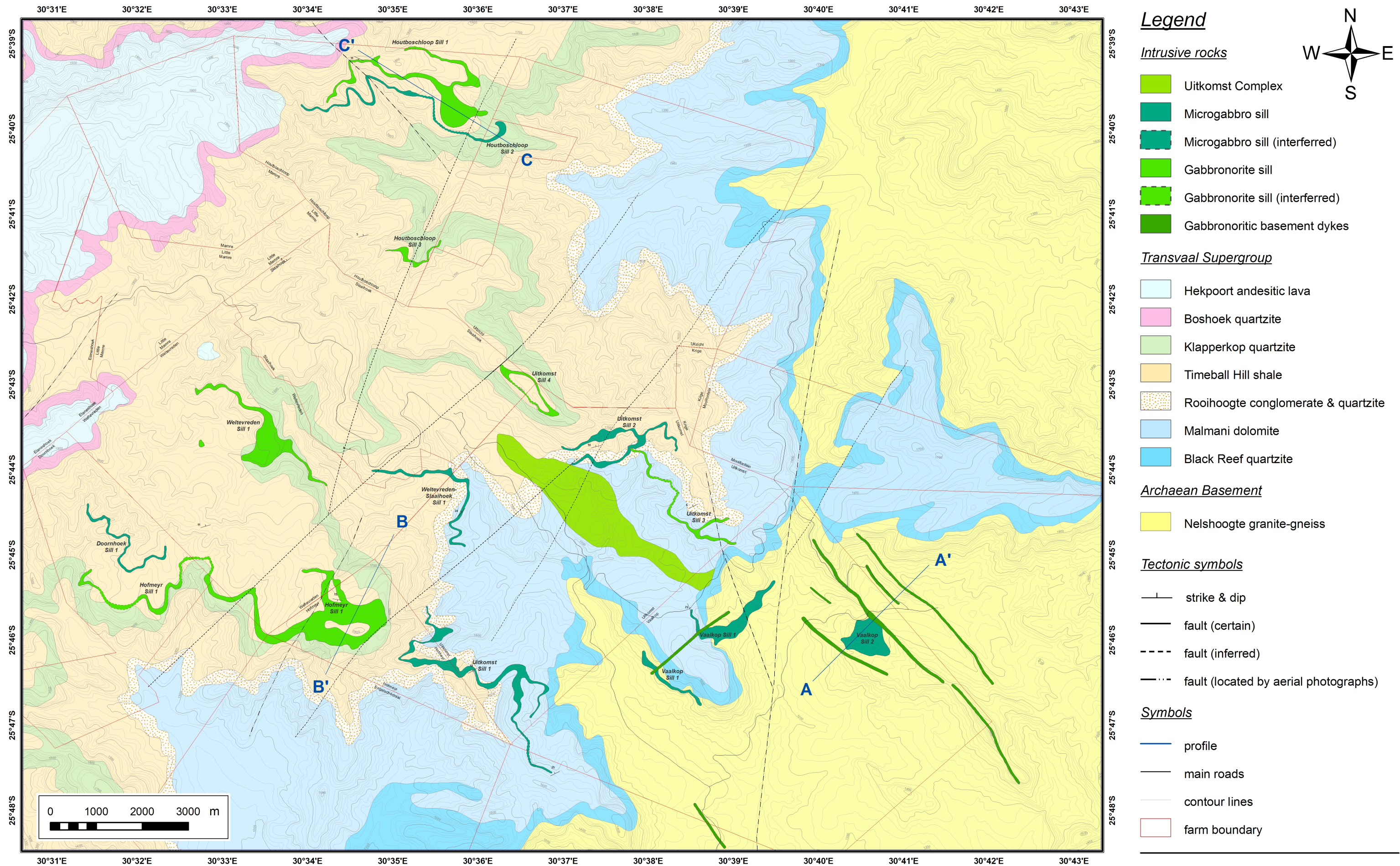
- Kruger, F.J. (2005): Filling the Bushveld Complex magma chamber: lateral expansion, roof and floor interaction, magmatic unconformities, and the formation of giant chromitite, PGE and Ti-V-magnetite deposits. – *Mineralium Deposita*, 40: 451-472.
- Layer, P.W., Lopez-Martinez, M., Kröner, A., York, D. & McWilliams, M. (1998): Thermochronometry and palaeomagnetism of the Archaean Nelshoogte Pluton, South Africa. – *Geophysical Journal International*, 135: 129-145.
- Le Maitre, R.W. (2002): *Igneous rocks: A classification and glossary of terms*. Cambridge University Press, Cambridge, UK. 236 pp.
- Li, C., Ripley, E.M., Maier, W.D. & Gomwe, T.E.S. (2002): Olivine and sulfur isotopic compositions of the Uitkomst Ni-Cu sulfide ore-bearing complex, South Africa: evidence for sulfur contamination and multiple magma emplacements. – *Chemical Geology*, 188: 149-159.
- Maier, W.D., Barnes, S.J. & De Waal, S.A. (1998): Exploration for magmatic Ni-Cu-PGE sulphide deposits: a review of recent advances in the use of geochemical tools, and their application to some South African ores. – *South African Journal of Geology*, 101 (3): 237-253.
- Maier, W.D., Li, C. & De Waal, S.A. (2001): Why are there no major Ni-Cu sulfide deposits in large layered mafic – ultramafic intrusions? – *The Canadian Mineralogist*, 39: 547-556.
- Maier, W.D., Gomwe, T.E.S., Barnes, S.J., Li, C. & Theart, H. (2004): Platinum Group Elements in the Uitkomst Complex, South Africa. – *Economic Geology*, 99: 499-516.
- Middlemost, E.A.K. (1985): *Magmas and magmatic rocks: an introduction to igneous petrology*. Longman, London. 266 pp.
- Miyashiro, A. (1974): Volcanic rock series in island arcs and active continental margins. – *American Journal of Science*, 274: 321-355.
- Morgan, G.E. & Briden, J.C. (1981): Aspects of Precambrian palaeomagnetism, with new data from the Limpopo Mobile Belt and Kaapvaal Craton in southern Africa. – *Physics of the Earth and Planetary Interiors*, 24: 142-168.

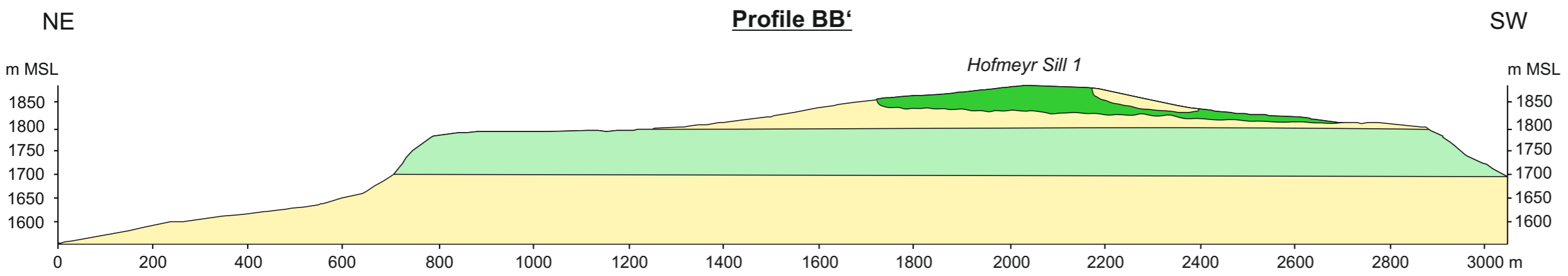
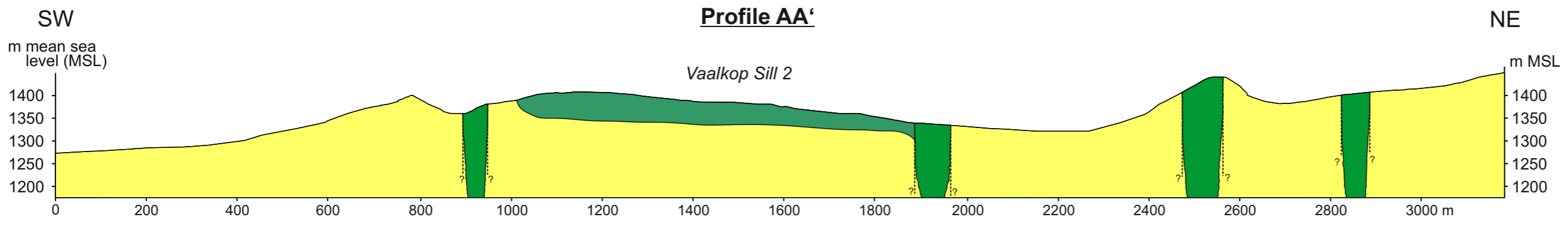
- Okrusch, M & Matthes, S. (2005): Mineralogie - Eine Einführung in die spezielle Mineralogie, Petrologie und Lagerstättenkunde. Springer Verlag, Heidelberg, Germany. 526 pp.
- Pearce, J.A. (1996): A users guide to basalt discrimination diagrams. – In: Wyman, D.A. (Ed.): Trace element geochemistry of volcanic rocks: applications for massive sulphide exploration. Geological Association of Canada, short course notes, 12: 79-113.
- Rollinson, H. (1993): Using geochemical data: evaluation, presentation, interpretation. Pearson Education, Essex, UK. 352 pp.
- Sakar, A., Ripley, E.M., Li, C. & Maier, W.D. (2008): Stable isotope, fluid inclusion, and mineral chemistry constraints on contamination and hydrothermal alteration in the Uitkomst Complex, South Africa. – *Chemical Geology*, 257: 129-138.
- Schweitzer, J & Kröner, A. (1985): Geochemistry and petrogenesis of early Proterozoic intracratonic volcanic rocks of the Ventersdorp Supergroup, South Africa. – *Chemical Geology*, 51: 265-288.
- Sharpe, M.R. (1978): “Cone-type” diabases from the Eastern Transvaal – Representatives of a quenched magma. - *Transactions of the Geological Society of South Africa*, 81: 373-378.
- Sharpe, M.R. (1980): A model for the emplacement of the eastern compartment of the Bushveld Complex. – *Tectonophysics*, 65: 85-110.
- Sharpe, M.R. (1981a): Petrology and geochemistry of Pre-Bushveld and Waterberg mafic sills. – *Transactions of the Geological Society of South Africa*, 84: 75-83.
- Sharpe, M.R. (1981b): Noble metals in the marginal rocks of the Bushveld Complex. – Research Report, Institute for Geological Research on the Bushveld Complex, University Pretoria, 30. 21 pp.
- Sharpe, M.R., Bahat, D. & von Gruenewaldt, G. (1981): The concentric elliptical structure of feeder sites to the Bushveld Complex and possible economic implications. – *Transactions of the Geological Society of South Africa*, 84: 239-244.
- Sharpe, M.R. & Chadwick, B. (1982): Structures in Transvaal sequence rocks within and adjacent to the Eastern Bushveld Complex. – *Transactions of the Geological Society of South Africa*, 85: 29-41.

- Sharpe, M.R. (1984): Petrography, classification and chronology of mafic sill intrusions beneath the eastern Bushveld Complex. Geological Survey of South Africa, Bulletin 77. 40 pp.
- Sharpe, M.R. & Hulbert, L.J. (1985): Ultramafic Sills beneath the Eastern Bushveld Complex: Mobilized Suspensions of Early Lower Zone Cumulates in a Parental Magma with Boninitic Affinities. – *Economic Geology*, 80: 849-871.
- Shervais, J.W. (1982): Ti-V plots and the petrogenesis of modern and ophiolitic lavas. – *Earth and Planetary Science Letters*, 59: 101-118.
- Streckeisen, A. (1976): To each plutonic rock its proper name. – *Earth-Science Reviews*, 12: 1-33.
- Uken, R. & Watkeys, M.S. (1997): An interpretation of mafic dyke swarms and their relationship with major mafic magmatic events on the Kaapvaal craton and Limpopo Belt. – *South African Journal of Geology*, 100: 341-348.
- Van Eeden, O.R. (1936): Geological map of the Eastern Transvaal 1: 100.000. – Geological Survey of South Africa.
- Viljoen, M.J. & Reimold, W.U. (1999): An introduction to South Africa's geological and mining heritage. Mintek, Randburg, South Africa. 193 pp.
- Visser, J.N.J. (1970): The Transvaal Basin - A new sedimentary model? – *Annual of the Geological Survey of South Africa*, 8: 75-85.
- Von Gruenewaldt, G., Sharpe, M.R. & Hatton, C.J. (1985): The Bushveld Complex: Introduction and Review. – *Economic Geology*, 80: 803-812.
- Von Scheibler, W.H.T.M., Cawthorn, R.G., Kenyon, A.K. & Allen, I.V.L. (1995): Ni-Cu sulphide mineralization in the Uitkomst Intrusion. – In: *Extended Abstracts of the Centennial Geocongress (1995)*. Geological Society of South Africa, Johannesburg: 133-136.
- Wagner, P.A. (1929): *The Platinum Deposits and Mines of South Africa*. Oliver and Boyd; Edinburgh, London. 326 pp.

- Walraven, F. & Martini, J. (1995): Zircon Pb-evaporation age determinations of the Oak Tree Formation, Chuniespoort Group, Transvaal Sequence: implications for Transvaal-Griqualand West basin correlations. – *South African Journal of Geology*; 98: 58-67.
- Ward, J.H.W. (2002): Explanation of the metallogenic map sheet 2530 Barberton. Council of Geoscience, South Africa. 67 pp.
- Willemsse, J. (1959): The “floor” of the Bushveld Igneous Complex and its relationships, with special reference to the eastern Transvaal. – *Transactions of the Geological Society of South Africa*, 62: 21-83.
- Woolfe, J.A.S. (1996): The Nkomati Joint Venture - A nickel mine in the making. – *Geobulletin*, 39 (1): 5-7.

Geological map of regional mafic sills and dykes in the vicinity of the Uitkomst Complex, South Africa

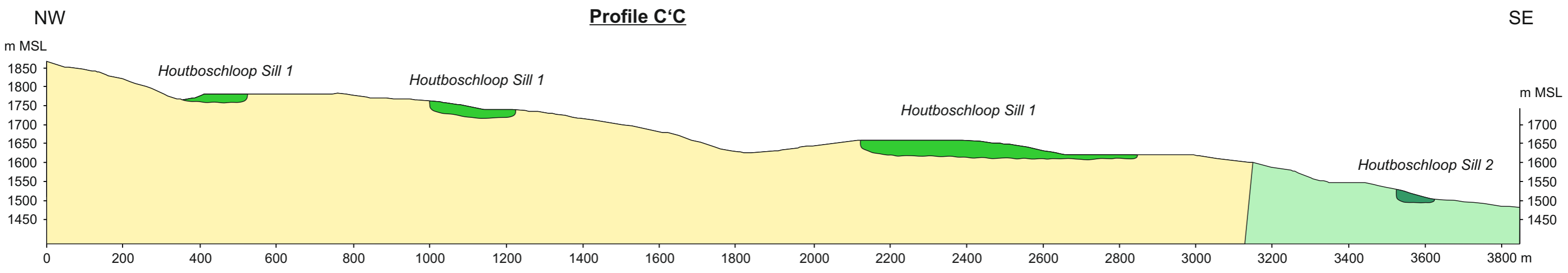




Legend

- Microgabbro sills
- Gabbro sills
- Basement dykes
- Klapperkop quartzite
- Timeball Hill shale
- Nelshoogte granite gneiss

1 : 10.000
scale for all profiles



APPENDIX

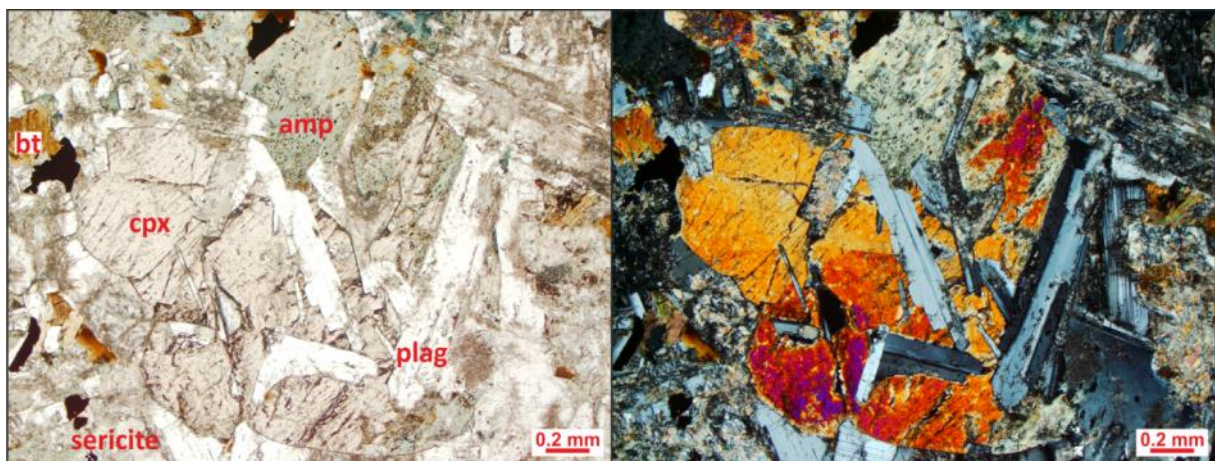
Thin section	U_11-7_3/1
--------------	------------

GENERAL DESCRIPTION	Medium grained, strong altered, idiomorphic to hypidiomorph rock of gabbronoritic composition. The typical gabbro texture shows subophitic to ophitic enclosed plagioclase laths in pyroxene or amphibole as well as intergranular pyroxene.
---------------------	--

mineral	%	grain size (mm)	comments
Plagioclase	30	≤ 2.0	euhedral - subhedral; fresh lath-shaped & prismatic crystals, which show polysynthetic twins and are subophitic - ophitic enclosed by px; also small tabular crystals as granular interstitial filling with strong centric alteration (saussuritisation), An-content: 60-65
Quartz	6	0.5	subhedral - anhedral, granular interstitial patches as well as single crystals between plag, yellowish (thick section)
Clinopyroxene	20	1.6	euhedral - subhedral, prismatic/tabular to granular, pale brown, low pleochroic, inclined extinction (43° → augite), twinning, marginal alteration to amp
Orthopyroxene	10	1.0	subhedral, stubby prismatic, colorless to pale green brown, low interference colors, cleavage angles near 90°, parallel extinction, marginal alteration to amp
Amphibole	10	≤ 1.2	subhedral, prismatic to short columnar, partly fibrous, greenbrown, strong pleochroic, hexagonal end section with 60°-120° cleavage angles, inclusions of fine magnetite
Biotite	8	≤ 0.8 (Ø 0.2)	euhedral - anhedral, tabular to platy/flaky, brown, pleochroic halos around zircons, birds-eye structure
Chlorite	4 - 6	≤ 0.2	anhedral, flaky to fibrous, green blue, pleochroic halos around zircon, anomalous yellow interfere. colors, intergrown with biotite
Calcite	1 - 2	0.4	anhedral, granular, colorless, parallel twins, high order interference colors, alteration product of plag
further alteration minerals	7	< 0.1	anhedral, sericite and clay minerals as further alteration-products of plag, intergrowth with biotite, chlorite & amphibole
Fe-Ti-oxides	2 - 3	0.5	multilateral, hackly to skeletal shapes, mixture of magnetite (isotropic), titanomagnetite (low anisotropic), ilmenite (anisotropic)
Sulphides	< 1	0.6 (Ø 0.1)	single pyrite cubes, framboidal aggregates as well as fine disseminated grains of pyrite, isotropic, light yellow

COMPOSITION	gabbronoritic
-------------	----------------------

CLASSIFICATION	medium grained, altered Microgabbro
----------------	--



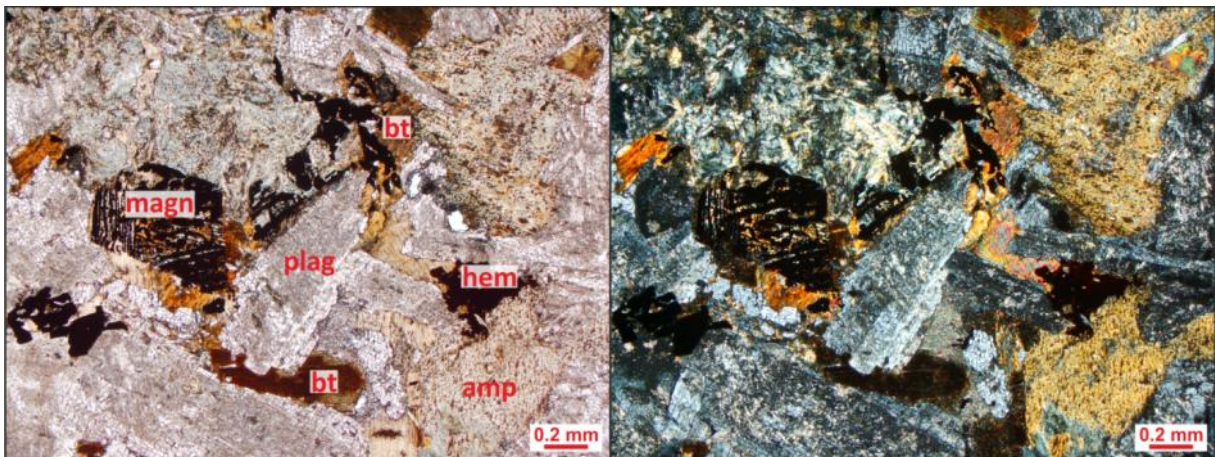
Plagioclase laths enclosed by clinopyroxene, which is altered to amphibole at the crystal margins.

Thin section	VK_13-6_3/1
--------------	-------------

GENERAL DESCRIPTION	Medium grained, highly altered, hypidiomorphic rock of gabbroic composition. Small plagioclase is subophitic to ophitic enclosed by pyroxene or amphibole, which fill also the interstices between larger plagioclase laths.
---------------------	--

mineral	%	grain size (mm)	comments
Plagioclase	30 - 35	≤ 3.2	euhedral - subhedral, prismatic to lath-shaped, polysynthetic twins, fresh as well as strong centric alteration to sericite, ophitic enclosed by px/amp, An-content: 45-55
Quartz	3	0.5	anhedral, granular, colorless, undulated extinction is rare, interstitial patches of quartz crystals between plag
Pyroxene	12	< 1.0	sub- to anhedral, stubby prismatic to short columnar, pale brown, only fragments are preserved, because of the strong alteration to amp, opx and cpx are difficult to difference, but probably more cpx
Amphibole	25	1.6	sub- to anhedral, prismatic to short columnar, green to brown, partly fibrous (actinolite), pleochroic, inclined extinction (15° - 22° → hbl, actinolite), pseudomorphic after px, inclusions of fine magnetite
Biotite	8 - 10	0.6	sub- to anhedral, tabular to platy/flaky, brown, pleochroic halos around zircons, birds-eye structure, intergrown with Fe-Ti-oxides
Calcite	3	0.5	anhedral, granular, colorless, parallel twins, high order interference colors, surrounded by plagioclase, alteration product
Further alteration minerals	10	≤ 0.1	anhedral, fine sericite and fibrous chlorite with anomalous interference colors
Fe-Ti-oxides	3	0.5 - 0.7	multilateral to skeletal shapes, mostly magnetite (isotropic), hematite (red reflections) and ilmenite (anisotropic)

COMPOSITION	gabbroic
CLASSIFICATION	medium grained, highly altered Microgabbro



A subhedral plagioclase crystal (middle) is surrounded by brown biotite, green-blue chlorite and skeletal opaque minerals, which could be identified as magnetite and hematite. The green brown amphibole crystal (top right) includes ophitic very small laths of plagioclase.

Thin section	W_17-7_7/1
--------------	------------

GENERAL DESCRIPTION	Medium grained, highly altered, hypidiomorphic to xenomorphic rock of original dioritic to gabbroic composition. The whole pyroxene is altered to secondary amphibole, but also primary hornblende occurs. The gabbroic texture is preserved; plagioclase is subophitic enclosed by amphibole. Orientated magnetite laths are remarkable.
---------------------	---

mineral	%	grain size (mm)	comments
Plagioclase	30 - 35	1.5	euohedral - subhedral, lath-shaped to short prismatic/tabular or interstitial filling, polysynthetic twins, strong altered to sericite and saussurite, subophitic to ophitic enclosed by amphibole
Quartz	3	< 0.2	anhedral, less single crystals between plag, no undulatory extinction
Amphibole	20 - 25	1.0	anhedral, stubby prismatic to columnar or fibrous (actinolite), pale green to greenblue, pleochroic, inclined extinction (25° → hornblende), fine magnetite inclusions in hbl, intergrowth with biotite and Fe-Ti-oxides, alteration product (uralitisation) of px (not in thin section)
Biotite	8	≤ 0.5	anhedral, platy to flaky, brown, pleochroic, birds-eyes extinction, pleochroic halos around zircon, intergrown with amp
Chlorite	12	0.3	an- to subhedral, flaky to fibrous, green, pleochroic, Mg-chlorite (anomalous yellow interfer. colors) is arranged in larger patches (up to 2.5 mm) and intergrown with bt & calcite, also small aggregates of Fe-chlorite (anomalous blue interference colors)
Epidote	4	0.4	sub- to anhedral, granular to short prismatic, colorless, shiny interference colors, alteration product of plag
Further alteration minerals	7	< 0.1	anhedral, mainly fine sericite enclosed in plag crystals, also calcite & zoisite together with bt, chl and epidote
Fe-Ti-oxides	5	0.1 - 2.4	relative high amounts, skeletal & multilateral shapes of magnetite with exsolution lamellae of ilmenite, also long magnetite laths (up to 2.4 mm), which are parallel arranged in groups
Sulphides	< 1	0.1	grains of light yellow pyrite and deep yellow to orange (tarnishing) anisotropic chalcopyrite

COMPOSITION	gabbroic (original)
CLASSIFICATION	medium grained, highly altered, hornblende bearing Microgabbro



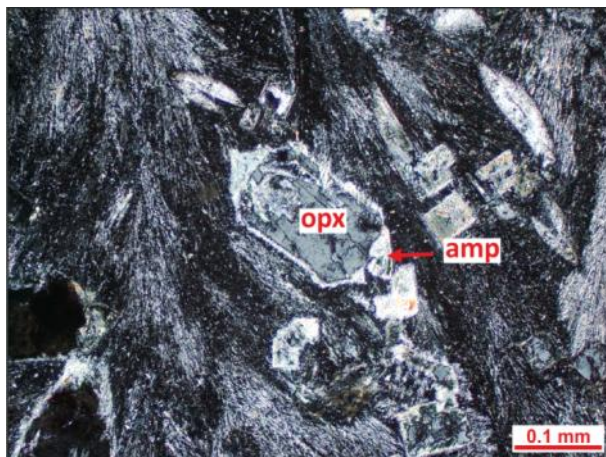
Short prismatic plagioclase crystals are surrounded and penetrated by chlorite, biotite, amphibole and Fe-Ti-oxides. A big anhedral biotite crystal (middle left) shows a pleochroic halo around a zirconium crystal. Groups of parallel orientated magnetite laths occur only in this thin section.

Thin section	VK_23-7_1/1
--------------	-------------

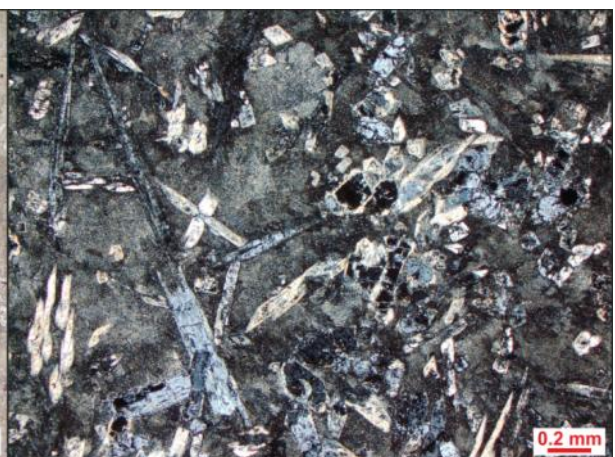
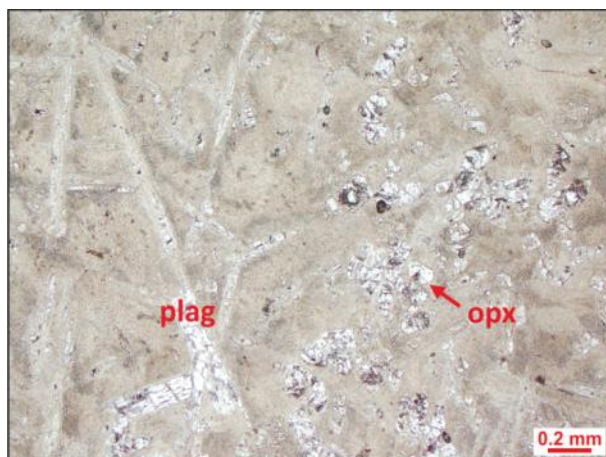
GENERAL DESCRIPTION	Chilled Margin. Very fine grained groundmass of variolitic plag, quartz, further alteration minerals and glass with elongated to lath-shaped as well as stubby prismatic phenocrysts of plagioclase and orthopyroxene. Microporphyritic texture.
---------------------	--

Mineral	%	grain size (mm)	comments
Plagioclase	12	≤ 1.2	euhedral - subhedral, lath-shaped to long prismatic phenocrysts, colorless, twinning, altered to sericite
Orthopyroxene	18	< 0.8	euhedral to anhedral, lath-shaped/long prismatic to stubby prismatic/short columnar phenocrysts, colorless, low order interference colors, square or octagonal basal sections, parallel extinction, marginal alteration to amp and clay minerals
Amphibole	5	-	euhedral - anhedral, only as rim/corona around opx crystals, which forms hexagonal basal sections around octagonal opx basal sections
Sulphides	< 1	< 0.05	very fine pyrite grains within the opx or amp crystals, not in groundmass
Groundmass	65	-	consist of very fine variolitic arranged plagioclase ± quartz ± sericite & clay minerals ± glass,

COMPOSITION	noritic
CLASSIFICATION	fine grained, low altered Chilled Margin



In picture left a subhedral orthopyroxene crystal, which forms an octagonal basal section, is surrounded by amphibole. Notice the hexagonal shape of cream white amphibole. The orthopyroxene phenocryst lies in a very fine groundmass of variolitic arranged plagioclase fibres. The lower pictures show lath-shaped plagioclase and stubby prismatic orthopyroxene phenocrysts in pale brown groundmass. The phenocrysts are often encircled by a rim of alteration minerals like amphibole or clay minerals.



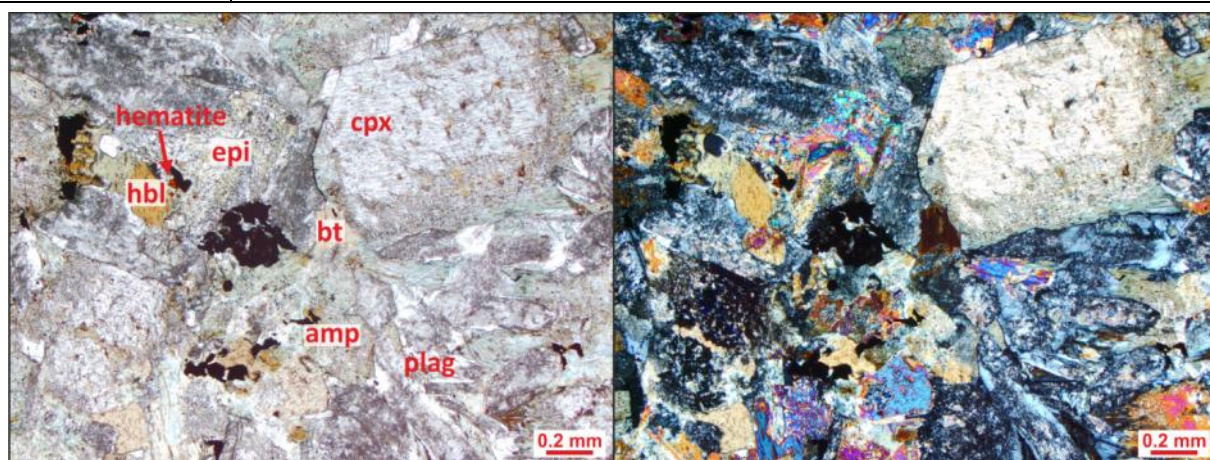
Thin section	VK_8-6_5/2
--------------	------------

GENERAL DESCRIPTION	Fine to medium grained, strong altered, hypidiomorph rock of gabbroic composition. Small plagioclase laths are subophitic to ophitic enclosed in px or amp. Some single euhedral cpx crystals are noticeable as well as the relative high amount of obvious primary hornblende.
---------------------	---

mineral	%	grain size (mm)	comments
Plagioclase	25 - 30	≤ 2.8 (Ø 1.2)	euhedral to subhedral, lath-shaped to prismatic crystals, many polysynthetic twins, zoning, subophitic - ophitic enclosed by px/amp, also small tabular crystals as granular interstitial filling, fresh as well as strong centric alteration (sericitisation), An-content: 65-75
Quartz	3	0.1	sub- to anhedral, granular, less single crystals between plag
Clinopyroxene	15	≤ 1.2	euhedral - subhedral, long prismatic to tabular, pale brown, inclined extinction (43° → augite), octagonal basal sections, twinning, marginal alteration to amp, also centric alteration to clay minerals, single larger euhedral crystals (up to 1.2 mm)
Orthopyroxene	< 5	0.5	anhedral, stubby prismatic, colorless to pale green brown, low order interference colors, parallel extinction, marginal alteration to amp
Amphibole	20	0.9	sub- to anhedral, long prismatic to short columnar, green-brown, strong pleochroic, inclined extinction (23° → hornblende), hexagonal end section with 60°-120° cleavage angles, inclusions of fine magnetite, alteration product as well as primary hornblende
Biotite	6	0.2	anhedral, platy to flaky, brown, pleochroic, parallel extinction, birds-eye structures, intergrowth with amp
Epidote	4 - 6	0.4	anhedral, granular, colorless to pale citreous, typical shiny interference colors with color-zonation from core to margin
Further alteration minerals	10	≤ 0.1	anhedral, next to biotite and epidote also fibrous chlorite, fine sericite and twinned calcite resulted from plag alteration
Fe-Ti-oxides	3 - 4	0.2	hackly to skeletal shapes, mixture of hematite (red reflections), magnetite, ilmenite and white leucoxene
Sulphides	< 1	≤ 0.1	light yellow, isotropic pyrite intergrown with magnetite, also fine disseminated grains of pyrite

COMPOSITION	gabbroic
-------------	-----------------

CLASSIFICATION	medium grained, strongly altered, hornblende bearing Microgabbro
----------------	---



In a mixture of nearly epigranular alteration minerals (epidote, biotite, sericite, amphibole), primary hornblende and plagioclase is one big cpx crystal, which altered marginal to amphibole. Notice the small red grains of hematite next to the opaque minerals.

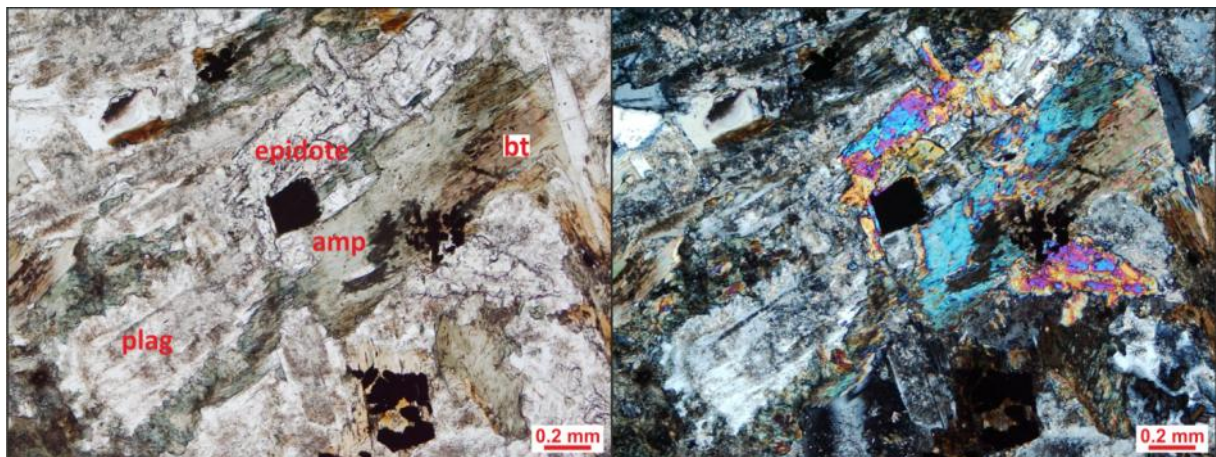
Thin section	U_19-6_7/1
--------------	------------

GENERAL DESCRIPTION	Medium grained, highly altered, hypidiomorph rock of original dioritic to gabbroic composition. Probably contact metamorphic affected. The whole pyroxene is altered to secondary amphibole, but also primary hornblende occurs. The gabbroic texture is preserved; plagioclase is ophitic enclosed by amphibole.
---------------------	---

mineral	%	grain size (mm)	comments	
Plagioclase	40	≤ 2.4	euhedral - anhedral, lath-shaped & prismatic crystals as well as granular interstitial filling, polysynthetic twins, mostly centric alteration (sericitisation & saussuritisation), subophitic to ophitic enclosed by amphibole, Anorthite-content: 40-50	
Quartz	5	0.4	anhedral, undulatory extinction, granular interstitial patches & single crystals between plag, yellowish (thick section)	
Amphibole	Actinolite	18	0.8	sub- to anhedral, fibrous, acicular, as aggregates, lightly green, inclined extinction, together with chlorite, alteration product of hornblende
	Hornblende	12	1 - 1.2	sub- to anhedral, prismatic, blue-green to green-brown, strong pleochroic, corroded margins, typical cleavage angles (60°/120°), altered to actinolite, magnetite & biotite
Biotite	8	0.6	sub- to anhedral, platy, flaky, brown, pleochroic, birds-eyes extinction, pleochroic halos around zircon, intergrown with amp & magnetite	
Chlorite	5	< 0.2	anhedral, flaky to fibrous, pale green, pleochroic, anomalous blue & yellow interference colors (Mg and Fe chlorite), arranged in bubble-like clusters, alteration product of plag	
Epidote	4	0.3	anhedral, granular, colorless, shiny interference colors with patchy color distribution, alteration product	
further alteration minerals	5	< 0.1	anhedral, mainly sericite and calcite, mostly in the centre of primary minerals like plagioclase	
Fe-Ti-oxides	3	≤ 0.8 (Ø 0.2)	skeletal or multilateral shapes, mainly magnetite with exsolution lamellae of ilmenite, intergrowth with bt, amp	
Sulphides	< 1	≤ 0.1	grains of light yellow pyrite, sometimes tarnishing, framboidal arranged	

COMPOSITION	gabbroic (original)
-------------	----------------------------

CLASSIFICATION	medium grained, highly altered, hornblende bearing Microgabbro
----------------	---



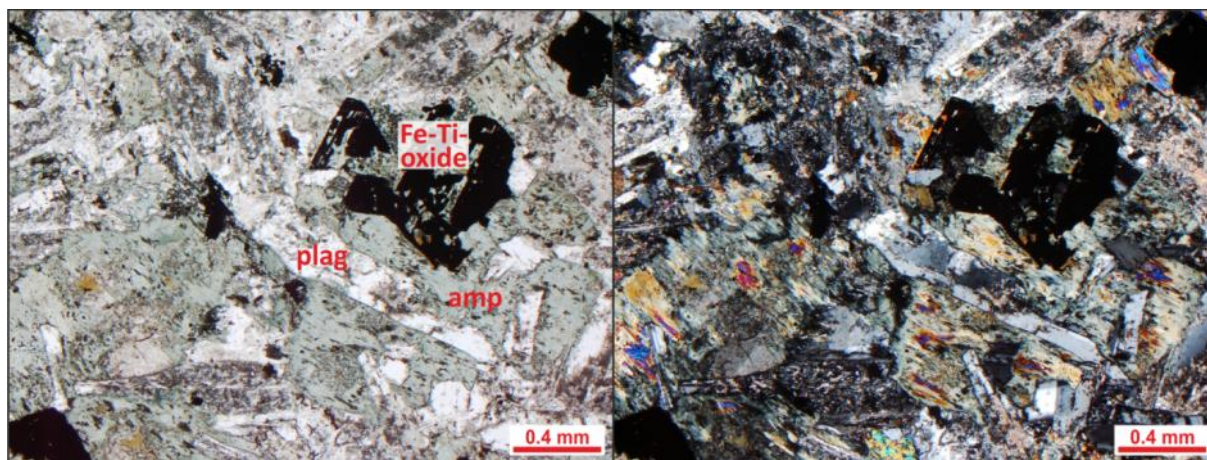
The prismatic plagioclase is saussurised into a mixture of epidote (shiny interference colors), sericite and chlorite. An amphibole crystal (hornblende) is intergrown with biotite at the margin. The opaque minerals are magnetite and ilmenite.

Thin section	UZ_8-7_6/1
--------------	------------

GENERAL DESCRIPTION	Medium grained, highly altered rock of gabbroic composition. Pyroxene is nearly completely replaced by amphibole. Subophitic to ophitic texture. Relative high amount of skeletal Fe-Ti-Oxides.
---------------------	---

mineral	%	grain size (mm)	comments
Plagioclase	35	< 2.0	euhedral - subhedral, lath-shaped to tabular, polysynthetic twins (An ₆₀ : Labradorite), fresh as well as altered (seritization), poikilitic enclosed by amp or px
Quartz	4	0.2	subhedral - anhedral, undulatory extinction, interstitial patches between plag
Amphibole	20	< 2.0	subhedral - anhedral, prismatic to columnar, marginal fibrous, green, tiny magnetite inclusions, alteration product of px (actinolite), partly pseudomorphic after px
Pyroxene	7	-	anhedral, highly altered to amp, extant as fragments surrounded by amp, mainly clinopyroxene
Biotite	3	0.2	anhedral, flaky, brown, strong pleochroic, birds-eyes structure, intergrown at amp-margins,
Chlorite	8	< 0.5	subhedral - anhedral, flaky, fibrous to felted, pale green to green blue, anomalous blue and yellow interference colors (Mg and Fe chlorite), alteration product of plag
Epidote	4	< 0.4	anhedral, pale yellow, intensive multiple interference colors, fine disseminated as well as irregular accumulations, alteration product
Saussurite & Sericite	10	< 0.2	alteration products of plag: Sericite, Zoisite, Calcite (additionally to chlorite & epidote)
Fe-Ti-oxides	5	< 1.2	skeletal, hackly-shaped or 3 to 4 sided shapes, mixture of primary magnetite, ilmenite, titanomagnetite and secondary leucoxene, mostly at amp-margins
Sulphides	< 1	0.3	fine disseminated or intergrown with oxides, light yellow (Pyrite) and deep yellow (Chalcopyrite)

COMPOSITION	gabbroic
CLASSIFICATION	medium grained, highly altered Microgabbro



Plagioclase is subophitic enclosed by amphibole, which is an alteration product of pyroxene. Magnetite appears as tiny inclusions in amphibole as well as multilateral shapes together with ilmenite (opaque minerals in thin section).

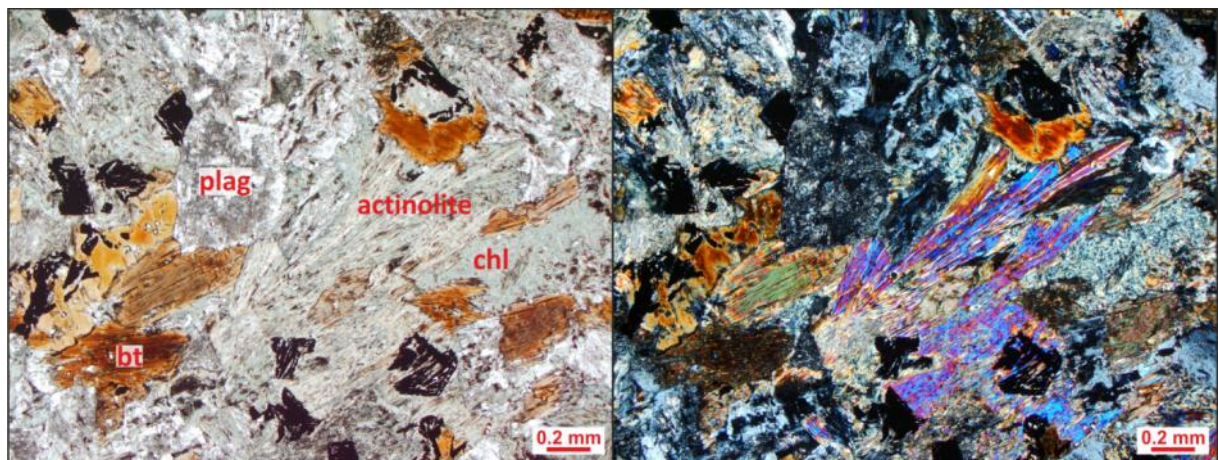
Thin section	U_22-6_3/1
--------------	------------

GENERAL DESCRIPTION	Medium grained, highly altered, hypidiomorph rock of original gabbro-noritic composition. The preserved gabbro texture shows subophitic to ophitic enclosed plagioclase laths in amphibole as well as intergranular mafic minerals.
---------------------	---

mineral	%	grain size (mm)	comments	
Plagioclase	35	3.0	euhedral - subhedral, lath-shaped to prismatic, polysynthetic twins, zonation, subophitic to ophitic enclosed by px or amp, strongly altered to sericite, An-content: 50-55	
Quartz	7	0.7	anhedral, granular, colorless, undulatory extinction, arranged in interstitial patches, corroded margins	
Pyroxene	< 6	0.5	anhedral, pale brown, only fragments preserved, nearly completely replaced by amphibole (uralitisation), probably more orthopyroxene (stubby prismatic, nearly parallel extinction)	
Amphibole	Actinolite	10	≤ 0.9	sub- to anhedral, fibrous, acicular, lightly green, inclined extinction (15°), intergrowth with biotite, alteration product
	Hornblende	12	2.4	sub- to anhedral, long prismatic to short columnar, green to brown, strong pleochroic, pseudomorph after px, inclined extinction (20°), tiny inclusions of magnetite
Biotite	8	≤ 0.8	euhedral - anhedral, tabular to platy/flaky, brown, hexagonal basal sections, pleochroic halos around zircons, birds-eye structure	
Calcite	3	0.5	anhedral, granular, colorless, parallel twins, high order interference colors, alteration product of plag	
Further alteration minerals	15	< 0.2	anhedral, sericite, chlorite and clay minerals as further alteration-products, intergrowth with biotite & plagioclase	
Fe-Ti-oxides	3 - 4	0.4	multilateral to skeletal shapes, mainly magnetite (isotropic) with exsolution lamellae of ilmenite (anisotropic), also tiny magnetite inclusions in amphibole	
Sulphides	< 1	0.3	light yellow isotropic pyrite cubes as well as deep yellow anisotropic chalcopyrite as fine disseminated grains	

COMPOSITION	gabbroic
-------------	-----------------

CLASSIFICATION	medium grained, highly altered, hornblende bearing Microgabbro
----------------	---



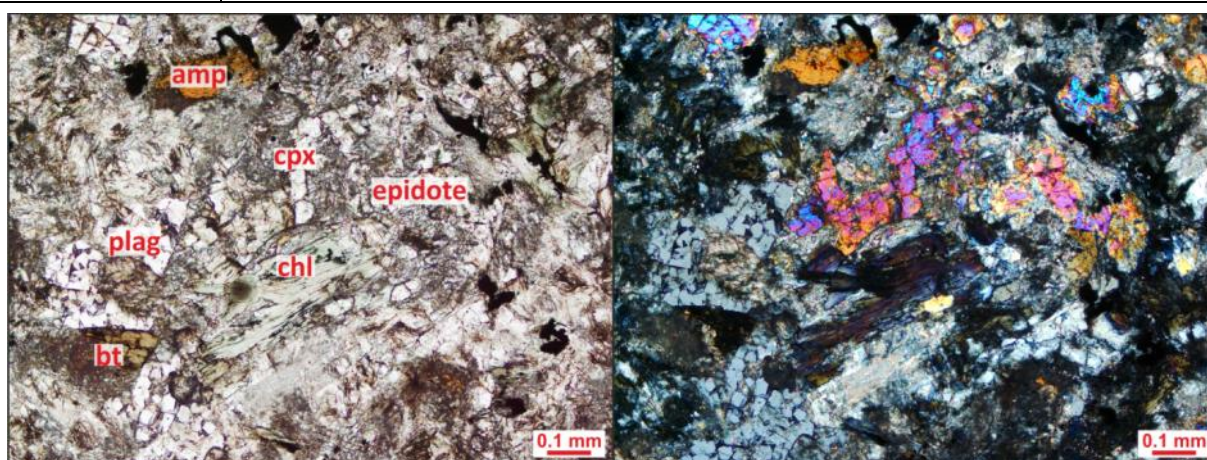
Intergrowth of fibrous actinolite, biotite, chlorite and magnetite (opaque minerals) between strong altered plagioclase crystals.

Thin section	D_20-6_6/1
--------------	------------

GENERAL DESCRIPTION	Fine grained, highly altered, epigranular hypidiomorphic to xenomorphic rock of gabbroic composition. Probably contact metamorphic affected. Mafic minerals (amp, bt, px) fill the interstices of small plagioclase laths. Relative high amount of opaque minerals.
---------------------	---

mineral	%	grain size (mm)	comments
Plagioclase	25 - 30	≤ 0.5	subhedral, small lath-shaped crystals as well as granular interstitial fillings, strong alteration (sericitisation & saussuritisation), mainly in the centre of the plag crystals
Quartz	8	0.2	sub- to anhedral, undulated extinction, in form of granular interstitial between plag, yellowish (thick section), relative high amount
Pyroxene	< 5	0.2	anhedral, pale brown to pale green, only fragments are preserved, because of the strong alteration to amp (uralitization), probably clinopyroxene
Amphibole	15 - 20	0.2 - 0.4	sub- to anhedral, prismatic to short columnar, green or brown, partly fibrous (actinolite), strong pleochroic, inclined extinction (20° → hornblende), hexagonal end section with 60°-120° cleavage angles, inclusions of fine magnetite
Biotite	3 - 5	0.15	sub- to anhedral, tabular to platy/flaky, brown, pleochroic, parallel extinction, pleochroic halos around zircons, birds-eye structure
Chlorite	12	0.5	sub- to anhedral, flaky to fibrous, green, pleochroic halos around zircon, anomalous yellow & blue interference colors, parallel extinction, alteration product
Epidote	5 - 7	0.3	sub- to anhedral, granular, colorless to pale citreous, typical shiny interference colors, surrounded by plagioclase, alteration product
further alteration minerals	10	0.1	sub- to anhedral, sericite, calcite and clay minerals as further alteration products of plagioclase
Fe-Ti-oxides	4	≤ 0.2	multilateral, hackly to skeletal shapes, mostly magnetite (isotropic), but also titanomagnetite, ilmenite, hematite
Sulphides	< 1	≤ 0.1	single pyrite cubes as well as fine disseminated grains of pyrite, isotropic, light yellow, sometimes tarnishing

COMPOSITION	gabbroic
CLASSIFICATION	fine grained, highly altered, quartz-bearing Micro-Gabbro



An anhedral clinopyroxene crystal (middle) is intergrown with chlorite and epidote. All of these are surrounded by plagioclase, which has a net like surface in due of the thickness of the thin section. The chlorite shows a pleochroic halo (dark-green spot within the crystal) and anomalous blue interference color.

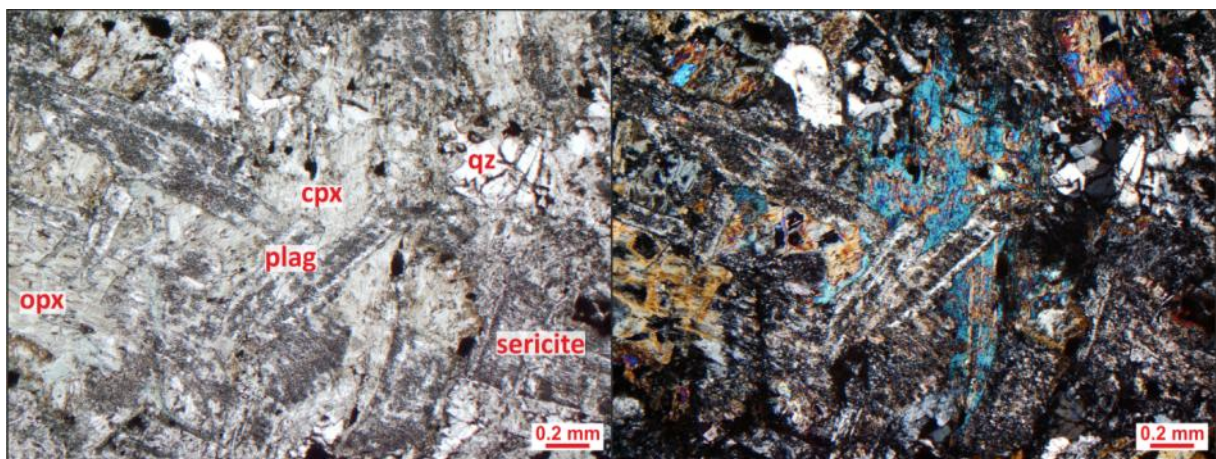
Thin section	HB_8-7_4/1
--------------	------------

GENERAL DESCRIPTION	Medium grained, highly altered hypidiomorphic rock of gabbronoritic composition. Plagioclase is subophitic to ophitic enclosed by pyroxene, which is partly replaced by amphibole. Interstitial plagioclase is variolitic or spherulitic arranged.
---------------------	--

mineral	%	grain size (mm)	comments
Plagioclase	30	≤ 1.2	euhedral - subhedral, lath-shaped to long prismatic crystals, which are strong altered (saussuritisation & sericitisation) and subophitic to ophitic enclosed by px, also interstitial plag partly arranged as variolites or spherulites
Quartz	8	0.2	anhedral, undulatory extinction, interstitial patches (up to 0.8 mm) of quartz crystals between plag
Orthopyroxene	13	4.0	euhedral - anhedral, short prismatic to lath-shaped, pale green, parallel extinction, strong altered to clay minerals, serpentine (bastite), carbonate and chlorite
Clinopyroxene	7	< 1.0	sub- to anhedral, prismatic to granular, inclined extinction (44° → augite), highly altered to amphibole, especially at the margins
Amphibole	10	0.8	euhedral - anhedral, green, strong pleochroic, surrounding px (corona texture) or forms pseudomorphs after px; also fibrous to columnar, pale green actinolite (inclined extinction 18°)
Chlorite	3	0.1	anhedral, flaky, fibrous to felted, green, anomalous blue interference colors, alteration product
Further alteration minerals	20	< 0.1	result of sericitisation and saussuritisation: sericite, epidote, zoisite, calcite (additionally to chlorite)
Fe-Ti-oxides	1 -2	< 0.2	3 to 4 sided shapes, no skeletal, mainly magnetite, ilmenite, rutile, surrounding the pyroxenes

COMPOSITION	gabbroic to noritic
-------------	----------------------------

CLASSIFICATION	medium grained, highly altered, quartz-bearing "Meta"-Gabbronorite
----------------	---



Plagioclase laths, which are altered to sericite in the centre, are subophitic enclosed by an anhedral clinopyroxene crystal (light blue interference color). Small quartz crystals are arranged in clusters (white fields on the top). On the left the fragments of an orthopyroxene crystal occur, whereas the central part of the crystal is replaced by alteration minerals.

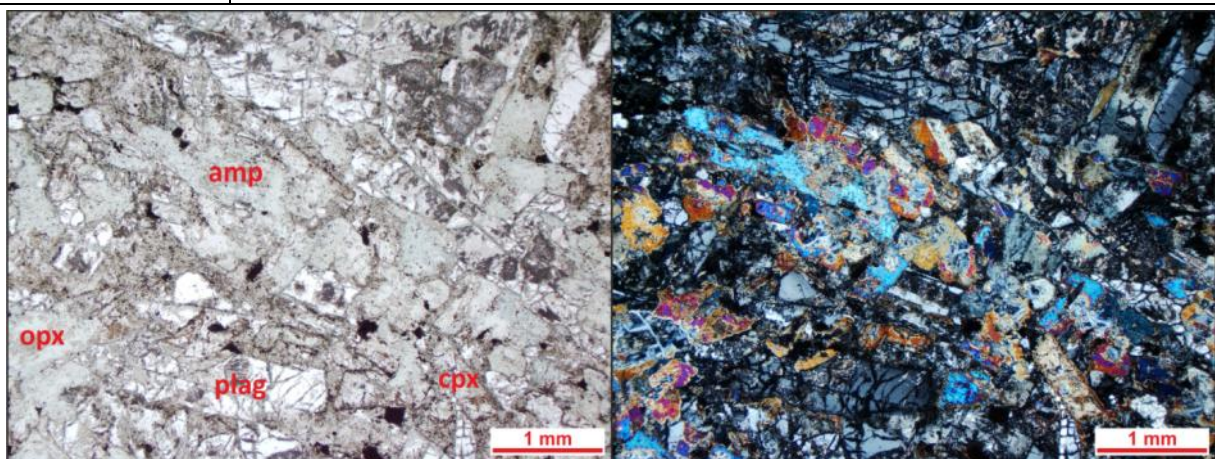
Thin section	HB_1-7_6/1
--------------	------------

GENERAL DESCRIPTION	Medium to coarse grained, strong altered hypidiomorph rock of gabbronoritic composition. Plagioclase is subophitic enclosed by pyroxene, which is partly altered to amphibole. Pyroxene is arranged intergranular between plagioclase laths.
---------------------	--

mineral	%	grain size (mm)	comments
Plagioclase	35	≤ 5.2	euhedral - subhedral, lath-shaped to tabular, partly arranged as spherulites, also in interstices, twinning, fresh as well as altered (seritisation & saussuritisation)
Quartz	5	0.3	anhedral, undulatory extinction, interstitial patches (up to 1 mm) between plag and pyroxenes
Orthopyroxene	12	1.2	subhedral - anhedral, prismatic to lath shaped, pale brown, parallel extinction, the core is strong altered to serpentine (bastite), margins altered to amph,
Clinopyroxene	18	2	subhedral, lightly brown, prismatic to tabular, inclined extinction (38° diopsid), perpendicular cleavage planes, twinning, intergranular between plag laths
Amphibole	15	2	sub- to anhedral, green, strong pleochroic, non-parallel extinction (10°-20° actinolite, hornblende), alteration product, partly pseudomorphic after cpx,
Chlorite	4	0.1	anhedral, flaky to fibrous, pale green to green blue, anomalous blue and yellow interference colors (Mg and Fe chlorite), alteration product of plag
Further alteration minerals	10	0.2	anhedral, alteration products of plag: sericite, zoisite, calcite, epidote (additionally to chlorite) as well as alteration products of pyroxene: serpentine, clay minerals
Fe-Ti-oxides	< 1	≤ 0.1	hackly-shaped or 3 to 4 sided shapes, sparse occurrence, mixture of magnetite, ilmenite, sphene with exsolution lamellae
Sulphides	< 1	< 0.05	fine disseminated grains of pyrite, insignificant amounts

COMPOSITION	gabbronoritic
-------------	----------------------

CLASSIFICATION	medium to coarse grained, strong altered gabbronorite
----------------	--



Pyroxene is partly replaced by green amphibole. An orthopyroxene crystal (bottom left) is strongly altered to a mixture of serpentine, clay minerals and amphibole. In contrast the plagioclase occurs relative fresh, sericitisation is limited to the centre of the crystals (bottom middle).

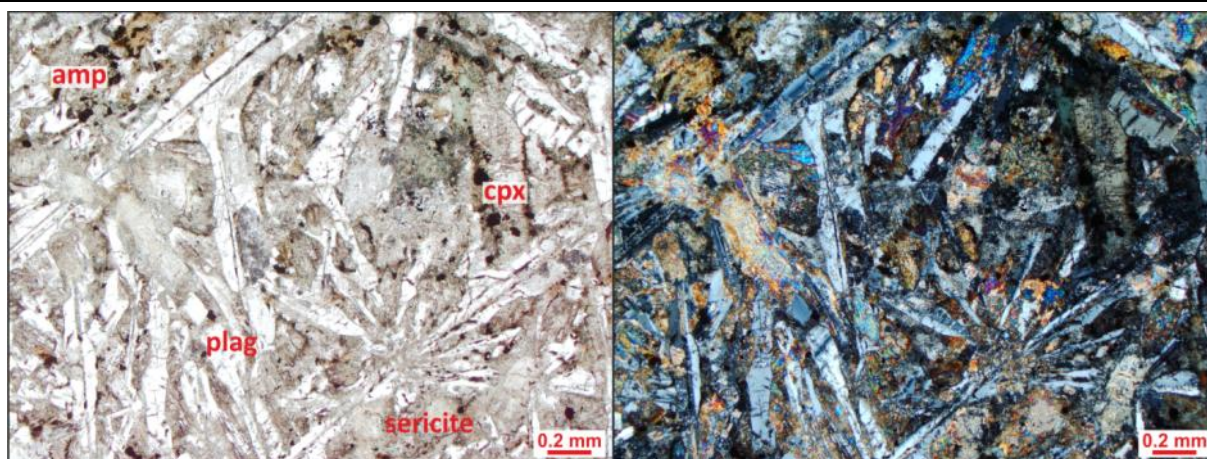
Thin section	U_22-6_7/1
--------------	------------

GENERAL DESCRIPTION	Medium grained, altered, idiomorphic to hypidiomorph rock of gabbronoritic composition. Plagioclase forms long lath shaped crystals arranged in spherulites, the interstitial space and the spherulites centers are filled with alteration minerals, pyroxene and amphibole. Small plagioclase crystals are ophitic enclosed in pyroxene.
---------------------	---

mineral	%	grain size (mm)	comments
Plagioclase	35 - 40	4.0	eu- to subhedral, lath-shaped to short prismatic, long laths form big spherulites, polysynthetic twins, zonation, also small tabular crystals as interstitial filling, fresh to low altered along cracks, An-content: 80-90
Quartz	3 - 4	0.2	anhedral, less single crystals between plagioclase laths, yellowish (thick section)
Clinopyroxene	18	0.8	subhedral, long prismatic to short columnar, pale brown, inclined extinction (44° → augite), cleavage angles near 90°, centric alteration to amphibole (uralitisation), intergranular between plag laths
Orthopyroxene	8	0.2	sub- to anhedral, stubby prismatic to granular, low interference colors, cleavage angles near 90°, parallel extinction, marginal alteration to amp
Amphibole	15	1.2	sub- to anhedral, prismatic to tabular, granular, partly fibrous, pseudomorphic after px, pale green to colorless actinolite/tremolite (inclined extinction 15°) as well as blue-green strong pleochroic hornblende with fine inclusions of magnetite
Chlorite	5	< 0.1	sub to anhedral, flaky to fibrous, green, anomalous yellow and blue interference colors (Mg and Fe chlorite), alteration product
Further alteration minerals	10	< 0.1	anhedral, sericite, epidote, clay minerals, biotite, basically along two long cracks, which get through the thin section
Fe-Ti-oxides	< 1	0.05	insignificant amounts of 3 to 4 sided shapes of grey isotropic magnetite, also tiny inclusions of magnetite in amphibole

COMPOSITION	gabbronoritic
-------------	----------------------

CLASSIFICATION	medium grained, altered gabbronorite
----------------	---



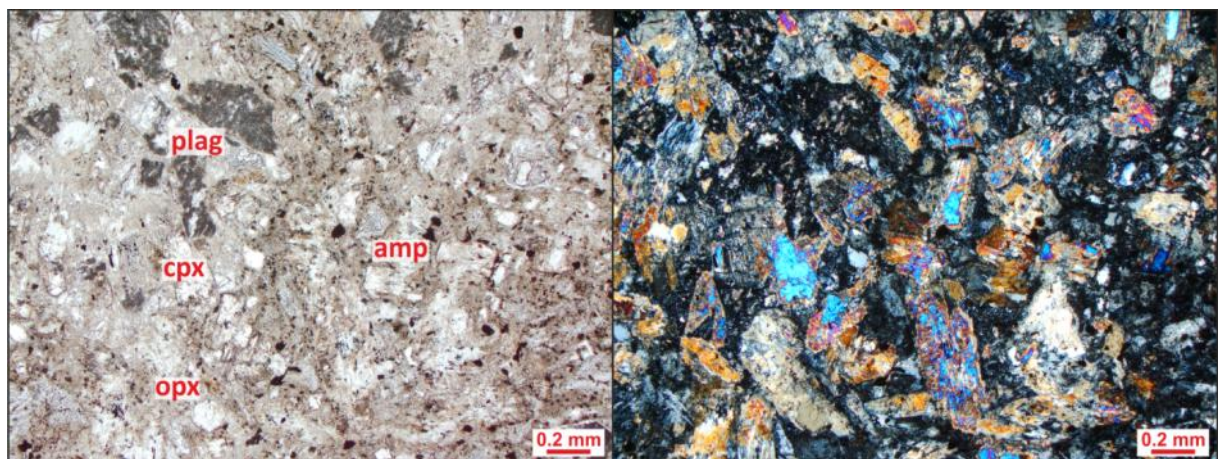
Plagioclase laths arranged as spherulites (bottom right), the space between is filled with amphibole and alteration minerals like sericite and talc (high order interference colors). A long prismatic clinopyroxene crystal (right) is marginal altered to amphibole and surrounded by small magnetite crystals (opaque phase).

Thin section	U_24-6_2/1
--------------	------------

GENERAL DESCRIPTION	Fine to medium grained, strong altered, hypidiomorph and epigranular rock of gabbronoritic composition. Ortho- and clinopyroxene are dominant, but also altered to amphibole. Granular plagioclase forms the intercumulus phase together with alteration minerals and Fe-Ti-oxides.
---------------------	---

mineral	%	grain size (mm)	comments
Plagioclase	25	1.2	sub- to anhedral, granular, lath-shape or prismatic crystals are rare and strong altered (seritisation, saussuritisation), as interstitial filling/ intercumulus phase between px, together with qtz & alteration minerals
Quartz	5	0.2	anhedral, undulatory extinction, colorless to yellowish (thick thin section), together with plag as interstitial filling
Clinopyroxene	20 - 25	0.8	subhedral, long prismatic to short columnar, pale brown, twinning, inclined extinction (45° → augite), cleavage angles near 90°, centric alteration to amphibole and clay minerals, exsolution lamellae of opx
Orthopyroxene	10	0.5	sub- to anhedral, stubby prismatic, quadratic or octahedral basal sections, colorless to pale brown, low order interference colors, parallel extinction, marginal alteration to amp
Amphibole	18	0.7	sub- to anhedral, prismatic to tabular or fibrous to columnar, pale green to colorless actinolite/tremolite (inclined extinction 15°) as well as blue-green strong pleochroic hornblende surrounding opx crystals
Epidote	3	0.1	anhedral, granular, colorless to pale yellow, intensive multiple interference colors, alteration product
Further alteration minerals	12	≤ 0.2	anhedral, including sericite, chlorite, clay minerals, result from plagioclase and amphibole alteration
Fe-Ti-oxides	< 1	0.05	few multilateral shapes of isotropic magnetite with exsolution lamellae of ilmenite, also tiny inclusions of magnetite in amphibole
Sulfides	< 1	< 0.05	insignificant amounts of fine disseminated light yellow pyrite grains and rare isotropic pyrite cubes

COMPOSITION	gabbronoritic
CLASSIFICATION	fine grained, strong altered gabbronorite



The epigranular gabbronorite consists basically of stubby prismatic orthopyroxene and elongated clinopyroxene, which are partly replaced by amphibole crystals. Plagioclase is strong altered to sericite and saussurite, and occurs mainly as interstitial filling between mafic minerals.

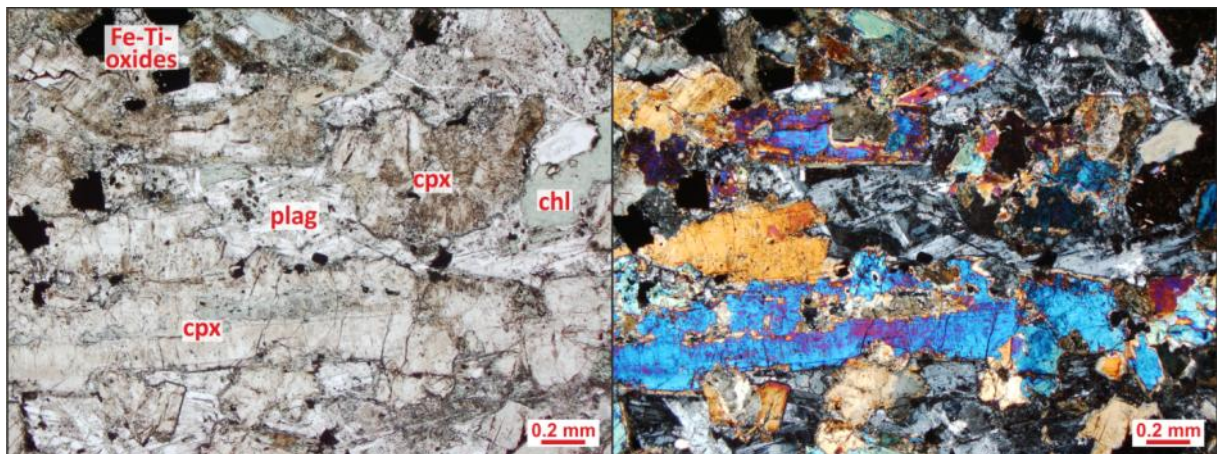
Thin section	BD_13-7_1/1
--------------	-------------

GENERAL DESCRIPTION	Medium grained, strongly altered hypidiomorphic basement dyke of gabbronoritic composition. Primary minerals are plagioclase (largely replaced by sericite) and clino- & orthopyroxene, which are marginal altered to amphibole. Micrographic intergrowth between plag and quartz. Intergranular/interstitial textures.
---------------------	---

mineral	%	grain size (mm)	comments
Plagioclase	25	< 0.7	subhedral, short prismatic to elongate crystals, polysynthetic twins, highly altered (mainly sericitisation in the centre), micrographic intergrowth with quartz
Quartz	7	0.2 - 0.4	anhedral, yellowish (section to thick), undulatory extinction, single crystals as well as interstitial patches, micrographic intergrowths
Clinopyroxene	20	< 1.5	sub- to anhedral, lath-shaped to short prismatic, pale brown, inclined extinction, twinning, strong altered to amphibole (especially at the margins), permeated by fractures
Orthopyroxene	13	0.2 - 1	euhedral - subhedral, stubby prismatic, pale brown or pale green, compositional zoned, parallel extinction, low order of interference colors, octagonal basal sections
Amphibole	5	0.6	sub- to anhedral, brown and green, strong pleochroic, inclined extinction, alteration product of px
Biotite	3 - 5	< 0.2	anhedral, flaky/platy, brown, birds-eyes extinction, intergrowth with amp and cpx
Chlorite	4	< 0.4	anhedral, flaky, green, anomalous yellow interference colors (Mg-rich), alteration product
Further Alteration minerals	18	0.3	anhedral, mainly very fine flaky sericite as alteration product of plag, also sub- to anhedral calcite (up to 1 mm) with typical parallel twins
Fe-Ti-oxides	2	≤ 0.4	multilateral shapes or cubes, mostly magnetite, but also ilmenite, hematite and rutile (red-brown, high relief, granular)

COMPOSITION	gabbronoritic
-------------	----------------------

CLASSIFICATION	medium grained, altered quartz-bearing basement dyke
----------------	---



Pale brown clinopyroxene occurs as subhedral laths and also as anhedral grains, which are deformed recognizable on the twin-like field division (middle right). Sub- to anhedral plagioclase crystals appear as interstitial filling.